Coastal Defence Vulnerability 2075

J Sutherland
J Wolf

Report SR 590
February 2002

Coastal Defence Vulnerability 2075

J Sutherland
J Wolf

Report SR 590
February 2002

HR Wallingford

Address and Registered Office: HR Wallingford Ltd. **Howbery Park, Wallingford, OXON OX10 8BA**
Tel: +44 (0) 1491 835381 Fax: +44 (0) 1491 832233

Contract - Research

This report describes work funded by the Department for the Environment, Food and Rural Affairs (DEFRA) through commission FD2303. The work was carried out by Dr J Sutherland, Mr RL Soulsby, Dr AH Brampton, Dr PJ Hawkes, Dr S Clarke and Mr BP Gouldby of HR Wallingford and Dr J Wolf, Dr RA Flather and Dr JC Hargreaves of the Proudman Oceanographic Laboratory. The project manager was Dr J Sutherland and the sponsor was Mr RL Soulsby. The HR Wallingford job number was CLS0045. Publication implies no endorsement by DEFRA of the report's conclusions or recommendations.

Prepared by ....

(name)

....

(Title)

Approved by ....

(name)

....

(Title)

Authorised by ....

(name)

....

(Title)

Date ....

Summary

Coastal Defence Vulnerability 2075

Report SR 590
February 2002

This report assesses the possible changes in coastal defence vulnerability (to overtopping or erosion) caused by global climate change over the next 75 years. The effects of climate change on waves and water levels were estimated using two thirty-year time slice simulations of a global climate model. The first simulation represented present day conditions and the second represented a future scenario, centred on 2075. The climate model produced meteorological forcing that was used to drive a wave hindcasting model and a tide-surge model. Hence wave and water level time series were derived for the present-day and future scenarios.

Three methods of estimating the changes in coastal defence vulnerability between now and 2075 were used. The methods use present and future simulations to calculate:

1. Coastal defence response to combined waves and water levels, using numerical models.
2. Longshore drift rates, to compare annual mean drift rates and their variance.
3. Statistical analysis of coastal defence response functions, derived from empirical equations.

The results were used to estimate changes in coastal defence vulnerability due to climate change at five test regions around the English and Welsh coastline. The results produced are not site specific but rather generic. Simplified bathymetries and typical structure types were used in an effort to provide results that are broadly representative of stretches of coastline, rather than specific locations. The results have also been driven by a single realisation of a single climate change scenario, run on a single climate model. Due to the variability between models and the range of scenarios considered possible by the IPCC, the modelled predictions do not give a definitive view of the changes that will occur and the results should be interpreted with caution.

Changes in wave climate around the UK are predicted to be small (generally less than 5% for wave height) and the increase in future extreme water levels will generally be within 20% of the increase in mean sea level. Sea level rise of 0.35m will cause average increases in overtopping volume of between 50% and 150%, depending on structure type, location and modelling approach and if present day defences are unchanged in 2075. If the observed coastal steepening continues it will increase overtopping rates by a further 15%, approximately. The inclusion of sea level rise predictions in design calculations should account for the majority of the predicted change in wave impact on coastal structures.

Summary *continued*

A formula was presented for the increase in crest elevation necessary to maintain present day overtopping rates when sea levels rise. It is based on well-established empirical overtopping formulae and shows that crest levels need to be raised by more than sea level rise to achieve this. Scour and damage potentials may increase or decrease as a result of climate change, depending on how the partial standing wave velocities at the coastal structure change. The average changes in scour potential were 16% for the seawall and less than 2% for the embankment and shingle beach.

In most cases the simulated future mean annual longshore drift rates were slightly greater than the present day rates (by an average of around 15%) but the standard deviations were all lower (also by around 15%). The greater volumes of material that may need to be re-nourished, but reduced inter-annual variability, would impact on the economic viability of beach nourishment and may necessitate a review of management options. However, as there is great uncertainty in the prediction of longshore transport, the work tends to show that future changes are unlikely to be greater than current levels of uncertainty and these should be considered in the normal course of sensitivity testing.

Qualitative and quantitative differences in future changes in vulnerability were found between the five sites examined around the coastline of England and Wales. This is because the sites have different tidal ranges, wave climates and surge levels. Moreover, the parameters have different joint probabilities at different sites. Thus results from one site cannot be transferred directly to other sites and individual assessments must be made for specific sites. Nonetheless, the modelled scenarios give an indication of the general extent of changes in coastal defence vulnerability that can be expected in the next 75 years.

Contents

Contents continued

Contents continued

Plates

Appendices

1. INTRODUCTION

Our climate is changing. Working Group I of the Intergovernmental Panel on Climate Change (IPCC) recently completed a comprehensive assessment of past, present and future climate change (IPCC, 2001a) as its contribution to the IPCC's Third Assessment Report (TAR). IPCC (2001a) catalogues increasing greenhouse gas concentrations. It tells us that sea level is rising and will continue to rise for hundreds of years even if greenhouse gas concentrations are stabilised during this century (Church *et al.*, 2001). Climate change will lead to altered wave heights and storm surges while sea level rise will increase mean and peak water levels and will change tidal ranges and storm surge amplitudes. These changes will affect the vulnerability of coastal defences to overtopping and damage. They will also affect beaches by altering longshore sediment transport rates and hence beach plan shapes.

These changes may produce considerable impacts at the coast. These impacts and possible adaptation strategies have been discussed in the contribution of Working Group II (IPCC, 2001b) to the IPCC's TAR. The possible impacts of climate change are, however, described in qualitative, general terms. Coastal zones contain large human populations and significant economic activity, from ports to tourism. Significant inhabited areas in the UK are below mean high water level. It is estimated that in 1990 approximately 25 million people in Europe lived beneath the 1 in 1,000 year storm surge level (IPCC, 2001b). These people are generally well protected from today's conditions but may become more vulnerable as a consequence of climate change.

This report seeks to assess the possible changes in coastal defence vulnerability (to flooding or erosion) caused by global climate change over the next 75 years. The effects of climate change were isolated by assuming that other factors (such as the shape of defence structures, beach level at the toe and offshore bathymetry) remain the same, although the effect of coastal steepening was included as its causes and relationship to climate change are not understood.

The project was carried out as a collaboration between HR Wallingford (HR) and the Proudman Oceanographic Laboratory (POL). A total of six HR staff and three POL staff (named on the contract page of this report) collaborated in the exchange of data and model results and in the linking of numerous numerical models. Indeed, the linking of models and multiple exchange of results between HR and POL was a notable feature of the project.

The effects of climate change on waves and water levels were estimated using two thirty-year time slice simulations of a global climate model. The first simulation represented present day conditions and the second represented a future scenario. In order to get a modelled climate suitable for detecting changes to the vulnerability of coastal defences, high spatial and temporal resolutions were required from the climate model. These are necessary to model storms which last from hours to days. The climate model produced meteorological forcing that was used to drive a wave hindcasting model and a tide-surge model. Hence wave and water level time series were produced for present day and future conditions. No swell was included in the wave modelling.

The response of beaches and structures to present and future conditions was then simulated and the changes in coastal defence vulnerability due to climate change were estimated. Three methods of determining the changes in coastal defence vulnerability between now and 2075 were used in this project. They are:

1. Coastal defence response to sea conditions with given joint exceedance probabilities. In this method a limited number of wave/water level combinations with a given return period were modelled to give overtopping rates and velocities. A number of state-of-the-art numerical models were used to transform the waves inshore and onto the structure.

2. Effects of changes in beach levels and plan shapes. Longshore drift calculations are used to compare annual mean drift rates and their variance for present and future conditions. The effect of these values on beach plan shape and beach management was discussed.
3. Statistical analysis of coastal defence response functions. In this analysis simple empirical equations were used to calculate overtopping rates for each wave/water level combination produced by a Monte-Carlo simulation. A full statistical analysis of the overtopping response was obtained, but the process modelling was simplified.

The methods were used at five test regions around the English and Welsh coastline. The results produced are not site specific. Simplified bathymetries and typical structure types were used in an effort to provide results that are broadly representative of stretches of coastline, rather then specific locations. The results are intended to inform the future planning of defence needs and any adaptation strategies. Preliminary results were presented in Sutherland and Wolf (2001).

2. SUMMARY OF TEST REGIONS

Five locations around the coast of England and Wales were selected to give a range of wave and tide conditions and also coastal types and defences. The locations are shown in Figure 1 and brief descriptions of the sites are given below.

2.1 Lincolnshire – East Coast

This has a long stretch of eroding beach in front of various types of seawall and has recently been the site of the largest beach nourishment so far undertaken in the UK. The hinterland is low-lying, and extensive flooding has occurred in the past, with loss of life in 1953. Maintaining adequate defences against wave overtopping is of crucial concern. Coastal steepening has been observed along much of this coastline, and the inter-tidal (and sub-tidal) clay seabed is being lowered by marine action. Long-term defence strategy plans are for continued beach recharge, so that any changes in longshore sediment transport rates are of interest, as well as any need to increase the beach height or width to deal with higher tidal levels or storm wave action. The frontage is east facing, onto the southern North Sea, and swell is present although unlikely to dominate coastal changes. Studies of this frontage would be potentially useful in assessing changes on similar types of coastline in East Norfolk and Northumberland.

2.2 Dungeness to Rye (Kent/Sussex, English Channel)

This frontage faces approximately south-west, and although some swell occurs, it is the storm waves generated in the English Channel that pose the greatest threat to coastal zone. The beaches are of shingle, although there is a large sand beach at Camber at the eastern end of the frontage. Coastal defence is achieved by a combination of measures including groynes, seawalls and beach re-cycling. The hinterland is low-lying, and parts of it are of great conservation value. The main economic assets are residential and commercial properties and valuable agricultural land, in areas reclaimed from the sea long ago. At the south-eastern end of this frontage lie the two nuclear power stations at Dungeness, and their presence significantly affects the long-term strategy for coastal defence. Drift rates are modest, and variable from year to year, so that changes in the average drift rate would be of considerable relevance to the continued usage of re-cycling beach sediment as an element of coastal defence management.

2.3 West Bay and Chesil Beach, Dorset (South coast)

This long gravel beach is largely in a natural state, although there are coastal defences at the extreme south-eastern end in front of Chiswell village. Longshore drift rates are generally low, and variable, although recent changes have had significant effects on the protection the beach provides to West Bay, Bridport, at the north-western end of the beach. Changes in the cross-section of this beach, or in the frequency and intensity of wave overtopping, will have the potential to cause major problems to the developments behind it, at West Bay and Chiswell. Quite conceivably, the recession of this beach and increased flooding could sever the road link between Portland and the mainland coast at Wyke Regis. The beach is susceptible to overtopping by swell waves approaching from the south-west, as well as to severe storm wave activity generated within the English Channel.

2.4 Swansea Bay – Mumbles to Porthcawl (South Wales)

This major south-west facing embayment has major commercial developments at risk at its northern end (Swansea, Neath, Port Talbot), an important conservation area in its centre (Kenfig Dunes) and a popular holiday destination further south (Porthcawl area). At times in the past, this coastline suffered from rapid accumulation of sand that overwhelmed agricultural land and several small villages. At present, however, there appears to be a long-term recession problem, threatening coastal assets. Waves are a mixture of swell and locally-generated, and the tidal range is large. Defences are largely near-vertical seawalls, and overtopping is a problem at several locations. A number of studies have been carried out in the past, aimed at understanding the hydrodynamic and sediment transport patterns in this area, partly in connection with dredging and the construction of Port Talbot. There is some information on coastal steepening data (for

Barry to Port Talbot). Note that sites further up the Bristol Channel would be more difficult to model due to concerns about the accuracy of future wind information from the ECHAM4 model.

2.5 Fylde, Lancashire (Irish Sea)

This frontage has a high tidal range, and experiences occasionally severe wave action. When these events occur together, flooding and damage results. Of all the potential sites chosen, this coast probably has the smallest occurrence of swell waves, so that predicting future wave climates is more straightforward here than elsewhere. The coastal defences along this frontage are typically vertical or near-vertical seawalls, often with a low beach at their toe (e.g. Blackpool). Sand beaches in front of high, impermeable seawalls are slowly lowering, as is the inter-tidal and sub-tidal seabed. Longshore drift rates, however, are low, so that any changes in the present balance between waves from different directions may cause more rapid changes in foreshore levels. Preservation of both the sandy beaches and the highly developed nearshore zone will be regarded as essential over the next 75 years, even if considerably more has to be spent on improving or rebuilding existing defences.

3. REVIEW OF RECENT RELEVANT RESEARCH

Various recent studies have aimed at understanding and quantifying changes in sea level, storm surge and wave climatology due to present and predicted climate change. Some studies have used meteorological data from climate models (known as general circulation models, or GCMs) to attempt to quantify changes associated with increases in atmospheric CO_2. Two sets of runs are typically carried out with “control" data representing present day conditions and with data from a "$2\times CO_2$" future climate scenario. Results are analysed to estimate extremes for each set and differences examined. The majority of these projects have used greenhouse gas emissions scenarios derived by the IPCC (Leggett *et al.*, 1992, Nakićenović *et al.*, 2000). Recently, two EU projects (WASA and STOWASUS-2100) have both produced multi-year time series of wave model and tide-surge model data over the NE Atlantic. WASA included present day wave and surge hindcasts for 1955-1995 and predictions for $2\times CO_2$. STOWASUS-2100 used meteorological data from the ECHAM4 GCM for “control” and “$2\times CO_2$” scenarios to investigate possible changes in the storm surge and wave climate. The JERICHO project (Cotton et al., 1999) examined trends in offshore wave climate from satellite and buoy data and used the SWAN wave model to transform offshore wave climate to the coast. Another EU project, Eurowave, (Cavaleri et al., 1999) also used SWAN to transform offshore waves to the coast for any location in NW Europe. Some of these studies are discussed further below.

3.1 Climate change 2001: The scientific basis

Working Group I of the Intergovernmental Panel on Climate Change (IPCC) has recently completed a comprehensive assessment of past, present and future climate change (IPCC, 2001a) as its contribution to the IPCC’s Third Assessment Report (TAR). This contribution analyses the increasing body of observations that gives a collective picture of a warming world with a changing climate. It notes that:

- “Concentrations of atmospheric greenhouse gases have continued to increase as a result of human activities.
- Confidence in the ability of models to project future climate has increased.
- There is new and stronger evidence that most of the warming observed over the last fifty years is attributable to human activities.
- Global average temperature and sea level are projected to rise under all IPCC SRES scenarios.
- Anthropogenic climate change will persist for many centuries.”

SRES is the IPCC Special Report on Emissions Scenarios (Nakićenović *et al.*, 2000). This has produced a new set of standard greenhouse gas emissions scenarios that will gradually replace the earlier set (Leggett *et al.*, 1992) that includes scenario IS92a used in this report. The SRES was published too late for its scenarios to be modelled here. IPCC (2001a) gives a range of possible future sea level rise, all calculated using scenario IS92a.

3.2 WASA

The WASA Project (Günther et al., 1998) produced hindcast waves for the North Atlantic and North Sea from 38°-77°N, 30°W-45°E. Forty years of hindcasts were produced, based on 100 years of observations, for the Northeast Atlantic. The WAM wave model was run on 2 nested grids: 1.5°×1.5° for the North Atlantic and 0.5°×0.75° for the Northeast Atlantic. Two sets of analysed wind fields from different weather centres were used to drive the models. The results do not support large increases in wave height. The mean significant wave height, *Hs,* appeared to be increasing by about 0.2% annually over the study period. The large variability spatially and temporally may be the cause of an apparent increase in “storminess”. Part of the variability is attributed to the North Atlantic Oscillation, which has increased over the past 30 years. There is only a very small change in mean significant wave height but significant increases in the 90 and 99th percentiles. (Whilst the authors claim that this result is real, it is just the effect that would be expected for a long dataset where resolution of events had considerably improved over the period in question).

3.3 JERICHO

The JERICHO project (Joint Evaluation of Remote sensing Information for Coastal defence and Harbour Organisations) was a BNSC Earth Observation LINK programme, funded by the British National Space Centre and the Environment Agency (Cotton et al., 1999). The principal objective of the JERICHO project was to investigate which parts of Britain's coastline may have experienced an increase in wave height similar to that observed by satellites in the surrounding seas. The satellite record of wave heights, measured almost continuously since 1985, shows a clear signal of an increase in winter of about 10% over the last decade. Satellites cannot measure right up to the shoreline because the offshore signal to the sensor becomes contaminated by land within the footprint. Procedures for comparing the buoy recordings with the satellite observations, and the methods for modelling wave behaviour at the coast from the wave field derived or observed in deeper water were tested. A database of satellite and buoy data was compiled. Two shallow water wave models, STORM and SWAN, were employed to transform the offshore waves to the coast. The former is based on a ray-tracing model. SWAN is a state-of-the-art 3rd-generation spectral wave model. STORM could be used to run long time series to derive the nearshore wave climate. SWAN was used to transform only the extreme events. The approach was to use the most likely and the worst case estimate for each extreme. Results suggested that an increase of offshore wave height would result in a lesser increase at the coast where waves are strongly controlled by water depth.

3.4 STOWASUS-2100

STOWASUS-2100 (Regional STOrm, WAve and SUrge Scenarios for the 2100 century*)* project looked at the changes in storm, surge and waves using two 30-year met. data sets from a time slice experiment with the ECHAM4 climate model run by the Danish Meteorological Institute (May 2001). Changes in extreme surge elevations caused by changing storminess were investigated by POL. Corresponding studies of waves were carried out by the Norwegian Meteorological Institute (DNMI). The overall objective of STOWASUS-2100 was to study severe storms, surges and waves in the present climate and in a scenario with increased CO_2-concentration. More specifically the project was a joint atmospheric/oceanographic numerical modelling effort aiming at constructing and analysing storm, wave and surge climatologies for the North Atlantic/European region in a climate forced by increasing amounts of greenhouse gases and comparing results with present day conditions. It investigated whether any systematic anomalies regarding frequency, intensity or area of occurrence are found for these extreme events. Also physical mechanisms responsible for possible scenario anomalies were investigated. The project included the use of the POL 2D tide-surge model to investigate changes in surge height and frequency (Flather and Williams, 2000).

3.5 Extreme surge elevations

A similar study of climate change effects on extreme surge elevations has been carried out by the Hadley Centre (Lowe et al. 2001). Met data from a high resolution regional climate model were used to force a POL tide-surge model (CSX; resolution ~35km). The results for extreme surges differed from those from STOWASUS; possibly because of differences in the climate model predicted changes in storm climatology or the different extreme value analysis approach applied to the surge model data.

3.6 Integrated effects of climate change on coastal extreme sea levels

A DEFRA funded project, "Integrated effects of climate change on coastal extreme sea levels" (FD1204), ran in parallel to CDV-2075, aimed to derive guidance on changes / trends in extreme sea levels from *existing* information. The work was carried out by POL, with inputs from external experts, and results were reported in Flather et al. (2001). Changes in extreme sea levels, as observed at the UK coast or just offshore, can arise from a number of inter-related components. These are:

(a) global mean sea level (MSL) change (Church *et al.,* 2001) and observed regional trends (Woodworth et al., 1999)
(b) regional land movements (Shennan 1989; Williams et al. 2001)
(c) tidal changes due to effects of increasing mean sea level on tidal dynamics (unpublished POL work).

(d) changes in extreme storm surge elevations due to effects of increasing mean sea level on surge dynamics
(e) effects on the surge climate of changes in the storm climate itself, e.g. storm tracks, intensity and frequency of occurrence, sometimes referred to as "storminess" (as studied in STOWASUS-2100)

The results for (e) suggest that the 50-year return-period surge, S50, could increase by about 10cm on the East coast south of Flamborough Head, and on the Lancashire coast, but decrease by about 10cm on the South coast. However, these results were subject to considerable uncertainty.

3.7 Coastal Steepening

Coastal steepening is the phenomenon whereby the cross-shore profile does not retreat or progress as an equilibrium profile, but develops towards a steeper profile. Soulsby et al (1999) shows evidence that the intertidal width is decreasing in many areas around the British coastline. This is one of the manifestations of coastal steepening and can be determined by comparing old maps and charts to recent ones. Repeat surveys of offshore bathymetry have not been analysed to search for possible steepening below the low water mark in Britain. Coastal steepening has, however, been observed around many North Sea countries (Verwaest et al, 1999, Laustrup et al., 2000) mainly in the subtidal zone. No satisfactory explanation has been provided for the phenomenon (although in some places it may be linked to the securing of the landward boundary by hard or soft flood defence measures on a naturally retreating beach). It cannot, therefore, be modelled to produce an estimate of coastal steepness in 2075. The future scenario chosen for coastal steepening was that historic rates of steepening continue until 2075. A non-steepened beach was also used for the future scenario.

Allsop et al (1995) performed tests in a wave flume that showed that the damage to beach control structures is significantly increased by steepening the (local) beach slope in front of a structure. Hawkes et al. (1998) also performed laboratory tests that showed overtopping rates increasing with beach slopes up to a steepness of between 1:20 and 1:10, before levelling out. The level of damage to a structure with a 1:20 beach was also far higher than the damage to the same structure fronted by a 1:50 beach. Soulsby et al. (1999) performed numerical model tests using COSMOS and OTT (details of the models are provided in Appendix 1 of this report). They showed overtopping rates increasing with beach slope and showed an example case where increasing the beach slope from 1:50 to 1:30 led to a greater increase in overtopping than raising the mean water level by 1m.

4. SIMULATING THE EFFECTS OF CLIMATE CHANGE ON WAVES AND WATER LEVELS

Climate change will lead to changes in the height and frequency of occurrence of waves and storm surges while sea level rise will increase mean and peak water levels and will change tidal ranges, storm surge amplitudes and nearshore wave heights. The effects of climate change on waves and water levels have been simulated by simulating thirty-year timeslices of present and future scenario climates. The thirty-year timeslices of wind speed and direction plus atmospheric pressure were used to drive wave and tide-surge models, which determined present and future conditions.

The IPCC's best estimate (Church *et al*, 2001) was used for sea level rise (0.35m by 2075) while changes in the climate were modelled using a global climate model, ECHAM4 (developed at the Max Planck Institute for Meteorology, Hamburg). Hulme and Jenkins (1998) recommended a number of scenarios (the UKCIP'98 scenarios) for use in the UK. These are named low, medium-low, medium-high and high. These were all modelled using UK Hadley Centre for Climate Predictions and Research model HadCM2. Both ECHAM4 and HadCM2 meet the IPCC criteria for climate modelling, were used in IPCC (2001a) and have their results stored by the IPCC's Data Distribution Centre (DDC). The ECHAM4 simulations used IPCC emissions scenario IS92a published in the 1992 Supplementary Report to the IPCC Assessment (Leggett et al., 1992). This is close to the emissions scenario used in the HadCM2 medium-high scenario model run and gives very similar global-mean temperature anomalies to it (Hulme and Jenkins, 1998, Figure 12).

Brampton and Harford (1999) showed that ECHAM4 models present-day high wind speeds better than HadCM2 (at one location) and it is necessary to model high wind speeds correctly to model extreme wave and surge events. Moreover, only monthly-averaged wind speeds were provided in the UKCIP'98 scenarios, while the ECHAM4 model run provided a high temporal resolution (six hours) so the development of storms could be resolved. ECHAM4 also gave a high spatial resolution (about 125km) so winds were supplied from grid cells close to the coast but mainly over the sea. The model runs used provided long timeseries (thirty years) so that a range of annual climates was modelled.

The methods used to simulate the effects of climate change on waves and water levels are described below. Sections 4.2 and 4.3 then give the simulated present and future conditions for wave heights and water levels. The present and future conditions are used in three methods of simulating the response to these conditions. The three response methods are described in Sections 5 to 7.

4.1 Method

The effect of climate change on waves and water levels was simulated as follows:

1. Thirty-year time series of pressure, wind speed and direction were extracted at points corresponding to the coastal sites from model runs of the ECHAM4 atmospheric general circulation model (Roeckner et al. 1996). The runs represented present day conditions and future conditions, assuming a doubling of $C0_2$ levels. Figure 2 shows the ECHAM4 output grid and CDV-2075 points, close to the sites selected. Table 1 gives the latitude and longitude of the grid points.
2. The ECHAM4 time series were used as atmospheric forcing for 30-year simulations of sea surface elevation (including the effect of mean sea level rise for the future case) made by the POL 2D-TS tide-surge model, NISE, run using a 12km grid (Flather & Williams, 2000). Thirty-year time series of water elevation were output at grid cells near the selected sites and the output point of the ECHAM4 model. Figure 3 shows the NISE model grid and location of water level output data points. Table 1 gives the latitude and longitude of the grid points.
3. The ECHAM4 time series of pressure, wind speed and direction were also used as atmospheric forcing for 30-year simulations of wave conditions using HR Wallingford's HINDWAVE wave hindcasting model (Hawkes, 1987).

4. The synchronous time series of wave height and water level were analysed using the JOIN-SEA joint probability method (Owen *et al*, 1997). The output of JOIN-SEA was analysed to provide:
   - marginal extremes for wave heights and water levels (i.e. plots of wave height and water level separately against return period)
   - contours of equal joint probability of exceedence of wave height and water level
   - thousands of years of simulated synchronous wave heights and water levels at each high tide.

Figure 4 shows how these models (and the models used to predict the response to changing conditions) are linked within CDV2075. Further descriptions of the models and how they were implemented can be found in Appendix 1.

4.2 Simulated marginal extreme wave heights

The present and future marginal extremes for wave heights and water levels at the five sites are shown in Figures 5 to 9. The results for Lincolnshire (Figure 5) show a reduction in extreme wave heights for the future scenario, although frequently occurring waves have similar heights. For example, the 200-year return period wave in 2075 is 0.65m smaller than the present day value, whereas the 1-year return period wave height in 2075 is only 0.08m smaller. A similar pattern, but with smaller differences in wave heights, is found at Lyme Bay (Figure 7) whereas at Swansea Bay (Figure 8) there are no significant changes in wave height between present and future scenarios. The results for Dungeness to Rye (Figure 6) and Fylde/Blackpool (Figure 9) show that extreme wave heights are up to around 0.3m lower in the future, but that frequently occurring wave heights (with return periods less than 1 year) are up to around 0.2m higher in the future.

The relative change in wave heights is shown in Figure 10, where the future significant wave heights is divided by the present day significant wave height and plotted against return period. The majority of future wave heights are within five percent of present day wave heights. The only simulation significantly outside this range is for Lincolnshire wave heights at high return periods, which reduce to 86% of the present day heights by 2075. There are small increases in wave heights for return periods less than 0.2 years for Lyme Bay and Swansea Bay, up to three years at Dungeness and Fylde and greater than about 90 years at Swansea. The future wave heights are lower than the present day wave heights in all other cases. The results for Dungeness, Fylde, Lyme Bay and Lincolnshire show reducing ratios of future/present wave heights as the return period increases. Only Swansea shows a generally increasing trend.

4.3 Simulated marginal extreme water levels

The plots of water levels (Figures 5 to 9) show that the input 0.35m sea level rise has the greatest effect on water levels – changes in tidal levels and surge heights play a secondary role. Figure 11 shows the relative increases in marginal extreme water levels between present and future plotted against return period. Here the relative increase is $(WL_f - WL_p)/SLR$ with WL_f = marginal extreme water level in future scenario, WL_p = marginal extreme water level in present day scenario and SLR = 0.35m sea level rise used in the POL 2D-TS model. A value of one implies that the linear addition of the expected sea level rise to present day water levels will be an accurate representation of the future water levels. Variations away from one are due to non-linear interactions, such as the effect of changes in water level on tidal range and surge dynamics.

The results vary around the 35cm increase in water level imposed in the POL 2D-TS model [$(WL_f - WL_p)/SLR = 1$]. The results for return periods lower than approximately thirty years are almost all within 20% of this figure. In other words, a sea level rise of 0.35m will produce changes in marginal water levels of between 0.28m and 0.42m in almost all cases, for return periods less than about 30 years. Note that these calculations allow no regional land movements so the variations between sites are not due to relative changes in land movement. The greatest deviations occur at the extreme return periods, several times the length of the model datasets used to generate the long-term simulations. They may be due to problems in fitting curves to the extreme distributions and so the results should be treated with caution. The greatest increases in water level occur off the Fylde coast, as expected, because of the relatively high correlation between storms and surge in the Irish Sea. The sea levels showed increases over and above sea level rise at Fylde, Dungeness and Swansea Bay and decreases for Lyme Bay and Lincolnshire (the more open coastal sites with lower tidal ranges).

It is also interesting to estimate the ratio of the present return period (prp) to the future return period (frp) associated with a given water level. Such ratios (prp/frp) give an indication of how many times more frequently a particular water level will occur. The values given below are only estimates (based on water levels associated with present day return periods between five and twenty years) as the ratio varies from water level to water level:

- Lincolnshire, prp/frp ≈ 6
- Dungeness to Rye, prp/frp ≈ 15
- Lyme Bay, prp/frp ≈ 5
- Swansea Bay, prp/frp ≈ 33
- Fylde, prp/frp ≈ 6.

The smallest changes in return period were from Lyme Bay, Lincolnshire and Fylde while the largest was for Swansea Bay, then for Dungeness to Rye. The smallest changes in return period are for the sites with the lowest tidal ranges and the steepest gradients in the marginal extreme water level graphs (Figures 5 to 9).

4.4 Joint probability contours

Figures 12 to 16 show contours of the joint probability of exceedance of wave height and water level with 20, 50 and 200-year return periods for the present and future scenarios at the five sites. The present day scenario contours are solid lines, the future scenario lines are dashed. The contours for 20, 50 and 200-year return periods are blue, red and green, respectively. A low level of correlation between wave height and water level is indicated by gently curving contours – the more angular contour lines with sharper bends are for cases where there is a higher correlation. In all cases the future water levels are greater than the present day levels so the future contours reach the water level axis at higher values than the present day contours. Where the future wave heights are lower than the present (such as for Lincolnshire) the contours cross. In some cases the contours are not smoothly-varying. Only 2,000 years of wave height/water level combinations were generated by the Monte-Carlo method for these cases. Running the simulations for longer periods (10,000 years, for example) could have produced smoother contours.

5. SIMULATION OF COASTAL DEFENCE RESPONSE TO JOINT PROBABILITY CASES

5.1 Method

This method, developed for CDV2075, calculates overtopping rates and velocities on the structure (as surrogates for scour and damage potential) for extreme sea conditions. The starting point is the joint-probability of exceedance plots produced by JOIN-SEA. A summary of the method is given below.

1. Contours of equal joint exceedance probability (with return periods of 20, 50 and 200 years) were calculated and plotted on wave height versus water level diagrams at each site. See Section 4.4 for details.
2. A number (normally four or six) of points on the contour were chosen as representative combinations of water level and waves to be used as inputs to the wave models that calculate the structural response (overtopping and/or velocity on the structure). Only one of these combinations will give the worst case response (the highest overtopping rate or rms velocity) and it can be a different combination for each response. The probability of occurrence of the structural response function calculated from the worst case combination of wave height and water level will be higher than the joint exceedance probability. This occurs because the same response may be obtained by other sea conditions in which only one parameter (wave height or water level) takes a very high value.
3. A most likely wave direction, wind direction and wind speed were assigned to each wave condition, by inspection of the extremes in the 30-year time series. A wave period was determined by assuming that the offshore wave steepness, $S = 2\pi H_s / gT^2$ equals 0.05. The extreme water level extrapolations recommended by Dixon and Tawn (1997) were used in deriving the extreme water level distributions.
4. The waves were transformed inshore, over a large area, using the third-generation coastal area wave model, SWAN (Booij et al, 1999, run by POL). Details of the SWAN modelling can be found in Appendix 2.
5. The inshore waves were taken through the surf-zone using HR Wallingford's coastal profile model COSMOS (Southgate and Nairn, 1993). COSMOS was run from approximately 1800m offshore to ensure that the entire surfzone was modelled using a fine grid (with decreasing spacing towards the shoreline) and to allow coastal steepening to be modelled. The COSMOS model included the structure (e.g. sea wall) and a simplified, linear, beach that was replaced by a steeper beach to represent the effects of coastal steepening. Thus, coastal steepening was included in the COSMOS and OTT models only.
6. The wave height and period from COSMOS were output at a point 60m in front of the structure and used as the input to a numerical model of wave run-up and overtopping, OTT (Dodd, 1998) that was run for 1000 peak wave periods. The structures were chosen to be representative of different general types of coastal structure: a smooth sloping sea wall, an embankment and a shingle beach.
7. Time series of surface elevation and velocity were output at the toe, midpoint and crest of the structure. These were analysed to produce overtopping rates and velocities on the structure (as surrogates for scour and damage potential).
8. Results were assessed in terms of the change in response between present and future scenarios.

Figure 4 shows how the models are linked within CDV2075. Further details on the models used and their implementation can be found in Appendix 1 and the results from the simulations are in Sections 5.3 to 5.4.

5.1.1 Coastal steepening

Coastal steepening was included in the future scenario modelling where there was evidence (collected in Soulsby *et al.*, 1999) that steepening is occurring now. The scenario for coastal steepening used was that the present rate of steepening continues until 2075. This is an extrapolation of a present trend, not a model output. The intertidal width is decreasing at about 2m per year along the Lincolnshire coast (Sir William Halcrow and Partners, 1988a and 1988b). The future scenario for coastal steepening at Lincolnshire assumed that this trend continues, so over 75 years the beach's slope increased from 1:144 to 1:115. BMT (1996) shows that over the period from 1945-1970 the width of the beach (here measured by taking the distance from high water to low water) between Port Talbot and Barry has been narrowing at about 2m per year. The period 1915 to 1945 showed slower change, but 1880 to 1915 was faster. Therefore 2m per year was taken as the average rate for the coastal steepening scenario at Swansea Bay. The authors are not aware of evidence for steepening at Lyme Bay, Dungeness or Fylde. However, there is evidence of steepening in Hampshire (Hooke and Riley, 1987) where the beach width at Crofton Cliffs has narrowed by between 0m and 90m over 95 years. An average value of 0.5m per year was taken as a representative value for the south coast and was used for Lyme Bay. The present and future beach slopes for the CDV2075 sites are given in Table 2.

5.1.2 Model output

The overtopping rates and velocities produced by OTT are stored and described in Appendix 3 to Appendix 7. Comparisons between present and future responses are required to assess the changes in coastal defence vulnerability between the present day and 2075. Three measures of the change in response were calculated:

1. Ratio of future mean overtopping rate (Q_f) to present day mean overtopping rate (Q_p): Q_f/Q_p
2. Percentage increase in scour potential. The potential for scour rises approximately as velocity to the power of three. Therefore the percentage increase in scour potential (*PISP*) is defined as:

$$PISP = \left\{ \left(\frac{u_{rms,f}}{u_{rms,p}} \right)^3 - 1 \right\} \times 100 \qquad (1)$$

   with $u_{rms,f}$ and $u_{rms,p}$ the future and present rms velocity at the toe of the structure respectively.

3. Percentage increase in damage potential. The potential for damage rises approximately as velocity to the power of two. Therefore the percentage increase in damage potential (*PIDP*) is defined as:

$$PIDP = \left\{ \left(\frac{u_{rms,f}}{u_{rms,p}} \right)^2 - 1 \right\} \times 100 \qquad (2)$$

   with $u_{rms,f}$ and $u_{rms,p}$ the future and present rms velocity at the toe of the structure respectively.

5.2 Choice of coastal structures

The overtopping, scour and damage responses are strongly determined by the type and design of coastal structures considered. Three structure types with simple cross-sections were used:

- Smooth sloping sea wall. The crest and toe levels and front slope were chosen by examining cross-sections of a number of existing seawalls in Lincolnshire. The chosen sea wall had a toe elevation of 0m ODN, a crest elevation of 6.47m ODN and a front slope of 1:1.6 (V:H). The same sea wall design was applied to the other sites to allow for a direct comparison between regions.
- Embankment. The crest elevation used was the 10,000-year return period water level for the site. The toe depth was the datum minus half the 1-year return period water level and the front slope was chosen to be 1:3.
- Shingle Beach. The crest elevation used was the 10,000-year return period water level for the site. The toe depth was the datum minus the 1-year return period water level and the front slope was chosen to be 1:5.

Details of beach slopes, toe depths and crest elevations are given in Table 2. NA = Not Applicable.

5.3 Simulated changes in overtopping

The simulated changes in response, calculated using the joint probability contours and using the standard scenarios in all five regions and three return periods are given in Table 3. This shows the ratio of future to present overtopping rates (Q_f/Q_p) the percentage increase in scour potential (PISP) and the percentage increase in damage potential (PIDP) for all three structure types. The ratio of future/present day mean overtopping rate (Q_f/Q_p) for the 20, 50 and 200-year return period wave and water level conditions are shown in Figure 17 for the seawall (top) embankment (middle) and shingle beach (bottom). All calculations were performed with the present day beach slope.

The vertical axis of the top plot has been truncated so the ratio from the 20-year return period at Lyme Bay is not displayed in full, as it is not reliable. It comes from two runs in which only one wave overtopped the seawall in each simulation. In fact, in some cases OTT did not predict any overtopping at all during the simulation of 1000 peak wave periods. The magnitudes of overtopping are so low because water levels are relatively low compared to the common seawall crest elevation (compare Figure 7 to Figure 5, 6, 8 and 9). Therefore this Q_f/Q_p ratio is unreliable so it is excluded from further analysis. The ratios from the 50 and 200-year return periods are considered representative, as they are derived from reasonable samples of overtopping events.

Future overtopping rates vary between 1.3 and 4.5 times the present day rates for the seawall (with the one exception). Lower ratios were recorded for the embankment (in the range 1.2 to 2.5) and the shingle beach (in the range 1.2 to 2.6). The average Q_f/Q_p ratios were 2.5 for the seawall (excluding the 20-year ratio at Lyme Bay) 1.6 for the embankment and 1.7 for the shingle beach. The embankment and shingle beach results are similar while the seawall results give a wider variation and larger ratios. This is a reflection of the methods used to devise the structures used. The seawall was a common structure, "designed" for Lincolnshire but used at all five sites to see how they compared. The embankment and shingle beach were different at each site, but "designed" to a common formula. The embankment and shingle beach had crest levels that corresponded to the 10,000-year return period water level, while the seawall crest level was 6.47m in all cases, irrespective of how that compared to the water level (hence the problems with the 20-year return period overtopping ratio at Lyme Bay). One of the consequences of the design of the embankment and shingle beach is that the overtopping rates calculated are very high (often of order 10^{-1} $m^3/s/m$)– large enough to cause structural damage to buildings. These rates would not be acceptable in many circumstances where assets are at risk. However, it is changes in the overtopping ratios that are of interest for the CDV2075 project, rather than the actual rates so this is not of great concern.

Most of the ratios of future to present overtopping rates (Q_f/Q_p) decreased as the return period increased. This is mainly because the models predict lower ratios of future to present wave heights at higher return periods. There was no significant change in the ratio of future to present overtopping rates at Swansea, which was the one region where there was a slight increase in the ratio of future to present day wave heights as return period increased (Figure 10).

There were noticeable variations in the overtopping ratios at the different sites, which are related to the tidal ranges and the tide/surge relationships. The highest overtopping ratios occur for Lincolnshire and Lyme Bay, which have the lowest tidal range, while the lowest ratios occur for Swansea Bay and Fylde, which have the highest tidal range, as shown in Table 4. This shows the mean Q_f/Q_p ratio for all return periods for the embankment. It also includes tidal range (taken as MHWS-MLWS at nearby standard ports) the 10,000 year return period water level (derived from the Monte-Carlo simulation in JOIN-SEA) and present and future water level differences. These are defined as the difference between future or present water levels with 50-year and 1-year return periods and are included as the tide-surge relationship has a marked effect on the distribution of extreme water levels.

The results show that the ratios are not solely dependent on tidal range. For example, the tidal range at Swansea is about 6.2m, while the water level difference (present) is about 0.9m. In contrast, the tidal range in Lincolnshire is about 5.7m but the water level difference is almost 2.5m. The small decrease in tidal range but large increase in water level with return period produces a large increase in overtopping ratio. The locations with the highest correlation between wave height and water level are Swansea Bay, Fylde and Dungeness. These have relatively low overtopping ratios.

5.3.1 Coastal steepening

The relative increase in future mean overtopping rates (Q_{fs}/Q_f) for all three regions with observed coastal steepening are shown in Figure 18 and tabulated in Table 5. Here Q_{fs} = future mean overtopping ratio, calculated with a steepened beach and Q_f = future mean overtopping ratio without steepening. The effect of coastal steepening, assuming that it continued at present day rates, was to increase future overtopping rates by around 15% ±10%. The percentage increase in scour potential caused by coastal steepening, assuming that it continued at present day rates, was about 25% to 50% at Lincolnshire, 20% to 25% at Lyme Bay and around 800% at Swansea Bay. The large percentage increase at Swansea is due to the small increase in scour potential in the present day scenario.

5.3.2 Additional scenarios modelled at Lincolnshire

A number of scenarios, including additional tests, were modelled using the representative sloping sea wall at Lincolnshire. The present day conditions were tested on the present day structure, the future conditions were tested with the present day structure and beach and the future conditions were also tested with a steepened beach (but present day seawall). In addition a number of tests were performed using the 50-year return-period wave/water level conditions and a modified structure. The additional tests all used the same structure slope and are detailed below.

1. Future conditions with present day beach but with the structure crest raised by 0.35m (an amount equivalent to the sea level rise). The value of 0.35m is a convenient one that maintains the same freeboard as before. It should not be seen as a recommendation, either from the authors or the funding body.
2. Present day waves but with water levels raised by 0.35m. This scenario represents a basic first guess at the future conditions by assuming that waves and water levels remain the same as at the present apart from the linear addition of sea level rise.
3. Present day conditions but with the toe of the structure lowered by 0.35m. In this scenario the water depth at the toe and the structure freeboard are similar to the conditions experienced in the future.
4. Future conditions, but with the toe of the structure lowered by 0.35m. Although many beaches are steepening, many beaches are also retreating. This may result in the drawing-down of beach levels in the future. The value of 0.35m was chosen to compare to the effect of sea level rise and is not a scientific evaluation of the possible beach draw-down that may occur.
5. Future conditions, but with the toe of the structure lowered by 0.35m and a steeper beach face (1:115). This represents in some ways the worst-case scenario. The steepening of the beach, lowering of the toe depth and increase in water levels all serve to increase the maximum wave heights that can exist at the structure toe. The increase in water levels reduces the freeboard, which also serves to increase the overtopping rate.

These tests were run with a 50-year return period, as the relationship between overtopping and return period was demonstrated by the standard tests. The results of the individual tests and some plots of the test results are given in Appendix 3. The changes in overtopping rates, scour and damage potential are given in Table 6, for 50-year return period offshore conditions. Figure 19 shows the relative overtopping rates, $Q/Q_{present}$ with Q the overtopping rate from the scenario named on the x-axis and $Q_{present}$ the present-day scenario mean overtopping rate.

Figure 19 shows that future mean overtopping rates are about four times the present day values. The future coastal steepening scenario increases the overtopping rate by a further 10%. Running the future waves and water levels at the structure with 35cm added to its crest height (an increase equivalent to the sea level rise) does not reduce the overtopping rates to present day levels. This is because the water depth at the structure toe is increased and so wave heights at the structure are greater, although the freeboard remains the same. Running the present waves with 35cm of water added to the present-day water levels gives a result that is close to the future conditions, showing that the change in water levels is dominant over the change in wave conditions, for the ECHAM4 model at this site.

Running present day waves at the structure with the lower toe depth gives similar mean overtopping rates to running the future condition with a raised crest level. Both these scenarios have the same toe depth and crest elevation, relative to Mean Water Level. The difference in the results could be due to:

1. Changes in the wave/water level combinations between present and future.
2. The relatively low number of scenarios tested. The highest overtopping rate of the 6 tested was used so testing a greater number of wave/water level combinations would give a finer resolution of the worst-case scenario.
3. The natural variability in the results from OTT that comes from running a numerical wave flume for 1000 peak wave periods per test. Running the same spectrum twice gives slightly different results as a different set of waves are generated each time.

The tests with the future wave/water level conditions, a steepened beach, the lowered toe depth and the standard crest elevation gave the highest overtopping rates (for the 50-year return period). Any such situation would develop over a period of many years, allowing time for measures to be taken to reduce the severity of the problem before it became too extreme. Such measures could include beach re-nourishment to raise the beach level and lower the beach slope immediately in front of the structure, or the raising of the seawall crest elevation. The results show that raising the crest elevation by an amount equivalent to the anticipated rise in mean sea level will not be sufficient to reduce future overtopping rates to present day levels. This occurs as the water depth at the structure toe is increased, even though the freeboard is the same. The greater water depth at the toe allows higher, depth-limited waves at the toe even when, as here, the future extreme wave heights offshore are expected to be lower than present day wave heights.

5.4 Simulated changes in scour and damage potential

The ability of OTT to record time series allows statistics of velocity and surface elevation to be calculated. These values serve as surrogates for scour and damage potential. The percentage increase in scour potential (PISP, Equation 1) and percentage damage potential (PIDP, Equation 2) were calculated. Figure 20 shows the percentage increase in scour potential at all five sites and all three return periods, for the standard beach and structure. Results are given for the seawall (top), embankment (middle) and shingle beach (bottom). The scour potential increases by between 5% and 27% for the seawall tests. Again the increase is lowest for Swansea Bay and highest for Lincolnshire and Lyme Bay. The increases are due to increases in velocity caused by the changes in the partial standing wave velocity field in front of the reflective seawall. The results for the embankment and shingle beach are lower than for the seawall and many of them are negative. These structures are much less reflective than the relatively steep seawall modelled. The lower scour potential is due partly to there being lower waves at some locations, partly to the increased water depths reducing velocities and partly to increased overtopping reducing the reflections from the embankment and seawall.

Table 6 and Figure 21 show the percentage increase in scour potential (relative to the present-day scenario) for the 50-year return period scenarios at Lincolnshire. Again, steepening the beach and lowering the toe produce increases (of 7% and 11%) in the scour potential above the standard future scenario. Using present day waves, but a raised water level gives a PISP = 19%, only 70% of the PISP for the standard future scenario. The percentage increases in damage potential (PIDP) are all lower than the corresponding PISP as the same velocities were used in the calculation. Therefore, the PISP values were discussed more.

5.5 Summary

The joint probability of exceedence contours have been used to determine worst-case overtopping rates and rms velocities for present and future conditions. Significant increases in the overtopping rates were predicted for each return period and structure. The higher return periods gave lower relative increases in overtopping when future extreme wave heights were predicted to be lower than present day wave heights (as is the case at all locations apart from Swansea Bay). However, these decreases were small and are due to small changes in wind speeds produced by the ECHAM4 model. There is sufficient variability between the results from different climate models and different greenhouse gas emission scenarios to conclude that these decreases are not significant. The overtopping response depended on tidal range and tide-surge relationship. Increases in beach steepness and toe depth both increased overtopping rates. Scour and damage potential behave similarly.

6. SIMULATING CHANGES IN BEACH LEVELS AND PLAN SHAPES

6.1 Introduction

Changes in beach levels can substantially alter the effectiveness of coastal defences, affecting both their functional performance (e.g. changing their overtopping rates) and their structural integrity (e.g. scour leading to undermining of the toe of a seawall). There are many possible causes of changes in beach levels. Common examples include:

- The short-term effects of a severe storm;
- Changes in the supply of sand from rivers;
- Changes in nearshore sandbanks or channels; and
- Anthropogenic activities such as mining of beach sediments, beach recharge operations and the construction of breakwaters, groynes or other structures.

In this project, the main emphasis is on changes in natural processes connected with climate change, rather than changes in anthropogenic activities. In considering natural beach changes, it is convenient to consider separately the changes in beach profile and in beach plan shape.

The former class of changes is dominated by sediment transport perpendicular to the beach contours, and changes can occur rapidly for example in a few days as a result of a single storm. Medium-term fluctuations in beach profiles also occur, for example over a spring-neap tidal cycle and seasonally, with typical winter beach profiles being less steep than in summer. While these fluctuations in level can amount to several metres in extreme cases, the underlying long-term changes in the profile of a beach, i.e. when profiles are averaged over several years, are often small and difficult to detect. These long-term changes in beach profile can affect both the average gradient of the beach, and its position. In the UK, the normal trend appears to be for both a landwards translation and for a steepening of the beach profile as described in Chapter 5 of this report. These changes can be expected to arise as a consequence of the gradual increase in sea level, the erosion of the rock strata underlying beaches and the occasional transport of sediment front the front face over the crest of a beach (over-washing). However, it is often difficult to quantify this type of effect, even when shoreline changes over many decades are compared.

Because of this, the major cause of long-term beach changes is usually connected to changes in their plan shape. These types of change are related to the transport of sediment along a coastline, the so-called "longshore drift". Where this volumetric rate of transport varies along a stretch of shoreline, then the beach plan shape alters in response. This is expressed by the following equation for continuity of mass of beach sediment:

$$\frac{dA}{dt} = \frac{dQ}{dx} \qquad (3)$$

where Q is the volumetric drift rate (e.g. in cubic metres/ second), A is the cross-sectional area of the beach, x is the longshore distance and t is time. The rate of change of shoreline position, y, is then given by:

$$D\frac{dy}{dt} = \frac{dQ}{dx} \qquad (4)$$

where D is the so-called "closure depth", the effective total depth of the profile, from the beach crest to its lower limit, usually below the low-tide mark. This equation holds for any instant in time, i.e. for any wave condition that occurs. For long term beach changes, however, it is convenient to interpret Q as the net annual longshore drift rate, i.e. the summation of the sediment transport caused by all the wave conditions during a year.

It can be seen from this equation that if the longshore drift rate, *Q*, is constant in value along a coast, so that *dQ/dx* is zero, then there is no induced change in beach position, however large the value of *Q*. However, if the longshore drift is interrupted, for example by the installation of a groyne or breakwater, producing a marked localised reduction in *Q*, then there will be a corresponding localised change in the beach plan shape. The beach levels will increase on the “updrift” side of the interruption, i.e. where *Q* reduces from it previous value, and there will be beach erosion of the opposite “downdrift” side of the obstruction. The importance of this mechanism to beach evolution, and hence to coastal defences, is emphasised by the following quotation from an eminent coastal engineer in the USA. Galvin (1990) wrote:

" ... all examples of shore erosion on non-subsiding sandy coasts are traceable to man-made or natural interruptions of longshore sediment transport".

This overstates the case somewhat, but in many situations, the cause of beach erosion (or accretion) is very similar to that described by Galvin. In the context of this research, therefore, it is important to consider how longshore drift rates along the shorelines of the UK are likely to alter as a consequence of climate change. This section of the report concentrates on just this issue.

6.2 The implications of longshore drift rate changes

Because of the fundamental importance of longshore drift in the evolution of beaches, deliberately modifying the natural drift rate has long been at the centre of beach management methods not only in the UK but also around the world. The most obvious examples of this are the large number of groyne systems along both sand and shingle beaches, designed to retain extra beach sediment, albeit often at the expense of adjacent beaches.

In more recent decades, alternative approaches to beach management have been adopted, namely beach recycling and beach recharge operations. A typical example of a recycling exercise is shown in Plate 1. This figure shows shingle, collected from the beach adjacent to the terminal groyne at the eastern end of Seaford beach (in the background), being carried by trucks to the updrift end of the beach, thus counteracting the effects of the longshore drift.

If drift rates along this beach were to alter as a consequence of climate changes, then so too would the intensity and/or frequency of the recycling operations. A reduction in drift rates would reduce the effort and expenditure with obvious economic benefits, while an increased drift rate would mean just the opposite.

This specific case is one example of a more general rule of thumb, namely that the management of beaches and coastal defences is likely to become more difficult and expensive if drift rates increase, less so if they decrease. More formally if *Q* at present changes to *kQ* in 2075, then *dQ/dx* will change to *k (dQ/dx)* and hence from equation 4, the rate of shoreline change *dy/dt* will also change to *k dy/dt*.

If *k* turns out to be significantly greater than unity, then this may require a change in management policy; for example at Seaford (see above) there might be an economic case for installing beach control structures to reduce the recurring cost of beach recycling operations. Elsewhere, existing groyne systems might need to be extended or improved in order to control the rate of beach erosion.

However, in the case of only minor changes in the wave climate, *k* will be close to unity, and changes in beach plan shape will continue to occur at much the same rate as today. There would therefore be little need, in most areas, to consider radical changes to the present methods of beach management. This conclusion will also generally hold for a reduction in *k* to a value between 0 and 1.

An interesting situation arises if *k* turns out to be negative, i.e. the drift direction in 2075 is opposite of the drift direction today. This is most likely to occur where the net annual longshore drift rate is presently low. If *Q* does reverse, then equation 4 indicates that areas presently eroding would tend to accumulate sediment and *vice versa*. There have been examples of this type of change in beach evolution in recent years, for example at West Bay, Dorset and along Montrose Links (eastern Scotland).

In the above discussion, it has tacitly been assumed that Q, the net annual longshore drift rate, is a well-defined quantity that does not change greatly from year to year. In reality, this is not true; Q will be a statistic with a Gaussian probability distribution. Accurately estimating the mean of this distribution requires a stationary wave climate and calculation of the annual drift rates for each year over several decades. These calculations will also provide information on the standard deviation of the Gaussian probability distribution, which is usually a large proportion of the mean value, even on coasts with a large longshore drift rate.

The variability in drift rates from year to year can have a number of implications for beach management. For example, a contract for recycling operations such as that at Seaford will have to be flexible in terms of arranging for the potentially very different amount of work required to restore the beach from one year to the next. On a beach with groynes, the variations in drift rate can cause short-term variations in beach plan shape that may have significant effects on coastal defences, e.g. because beach levels on the downdrift side of groynes are lower for longer when drift rates are larger. As with the mean annual longshore drift, therefore, it is likely that an increase in the inter-annual variability of drift rates will lead to greater problems for beach management. This aspect was therefore also investigated in this research study.

6.3 The methods used to calculate longshore drift rate changes

From the foregoing discussion, it was decided that calculating the changes in both the mean annual longshore drift rate, and its inter-annual variability, would both be helpful in assessing how coastal defence vulnerability might alter in the coming years.

Calculating the volumetric longshore drift rate along a coastline has been a part of the scientific study of beaches and coastal defences for almost fifty years, and over that time, a large number of different formulae have been developed for this purpose. The earliest research and development for this appears to have been carried out on the long, straight and sandy beaches of California where swell waves from the Pacific Ocean produce a very regular wave pattern. The formula developed in this early work was refined by Komar and Inman (1970) and is widely known as the CERC formula. Despite the subsequent research, this formula is still regarded as being as, or more, reliable than many more complicated methods, at least for sand beaches.

In the UK, there are often a large number of factors that complicate the calculation of longshore drift rates, including:

- The presence of groynes, breakwaters, seawalls and other structures that affect drift rates;
- Mixed sediment types, e.g. sand and shingle, that move at different rates along a coast;
- A lack of beach sediment in the lower inter-tidal zone reducing the volumetric drift rate;
- Tidal currents that affect both waves and the longshore currents that they produce; and
- Uneven seabed bathymetry causing spatial variations in wave conditions along a beach.

The importance of these factors can vary considerably over a short length of coast, further complicating the calculations. In this project, the main interest is in the scale of changes in longshore drift rates rather than in trying to precisely calculate (and verify) those rates for a particular location. The CERC formula has been used, albeit with a different time-scale constant to account for differences between beaches in California and those in the UK.

The CERC formula can be written as follows;

$$Q = K \frac{H_b^2}{8\gamma_s} C_{gb} \sin(2\alpha_b) \qquad (5)$$

where: Q is the volumetric longshore drift rate, K is a time-scale constant, γ_s is the specific weight of beach material *in situ*, H is the wave height, C_g is the wave group velocity, α is the angle between the wave crest and the beach contours and the subscript b indicates quantities that are evaluated at the breaker line. For conditions along the California coastline, Komar and Inman (1970) suggested a value for K of 0.385. On sand beaches in the UK, a value of approximately 0.3 usually provides more accurate predictions of the drift rate, and for shingle beaches a value for K of about 0.015 is a reasonable first approximation.

This formula lies at the heart of a straightforward numerical model, DRCALC, used in this project for calculating longshore beach sediment transport. This model was developed at HR Wallingford and can deal with a variety of different types of wave data, producing information on annual net drift rates and their variations with time.

In this project, the six-hourly time-series of (synthetic) wave conditions were used as the primary input to the DRCALC program, rather than using the statistical summary of those waves as presented in the format of wave roses, scatter diagrams or probability tables. The use of the sequential data has two main advantages, namely:

1. It is possible to calculate the longshore transport for each year, providing information on inter-annual variability in drift rates;
2. The sequential data retains the precise wave heights and directions calculated by the forecasting model, whereas using the probability tables results in error due to "discretisation" of these quantities, e.g. directions only stored to the nearest 5° or 10°.

Prior to calculating a longshore drift rate for a particular wave condition, the DRCALC model carries out a wave refraction calculation. It uses a simplified method to convert offshore wave conditions to corresponding breaking waves conditions along the shoreline. The method used assumes that the seabed contours are straight and parallel to the shoreline; although simple, this technique is appropriate for the present study where a broad-brush approach to assessing change in coastal processes have been taken.

The main inputs to the DRCALC modelling were the offshore wave conditions estimated for the five sites around the coastline of the UK as described previously in this report. However, these offshore wave conditions are suitable for estimating longshore drift rates over substantial lengths of coastline, and hence for differing beach orientations along each length. In order to maximise the value of the DRCALC modelling, it has therefore been possible to consider longshore drift rates, and their changes, for more than one beach for some of the five areas considered.

6.4 Simulated drift rates

For each of the beach lengths studied, the DRCALC model provides the following information for both present-day and future (2075) conditions:

1. Calculations of the net longshore drift rate for each year;
2. An estimate of the overall mean annual longshore drift rate;
3. An estimate of the standard deviation in the annual drift rate, and
4. A mean wave direction, i.e. the beach normal direction that would reduce Q to zero.

The summary statistics of the DRCALC runs are detailed in Table 7. The year by year drift results for the present and future scenarios are presented in Appendix 8, Longshore Drift Rates. Figure 22 shows the percentage change in mean annual drift rates (between present and future) and their standard deviation. The numbers after a location name give the shore-normal direction. Two sets of results are given for Dungeness to Rye and Lyme Bay because of the changing beach orientation along these frontages.

6.4.1 Lincolnshire

The wave climate for this site was derived approximately 30km offshore of Mablethorpe. However, the results can be considered broadly representative for the area of coast stretching from the Humber Estuary in the north, to The Wash in the south. This stretch of coastline is primarily low lying land, and the flood defences consist of dunes and man-made defences. The beaches in this area have undergone extensive renourishment in the recent past and this has been identified as the preferred beach management option for the foreseeable future. The beach orientation was considered to be on a north-south alignment, to provide broadly representative results for this area, although the coastline does vary in alignment.

The most noticeable difference in the present/future results are the less variable (lower standard deviation) future drift results (27% decrease) and the lack of reverse drift in the future conditions for the chosen angle of beach orientation. Consequently, if this situation were to arise, the management of beach re-nourishment in this area would be simplified.

6.4.2 Dungeness

The wave climate for this site was derived approximately 20km offshore of Dungeness. This climate can be considered broadly representative for the area of coast from Dover in the east, to Eastbourne in the west. This stretch of coastline primarily consists of shingle upper beaches and varying amounts of shingle/sand mixture on the foreshore. The sea defences in this area are generally groyned beaches, backed by seawalls of various profiles, although Dungeness itself is a succession of shingle ridges. Beach re-nourishment is common and shingle recycling is apparent at several locations. As the coastline varies significantly in orientation, DRCALC was run with the beach facing southwards (180°) and to the south west (225°).

The results for the south facing beach show a slight (approxmately 10%) increase in the mean annual drift but less (6%) year by year variability. Similarly the south west beach shows an increase of approximately 15% with a standard deviation reduction of 10%. Future changes such as these would result in comparatively small modifications to the current beach management strategies, with recycling and re-nourishment programs adjusted accordingly.

6.4.3 Lyme Bay

The wave climate for this site was obtained approximately 30km offshore of Lyme Regis. This offshore climate could feasibly be applied along the coast from Portland Bill in the east, to Exmouth in the west. Shingle beaches backed by cliffs are a prominent feature along this stretch of coastline. These shingle beaches, together with sea walls, characterise much of the sea defences in this area. Re-nourishment has been carried out within this area in the past. As for Dungeness, DRCALC was run with the beach facing southwards and to the south west.

The results for Lyme Bay are similar to those obtained at Dungeness for the south facing beach, whereby the mean annual nett drift increases by 10%. However, the south west facing beach sees an increase of nearly 30% from the present to the future. This is accompanied by a 20% reduction in the year by year variability. The reduced variability would mean a more consistent year by year approach to managing any re-nourishment schemes. However, the significantly greater volumes of material that may need to be re-cycled or re-nourished could impact on the economic viability of such activities, leading to a change in management strategy.

6.4.4 Swansea Bay

The wave climate for this area is representative of the central Severn Estuary, approximately 20km offshore. Although noted as Swansea, the wave climate changes would be generally applicable along the north coasts of Devon as well as much of the south coast of Wales. Swansea Bay hosts a variety of sand and shingle beaches, backed by urban areas and industrial developments and also dune systems fronting a nature reserve. As a consequence of the mixture of land uses, the sea defences are equally diverse. Concrete walls backing eroding beaches form the protection of much of the urban and industrial areas, whilst the dune systems offer a more natural form of protection.

DRCALC was run for a beach angle of 245^{o}N, which is approximately the orientation of the coast towards the east of Swansea Bay. This is the most exposed area of the frontage. The results for Swansea show an increase of 30% in the mean annual net drift and a reduction in the variability of approximately 10%. This significant increase in drift rates could cause accelerated erosion of downdrift areas already undergoing recession.

6.4.5 Fylde

The wave climate for this site was derived approximately 20km offshore and can be considered representative of the area stretching from Lytham St Anne's in the south to Fleetwood in the north. This area of coast primarily consists of sand beaches backed by low-lying land. Protection for the low-lying land typically consists of sea walls and sand dunes.

The results for Fylde show an increase in the mean annual drift of approximately 20% and a reduction in the year by year variability of approximately 13%. Re-nourishment and recycling schemes are not prevalent along this area. Thus, if these relatively modest predicted changes did occur, no substantial changes to the management schemes in this area are anticipated.

6.5 Summary

The percentage changes in mean annual nett drift and the standard deviation of the annual nett drift are shown in Figure 22. Two beach directions (180° and 225°) were used for Dungeness and Lyme Bay. In all but one case the future mean annual drift rates are greater than the present day rates, by an average of 15% (although the one exception, Lincolnshire, was the one presented in Sutherland and Wolf, 2001). The standard deviations are all lower, by an average of 14%. The reduced variability would mean a more consistent year by year approach to managing any beach nourishment schemes. However, the greater volumes of material that may need to be re-nourished could impact on the economic viability of such activities and may necessitate a review of management options. Nevertheless, the work tends to show that future changes are unlikely to be greater than current levels of uncertainty and these should be considered in the normal course of sensitivity testing.

7. STATISTICAL ANALYSIS OF SIMULATED COASTAL DEFENCE RESPONSE FUNCTIONS

An alternative method of calculating the structural response is to use simple empirical equations to calculate the overtopping rate for each wave/water level combination in a simulation. Here the Monte-Carlo simulation of waves and water levels at each high tide for thousands of years, produced by the JOIN-SEA method, was used to create hundreds of thousands of combinations of wave height and water level for each of the present and future scenarios at each of the five sites. Empirical formulae for inshore wave height and overtopping rates (EA, 1999, Owen, 1980) were then used to calculate overtopping rates at each high tide. A statistical analysis (sorting and counting back) of the overtopping response was used to calculate the overtopping rate at a number of return periods.

Wave period is a key variable in overtopping calculations. JOIN-SEA incorporates the variability in wave period by modelling the wave steepness. An appropriate wave height threshold is selected (typically 95%). Below the threshold the empirical distribution of wave steepness is used, above the threshold the normal distributions conditional on wave height is used. This approach models the wave steepness better than the joint probability approach where steepness is assumed constant.

7.1 Empirical formulae for overtopping

Well-established empirical methods for determining the wave height at the structure toe and the overtopping rate were used. They are described in EA (1999). The breaking wave height at the toe of the structure is given by an equation of the form:

$$\frac{H_{sb}}{h} = a - b\frac{h}{gT_m^2} + c\left(\frac{h}{gT_m^2}\right)^2 \qquad (6)$$

with H_{sb} the significant wave height at the structure toe (*m*), h the total water depth at the structure toe (*m*), g the gravitational acceleration (ms^{-2}), T_m the average wave period (*s*) and *a, b* and *c* are empirical coefficients that depend on the beach slope. The overtopping rates are calculated by the Owen (1980) formula for smooth sloping sea walls. In this method the discharge and freeboard are non-dimensionalised:

$$Q^* = \frac{Q}{T_m g H_{sb}} \qquad (7)$$

$$R^* = \frac{R}{T_m \sqrt{gH_{sb}}} \qquad (8)$$

with Q^* and R^* the non-dimensionalised discharge and freeboard, Q the mean wave overtopping discharge per metre of sea wall ($m^3/m/s$) and R the freeboard of the seawall (the height of the wall crest above water level, *m*). The overtopping rates are then given by:

$$Q^* = A\exp\left(-BR^*\right) \qquad (9)$$

where A and B are non-dimensional empirical coefficients that depend on wall slope.

7.2 Effect of sea level rise

The effect of an increase in sea level is to reduce the future freeboard, R_f, and increase the future depth-limited breaking wave height, H_{sf}, at the structure toe. Here it is assumed that there are depth-limited wave heights at the structure toe and that the beach has not altered as a response to rising sea level. The increased wave height is calculated by replacing h by $h+\delta h$ in Equation 6, where δh is the increase in water depth at the structure toe due to sea level rise. It follows from Equations 7, 8 and 9 that the overtopping rate will increase due to the increase in H_{sf} and the decrease in R_f.

7.3 Increase in crest elevation to maintain present-day overtopping rates

In order to counter the effects of sea level rise and ensure that the future overtopping rate is no higher than the present rate the crest elevation of the sea wall may be raised by an amount r_c, to give a future-scenario freeboard of

$$R_f = R - \delta h + r_c \tag{10}$$

This section derives a formula for r_c that will maintain the future overtopping rate, Q_f, at the present rate, Q, assuming depth-limited wave heights at the structure toe, given by Equation 6. The condition $Q_f = Q$ implies the following:

$$T_m g H_{sf} A \exp\left\{ -B \frac{R_f}{T_m \sqrt{g H_{sf}}} \right\} = T_m g H_{sb} A \exp\left\{ -B \frac{R}{T_m \sqrt{g H_{sb}}} \right\} \tag{11}$$

Assuming that the wave period does not change gives:

$$\ln\left(\frac{H_{sf}}{H_{sb}} \right) - \frac{B R_f}{T_m \sqrt{g H_{sf}}} = -\frac{BR}{T_m \sqrt{g H_{sb}}} \tag{12}$$

Substituting for R_f using (10), multiplying through by $-T_m(gH_{sf})^{0.5}/B$, and re-arranging gives

$$r_c = \delta h + R\left(\sqrt{\frac{H_{sf}}{H_{sb}}} - 1 \right) + \frac{T_m}{B} \sqrt{g H_{sf}} \ln\left(\frac{H_{sf}}{H_{sb}} \right) \tag{13}$$

Equation 11 is an explicit equation for the increase in crest elevation needed to maintain the present overtopping rate in the future (subject to the assumptions above and using the formulae in EA (1999)) providing sea level rise can be estimated. The necessary crest level increase is given by sea level rise plus two other terms. The assumptions made above imply that $H_{sf}/H_{sb} > 1$ so the second and third terms on the right hand side of Equation 13 both require further increases in crest elevation above the allowance for sea level rise if the present-day overtopping rate is to be maintained in future.

7.4 Simulated changes in overtopping

The statistical analysis of coastal defence response functions method was used to calculate present day and future overtopping rates at a vertical seawall, an embankment and a shingle beach in the DEFRA-funded project ‘National Appraisal of assets at risk from flooding and coastal erosion, including the potential impact of climate change’. The embankment and shingle beach were the same as for this project and the same results are used here. The vertical wall results are not included here as OTT cannot be used on steep or vertical walls so there are no joint probability method results for a vertical wall. Note, however, that the beach slope was taken to be 1:50 in all cases here. Tables of present and future overtopping rates and their ratios for the embankment and shingle beaches at all five sites can be found in Appendix 9. Table 8 gives the ratio of future to present-day embankment overtopping rates (Q_f/Q_p) for a number of return periods for all sites. Note that these return periods are the return period of the overtopping rate, not the return period of the offshore wave/water level combination, as used in the joint probability method (Section 5). Table 9 gives the same information for the shingle beach. The results are plotted in Figure 24. Most of the ratios are between 1.2 and 2, indicating increases of between 20% and 100% in the overtopping ratio. The average of the plotted values for the embankment is 1.5 and for the shingle beach it is 1.8. There is also a wider variation in the future/present overtopping ratios for the shingle beach compared to the embankment. There are only small variations in the overtopping ratio with return period. Higher ratios tend to occur for the lowest and the highest return periods (especially for the shingle beach). The highest ratios occur for Dungeness and Lyme Bay, while the lowest are mainly for Swansea Bay and Lincolnshire.

7.4.1 Effect of raising the crest level.

Equation 13 gives an expression for the increase in crest level necessary to maintain present day overtopping rates. This section gives a worked example for the Lyme Bay embankment. In this case the present-day 50-year return period overtopping rate was $Q = 0.307m^3/s/m$. The combination of 20-year return period water level, 2.77m and the 5-year return period offshore wave height, 5.02m give a present day wave height $H_{sb} = 2.07m$, using Equation 6, assuming an offshore wave steepness, $s = 0.05$ and a beach slope of 1:50. The water level gives a freeboard $R = 1.78m$ and $Q = 0.304m^3/s/m$ (using equations 7, 8 and 9, with $B = 28.7$). This is close to the 50-year return period and will be taken as a representative condition for that return period. Assuming a 0.35m sea level rise in the future, but maintaining the present day waves and crest elevation would give an overtopping rate of $0.483m^3/s/m$, an increase of almost 60% on the present day rate. The present-day offshore wave heights were used in the future scenario as only small changes between present and future wave conditions were simulated. The future-scenario wave height at the embankment toe was $H_{sf} = 2.21m$. Applying Equation 13 gave an increase in the crest elevation of $r_c = 0.35 + 0.062 + 0.090 = 0.502m$. Using this increase in crest elevation, with 0.35m sea level rise, but present day offshore wave heights gave an overtopping rate of $0.298m^3/s/m$, close to the desired value.

The statistical analysis of simulated coastal defence response functions method was then run for the Lyme Bay embankment for the future wave and water level conditions, but with the embankment crest raised by 0.502m. Figure 24 shows the overtopping rates presented against return period. Results are shown for present and future conditions using the present day embankment (curves labelled 'present' and 'future') and for future conditions using the embankment with the crest raised by 0.502m (curve labelled 'Future – raised crest'). The future conditions run with the present day embankment show overtopping increases of about 60% over present day results. The future conditions run with the raised embankment show simulated overtopping rates almost exactly the same as for the present day case for return period lower than about 20 years. At higher return periods the future overtopping rates are lower than the present day rates. The match is not exact at the 50-year return period used to derive the crest level increase. This difference has three main causes:

- The wave steepness, which determines wave period and influences wave height, was assumed.
- Different combinations of water level and wave height give the same overtopping rate, and these combinations will respond differently to the increase in crest level. Only one combination was used to derive the imposed crest level increase.
- Present day waves and water levels were used (with sea level rise) to simulate the future conditions in deriving the crest level increase. The simulation was run using the future waves and water levels, which are close to, but not the same as present-day waves and water levels combined with sea level rise. In particular, the simulated future wave heights are lower than the present day wave heights for return periods greater than about 10 years (Figure 7). This may account for the lower overtopping rates at high return periods in the raised-crest simulation. Under normal circumstances, only present-day conditions will be available in the design of a structure and such problems will not be apparent.

These results indicate that Equation 13 can be used to give a first estimate of the increase in crest elevation needed to maintain future overtopping rates close to their present rates. Should there be a need to produce a future overtopping rate closer to the present day one, this can be achieved by iterating the crest level increase between 0 (the 'future' run) and the level given by Equation 13.

7.4.2 Comparison between statistical analysis and joint probability methods

The overtopping ratios from the statistical analysis of coastal defence response functions (SA) method (Section 7.4) and the joint probability of exceedence (JP) method (Section 5.4) can now be compared. Note that this is not a comparison of like with like. In the joint probability method, a number of offshore wave and water level combinations with the same joint probability were chosen as representative combinations to be used as inputs to the wave models that calculate the structural response (overtopping). The worst case response (the highest overtopping rate) was used as the overtopping rate associated with the offshore joint probability. However, the probability of occurrence of the structural response function calculated from the worst case combination of wave height and water level will be higher than the joint probability of that combination. This is because the same structural response function may be obtained by other sea conditions in which only one parameter (wave height or water level) takes a very high value. Therefore, joint-probability return-period sea conditions will under-predict the response, if the response is assumed to have the same return period.

The overtopping ratios (Q_f/Q_p) from the joint probability (JP) method and the statistical analysis (SA) method for embankment (bank) and shingle beach (shingle) are given in Table 10 and are plotted against one another in Figure 25. The solid diagonal line is the Y = X line, signalling complete agreement between the two methods. The results for the embankment are clustered around this line. The results for Swansea and Dungeness (where there is little change in overtopping with return period) are particularly good. The results for Fylde and Lincolnshire show higher ratios from the joint probability method than for the statistical analysis method, as would be expected when the overtopping ratio decreases with increasing return period. The results for Lyme Bay are the worst. In this case the joint probability method shows a large variation in overtopping ratio with return period. This variation is not nearly so evident in the statistical analysis method.

The results for the shingle beach are worse than for the embankment. Nevertheless, the results are still scattered about the Y = X line. The increased scatter may be due to methods used to model the shingle beach. The OTT numerical model used in the joint probability method treats the shingle as a rough, impermeable bank, not as a porous beach. The physical model tests used to calibrate the empirical equations for the overtopping of shingle banks used a porous bed.

7.5 Summary

The results from the statistical analysis method are broadly in line with those from the joint probability of response method. Future overtopping rates are simulated to be typically 50%and 80% higher than present day rates for the embankment and shingle beach. An explicit equation has been formulated to calculate the increase in crest level necessary to maintain future overtopping rates at the present day values. An example indicates that using this equation with a single representative set of conditions gives a crest level increase that produces similar overtopping rates to present day rates when run with a two thousand year simulation.

Differences between the statistical analysis and joint probability methods were partly due to the fact that the two methods determine statistically different quantities and partly due to the fact that the different overtopping calculation methods gave different results for the same overtopping cases. The main advantage of the statistical analysis method was that a full representation of the offshore wave and water level climate was used to derive overtopping rates with return periods that refer to the overtopping rates, not to the offshore sea conditions. The disadvantage was that rather simple, although well-established formulae were used for determining wave height and overtopping. The main advantage of the joint probability method was that advanced numerical models were used to model nearshore processes, such as refraction and wave-wave interaction that were left out of the other method. The main disadvantage was not knowing what the return period of the overtopping was – only the return period of the waves and water level combination that produced the overtopping was known. The numerical models used in the joint probability method could not be used to perform a statistical analysis due to the excessive computing power that that would have required.

8. CONCLUSIONS

CDV2075 has assessed the effects of climate change on the vulnerability of coastal defences between the present day and 2075. The results have been derived using a single realisation of a single climate change scenario, run on a single climate model. Due to the variability between climate models and the range of scenarios considered possible by the IPCC, the modelled predictions do not give a definitive view of the changes that will occur and the results should be interpreted with caution. The main conclusions that can be drawn from the modelled scenarios are set out below.

8.1 Waves and water levels

- Changes in wave climate around the UK are predicted to be small. The majority of future-scenario extreme wave heights are within 5% of the present day values. The changes in the mean annual offshore wave angles are all less than 5° and are all less than the standard deviation in the mean annual offshore wave angle. There is sufficient variability between the results from different climate models and different greenhouse gas emission scenarios to conclude that this predicted level of change is not significant.
- The project has demonstrated that for most structures even if changes in offshore waves are larger this will not have a significant effect on overtopping due to depth limitation effects at the structure toe.
- The effect of climate change (including sea level rise) on tide and surge amplitudes will be relatively small. The increase in future extreme water levels is generally expected to be within 20% of the increase in mean sea level.

8.2 Effects on beaches and coastal sediment movement

- In most cases the simulated future mean annual longshore drift rates were slightly greater than the present day rates (by an average of around 15%) but the standard deviations were all lower (also by around 15%). These changes were driven by small changes in wave climate and imply that greater volumes of material may need to be re-nourished, but with reduced inter-annual variability.
- If the observed coastal steepening continues it will serve to increase overtopping rates by around 15% ± 10% over that caused by climate change. It is not possible to estimate changes in the rate of coastal steepening as its causes are not sufficiently understood.

8.3 Implications for design of coastal defences

- The inclusion of sea level rise predictions in design calculations (including the effect this has on increasing wave heights at the toe of structures) should account for the majority of the predicted change in wave impact on coastal structures.
- The results indicate that there will be considerable increases in overtopping rates caused mainly by sea level rise if present day defences are unchanged in 2075. Using an illustrative estimate of 0.35m sea level rise between the present day and 2075 gave average percentage increases in overtopping due to climate change of 150% for the seawall, 60% for the embankment and 70% for the shingle beach using the joint probability approach. The statistical analysis approach gave average increases of 50% for the embankments and 80% for the shingle beach. The seawall was treated in a different way to the embankment and shingle beach and this may partly explain the larger predicted increase in the overtopping rates
- A formula has been derived for the increase in crest elevation necessary to maintain present day overtopping rates when sea levels rise. It is based on well-established empirical overtopping formulae and shows that, as expected, crest levels need to be raised by more than sea level rise to achieve this.
- There is great uncertainty in the prediction of longshore transport under current conditions. The work tends to show that future changes are unlikely to be greater than current levels of uncertainty and these

should be considered in the normal course of sensitivity testing which should guide the choice of beach management options.

- The scour and damage potentials may increase or decrease as a result of sea level rise. The scour potential increased for the seawall, by an average of 16%, but both increased and decreased for the embankment and shingle beach and gave average changes less than 2% for each. These changes are not linked to the changes in overtopping in a simple way and are due to changes in the partial standing waves in front of the structure. These potential changes are within the range that should be taken into account in normal sensitivity testing.

8.4 Overall changes in vulnerability

- Qualitative and quantitative differences in future changes in vulnerability were found between the five sites examined around the coastline of England and Wales. This is because the sites have different tidal ranges, wave climates and surge levels. Moreover the parameters have different joint probabilities at different sites. Thus results from one site cannot be transferred directly to other sites and individual assessments must be made for specific sites. For most practical purposes these individual assessments can be considerably simplified on the basis of the conclusions above.
- The modelled scenarios give an indication of the general extent of changes in coastal defence vulnerability that can be expected in the next 75 years.

9. REFERENCES

Allsop, N.W.H., Jones, R.J. and Bradbury, A.P., 1995. Design of beach control structures on shingle beaches. Proc ICE, Water, Maritime and Energy, April 1995.

BMT, 1996. Nash Bank environmental assessment.

Booij, N., R.C. Ris and L.H. Holthuijsen 1999. A third-generation wave model for coastal regions, Part I, Model description and Validation. J.Geophys. Res. 104, C4, 7649-7666.

Brampton, A.H. and Harford, C. M., 1999. Wave Climate change indications from simple GCM outputs. HR Wallingford Report TR80.

Cavaleri, L., Athanassoulis, G.A. and Barstow, S. 1999 Eurowaves, a user-friendly system for local wave climatology. Proc. 9th Int. Offshore and Polar Engineering Conf. ISOPE, Brest, France May 30-June 4 1999.

Church, J.A., Gregory, J.M., Huybrechts, P., Kuhn, M., Lambeck, K., Nhuan, M.T., Qin, D. and Woodworth, P.L., 2001. Changes in sea level. In: *Climate Change 2001: the scientific basis. Contribution of Working Group I to the Third Assessment Report of the Intergovernmental Panel on Climate Change.* Cambridge University Press, Cambridge, UK and New York, NY, USA. 881pp.

Cotton, P.D., Carter, D.J.T., Allan, T.D., Challenor, P.G., Woolf, D., Wolf, J., Hargreaves, J.C., Flather, R.A., Bin, L., Holden, N. and Palmer, D. 1999 JERICHO – The impact of a changing wave climate on our coasts, Technical report, BNSC LINK project R3/003, Satellite Observing Systems, UK.

Dixon and Tawn, 1997. Spatial analysis for the UK coast. Proudman Oceanographic Laboratory internal document 112, June 1997

Dodd, N., 1998. Numerical model of wave run-up, overtopping and regeneration. J. Waterway, Port, Coastal and Ocean Engineering, 124(2): 73–81.

EA, 1999. Overtopping of seawalls: design and assessment manual. Prepared by HR Wallingford.

Flather, R.A. & Williams, J.A. 2000. Climate change effects on storm surges: methodologies and results. pp. 66-78 in Beersma, J., Agnew, M., Viner, D. and Hulme. M. (eds.) *Climate scenarios for water-related and coastal impact*. ECLAT-2 Workshop Report No. 3, KNMI, the Netherlands, 10-12 May 2000. CRU, Norwich, UK. 144pp.

Flather, R.A., Baker, T.F., Woodworth, P.L., Vassie, J.M. & Blackman, D.L. 2001. Integrated effects of climate change on coastal extreme sea levels. Proceedings of the 36th MAFF Conference of River and Coastal Engineers, Keele, UK. Paper 03–4.

Günther, H., Rosenthal, W. Stawarz, M, Carretero, J.C., Gomez, M., Lozano, I., Serrano, O. and Reistad, M. (1998) The Wave Climate of the North-East Atlantic over the period 1955-1994: the WASA Wave Hindcast. The Global Atmosphere and Ocean System, 6, 121-163.

Hawkes, P.J., 1987. A wave hindcasting model. In 'Advances in underwater technology, ocean science and offshore engineering, Volume 12: Modelling the offshore environment', Society for Underwater Technology, April 1987.

Hawkes, P.J., Coates, T.T. and Jones, R.J., 1998. Impact of bi-model seas on beaches and control structures. HR Wallingford Report SR 507.

Hooke, J. and Riley, R., 1987. Historical changes in the Hampshire coast, 1870–1965. Dept. of Geography, Portsmouth Polytechnic.

Hulme, M. and Jenkins, G.J., 1998. Climate change scenarios for the UK: scientific report. UKCIP Technical Report No. 1, Climate Research Unit, Norwich, 80pp.

IPCC, 2001a. Climate Change 2001: The Scientific Basis. Contribution of Working Group I to the Third Assessment Report of the Intergovernmental Report on Climate Change [Houghton, J.T., Y. Ding, D.J. Griggs, M. Noguer, P.J. van der Linden, X. Dai, K. Maskell, and C.A. Johnson (eds.)]. Cambridge University Press, Cambridge, UK and New York, NY, USA, 881pp.

IPCC, 2001b. Climate Change 2001: Impacts, Adaptation and Vulnerability. Contribution of Working Group II to the Third Assessment Report of the Intergovernmental Report on Climate Change [McCarthy, J.J., O.F. Caniziani, N.A. Leary, D.J. Dokken and K.S. White (eds.)]. Cambridge University Press, Cambridge, UK and New York, NY, USA, 1032pp.

Komar, P.D. and Inman, D.L., 1970. Longshore sand transport on beaches. J Geophysical Research, 75(30): 5914–5927.

Laustrup, C., Toxvig Madsen, H., Bjerre Knudsen, S. and Sørenson, P., 2000. Coastal Steepening in Denmark. Proceedings of the 27th International Conference on Coastal Engineering, Sydney, Australia. ASCE 2428–2438.

Leggett, J., Pepper, W., Swart, R.J., Edmonds, J., Meira Filho, L.G., Mintzer, I., Wang M.X., and Watson, J., 1992. Emissions scenarios for the IPCC: an update. In Climate Change 1992: the supplementary report to the IPCC Scientific assessment. Cambridge University Press, Cambridge, UK.

Lowe, J.A., Gregory, J.M. and Flather, R.A. 2001. Changes in the occurrence of storm surges around the United Kingdom under a future climate scenario using a dynamic storm surge model driven by Hadley Centre climate models. Journal of Climate (in press).

May, W. 2001. The impact of horizontal resolution on the simulation of seasonal climate in the Atlantic/European area for present and future times. Climate Research, (in press).

Nakićenović, N., Alcamo, J., Davis, G., de Vries, B., Fenhann, J., Gaffin, S., Gregory, K., Grubler, A., Jung, T.Y., Kram, T., La Rovere, E.L., Michaelis, L., Mori, S., Morita, T., Pepper, W., Pitcher, H., Price, L., Raihi, K., Roehrl, A., Rogner, H-H., Sankovski, A., Schlesinger, M., Shukla, P., Smith, S., Swart, R., van Rooien, S., Victor, N. and Dadi, Z., 2000. IPCC Special Report on Emissions Scenarios, Cambridge University Press, Cambridge, UK and New York, NY, USA, 599pp.

Owen, M.W., 1980. Design of sea walls allowing for wave overtopping. HR Wallingford Report EX 924

Owen, M.W., Hawkes, P.J., Tawn, J.A. and Bortot, P., 1997. The joint probability of waves and water levels: A rigorous but practical new approach. MAFF Conference of River and Coastal Engineers, Keele, July 1997.

Roeckner E, Arpe K, Bengtsson L, Christoph M, Claussen M, DuÈmenil L, Esch M, Giorgetta M, Schlese U, Schulzweida U (1996) The atmospheric general circulation model ECHAM-4: Model description and simulation of present-day climate. MPI-Report 218: 90 pp

Shennan, I. 1989. Holocene crustal movements and sea-level changes in Great Britain. Journal of Quaternary Science, 4, 77-89.

Sir William Halcrow and Partners Ltd, 1988a. The sea defence management study for the Anglian Region. Strategy report for Anglian Water.

Sir William Halcrow and Partners Ltd, 1988b. The Anglian Coastal Management Atlas. Prepared for Anglian Water.

Soulsby, R.L., Sutherland, J. and Brampton, A.H., 1999. Coastal Steepening, the UK view. HR Wallingford Report TR 91.

Southgate, H.N. and R.B. Nairn, 1993. Deterministic profile modelling of nearshore processes. Part 1. Waves and Currents. Coastal Engineering 19: 27–56.

Sutherland, J. and Wolf, J., 2001. Coastal defence vulnerability 2075. Proceedings of the 36th DEFRA Conference of River and Coastal Engineers, Keele, UK. Paper 03–6.

Verwaest, T., Kunz, H., Hüttermeyer, P., Stam, J.-M., Soulsby, R.L., Laustrup, C. and Madsen, H.T., 1999. Profile steepening: a report prepared for the North Sea coastal management group. Kystinspektoratet, Denmark.

Williams, S.D.P., Baker, T.F., and Jeffries, G. 2001. Absolute gravity measurements at UK tide gauges. Geophysical Research Letters, (in press).

Woodworth, P.L., Tsimplis, M.N., Flather, R.A., & Shennan, I. 1999. A review of the trends observed in British Isles mean sea level data measured by tide gauges. Geophysical Journal International, **136**, 651-670.

Tables

Table 1 ECHAM4 and NISE locations for the 5 selected model areas

Location	ECHAM4		NISE	
	longitude	latitude	Longitude	Latitude
Lincolnshire	1° 07.5' E	53° 16.2'N	0° 35' E	53° 16.7'N
Fylde coast	3° 22.5' W	54° 23.5' N	3° 15' W	53° 50' N
Swansea Bay	4° 30' W	51° 01.6' N	3° 55' W	51° 30' N
Lyme Bay	3° 22.5' W	49° 54.4' N	2° 45' W	50° 30' N
Dungeness	1° 07.5' E	51° 01.6' N	0° 45' E	50° 43.33'N

Table 2 Details of coastal structures

Quantity	Units	Linconshire	Dungeness	Lyme Bay	Swansea Bay	Fylde
Beach slope	1:N	144	142	206	54	100
Steepened beach slope	1:N	115	NA	191	30	NA
Seawall toe depth	[m]	0	0	0	0	0
Seawall crest elevation	[m]	6.47	6.47	6.47	6.47	6.47
Embankment toe depth	[m]	-1.815	-1.965	-1.11	-2.56	-2.3
Embankment crest elevation	[m]	5.38	5.55	4.56	6.14	6.93
Shingle beach toe depth	[m]	-3.63	-3.93	-2.22	-5.12	-4.6
Shingle beach crest elevation	[m]	5.38	5.55	4.56	6.14	6.93

Table 3 Responses for all sites using standard structures and beaches

Location	RP [years]	Seawall			Embankment			Shingle Beach		
		Qf/Qp	PISP	PIDP	Qf/Qp	PISP	PIDP	Qf/Qp	PISP	PIDP
Lincolnshire	20	4.50	26	16	1.86	4	2	1.86	4	2
Lincolnshire	50	3.93	27	17	1.75	2	1	1.75	2	1
Lincolnshire	200	3.63	22	14	1.71	1	1	1.71	1	1
Dungeness	20	2.60	19	13	1.65	-5	-4	1.74	0	0
Dungeness	50	2.34	17	11	1.58	-5	-4	1.68	0	0
Dungeness	200	2.09	14	9	1.53	-5	-4	1.61	0	0
Lyme Bay	20	29.8	25	16	2.47	10	7	2.59	6	4
Lyme Bay	50	2.90	22	14	2.01	6	4	1.52	5	3
Lyme Bay	200	2.76	12	8	1.33	2	1	1.57	5	4
Swansea Bay	20	1.41	6	4	1.20	-3	-2	1.20	0	0
Swansea Bay	50	1.40	6	4	1.23	-3	-2	1.25	0	0
Swansea Bay	200	1.33	5	3	1.20	-3	-2	1.23	0	0
Fylde	20	2.00	13	9	1.69	-5	-4	1.91	2	1
Fylde	50	1.83	12	8	1.65	-5	-4	1.88	1	1
Fylde	200	1.66	8	5	1.51	-5	-4	1.66	0	0

Table 4 Overtopping ratios, tidal ranges and water levels

Location	Embankment average Qf/Qp	Tidal range [m]	10,000 year water level [m]	Water level difference, present [m]	Water level difference, future [m]
Lincolnshire	1.77	5.7	5.38	2.48	2.01
Dungeness	1.59	5.85	5.55	1.02	0.69
Lyme Bay	1.94	4.2	4.56	1.05	0.82
Swansea Bay	1.21	6.2	6.14	0.92	0.96
Fylde	1.62	8.2	6.93	0.93	0.69

Table 5 Summary statistics for coastal steepening scenario

Location	RP [years]	Standard beach slope			Steepened beach slope		
		Qf/Qp	PISP	PIDP	Qf/Qp	PISP	PIDP
Lincolnshire	20	4.5	26	16	5.5	40	25
Lincolnshire	50	3.9	27	17	4.3	34	22
Lincolnshire	200	3.6	22	14	4.4	32	20
Lyme Bay	20	29.8	25	16	32.5	30	19
Lyme Bay	50	2.9	22	14	3.5	26	17
Lyme Bay	200	2.8	12	8	3.2	15	10
Swansea Bay	20	1.4	6	4	1.6	55	34
Swansea Bay	50	1.4	6	4	1.6	54	33
Swansea Bay	200	1.3	5	3	1.6	49	30

Table 6 Summary statistics for scenarios at Lincolnshire, including additional cases

Location	RP [years]	Scenario	Qf/Qp	PISP	PIDP
Lincolnshire	50	future	3.9	27	17
Lincolnshire	50	future -steepened	4.3	34	22
Lincolnshire	50	future - raised crest	2.1	17	11
Lincolnshire	50	present waves - raised wl	3.2	19	12
Lincolnshire	50	present - lowered toe	1.7	14	9
Lincolnshire	50	future, lowered toe	5.5	38	24
Lincolnshire	50	future, low toe, steepened	6.6	57	35

Table 7 Longshore drift rates

	Units	Lincolnshire	Dungeness	Dungeness	Lyme Bay	Lyme Bay	Swansea Bay	Fylde
Beach-normal direction	[deg]	90	180	225	180	225	245	270
Present mean annual net drift	[m^3/year]	-356000	114000	27000	111487	24000	219000	-589000
Future mean annual net drift	[m^3/year]	-324000	126000	31000	121491	31000	284000	-714000
Direction of positive drift (towards)	[deg]	North	East	East	East	East	East	South
Percentage increase in net drift	[%]	-9	11	15	9	29	30	21
Present standard deviation of net drift	[m^3/year]	310000	29000	15000	36886	20000	147000	262000
Future standard deviation of net drift	[m^3/year]	227000	27000	13000	34714	15000	134000	227000
Percentage increase in std deviation	[%]	-27	-7	-13	-6	-25	-9	-13
Zero drift wave direction	[deg]	81	206	229	200	228	247	266

Table 8 Ratios of future to present day overtopping rates for embankment, calculated using statistical analysis method

Return period [years]	Lincolnshire	Dungeness to Rye	Lyme Bay Bay	Swansea Bay	Fylde
	Qf/Qp	Qf/Qp	Qf/Qp	Qf/Qp	Qf/Qp
0.1	1.53	1.86	1.95	1.47	1.63
0.2	1.40	1.83	1.80	1.39	1.58
0.5	1.37	1.77	1.71	1.32	1.50
1	1.39	1.73	1.66	1.29	1.47
2	1.35	1.70	1.62	1.27	1.45
5	1.33	1.70	1.55	1.26	1.45
10	1.36	1.65	1.53	1.27	1.45
20	1.33	1.65	1.51	1.28	1.44
50	1.35	1.67	1.33	1.27	1.44
100	1.22	1.68	1.27	1.24	1.44
200	1.15	1.64	1.28	1.25	1.46
500	1.27	1.56	1.26	1.36	1.60

Table 9 Ratios of future to present day overtopping rates for shingle beach, calculated using statistical analysis method

Return period [years]	Lincolnshire	Dungeness to Rye	Lyme Bay Bay	Swansea Bay	Fylde
	Qf/Qp	Qf/Qp	Qf/Qp	Qf/Qp	Qf/Qp
0.1	1.60	2.78	2.71	1.90	2.38
0.2	1.57	2.59	2.42	1.74	2.06
0.5	1.55	2.42	2.10	1.60	1.97
1	1.54	2.31	2.07	1.53	1.81
2	1.58	2.25	2.03	1.48	1.75
5	1.51	2.17	1.90	1.45	1.68
10	1.53	2.17	1.86	1.43	1.67
20	1.50	2.21	1.83	1.46	1.75
50	1.54	2.11	1.58	1.44	1.73
100	1.34	2.13	1.46	1.38	1.86
200	1.24	2.14	1.42	1.48	2.36
500	1.39	2.44	1.31	1.67	2.53

Table 10 Comparison between results from joint probability (JP) and statistical analysis (SA) methods for calculating overtopping ratios

Location	Return period [years]	JP bank Qf/Qp	JP shingle Qf/Qp	SA bank Qf/Qp	SA shingle Qf/Qp
Lincolnshire	20	1.86	1.86	1.65	1.50
Lincolnshire	50	1.75	1.75	1.67	1.54
Lincolnshire	200	1.71	1.71	1.64	1.24
Dungeness	20	1.65	1.74	1.65	2.21
Dungeness	50	1.58	1.68	1.67	2.11
Dungeness	200	1.53	1.61	1.64	2.14
Lyme Bay	20	2.47	2.59	1.51	1.83
Lyme Bay	50	2.01	1.52	1.33	1.58
Lyme Bay	200	1.33	1.57	1.28	1.42
Swansea Bay	20	1.20	1.20	1.28	1.46
Swansea Bay	50	1.23	1.25	1.27	1.44
Swansea Bay	200	1.20	1.23	1.25	1.48
Fylde	20	1.69	1.91	1.44	1.75
Fylde	50	1.65	1.88	1.44	1.73
Fylde	200	1.51	1.66	1.46	2.36

Figures

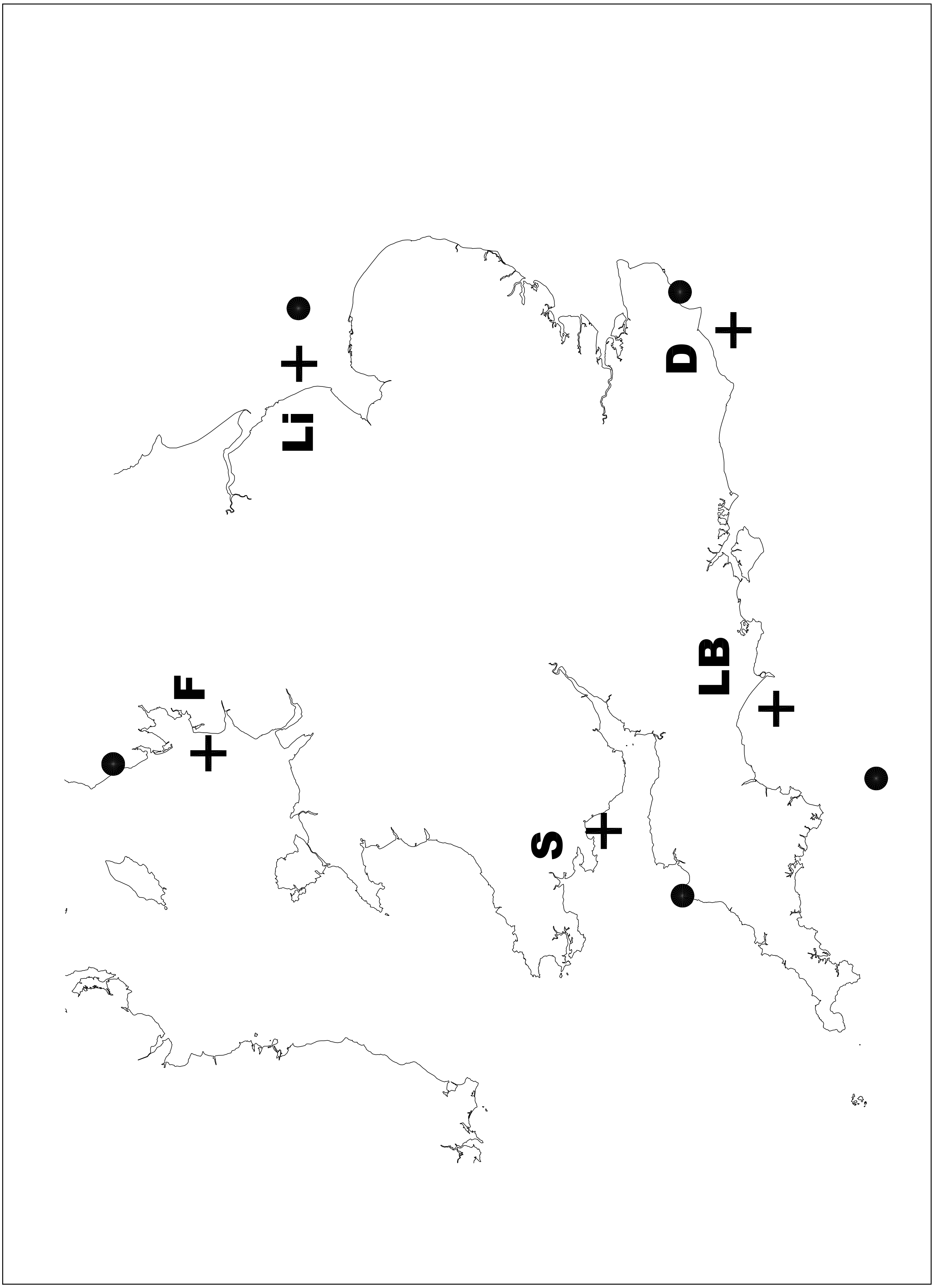

Figure 1 **Location of modelled sites. Li = Lincolnshire, D = Dungeness to Rye, LB = Lyme Bay, S = Swansea Bay and F = Fylde. The circles and crosses mark the centres of the ECHAM4 and NISE output cells**

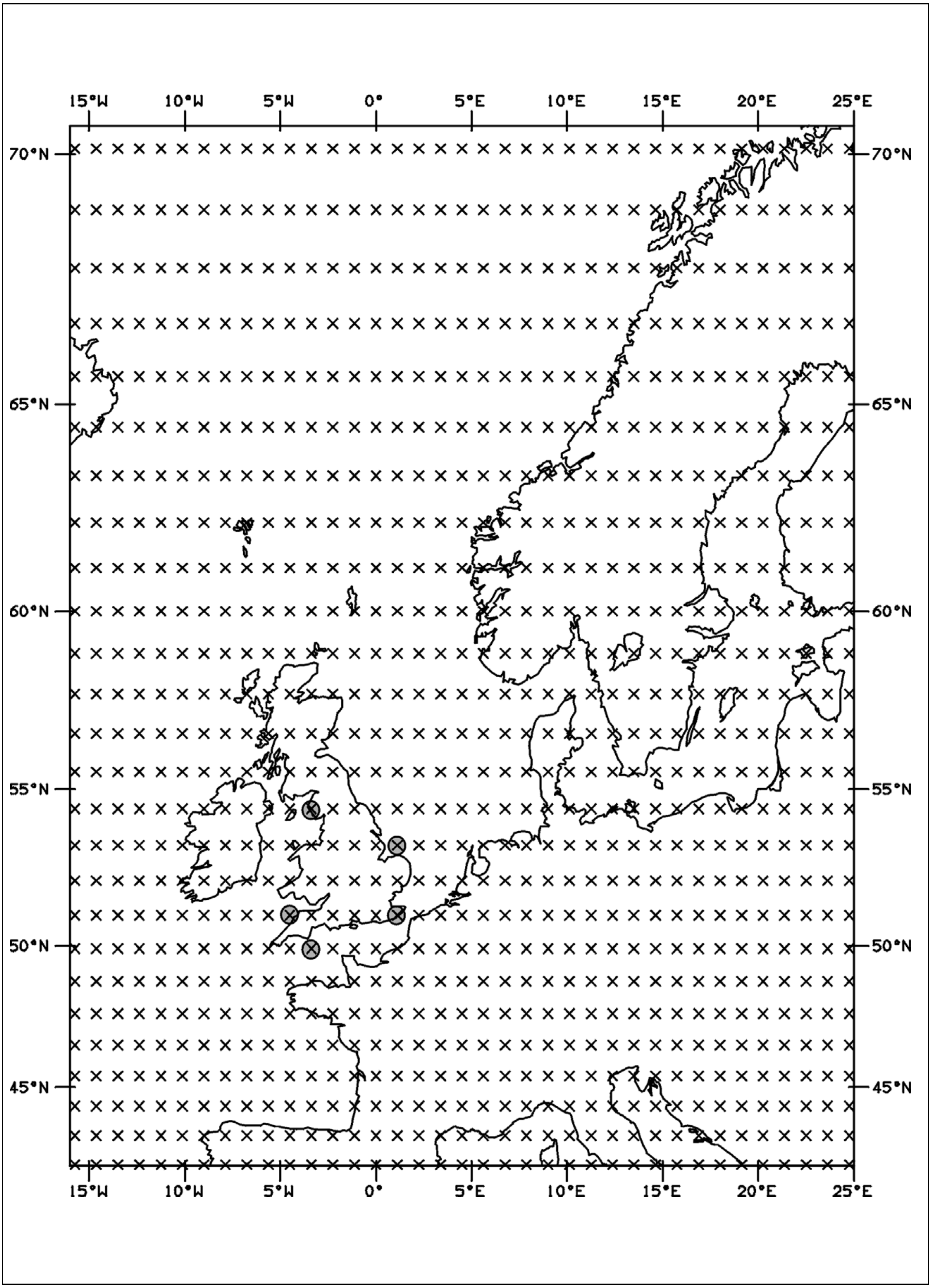

Figure 2 ECHAM4 grid and selected points used for CDV2075

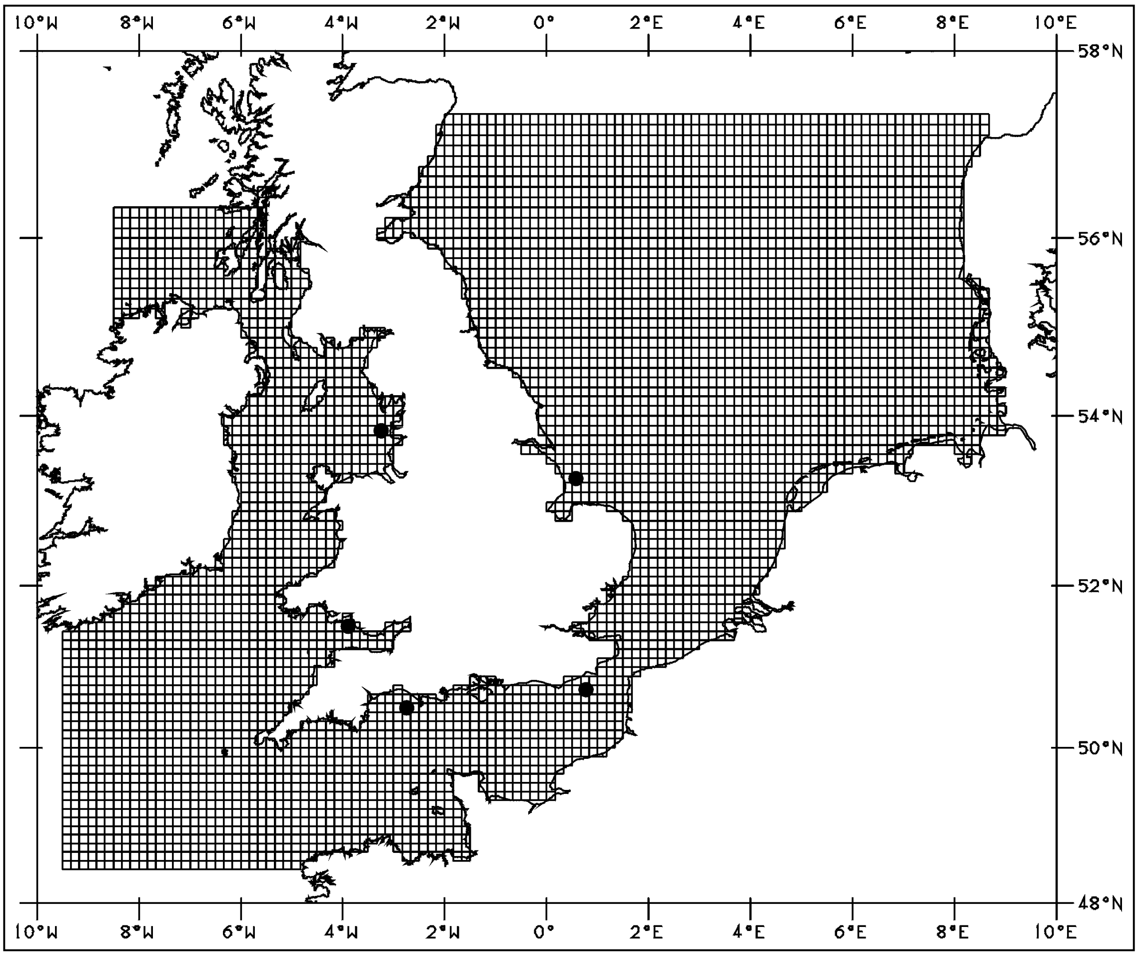

Figure 3 POL 2D-TS tide-surge model grid and points selected for CDV2075

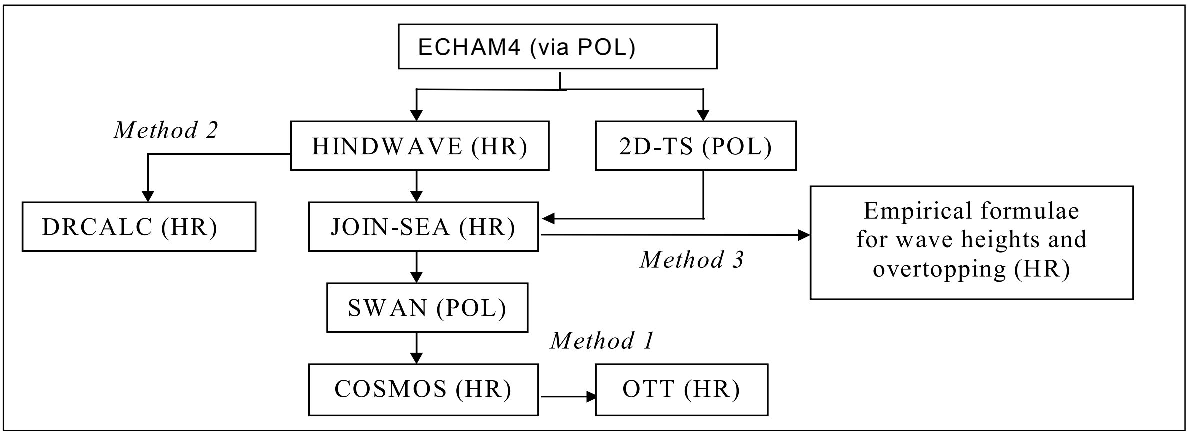

Figure 4 Linkage of models in CDV2075

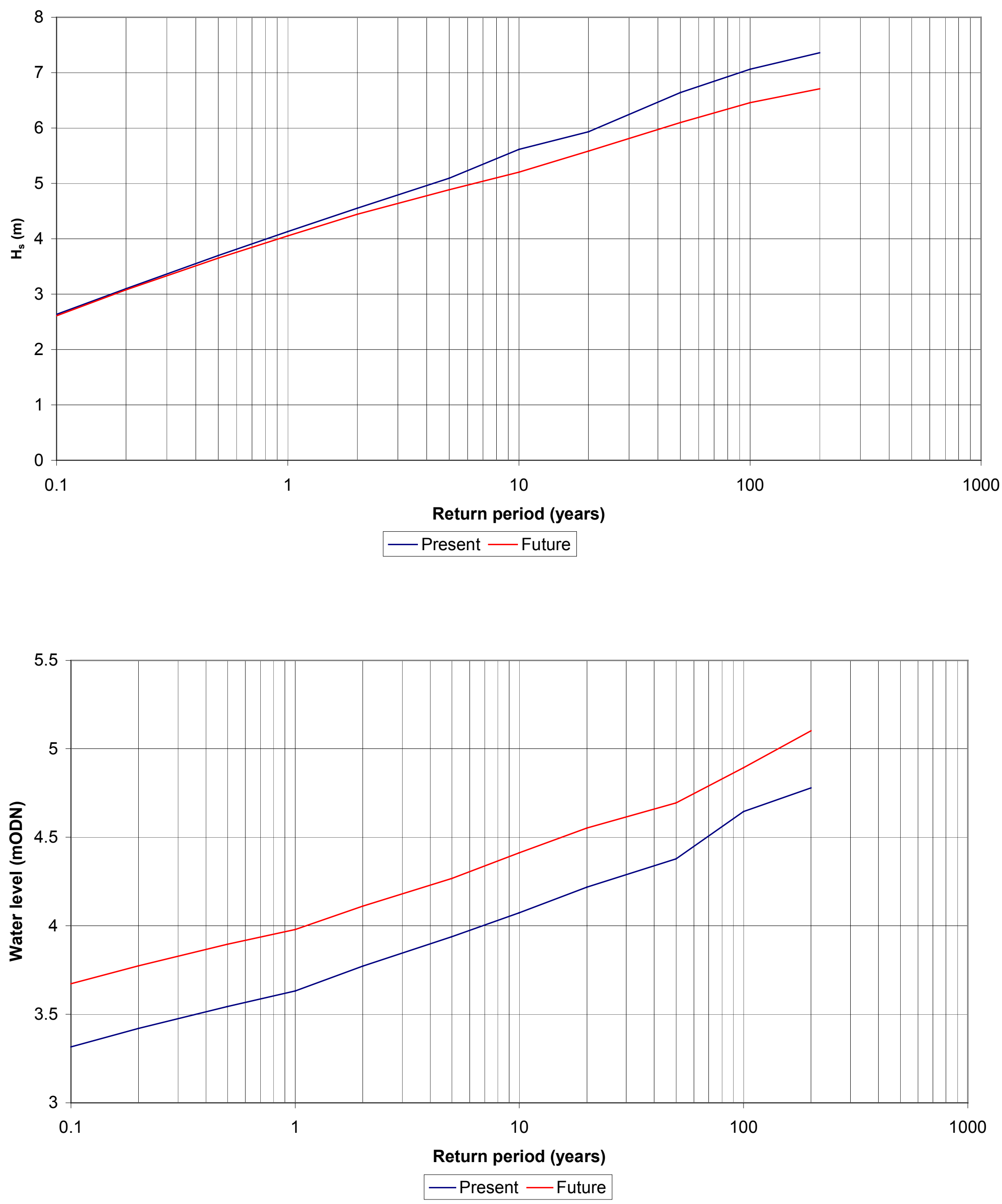

Figure 5 Marginal extreme wave height and water level for Lincolnshire

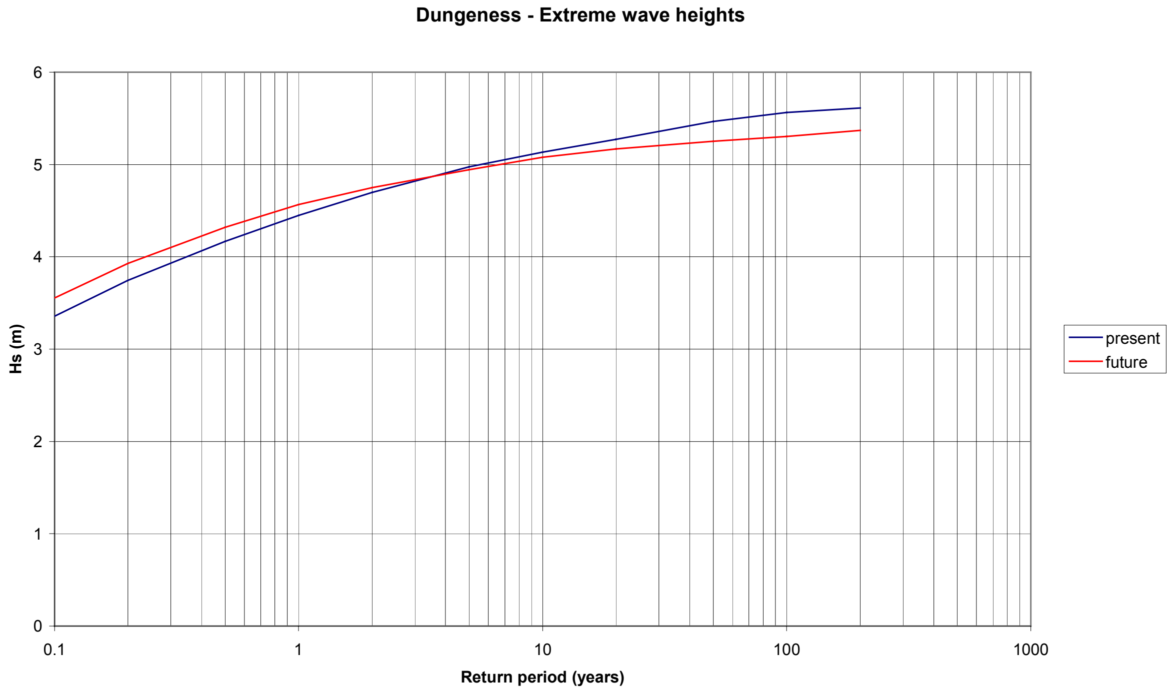

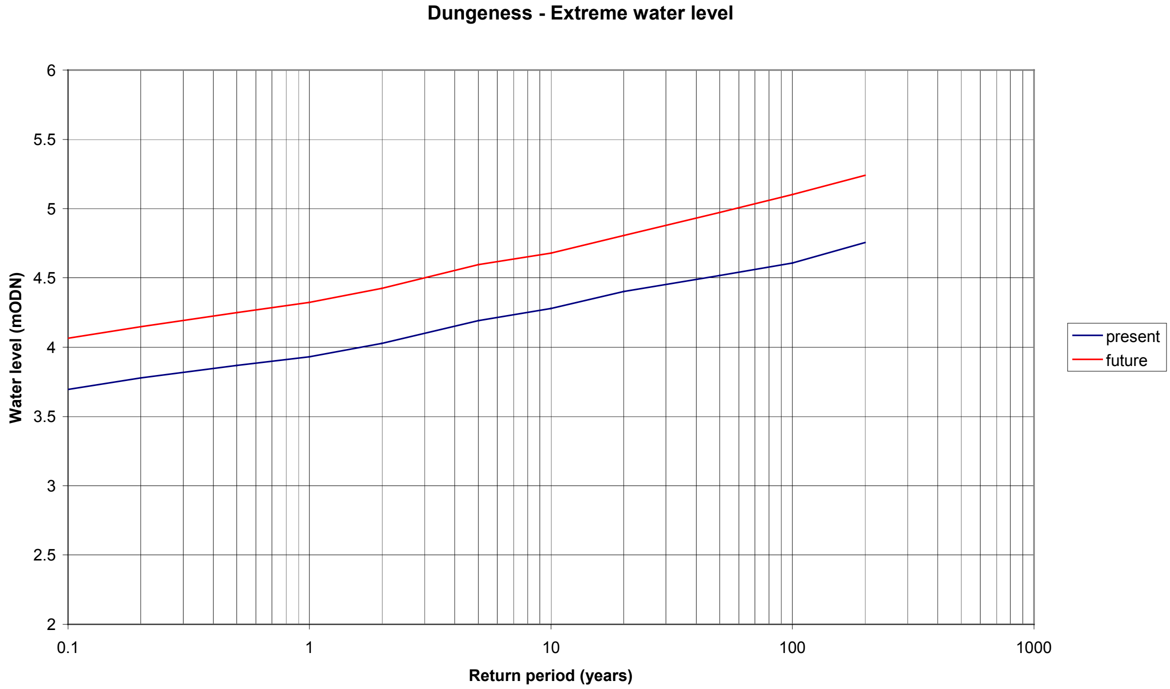

Figure 6 Marginal extreme wave heights and water levels for Dungeness to Rye

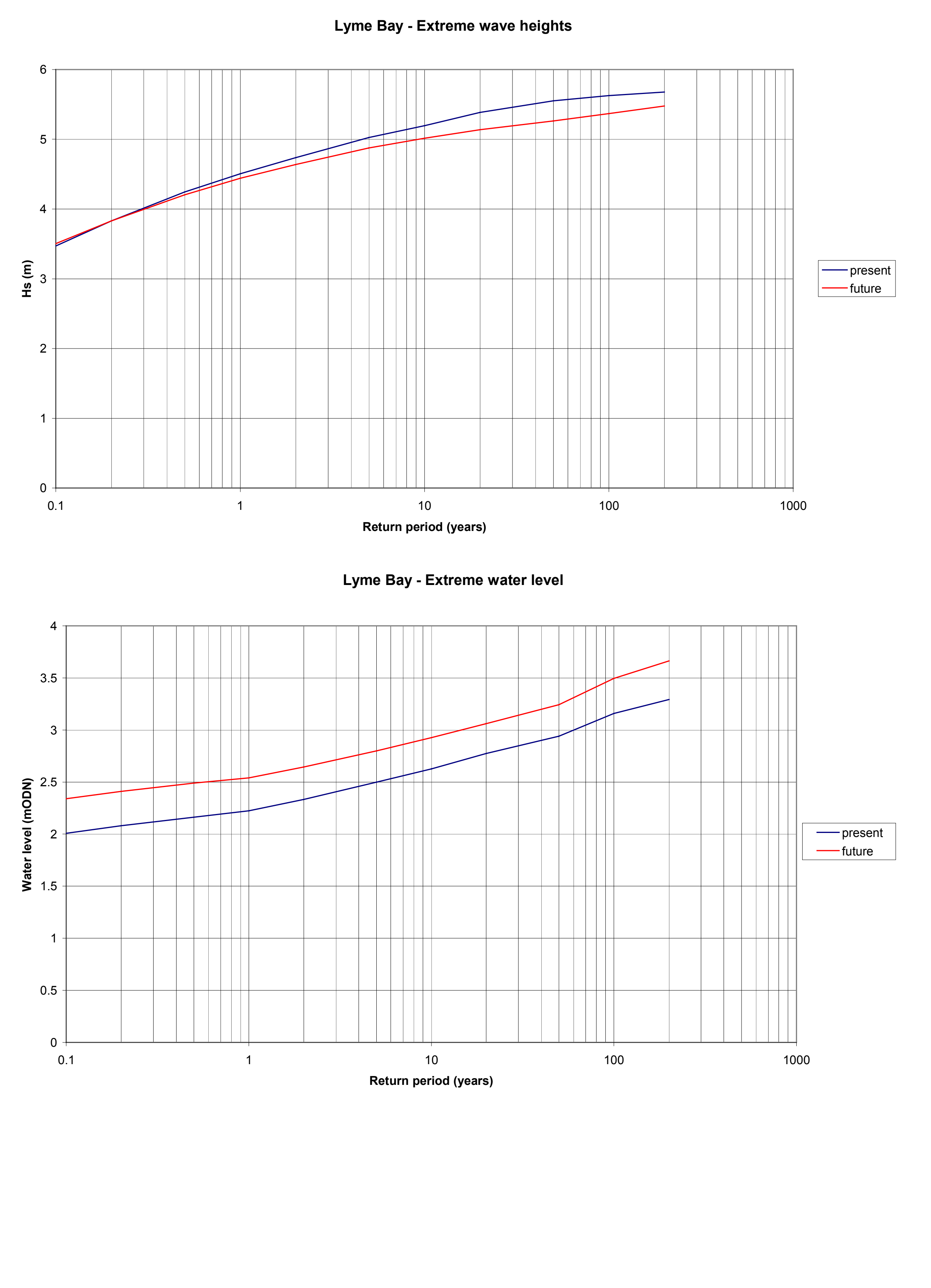

Figure 7 Marginal extreme wave heights and water levels for Lyme Bay

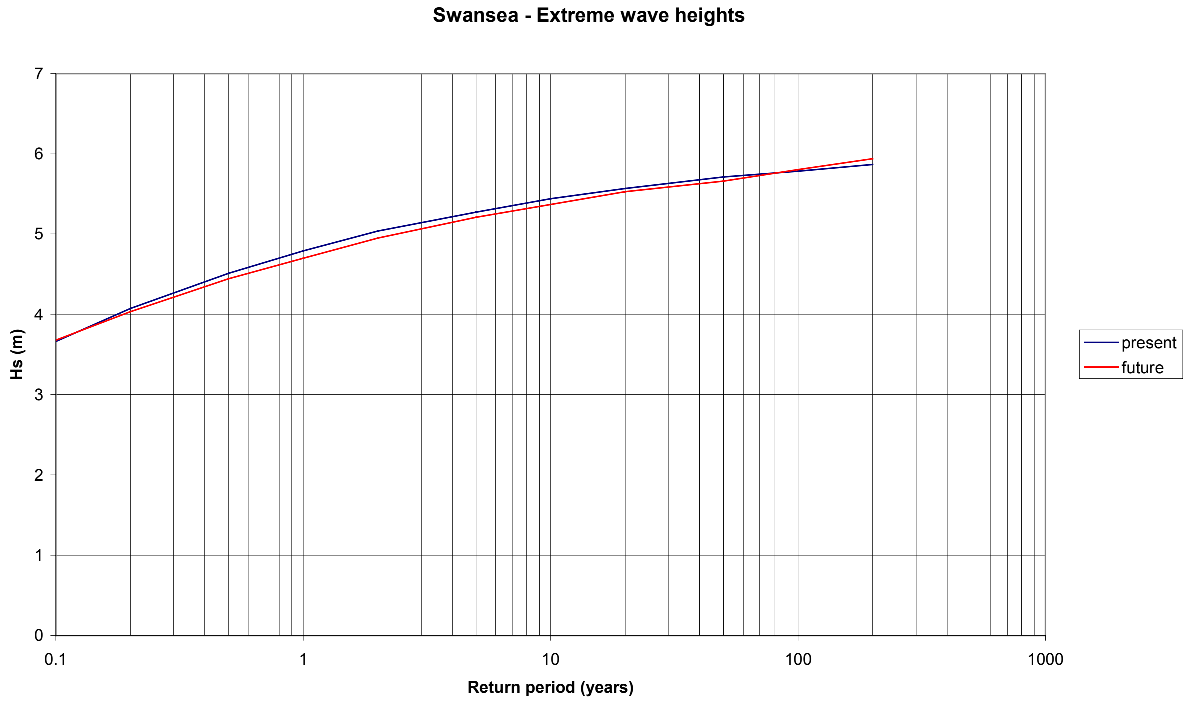

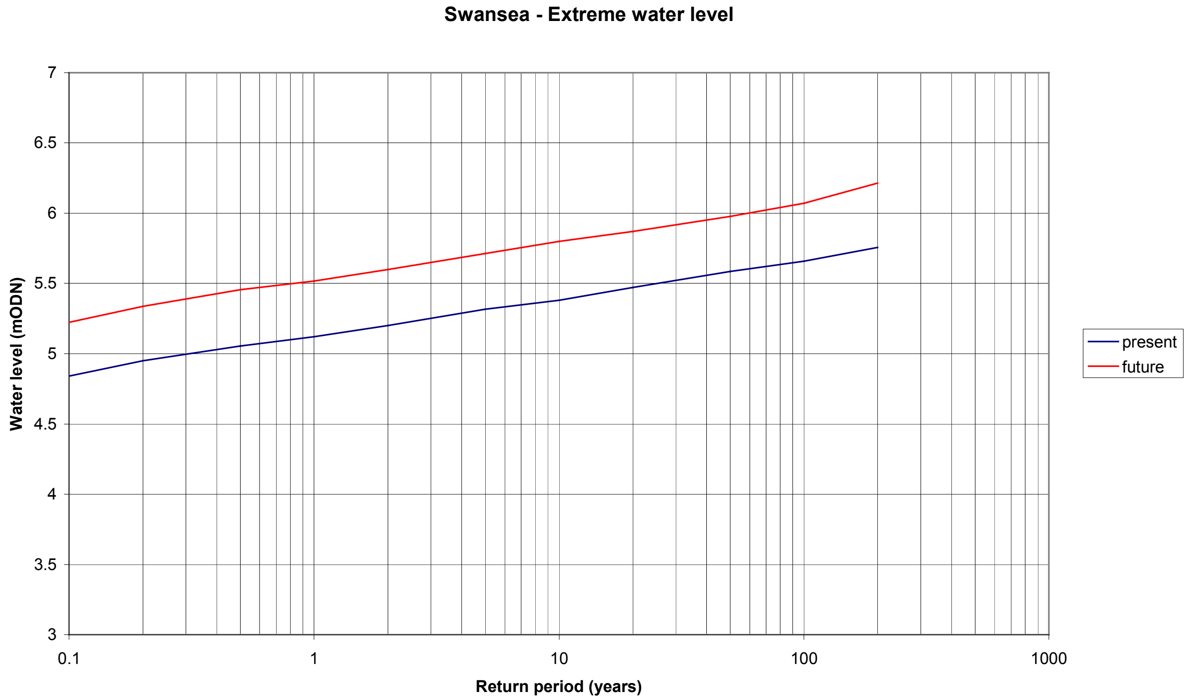

Figure 8 Marginal extreme wave heights and water levels for Swansea Bay

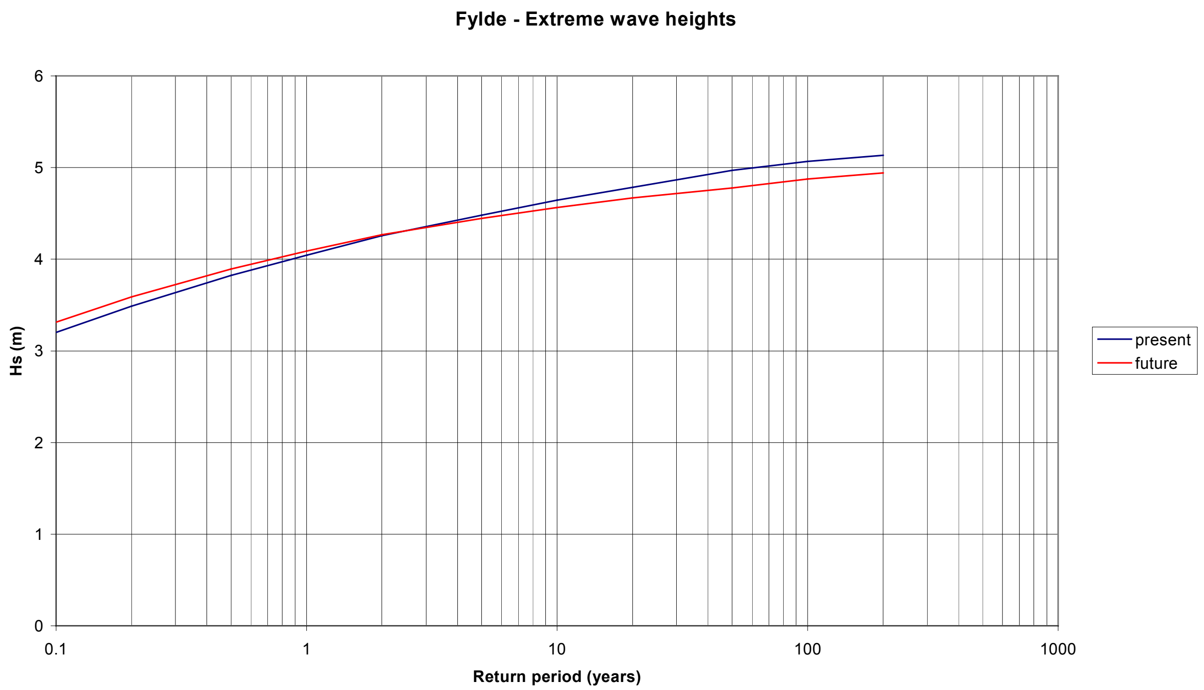

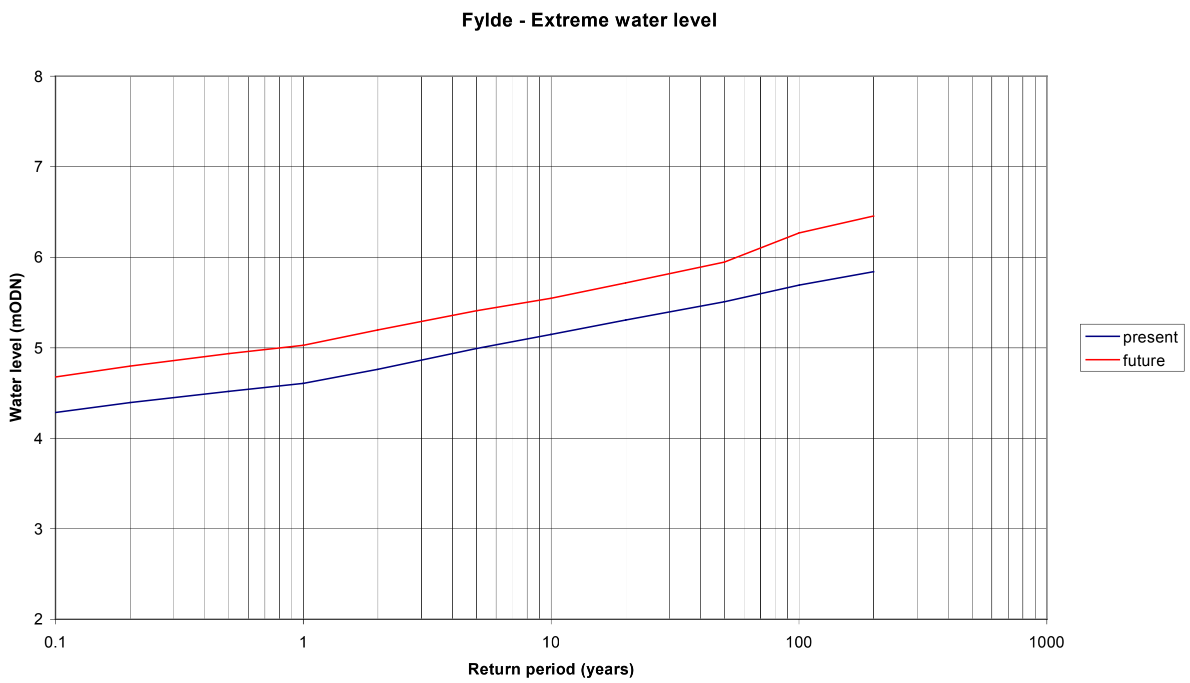

Figure 9 Marginal extreme wave heights and water levels for Fylde

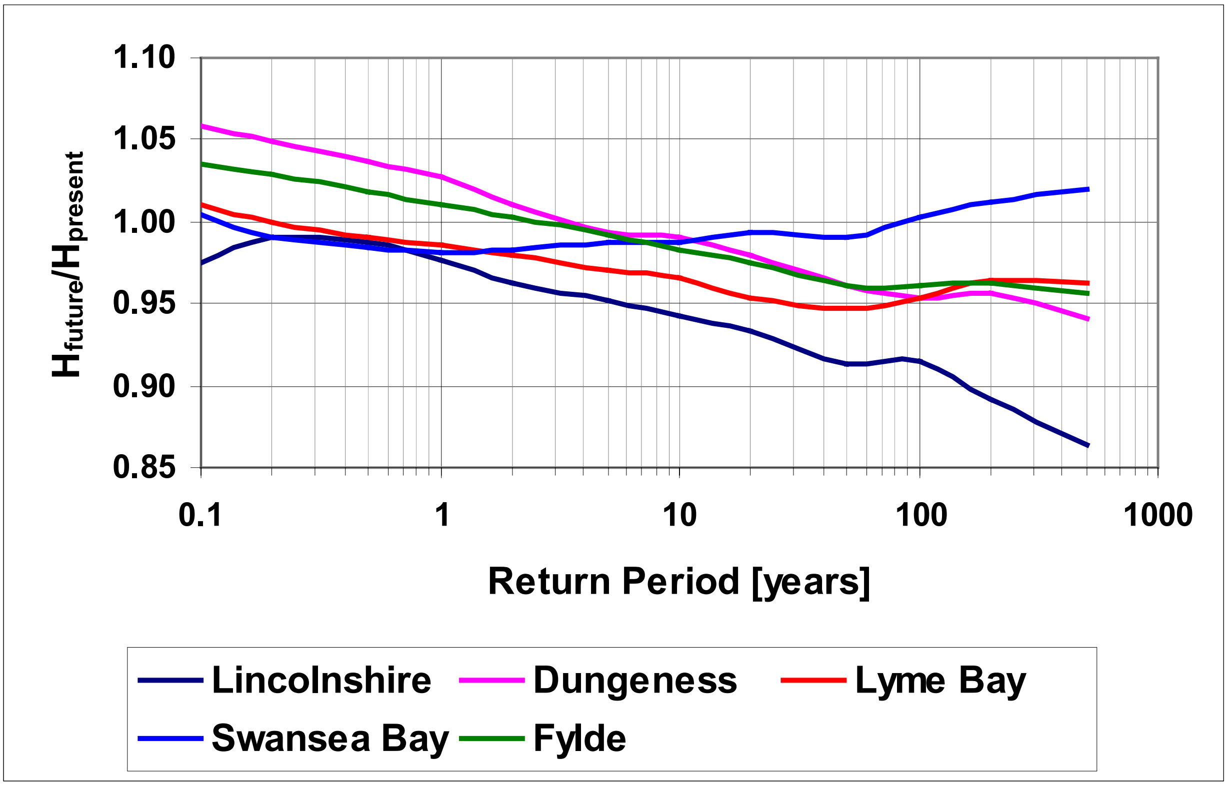

Figure 10 Relative change in wave height against return period

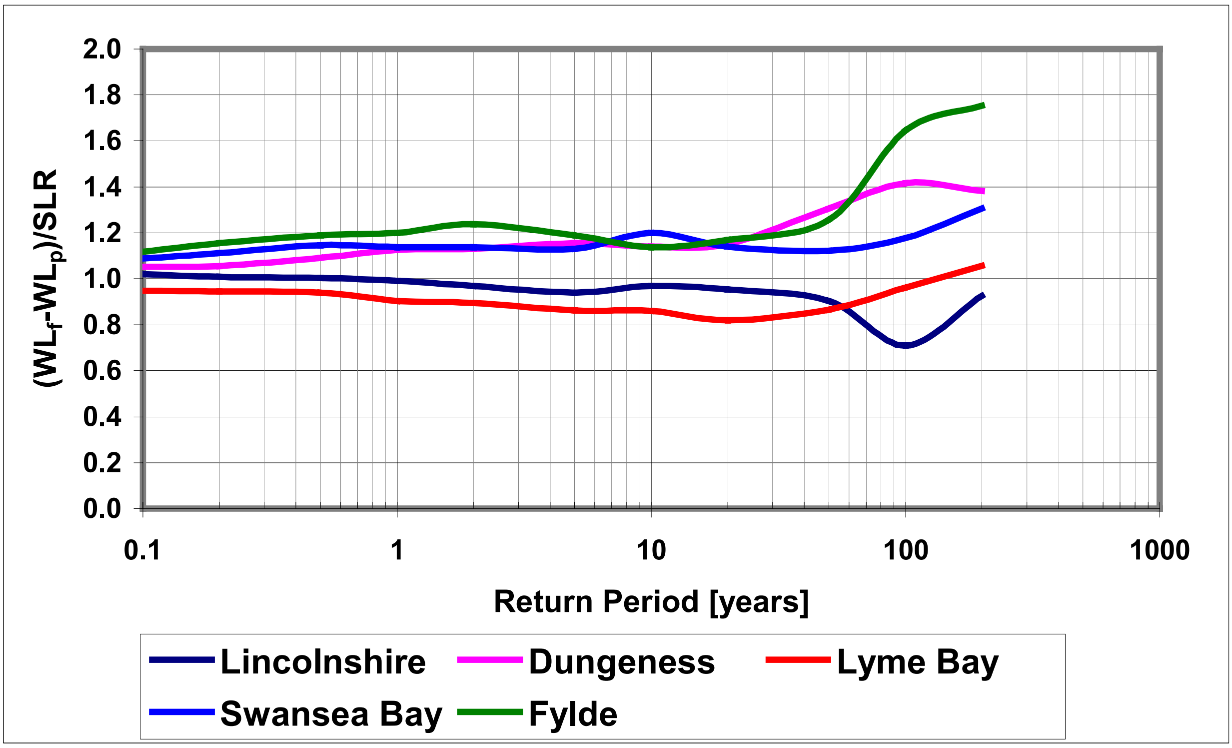

Figure 11 Relative increase in water level against return period. WL_f = future water level, WL_p = present water level and SLR = sea level rise

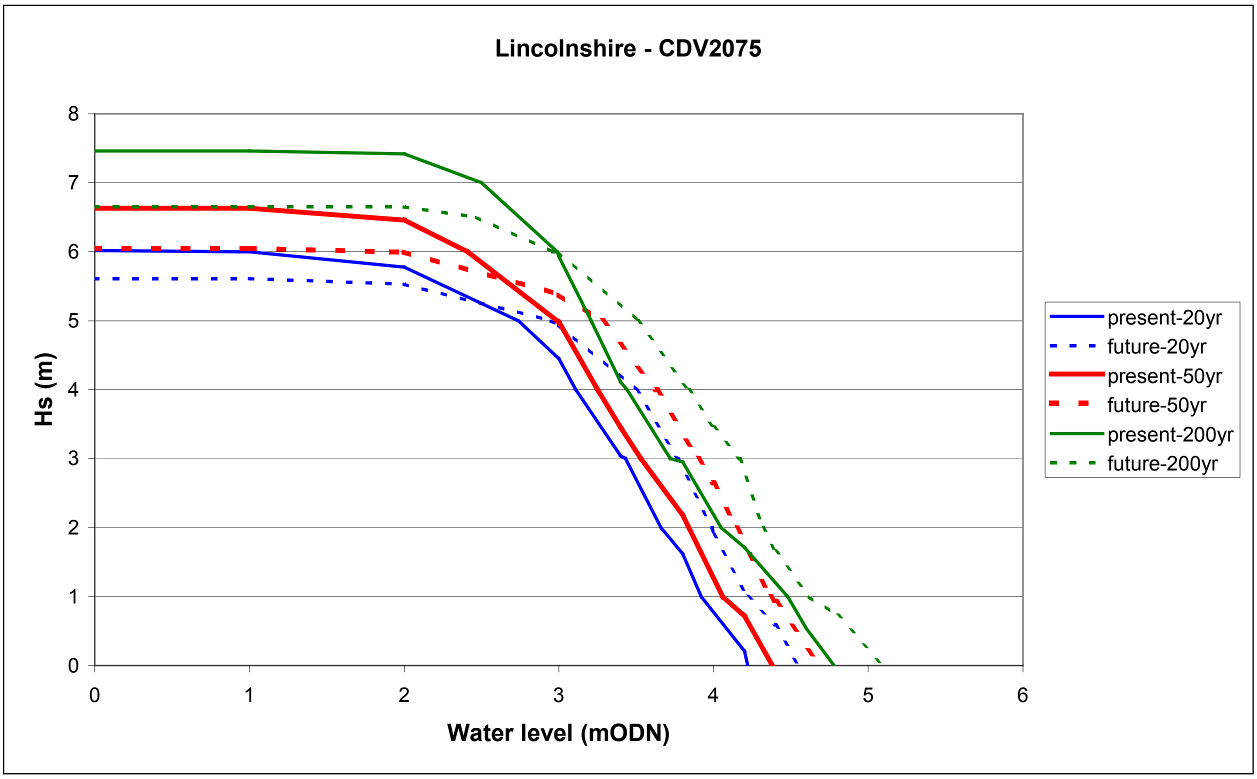

Figure 12 Joint probability of exceedance contours for Lincolnshire

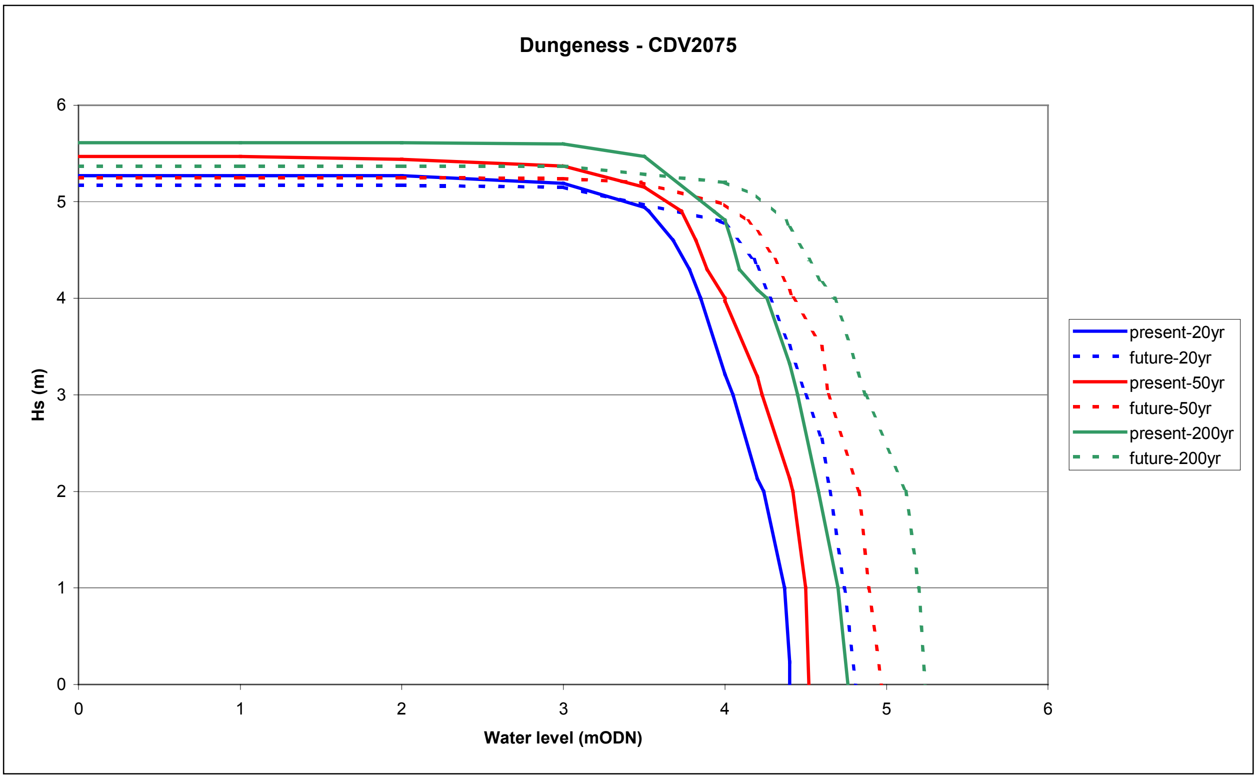

Figure 13 Joint probability of exceedance contours for Dungeness to Rye

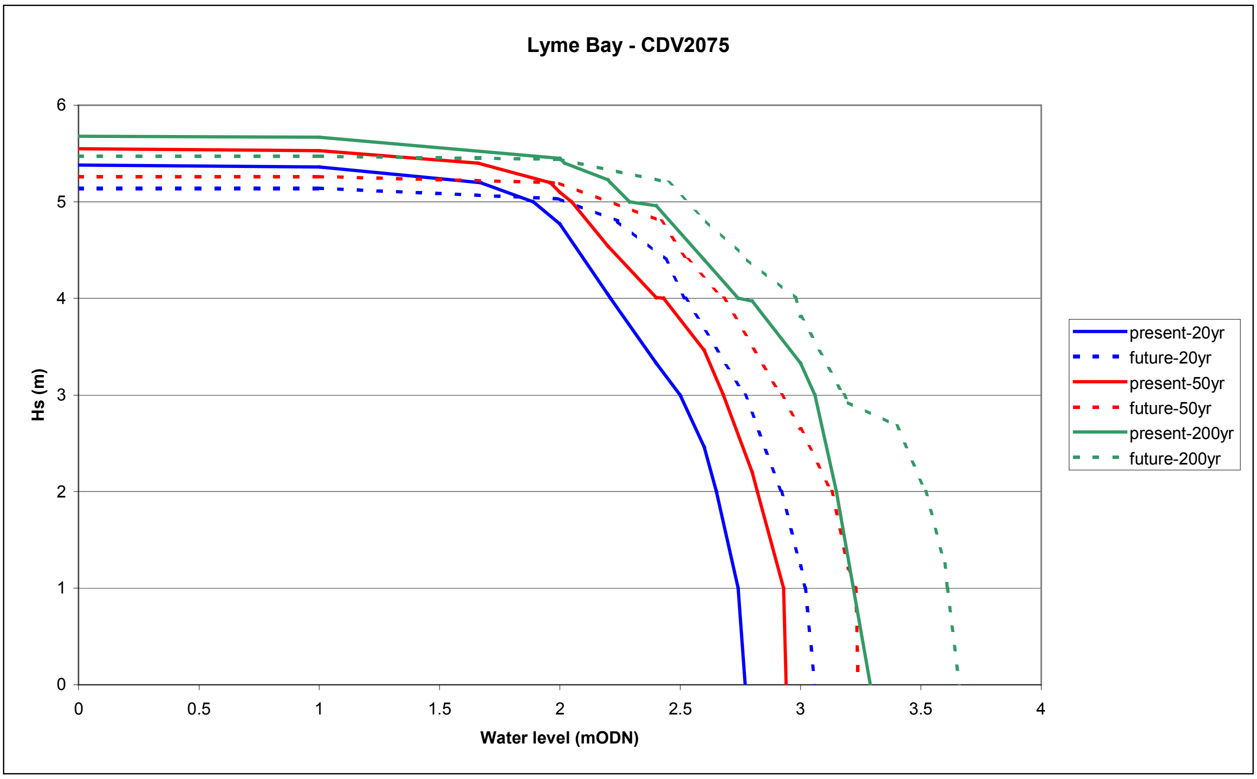

Figure 14 Joint probability of exceedance contours for Lyme Bay

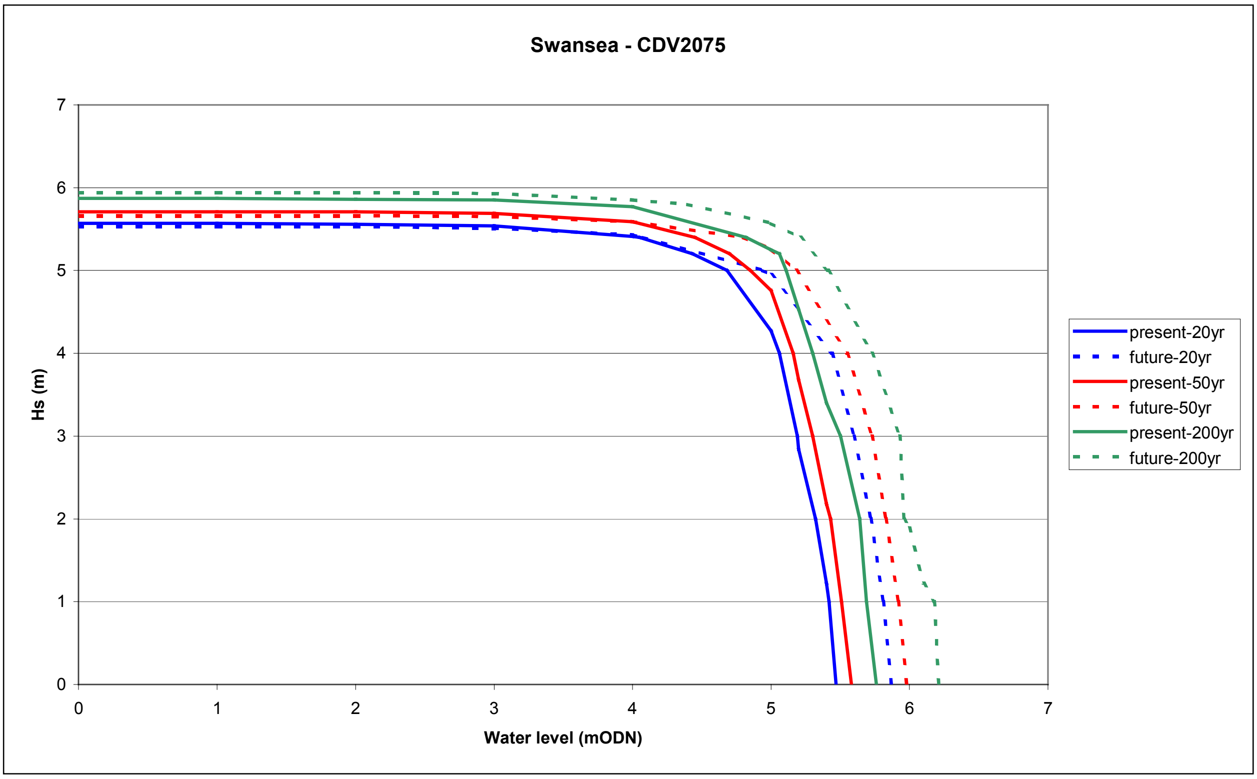

Figure 15 Joint probability of exceedance contours for Swansea Bay

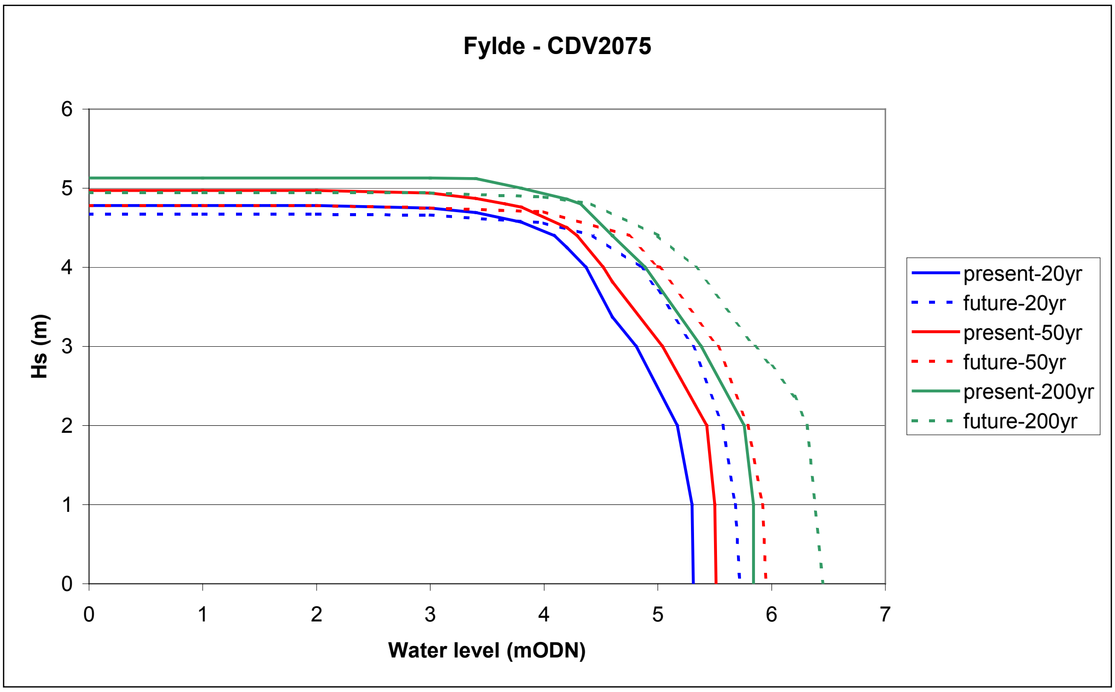

Figure 16 Joint probability of exceedence contours for Fylde

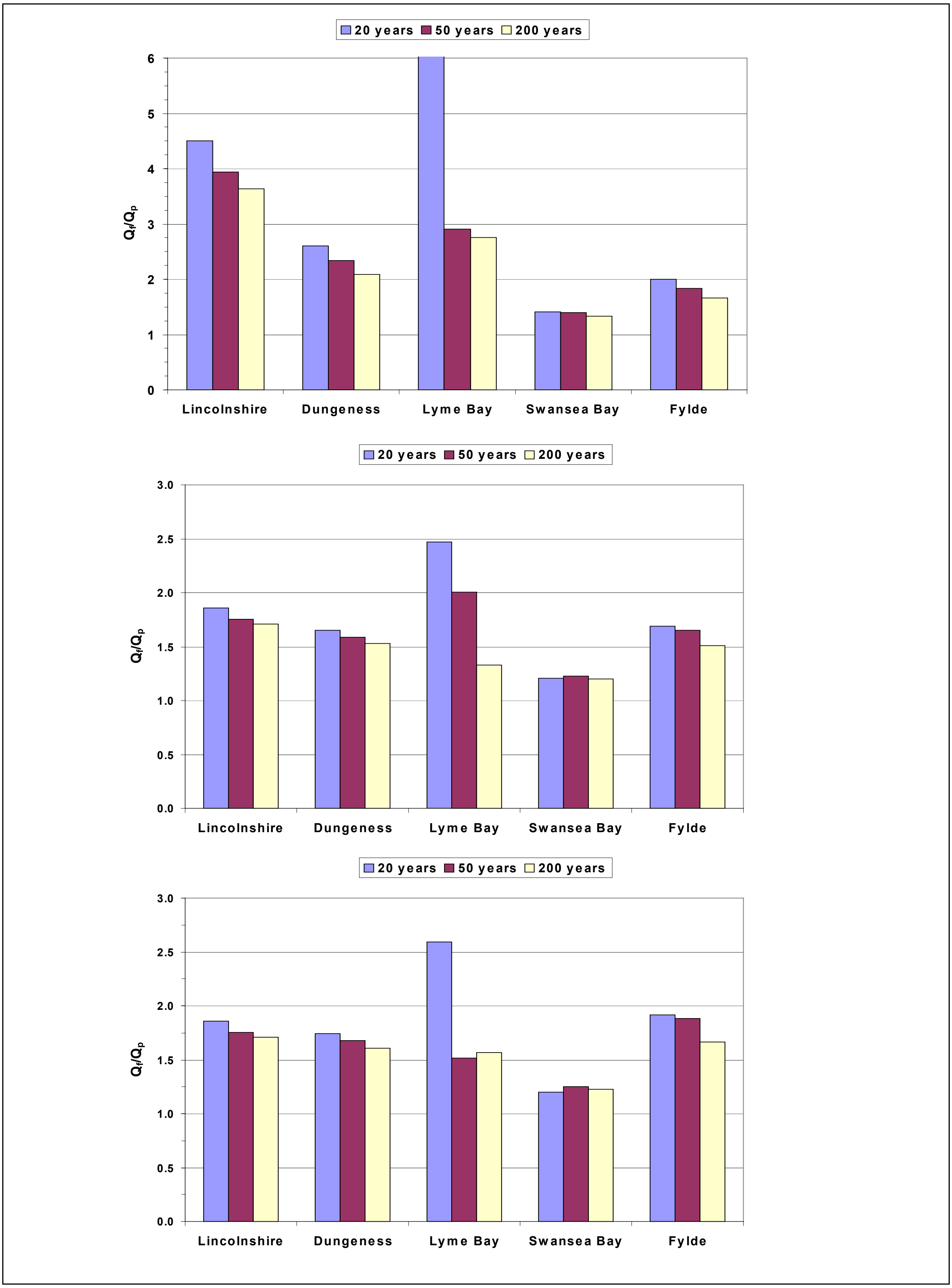

Figure 17 Relative increase in mean overtopping rates due to climate change at all sites and return periods for seawall (top) embankment (middle) and shingle beach (bottom)

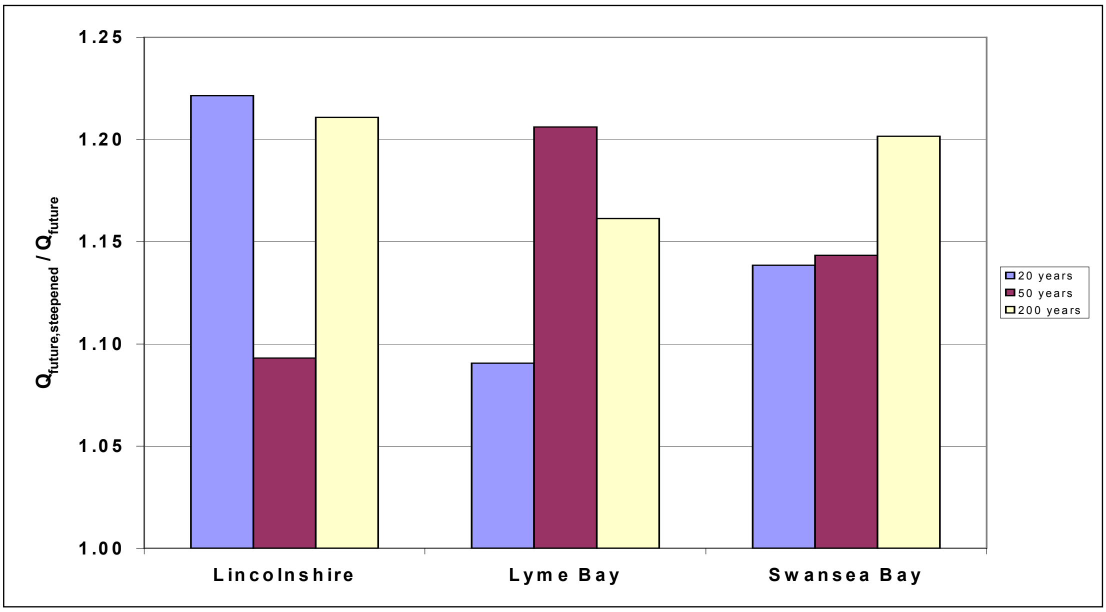

Figure 18 Relative increases in future mean overtopping rate due to coastal steepening

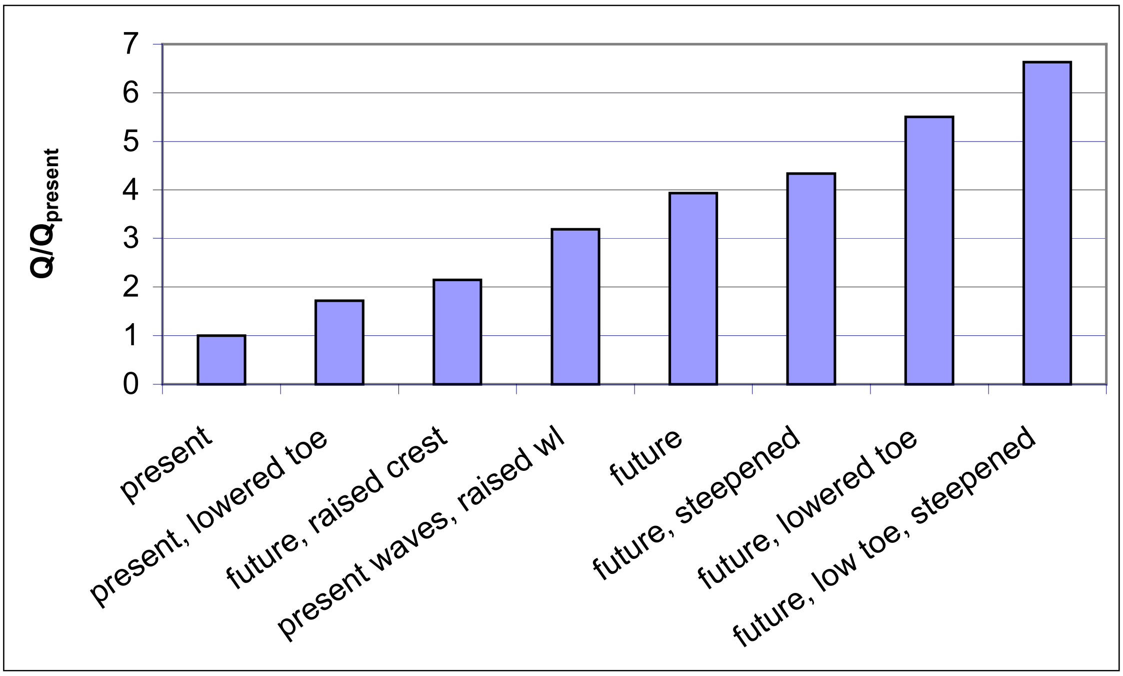

Figure 19 Relative overtopping rates from tests at Lincolnshire, including additional scenarios. Results were non-dimensionalised by the present-day scenario mean overtopping rate at Lincolnshire

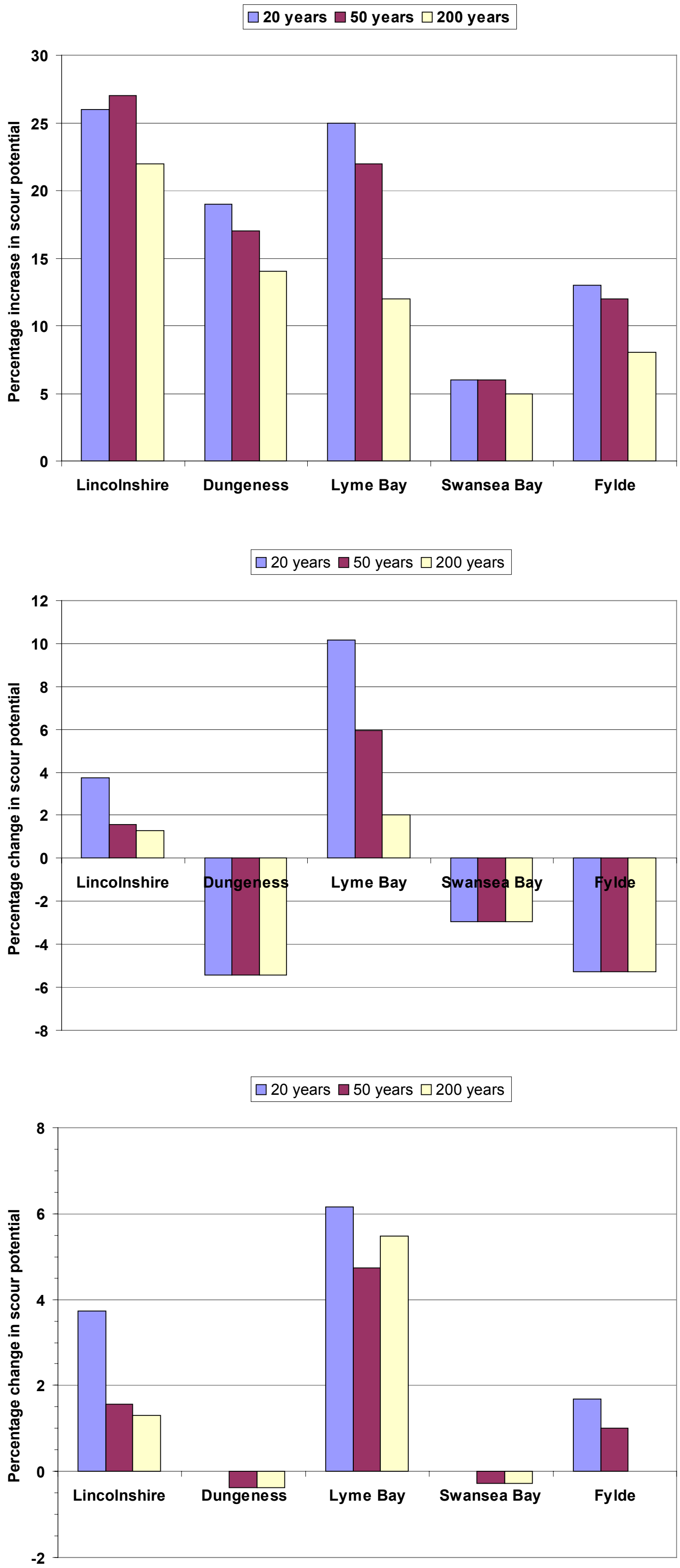

Figure 20 Percentage increase in scour potential at all sites and for all return periods, calculated for a seawall (top) embankment (middle) and shingle beach (bottom)

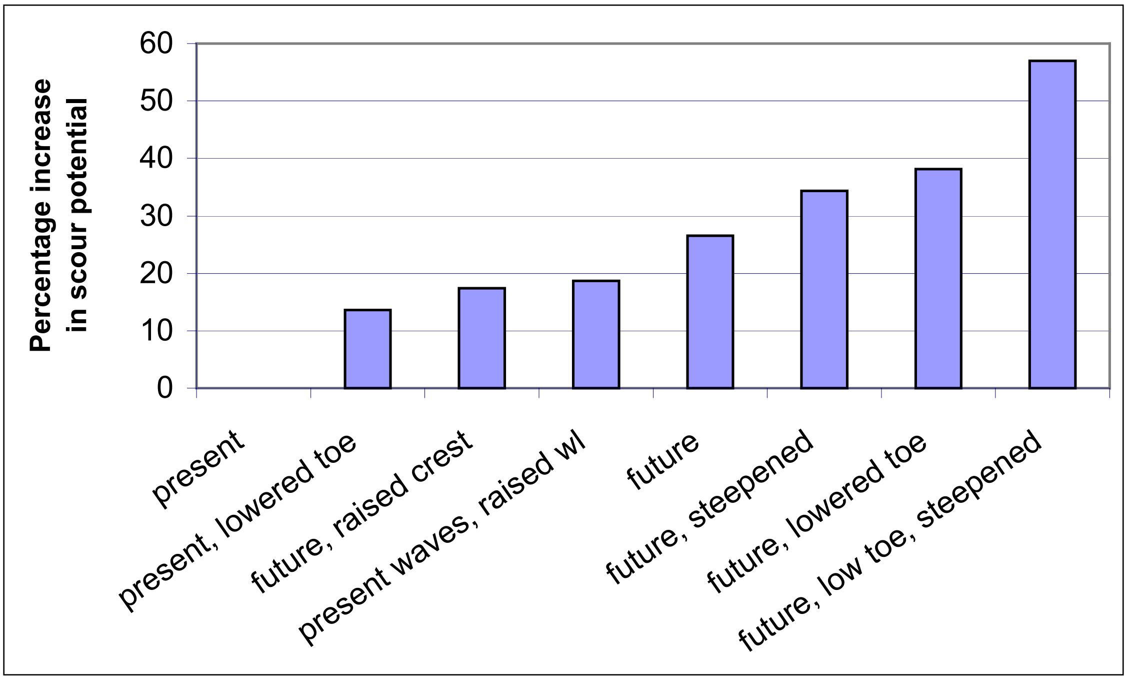

Figure 21 Percentage increase in scour potential (relative to present-day conditions) at Lincolnshire

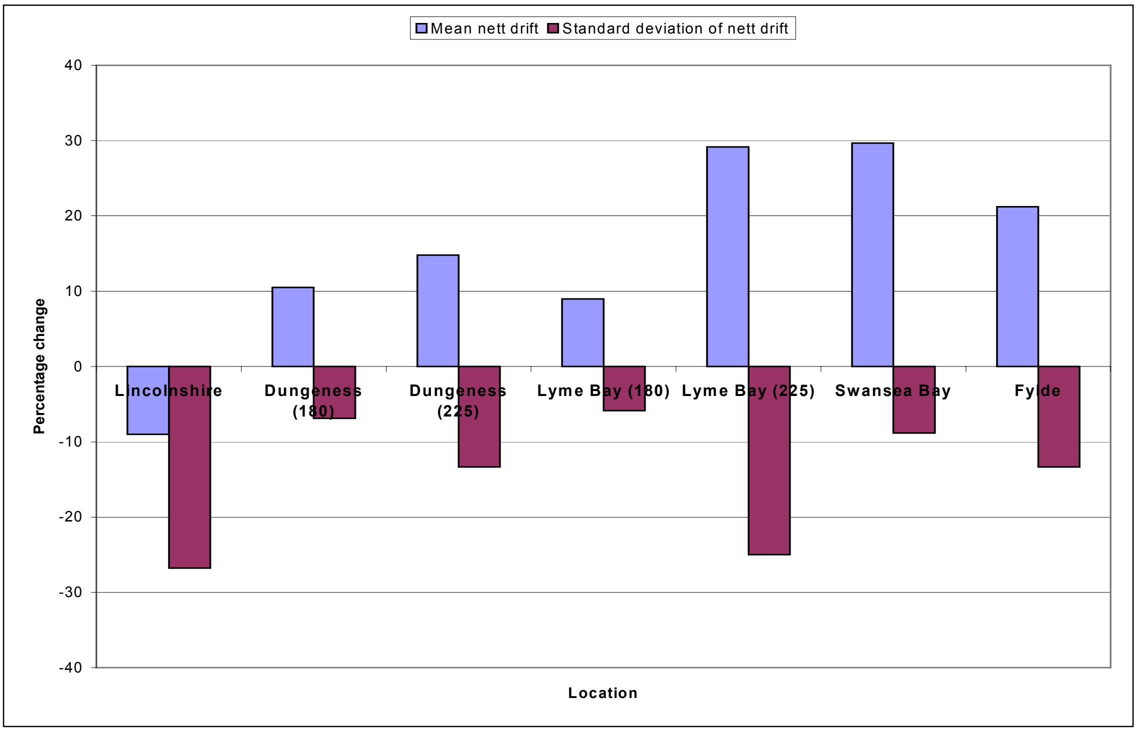

Figure 22 Percentage change in mean annual drift rates and their standard deviation. Numbers after a location name give the shore-normal direction

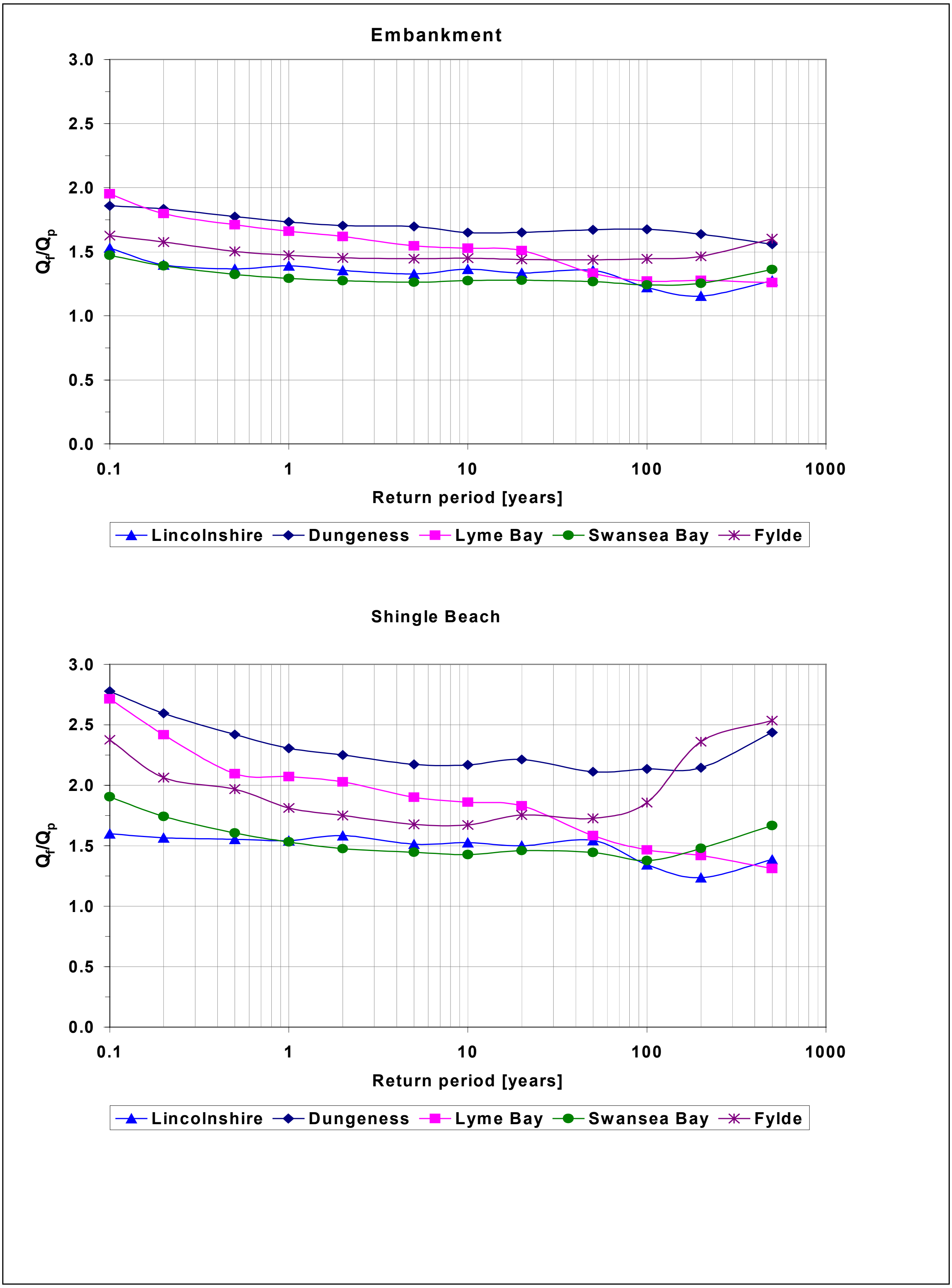

Figure 23 Ratio of future to present day overtopping rates versus return period for embankment and shingle beach

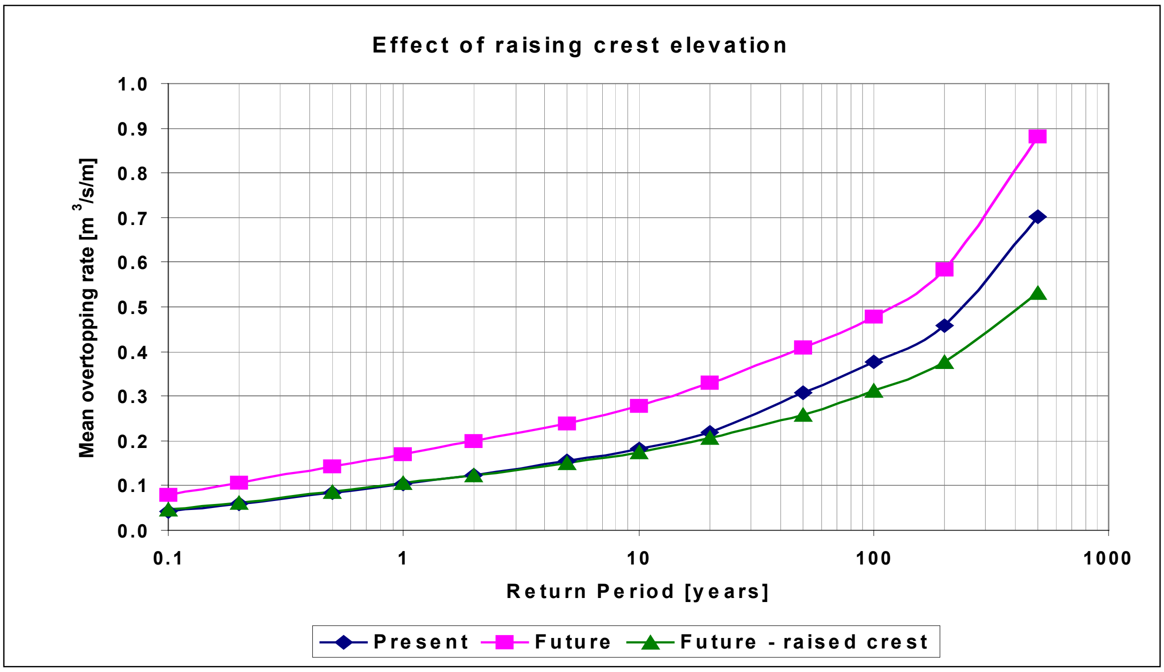

Figure 24 Effect of raising crest elevation by amount given by Equation 13

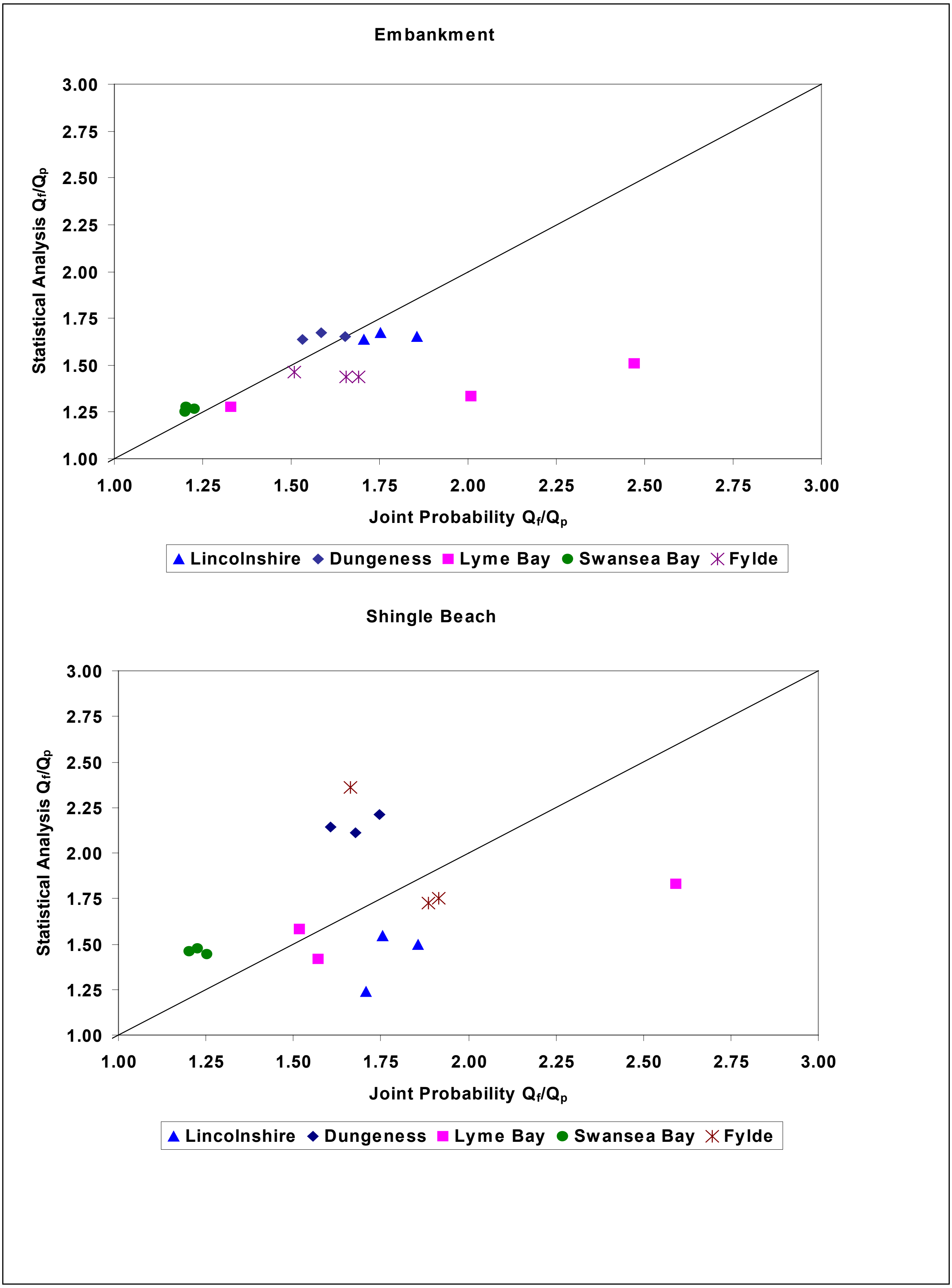

Figure 25 Comparison between joint probability and statistical analysis methods of determining overtopping ratios

Plates

Plate 1 Beach recycling at Seaford, East Sussex

Appendices

Appendix 1

Numerical Models

Appendix 1 Numerical Models

ECHAM4

The ECHAM4/OPYC coupled general circulation model of the atmosphere and ocean (AOGCM) was used to assess future climate change as a result of the expected increase in anthropogenic emissions (May and Roeckner, 2001). The highest horizontal resolution currently affordable in such coupled atmosphere-ocean models is T42 resolution (2.8° latitude/longitude). In order to obtain better resolution of the atmospheric dynamics a higher resolution, T106 (1.1° latitude/longitude) atmosphere-only general circulation model, ECHAM4, was forced by sea surface temperatures and sea-ice derived from the T42 resolution ECHAM4/OPYC AOGCM, for multi-year “time slices”. IPCC scenario IS92a was used. Bengtsson et al. (1995) showed that a T106 model was able to capture the structure and frequency of hurricane-type vortices quite realistically, while a T42 model was not. A finer resolution (down to tens of kilometres) can be obtained by driving a regional climate model using the AOGCM, but the main disadvantage is that there are no interactions between the regional and global scales. Another method of deriving local predictions from large-scale models is statistical downsizing, which is computationally inexpensive but relies on ill-defined empirical relationships between regional model values and local ones. Therefore the T106 global climate model was used to combine a relatively fine resolution with large-scale interactions.

ECHAM4 is an atmospheric general circulation model (AGCM) developed at the Max-Planck-Institute for Meteorology. The model uses a 19-level hybrid sigma-pressure coordinate system, and the vertical domain extends up to a pressure level of 10 hPa. Prognostic variables are vorticity, divergence, logarithm of surface pressure, temperature, specific humidity and water vapour. Apart from positive definite quantities, the prognostic variables are represented by spherical harmonics with triangular truncation. Two time slices of 30 years each were modelled, representing the present-day period (1970-1999) and a future period (2060-2089), centred on the time when it is estimated that the CO_2 concentration will have doubled. Surface atmospheric pressure fields and 10-metre wind vectors were extracted at 6-hourly intervals extracted at six-hourly intervals on a Gaussian spatial grid of about 1.1° (giving approximately 125km resolution over the UK) for each time slice and used in STOWASUS-2100. Data for points corresponding to the coastal sites studied were extracted by POL from this dataset.

POL 2D-TS

POL 2D tide-surge models were run in STOWASUS-2100 producing hourly total water level fields (relative to present day mean sea level) from the ECHAM4 meteorological forcing described above. Thirty-year time series of data from a 12km model of the North and Irish Seas and English Channel (NISE) were extracted for use in CDV-2075.

Corrections were applied for mean sea level rise and its effects on tidal levels as follows. The mean (undisturbed) water depth for the two scenarios was taken as present-day and present-day + 35cm, respectively. The latter increment was derived by reference to the Intergovernmental Panel on Climate Change (IPCC) Third Assessment Report (Church *et al*., 2001) as the best estimate for the time of $2\times CO_2$ i.e. 2075. This is the upper limit for the worst case scenario (predicted by averaging different AOGCMs) of global-average sea-level rise for the time when carbon dioxide reaches twice the present day levels, which is estimated to occur in the year 2075. A maximum prediction from looking at the range of individual AOGCMs would be about 50cm. Possible variations in the mean sea level over the model area could occur, due to differential land movement and regional differences in oceanographic effects, but have not been included. These relative differences are possibly of the order of 1mm/year.

Effects of this increase in sea level on the tides were computed by first running the POL CS3 model (as currently used for operational surge forecasts) to compute tidal elevations with present MSL and with MSL raised by 35cm. Hourly differences were then analysed and the major tidal harmonics of the difference determined. These harmonics and the assumed MSL change were then used to compute, for each CDV-2075 location, hourly corrections, which were added to water levels from the STOWASUS "$2\times CO_2$"

scenario. The result was 30-year time series of hourly water levels at the 5 CDV-2075 locations (Figure 3), together with corresponding time series from the "control" run.

Discussion of sea level effects

Of course, these sea level time series are approximations to what may happen towards the end of this century and are subject to considerable uncertainty in all elements as discussed above. Also some effects are at present neglected; in particular those due to land movements caused e.g. by glacial isostatic adjustment of the Earth following the last ice age, which may be of the order of 1mm/year.

However, the results are broadly in line with current DEFRA advice on effects of climate change on sea levels as given in Section 4.6 of DEFRA (2000). This is based on trends in MSL from the 1990 report of IPCC combined with assumed rates of large-scale land movement in England and Wales from previous research (Shennan 1989). The average predicted sea level rise was 4.5mm/yr over the next 40 to 50 years and, including land movements, the regional rates of relative sea level rise were:

- 6mm/yr for the E coast south of Flamborough Head and the S coast;
- 5mm/yr for the South West and Wales; and
- 4mm/yr for the North West and the E coast north of Flamborough Head.

So 5mm/yr for 75 years gives a MSL rise of 37.5cm which is close to the assumption used.

Furthermore, the 2001 IPCC estimates of global absolute MSL rise are lower than the 1990 values, partly compensating for the effects of land movements. Also, DEFRA advice does not account for effects of MSL rise on tidal dynamics nor possible effects of changes in storminess.

Local sea level variations

A further assumption in using the sea level data described above is that it is uniform within the areas used to compute wave transformations. This of course is incorrect: in fact sea level will vary locally depending on site and time. Some assessment of sea level variability within these areas could be derived by running local (O(1km) grid) tide-surge models for the two scenarios, analysing results, and using in the wave transformation calculations the space and time-dependent water level fields. This is feasible but was not possible within the constraints of the present project.

HINDWAVE

HINDWAVE (Hawkes, 1987) is a practical and well-established method of determining the wave spectrum at a point, given a time series of wind speeds at that point. The method assumes that the wind speed is constant over the whole fetch length at any one time, but varies in time. Fetch lengths are specified at angular intervals of 10° about the point of interest. The depth (often simply specified as deep water) is assumed constant along the fetch. Wind speeds over the previous 36 hours are used to construct the wave spectrum at the specified point. The output is a significant wave height, period and direction at each time-step, plus the input wind speed and direction. Since only local wind information is used to derive the offshore waves, the results do not include the effects of swell, which are likely to be significant particularly on the south and west coasts of England and Wales. Swell may contribute to overtopping due to its long period, despite its relatively low wave height: however storm waves only are considered here.

JOIN-SEA

JOIN-SEA is a rigorous but practical approach to calculating the joint probability of waves and water levels (HR Wallingford, 1998, Owen et al., 1997). Joint probability refers to the chance of two or more partially related variables occurring simultaneously. Damage to sea defences often occurs when high water levels and high wave heights occur simultaneously. The joint probability of water levels and wave heights is therefore important in determining the design of a structure. JOIN-SEA analyses the extremes and dependencies in the synchronous time series. It then uses a Monte-Carlo simulation technique to generate thousands of years worth of wave and water level data. The simulations for CDV2075 were based on the values of wave height and water level at each high water in the 30-year synchronous time series of wave heights and water levels from the POL 2D-TS and HINDWAVE models. The outputs of the Monte-Carlo simulations are listed in Section 4.1.

SWAN

SWAN (Simulating Waves Nearshore) is a 3rd-generation (3-G) phase-averaged spectral wave model, specifically designed for modelling shallow water coastal regions (Booij et al., 1999; Ris et al., 1999). SWAN is applicable to shallow water and typically runs on fine grids (resolution 50m-1km) over small areas (a few kilometres square). The model is termed 3-G because it includes explicit redistribution of the wave energy within the wave spectrum, by non-linear wave-wave interactions i.e. it does not assume a prescribed spectral shape. The model does not compute the full exact solution for non-linear interactions but uses the so-called discrete interaction approximation (DIA) developed for the WAM model (Komen et al. 1994). It models the two-dimensional wave frequency-direction energy density spectrum prognostically over a regular spatial grid.

One of the benefits of SWAN is that it produces a 2-D map of wave heights over the whole model area rather than just predictions for a single location as in ray-tracing models. It can be applied on grids ranging from kilometres down to a few metres and on rectangular or curvilinear grids.

The SWAN model is still under development by the Delft University of Technology, funded by the US Office of Naval Research, and the international user community, including POL. For example, SWAN does not include wave-current interaction in the bottom friction term, which is probably important. A very detailed review of the physics of SWAN has been carried out by Dingemans (1998), who recommends further developments which need to be carried out to improve the accuracy of forecasts in the coastal zone, especially if these are to be applied in morphodynamic models. He identifies some terms as not being correctly derived, including the depth-limited breaking. This model is likely to provide the basis for the next generation of shallow water wave models. SWAN version 40.01 was used for this project.

Some results of the experience of using SWAN in the JERICHO project were applied here (Wolf *et al*., 2000). At Holderness there were sufficient data to test and validate the model. SWAN was run at three-hourly intervals over a two-day storm event in January 1995. The results showed that varying the bottom friction formulation had a significant effect on the results, with the Madsen formulation producing better results than the (default) JONSWAP formulation. Triad interactions (see below) were somewhat suspect and switched off. To use SWAN for extreme value analysis it is possible to transform the statistical extreme events, but interpretation of the resulting transformed event is more problematic. The return period of the response will not correspond to that of the boundary forcing. Specific technical aspects of SWAN are discussed below.

Nonlinear interactions

These are what make the model "3rd-generation". The quadratic interactions are as developed for WAM in deep water, converted to wave-number scaling and approximated using the Discrete Interaction Approximation (DIA) which only considers the first set of interactions. SWAN also has the option to include triad interactions, which become important in very shallow water (when the Ursell number exceeds 0.1). These were switched off for the runs presented here. This should make little difference except very near shore, inshore of the output points selected.

Wind input and white-capping dissipation

Two options are included: Komen and Janssen with corresponding white-capping terms. The default Komen term was used.

Bottom Friction

In SWAN there are three possible formulations for the bottom friction term. The user may choose some parameters or the default values can be used. These parameters are, in theory, influenced by the sediment grain size and the presence of ripples on the seabed and so may reasonably be expected to be different for different implementations of the model.

The default formulation is the empirical model of JONSWAP (Hasselmann et al., 1973). Other options are the drag law model of Collins (1972) and the eddy-viscosity model of Madsen et al. (1988). All three formulations may be expressed in the following form:

$$S(\sigma,\theta) = -C_{bottom} \frac{\sigma^2}{g^2 \sinh^2(kd)} E(\sigma,\theta)$$

where $S(\sigma,\theta)$ is the bottom friction source term and $E(\sigma,\theta)$ is the wave energy spectrum. C_{bottom} is the bottom friction coefficient, which depends in some functional way on the bottom orbital motion. It is the formulation of this coefficient which varies between the different models, and for which the user can change the inherent empirical constants.

The Madsen bottom friction formulation was used with the default Nikuradse length scale (k_N=0.05m). This was found to be preferable in the JERICHO project although it is possible that an even higher value of k_N might be necessary.

Shallow water wave breaking

In very shallow water the waves would increase in wave height due to shoaling was it not for an extra term which is introduced for the depth-limited wave breaking. The default settings for this parameter were used. This term is only important in less than about 10m of water depth.

SWAN implementation

Discrete, extreme events were modelled in this project, so the model was run in time-independent mode. The assumption made when using this mode is that the boundary conditions evolve more slowly than the time it takes for the waves to propagate across the grid. This is a reasonable assumption for the cases described here since the model domains extend to only a maximum of 20km off-shore. The most energetic waves (8-10s period) cross the grid in about half an hour and even very short (2s) waves take less than 2 hours.

The offshore boundary of the SWAN model grid was positioned so as to intersect the centre of the POL storm-surge model's grid point at each of the five sites. SWAN models the full 2D wave spectrum, but HINDWAVE produces information for only the wave parameters of significant wave height and mean period. It was, therefore, necessary to make some assumption about spectral shape before SWAN could use the information. When looking at the water level at mean sea level, the SWAN offshore model boundaries are undoubtedly in sufficiently shallow water that a JONSWAP spectrum would be inaccurate. However, for the extreme events studied here, the water levels are mostly sufficiently high, and the waves sufficiently low that a JONSWAP spectrum is a reasonable assumption. The exception to this is the Lincolnshire model where the offshore depth is only about 20m even for the extreme events. Techniques exist for scaling the spectra (Bouws et al., 1985), but these would have changed the offshore significant wave-height, so this scaling was not performed. The consequences of this decision are discussed further in the Results section of this report. The directional spread was assumed to be the same for all cases and set to 31.5^o, which was a typical value for wind-sea conditions.

The bathymetry was obtained from a variety of sources, but for all locations the highest resolution of any of the depth data was about 1km. Interpolating the data onto a finer grid is worthwhile because, for any time-independent finite difference scheme with variables x and y, as the grid size, Δx and Δy, decrease, the solution more closely approximates the solution to the continuous equations.

The model resolution used for each case described in Table 2 was constrained by the computational limits imposed by the available computer resources (256-384MB Unix workstations).

A range of combined wave and water level events, were chosen from the JOINSEA output for each of the return periods (20, 50 and 200 years). In each case a steady-state solution was obtained over the whole model area. Wave height, period and direction, as well as water depth were output along a single line at 100 or 200m intervals across the model and approximately perpendicular to the shoreline. The significant wave height, peak period and mean wave directions were extracted from the full inshore directional spectra.

COSMOS

COSMOS is a coastal profile model of nearshore hydrodynamics and sediment transport that includes linear wave transformation by refraction, shoaling, Doppler shifting, bottom friction, depth-limited wave breaking and set-up from the radiation stress gradient. The model also includes a transition zone, representing the delay between waves breaking and the start of energy dissipation. In addition the model also includes driving forces for longshore wave-induced currents from the spatial distribution of wave energy dissipation, longshore currents from pressure-driven tidal forces and wave-induced forces, a three-layer model for cross-shore undertow, cross-shore and longshore sediment transport rates using Baillard's energetics approach and seabed level changes due to cross-shore sediment transport.

The model assumes a straight coastline with parallel depth contours. Here only the wave shoaling and breaking modules are used to transform the waves into and through the surfzone, up to the structure. Results for wave height, setup and water depth are output along a single cross-shore profile. COSMOS is quick to run and relatively simple to setup and operate. A detailed model description can be found in Southgate and Nairn, 1993.

COSMOS was run assuming that the waves were shore-normal, although oblique-incidence waves can be included in the model. The bathymetry used by COSMOS was a simplification of the actual bathymetry. Two straight lines were fitted to the last 2km of the SWAN output line. The offshore line had a lower gradient than the inshore line. The structure was placed where the inshore line crossed the toe-depth of the structure. In cases of coastal steepening, the inshore point of the inshore line was held in the same position, while its gradient was increased, based on historical trends extrapolated to 2075. This simplification of the bathymetry allowed coastal steepening to be included in the COSMOS and OTT models only.

OTT

OTT is a numerical model of wave run-up, overtopping and regeneration (Dodd, 1998). It is based on the one-dimensional nonlinear shallow water equations on a sloping bed, including the effects of bed shear stress. The equations are solved using a shock-capturing upwind finite-volume technique incorporating a Roe-type Riemann solver. No special shoreline-tracking algorithm is required, so that non-contiguous flows can easily be simulated. Therefore this model can be used to simulate the transmission of waves over water surface-piercing obstacles. The model has been validated against random wave experiments, for smooth slopes up to 1:1. The model is valid for shallow water only (e.g. water depth less than on tenth of the wavelength).

The model generates a time-series of waves at the offshore boundary. A JONSWAP spectrum is used to generate a time-series of random waves, lasting 1000 peak periods. The spectrum is derived from the wave height, period and water depth (including wave setup) output by COSMOS 60m from the toe of the structure. This distance is roughly one wavelength in front of the structure (calculated by linear theory in shallow water). The small distance allows the waves to steepen (from their original smooth profiles) or even break before reaching the structure. If the waves are generated too far from the structure, they will break and dissipate too much of their energy before reaching the structure. OTT and COSMOS were run with the structure removed (leaving only the dissipative beach) in order to check the dissipation in OTT.

The wave heights at the toe depth of the structure were compared in COSMOS and OTT and using a simple depth-limited formula and were found to be similar, indicating that OTT was started from a reasonable distance offshore.

The output from OTT is time series of surface elevation and horizontal velocity at the toe, centre and crest of the breakwater. There are analysed to produce statistics for root-mean-square velocity and overtopping discharge.

References

Bengtsson L, Bozet M and M Esch, 1995. Hurricane-type vortices in a general circulation model. Tellus 47A: 175-196.

Booij, N., R.C. Ris and L.H. Holthuijsen 1999. A third-generation wave model for coastal regions, Part I, Model description and Validation. J.Geophys. Res. 104, C4, 7649-7666.

Bouws, E., Günther, H., Rosenthal, W. and Vincent, C.L. 1985 Similarity of the wind wave spectrum in finite depth water 1. Spectral form. Journal of Geophysical Research, 90, C1, 975-986.

Church, J.A., Gregory, J.M., Huybrechts, P., Kuhn, M., Lambeck, K., Nhuan, M.T., Qin, D. and Woodworth, P.L., 2001. Changes in sea level. In: *Climate Change 2001: the scientific basis. Contribution of Working Group I to the Third Assessment Report of the Intergovernmental Panel on Climate Change.* Cambridge University Press, Cambridge, UK and New York, NY, USA. 881pp.

Collins, J.I., 1972: Prediction of shallow water spectra, *J. Geophys. Res.*, **77**, No. 15, 2693-2707

Dingemans, M.W. 1998 A review of the physical formulations in SWAN, Delft Hydraulics Report H3306, 69pp.

DEFRA, 2000. Flood and coastal defence project appraisal guidance: economic appraisal (FCDPAG3), 104pp, PB4650.

Dodd, N., 1998. Numerical model of wave run-up, overtopping and regeneration. J. Waterway, Port, Coastal and Ocean Engineering, 124(2): 73–81.

Hasselmann, K., T.P. Barnett, E. Bouws, H. Carlson, D.E. Cartwright, K. Enke, J.A. Ewing, H. Gienapp, D.E. Hasselmann, P. Kruseman, A. Meerburg, P. Müller, D.J. Olbers, K. Richter, W. Sell and H. Walden 1973: Measurements of wind-wave growth and swell decay during the Joint North Sea Wave Project (JONSWAP), Dtsch. Hydrogr. Z. Suppl., 12, A8

Hawkes, P.J., 1987. A wave hindcasting model. In 'Advances in underwater technology, ocean science and offshore engineering, Volume 12: Modelling the offshore environment', Society for Underwater Technology, April 1987.

HR Wallingford, 1998. The joint probability of waves and water levels: JOIN-SEA, a rigorous but practical approach. HR Report SR 537, 244pp.

Komen, G.J., Cavaleri, L., Donelan, M., Hasselmann, K., Hasselmann, S. & Janssen, P.A.E.M. 1994 Dynamics and modelling of ocean waves. Cambridge University Press. 532pp.

Madsen, O.S., Poon, Y.-K. and Graber, H.C., 1988. Spectral wave attenuation by bottom friction: theory. Proceedings, 21st International Conference on Coastal Engineering, ASCE, New York, pp 492–504.

May, W. and Roeckner, E. 2001 A time-slice experiment with the ECHAM4 AGCM at high resolution: the impact of horizontal resolution on annual mean climate change. Climate Dynamics, (in press).

Owen, M.W., Hawkes, P.J., Tawn, J.A. and Bortot, P., 1997. The joint probability of waves and water levels: A rigorous but practical new approach. MAFF Conference of River and Coastal Engineers, Keele, July 1997.

Ris, R.C., Holthuijsen, L.H. and N. Booij, 1999. A third-generation wave model for coastal regions, part 2: verification. J. Geophys. Res., 104(C4): 7667–7681.

Southgate, H.N. and R.B. Nairn, 1993. Deterministic profile modelling of nearshore processes. Part 1. Waves and Currents. Coastal Engineering 19: 27–56.

Wolf, J., Hargreaves, J.C. & Flather, R.A. 2000 Shallow water wave modelling for the JERICHO Project. POL Report No. 57

Appendix 2

SWAN Modelling

Appendix 2 SWAN Modelling

Area Modelling

The offshore boundary for the SWAN area models was the POL 2D-TS model grid point. The model resolution used for each site is given in Table 2.1 and was constrained by the computational limits imposed by the available computer resources (256-384MB Unix workstations). The input conditions for the model runs that were performed with SWAN are recorded in Tables 2.2 to 2.6. For each of the return periods (20, 50 and 200 years), a range of combined wave and water level events, were chosen from the JOINSEA output. Some of the results are displayed in Figures 2.1 to 2.7. The bottom subplot of each figure shows the water level over the computational grid for the particular run. The central plot shows the significant wave-height and mean wave direction. The top plot shows the rate at which energy is lost from the wave-field by the combined effects of bottom friction and depth-induced breaking. It is this top subplot which most clearly illustrates the differences between the different runs. Figures 2.3 to 2.7 show the results for high wave events run through the models (two bigger events were later run for Lincolnshire – see Table 2.2). These events were the 200-year return events for a future raised water level with either 4 or 5 metre significant wave-height input at the SWAN boundary.

A comparison of Figures 2.2 and 2.4 highlights the difference between low and high wave-height events for the same return period (future scenario, 200y event). It is clear that there is much more wave energy dissipated by the seabed throughout the whole computational domain for the event with the higher wave height imposed at the boundary. For the same return period lower wave-height events coincide with higher water, but the actual effect of this change in water level (on dissipation by friction) is small compared to the change in wave-height. A comparison of Figures 2.1 and 2.2, which show results from the 200-year low wave-height events for present day and future water levels, shows that the predicted future rise in water level alone has a very small effect on the waves outside the surfzone.

The energy dissipation rate is highly spatially variable, even within these small model domains, and depends to a large extent on the bathymetry. This illustrates the importance of obtaining accurate bathymetry around the whole area for accurate modelling of a particular region. This is not of great concern here since the main interest lies in theoretical application of the model, but it will become very important once these methods are put into practice in "real-life" situations. The destructive effect of the waves on the seabed is dependent on the mobility of the sediment. The thin bands of high dissipation very near-shore and little dissipation offshore (compare Figures 2.5, 2.6, and 2.7 with Figure 2.3 and 2.4) indicate that a relatively large proportion of the offshore wave energy is propagating to very near the coast. If the seabed is mobile in these regions then these areas are likely to be susceptible to effects such as coastal steepening. The high dissipation right at the offshore boundary at Lincolnshire shown in Figure 2.3 occurs in an area where there is a relatively rapid decrease in depth, as shown by Figure 2.8.

SWAN Results along a Profile

The main output supplied from the SWAN runs consisted of cross-shore sections with wave parameters output along a single line, approximately perpendicular to the shoreline. Significant wave height, peak period and mean wave directions were extracted from the full inshore directional spectra at 100 or 200m intervals across the section. The locations of the chosen sections are drawn on the water level subplots in Figures 2.1-2.7.

Results from the cross-shore sections are shown in Figures 2.8-2.13, for a range of events. Again it is clear that, as far as the waves are concerned, changes in water level between different events have little bearing on the energy that is transported near-shore compared with the different wave heights input at the boundary. It is also clear that the bathymetry has a high bearing upon the near-shore wave height. Possible bathymetric erosion due to changes in climatology (e.g. increased storminess) may therefore be more important for the development of the subtidal bathymetry than the effect of rising sea levels per se.

The HR model HINDWAVE is tuned to produce accurate results at about 20km offshore, and there was concern that the same technique be applied to all locations, which meant placing SWAN's offshore boundary at the centre of the storm-surge model's grid. The problem with the Lincolnshire area is that it is not typical of much of the UK coastline, being shallow for many kilometres offshore. Moreover, there is a shoal just inshore of the model boundary, and the dissipation rate peaks at the top of the shoal.

In order to demonstrate the possible error involved in the approach taken, another model run was performed, but this time using a model which extended to 40km offshore. Results from the two runs are shown together in Figure 2.14. The run with the boundary further offshore also exhibits dissipation over the shoal, situated at just over 17km offshore. The dissipation rate over the shoal is lower for the model starting 40km offshore, but the wave height offshore of this was lower due to dissipation between the shoal and the offshore boundary. It is clear that taking the offshore boundary further offshore reduces the inshore wave height until the waves become depth-limited close to the shore. The wave period is reduced by non-linear interactions during the shoaling, so is lower at all locations for the model starting further offshore.

What is not clear is which result is the more accurate. The only way to calculate the correct offshore boundary position for this area would be to compare HINDWAVE results for actual events with wave data at a number of locations in this region, using, for example, satellite altimeter wave heights. Then the appropriate location for the SWAN boundary could be readily estimated.

Figure 2.15 is included to show some of the benefits in using the SWAN model. In this case the largest storm event observed at Holderness (Wolf, 1998) has been modelled. A comparison is made of the predicted wave height with the observations at stations N1, N2 and N3. The triads, depth-limited breaking and bottom friction have been switched off in turn in SWAN and experiments carried out using different values for the bottom friction. This shows that bottom friction is the controlling dissipation process over most of the near-shore region, for depths greater than 10m. Within the last 1km depth-limited breaking does become significant.

SWAN output to COSMOS

Wave height, period and direction, as well as water depth were output along a single line at 100 or 200m intervals across the model and approximately perpendicular to the shoreline. The significant wave height, peak period and mean wave directions were extracted from the full inshore directional spectra.

References

Wolf, J. 1998 Waves at Holderness: results from in-situ measurements, pp. 387-398 in Proceedings of Oceanology'98, Brighton, UK, March 1998.

Table 2.1 SWAN model setup configurations. Nf is the number of frequency bins and Nθ the number of directional bins in the wave spectrum

Location	Model resolution		Size of computational domain			
	Δx(m)	Δy(m)	Nx	Ny	Nf	Nθ
Lincolnshire	200	200	135	266	25	36
Fylde	100	100	203	421	25	36
Swansea Bay	100	100	219	155	25	48
Lyme Bay	200	200	340	129	25	36
Dungeness	200	200	266	145	25	48

Table 2.2 SWAN input conditions for Lincolnshire. Hs and Tp are the significant waveheight and peak period of the JONSWAP spectrum input at the model boundary; WL is water level above mean sea level; and the directions are directions the wind or waves are coming from, clockwise from North

Lincolnshire	Present Day					
Return period (years)	Hs (m)	Tp (s)	Wave direction (^{o})	Water level (m)	Wind speed (ms)	Wind direction (^{o})
20	2	6.9	60	3.66	9	60
	3	8.0		3.43	13	
	4	9.2		3.11	16	
	5	10.3		2.74	20	
	5.4	10.6		2.36	22	
	5.8	11.0		1.9	23	
50	2	6.9		3.84	9	
	3	8.0		3.53	13	
	4	9.2		3.25	16	
	5	10.3		2.99	20	
	5.4	10.6		2.76	22	
	5.8	11.0		2.53	23	
200	2	6.9		4.05	9	
	3	8.0		3.72	13	
	4	9.2		3.44	16	
	5	10.3		3.21	20	
	5.4	10.6		3.12	22	
	5.8	11.0		3.03	23	
Lincolnshire	Future					
20	2	6.9	60	3.99	9	60
	3	8.0		3.77	13	
	4	9.2		3.5	16	
	5	10.3		2.95	20	
	3.5	8.59		3.64	15	
	4.5	9.74		3.23	18	
50	2	6.9		4.15	9	
	3	8.0		3.9	13	
	4	9.2		3.63	16	
	5	10.3		3.28	20	
	3.5	8.59		3.77	15	
	4.5	9.79		3.46	18	
200	2	6.9		4.32	9	
	3	8.0		4.17	13	
	4	9.2		3.84	16	
	5	10.3		3.51	20	
	3.5	8.59		3.99	15	
	4.5	9.74		3.68	18	

Table 2.3 SWAN input conditions for Dungeness to Rye

Dungeness	**Present Day**					
Return period (years)	**Hs (m)**	**Tp (s)**	**Wave direction (^{o})**	**Water level (m)**	**Wind speed (ms)**	**Wind direction (^{o})**
20	1	4.4	236	4.37		240
	2	6.2		4.24		
	3	7.6		4.05		
	4	8.7		3.85		
50	1	4.4		4.5		
	2	6.2		4.42		
	3	7.6		4.23		
	4	8.7		4		
200	1	4.4		4.7		
	2	6.2		4.58		
	3	7.6		4.45		
	4	8.7		4.26		
Dungeness	**Future**					
20	1	4.4	236	4.74		240
	2	6.2		4.65		
	3	7.6		4.5		
	4	8.7		4.28		
50	1	4.4		4.89		
	2	6.2		4.83		
	3	7.6		4.64		
	4	8.7		4.42		
200	1	4.4		5.2		
	2	6.2		5.12		
	3	7.6		4.87		
	4	8.7		4.68		

Table 2.4 SWAN input conditions for Lyme Bay

Lyme Bay	Present Day					
Return period (years)	**Hs (m)**	**Tp (s)**	**Wave direction (^{o})**	**Water level (m)**	**Wind speed (ms)**	**Wind direction (^{o})**
20	1	4.4	228	2.74		240
	2	6.2		2.65		
	3	7.6		2.5		
	4	8.7		2.21		
50	1	4.4		2.93		
	2	6.2		2.82		
	3	7.6		2.68		
	4	8.7		2.43		
200	1	4.4		3.29		
	2	6.2		3.15		
	3	7.6		3.06		
	4	8.7		2.74		
Lyme Bay	**Future**					
20	1	4.4	228	3.01		240
	2	6.2		2.92		
	3	7.6		2.77		
	4	8.7		2.52		
50	1	4.4		3.23		
	2	6.2		3.13		
	3	7.6		2.92		
	4	8.7		2.68		
200	1	4.4		3.61		
	2	6.2		3.52		
	3	7.6		3.18		
	4	8.7		2.98		

Table 2.5 SWAN input conditions for Swansea Bay

Swansea Bay	**Present Day**					
Return period (years)	**Hs (m)**	**Tp (s)**	**Wave direction (^{o})**	**Water level (m)**	**Wind speed (ms)**	**Wind direction (^{o})**
20	2	6.5	243	5.32	12	240
	3	8.1		5.19	17	
	4	9.2		5.06	20	
	5	10.4		4.68	24	
50	2	6.5		5.43	12	
	3	8.1		5.3	17	
	4	9.2		5.16	20	
	5	10.4		4.85	24	
200	2	6.5		5.64	12	
	3	8.1		5.5	17	
	4	9.2		5.3	20	
	5	10.4		5.11	24	
Swansea Bay	**Future**					
20	2	6.5	243	5.72	12	240
	3	8.1		5.6	17	
	4	9.2		5.44	20	
	5	10.4		4.94	24	
50	2	6.5		5.83	12	
	3	8.1		5.73	17	
	4	9.2		5.55	20	
	5	10.4		5.18	24	
200	2	6.5		5.96	12	
	3	8.1		5.93	17	
	4	9.2		5.73	20	
	5	10.4		5.41	24	

Table 2.6 SWAN input conditions for Fylde

Fylde	**Present Day**					
Return period (years)	**Hs (m)**	**Tp (s)**	**Wave direction (^{o})**	**Water level (m)**	**Wind speed (ms)**	**Wind direction (^{o})**
20	1	4.1	250	5.3	7	240
	2	5.9		5.17	12	
	3	7.2		4.81	17	
	4	8.3		4.37	22	
50	1	4.1		5.5	7	
	2	5.9		5.43	12	
	3	7.2		5.04	17	
	4	8.3		4.52	22	
200	1	4.1		5.84	7	
	2	5.9		5.76	12	
	3	7.2		5.38	17	
	4	8.3		4.89	22	
Blackpool	**Future**					
20	1	4.1	250	5.68	7	240
	2	5.9		5.57	12	
	3	7.2		5.31	17	
	4	8.3		4.85	22	
50	1	4.1		5.92	7	
	2	5.9		5.79	12	
	3	7.2		5.53	17	
	4	8.3		5.01	22	
200	1	4.1		6.45	7	
	2	5.9		6.31	12	
	3	7.2		5.85	17	
	4	8.3		5.33	22	

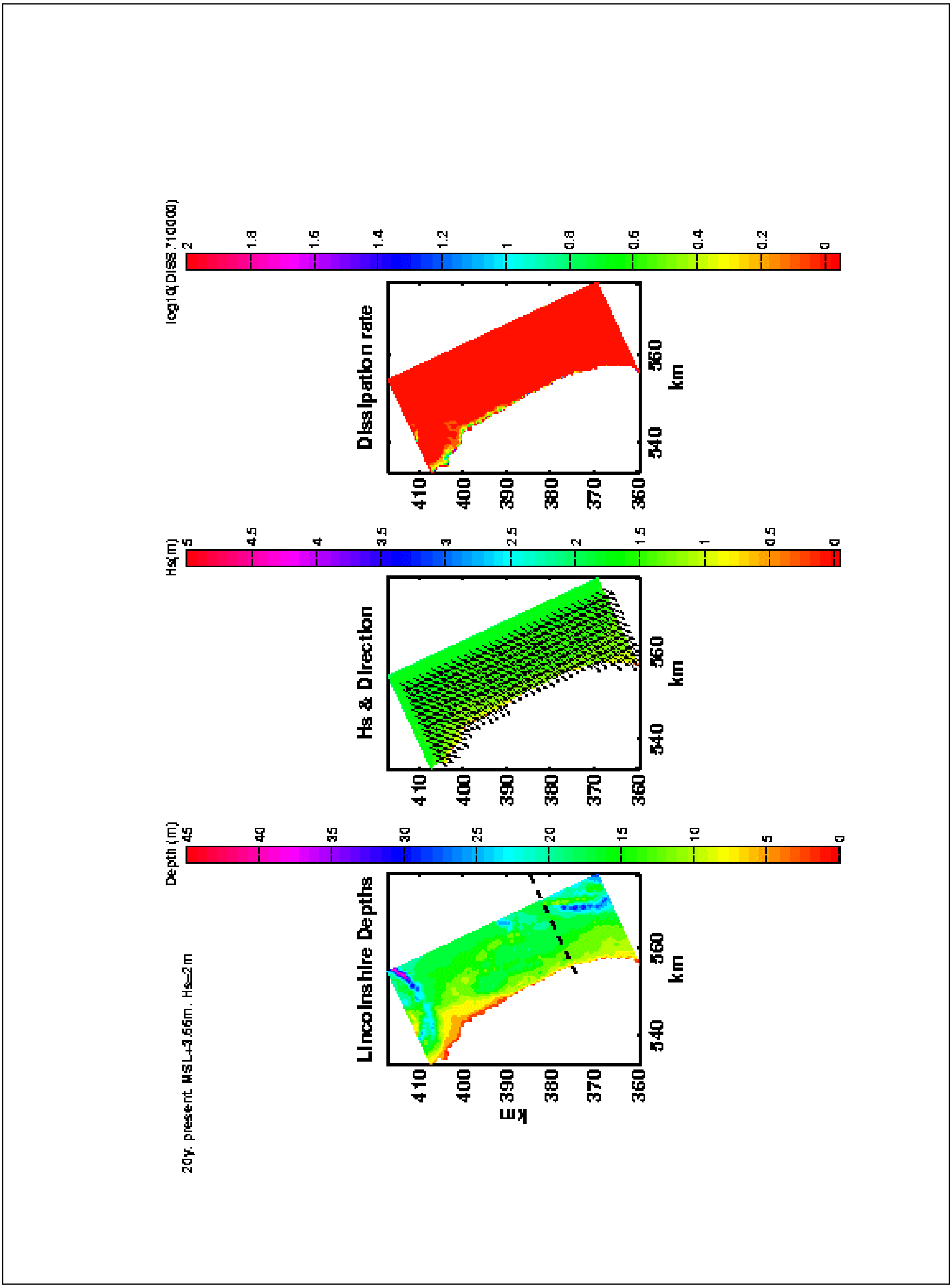

Figure 2.1 The smallest wave event at Lincolnshire: the present day 20 year return period event, with offshore wave height of 2m and water level of MSL+3.66m

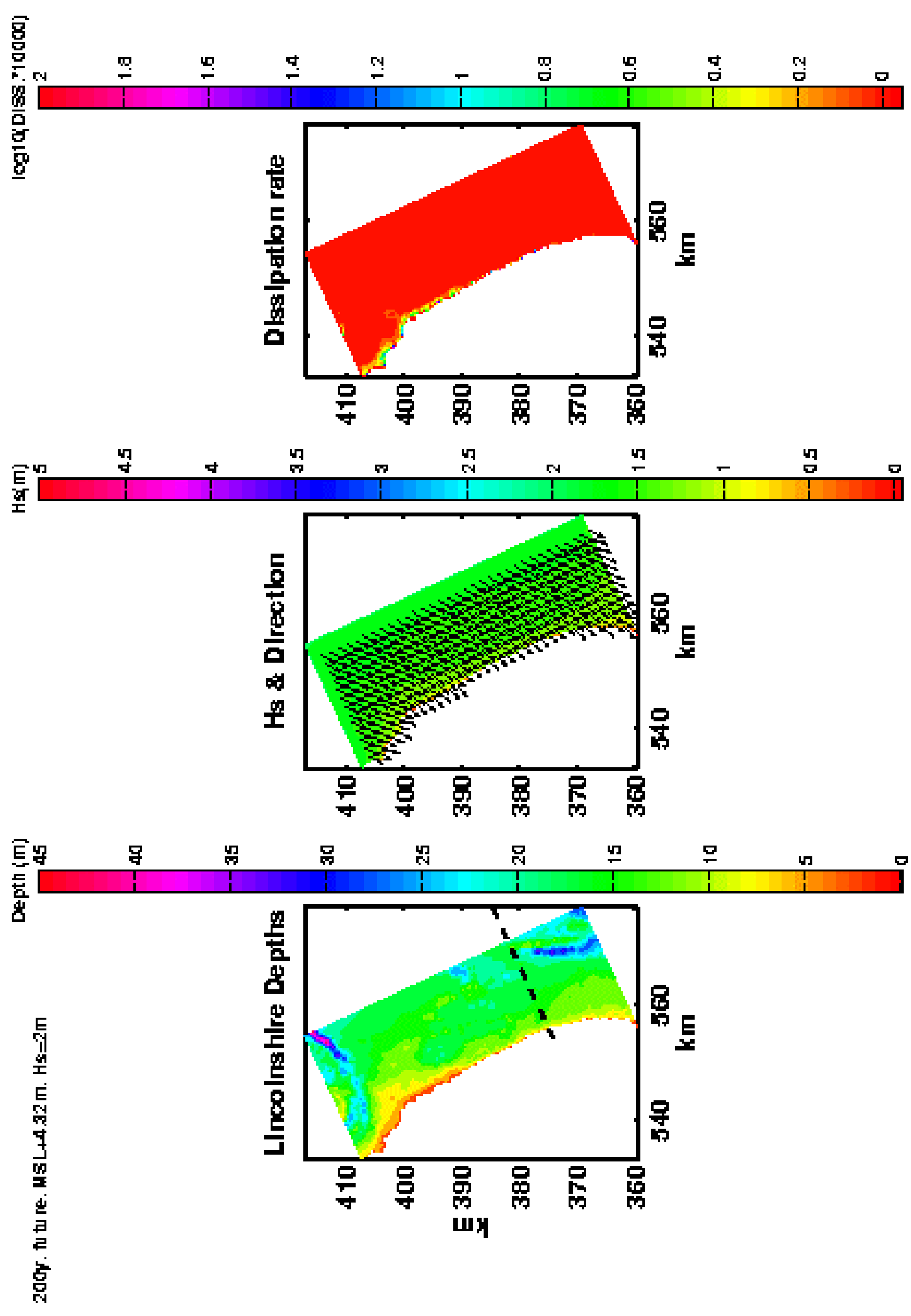

Figure 2.2 **The future 200-year return period event, with offshore wave height of 2m and water level of MSL+4.32**

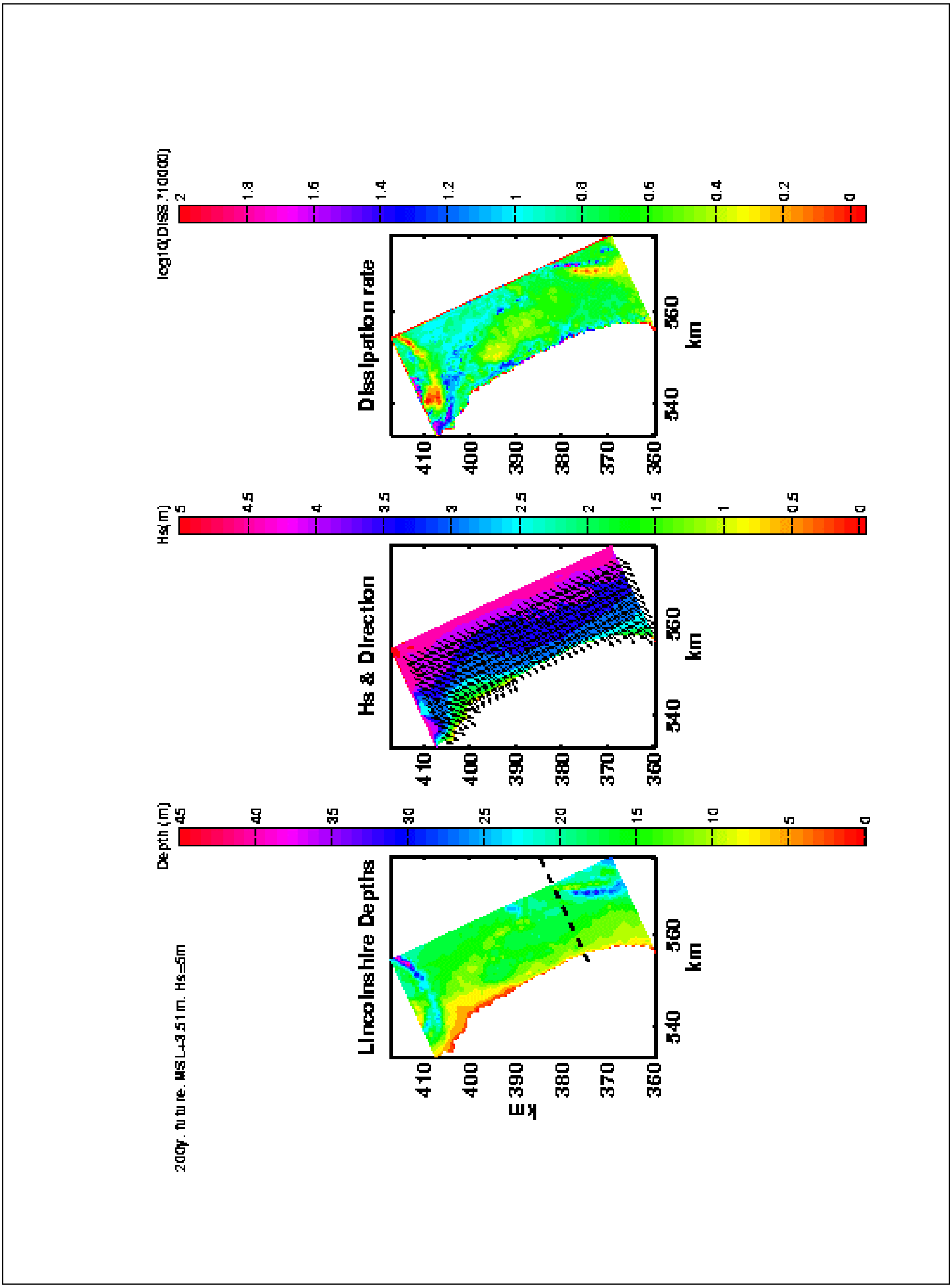

Figure 2.3 The future scenario 200-year return period event, with offshore wave height of 5m, and water level of MSL+3.51m

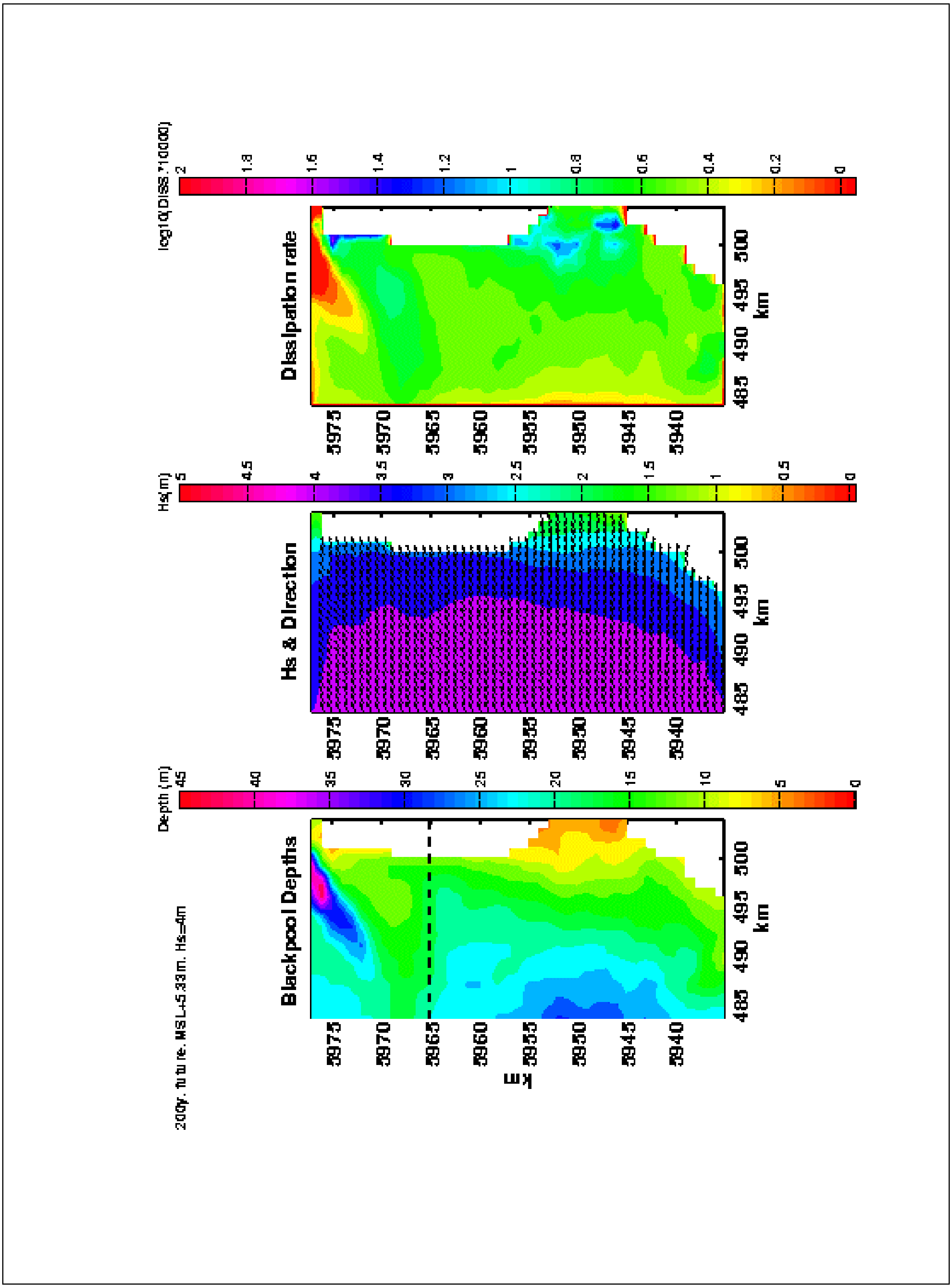

Figure 2.4 The largest event at Blackpool: the future scenario 200-year return period event, with offshore wave height of 4m, and water level of MSL+5.33m

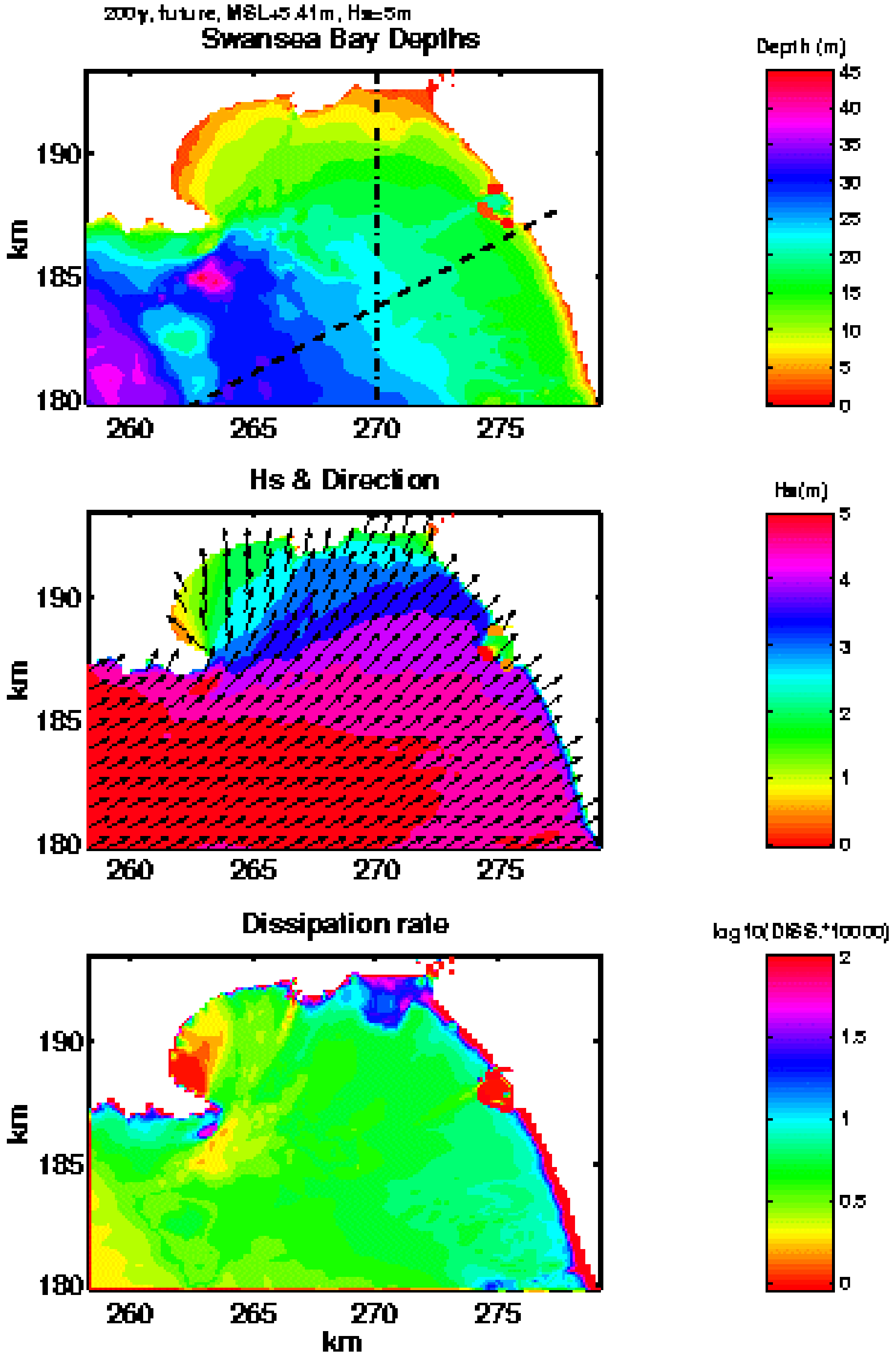

Figure 2.5 The largest event at Swansea: the future scenario 200 year return period event, with offshore wave height of 5m, and water level of MSL+5.41m

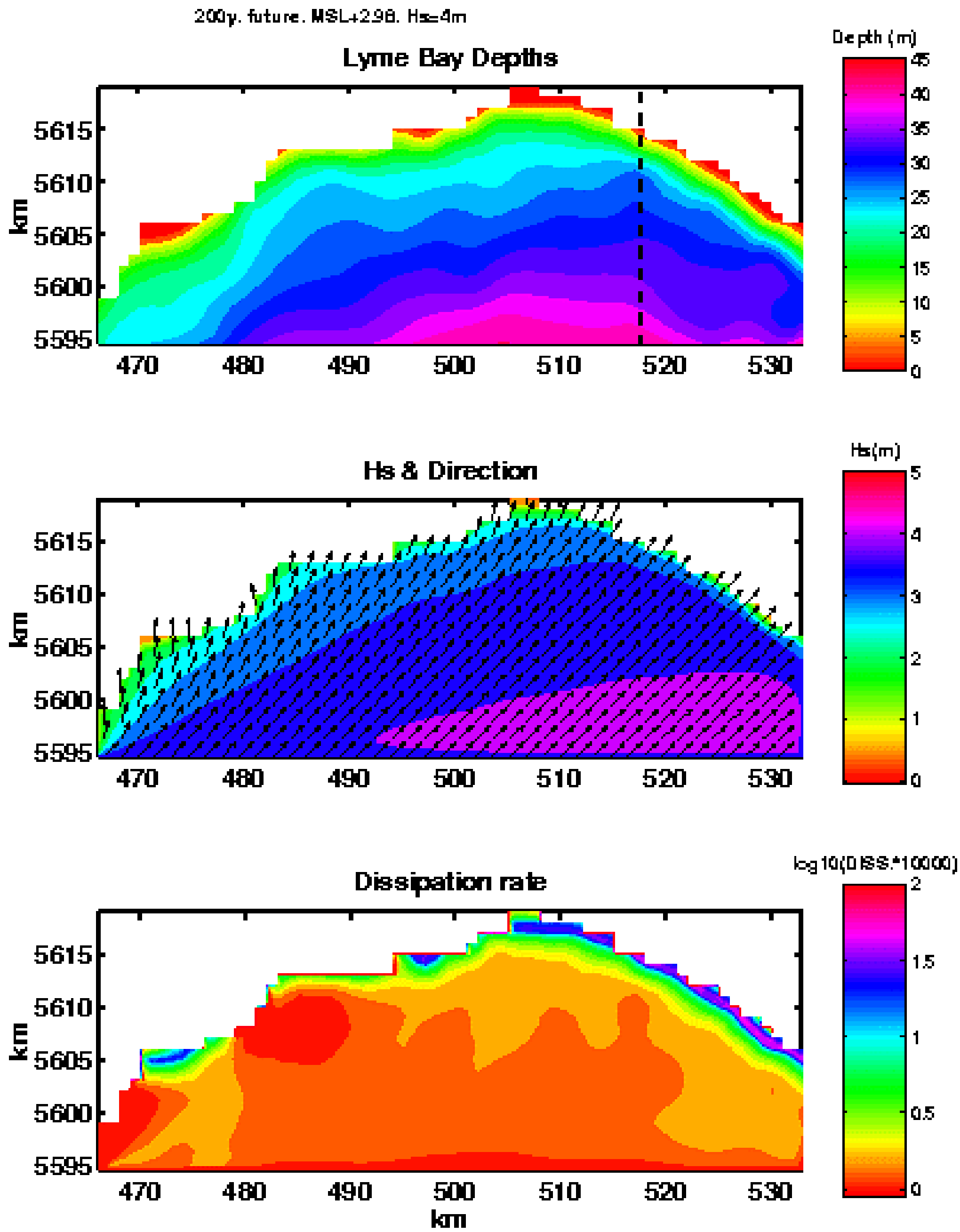

Figure 2.6 The largest event at Lyme Bay: the future scenario 200-year return period event, with offshore wave height of 4m, and water level of MSL+2.98m

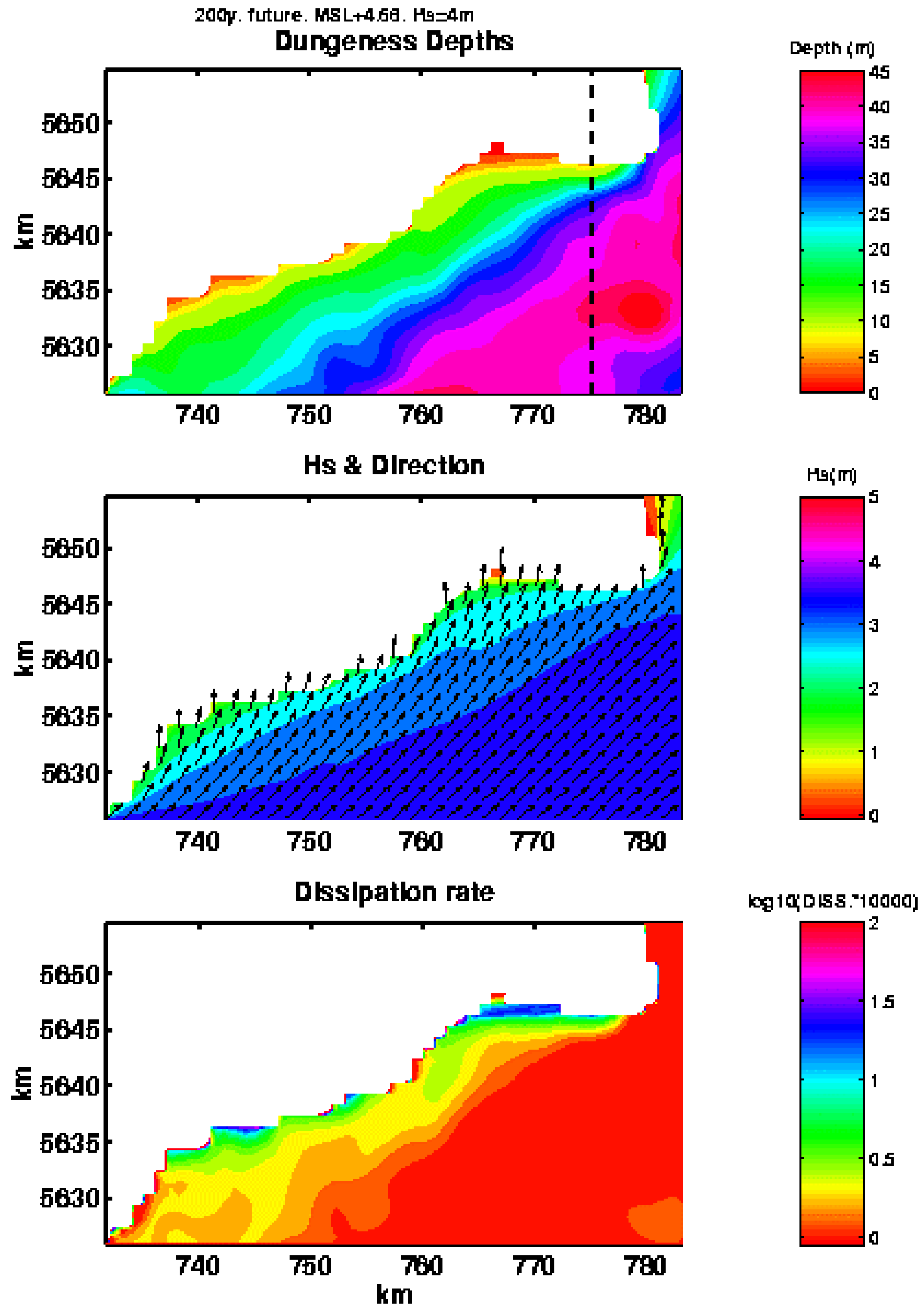

Figure 2.7 The largest wave event at Dungeness: the future scenario 200 year return period event, with offshore wave height of 4m, and water level of MSL+4.68m

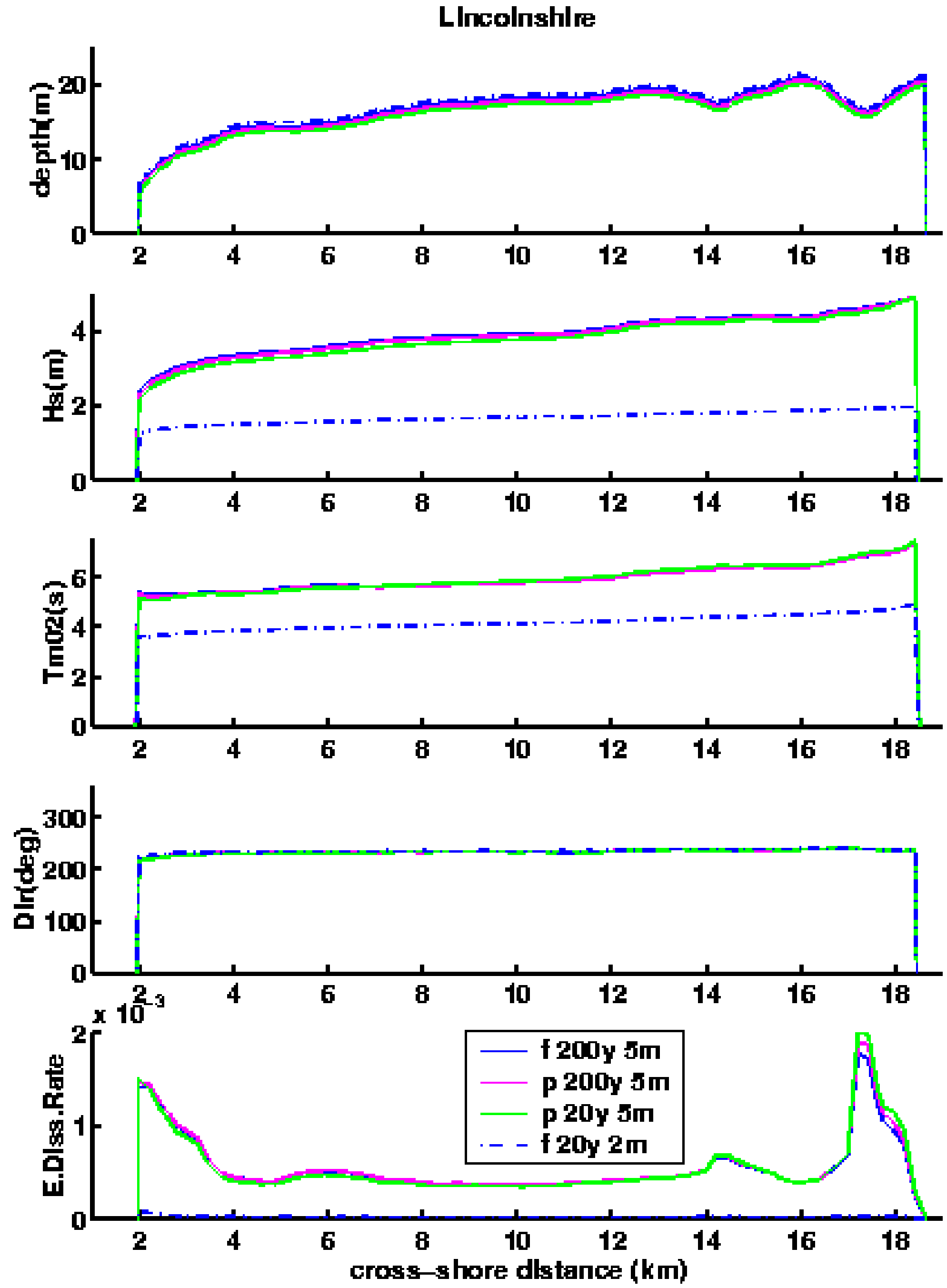

Figure 2.8 cross-shore sections, showing water depth, wave height, mean wave period ($T_{0,2}$), mean wave direction and energy dissipation rate, for Lincolnshire

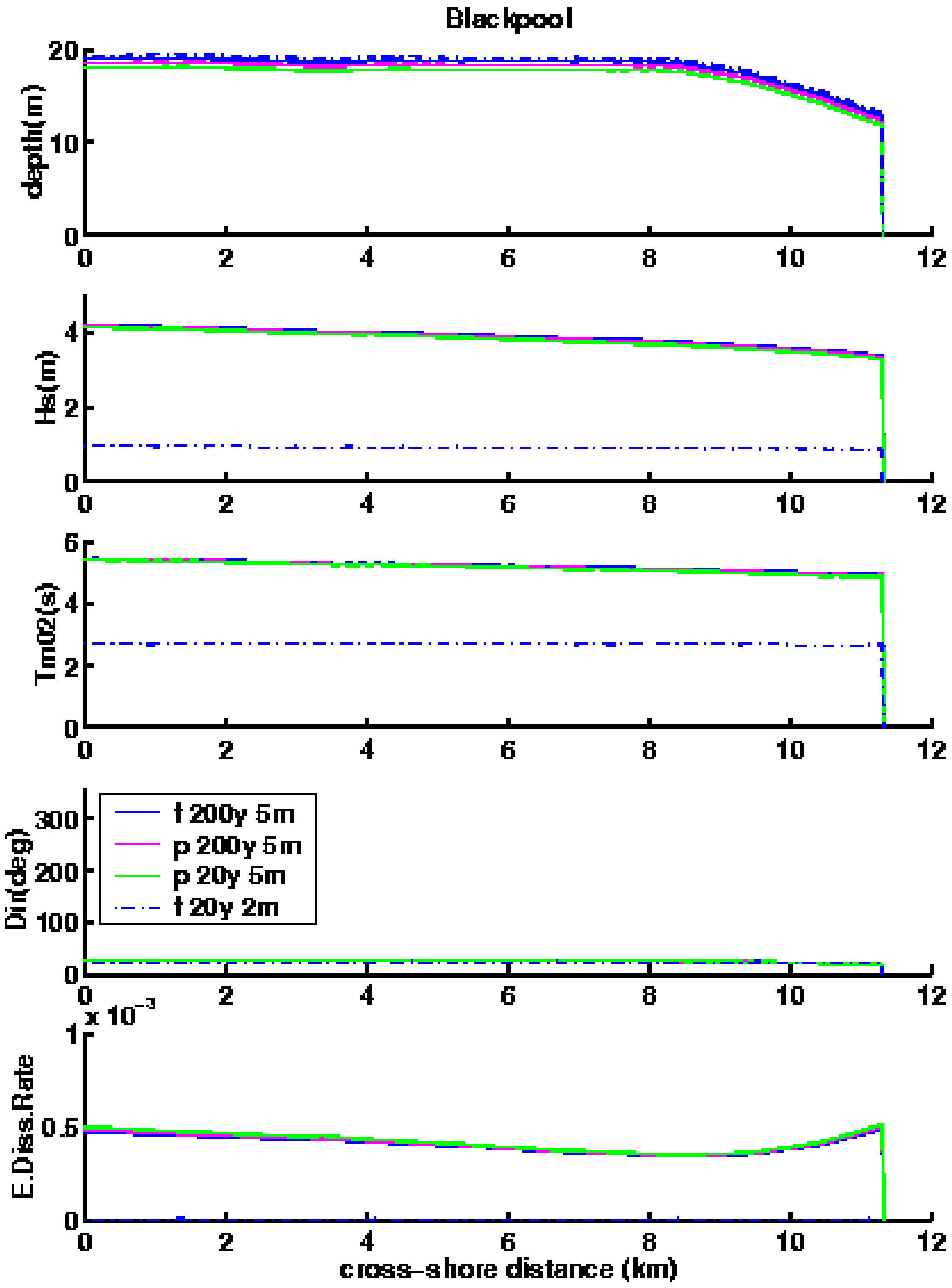

Figure 2.9 **cross-shore sections, showing water depth, wave height, mean wave period ($T_{0,2}$), mean wave direction and energy dissipation rate, for Blackpool (Fylde coast)**

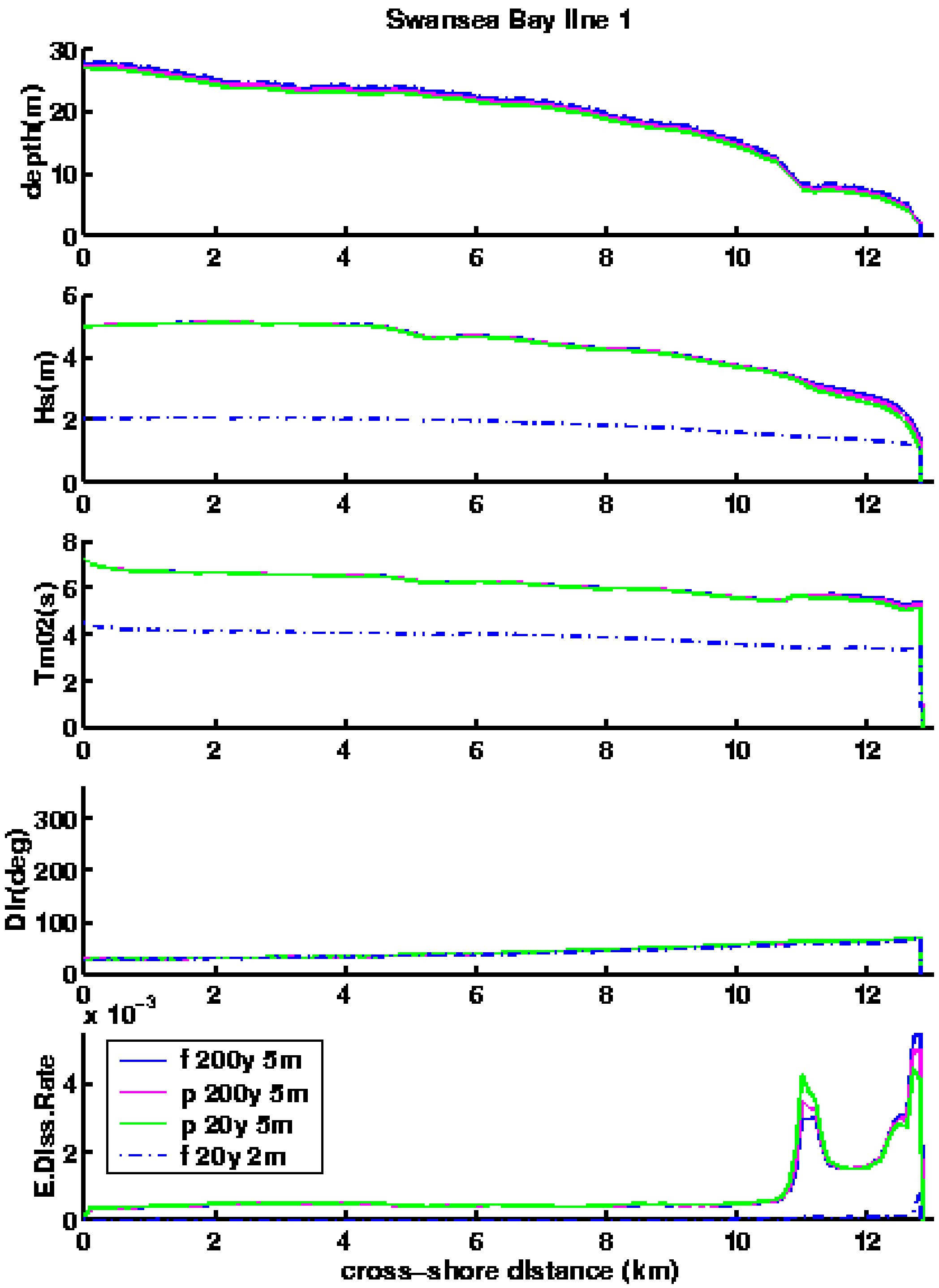

Figure 2.10 cross-shore sections, showing water depth, wave height, mean wave period ($T_{0,2}$), mean wave direction and energy dissipation rate, for Swansea Bay line 1

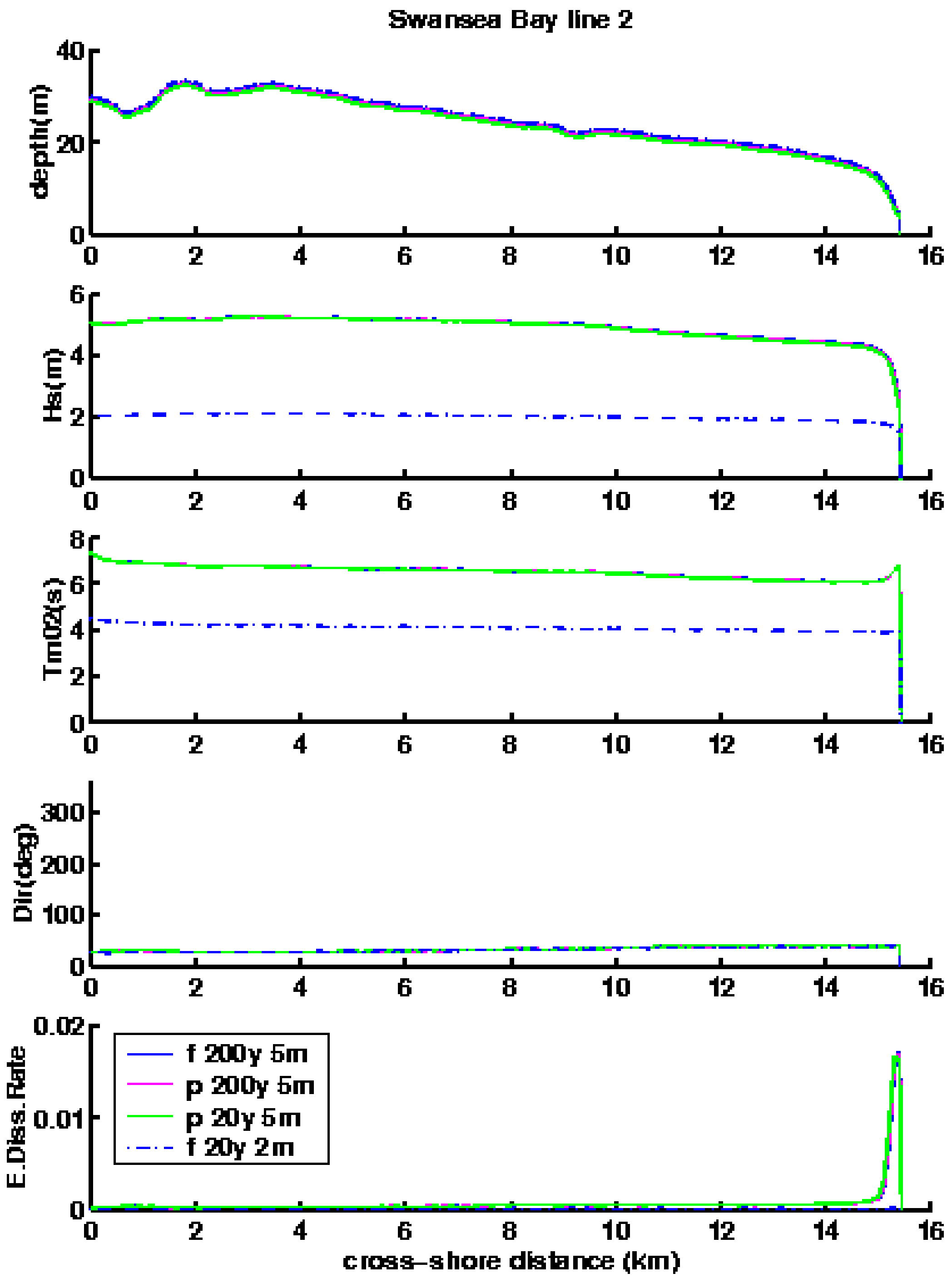

Figure 2.11 Cross-shore sections, showing water depth, wave height, mean wave period ($T_{0,2}$), mean wave direction and energy dissipation rate, for Swansea Bay line 2

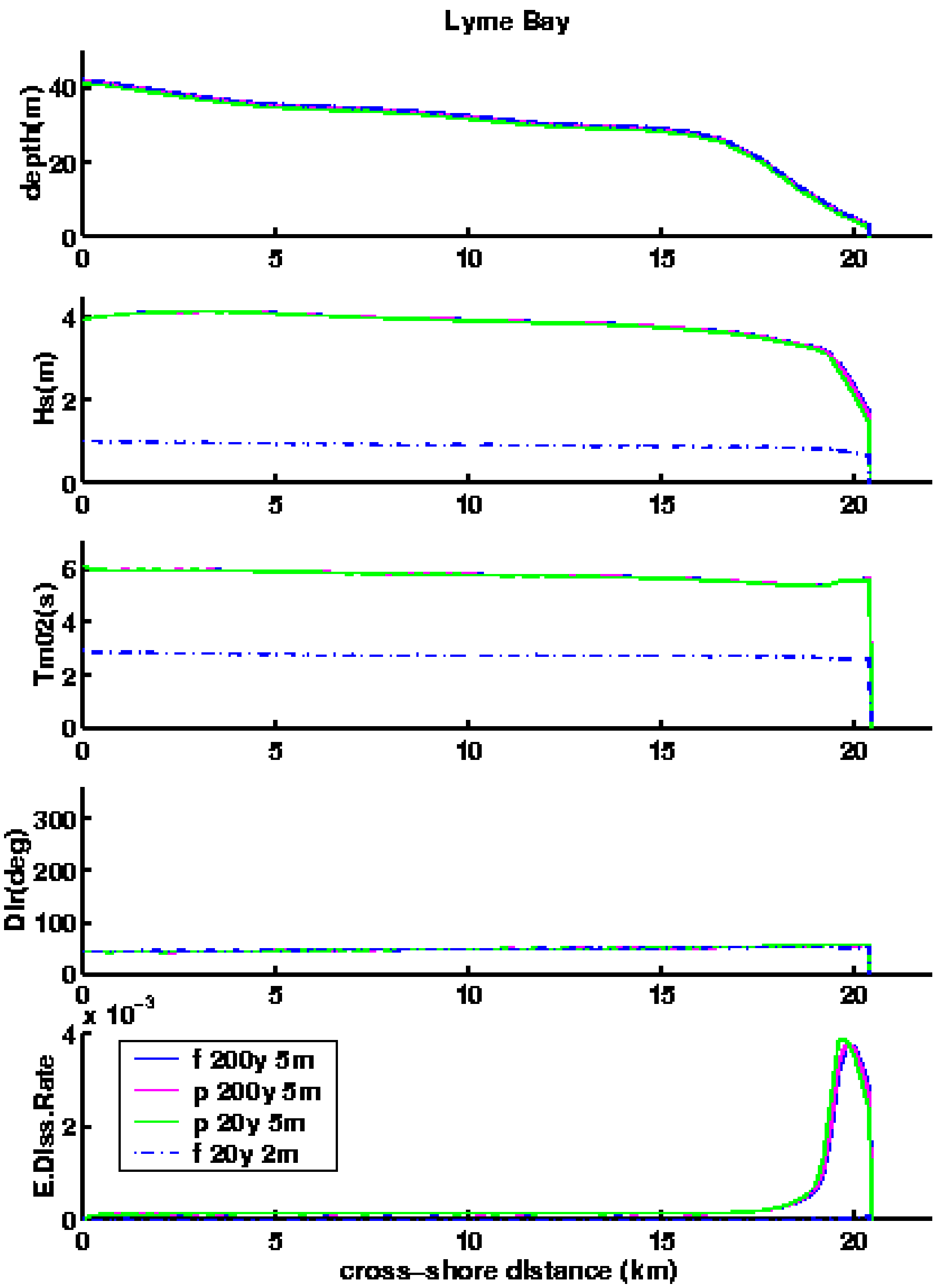

Figure 2.12 **Cross-shore sections, showing water depth, wave height, mean wave period ($T_{0,2}$), mean wave direction and energy dissipation rate, for Lyme Bay**

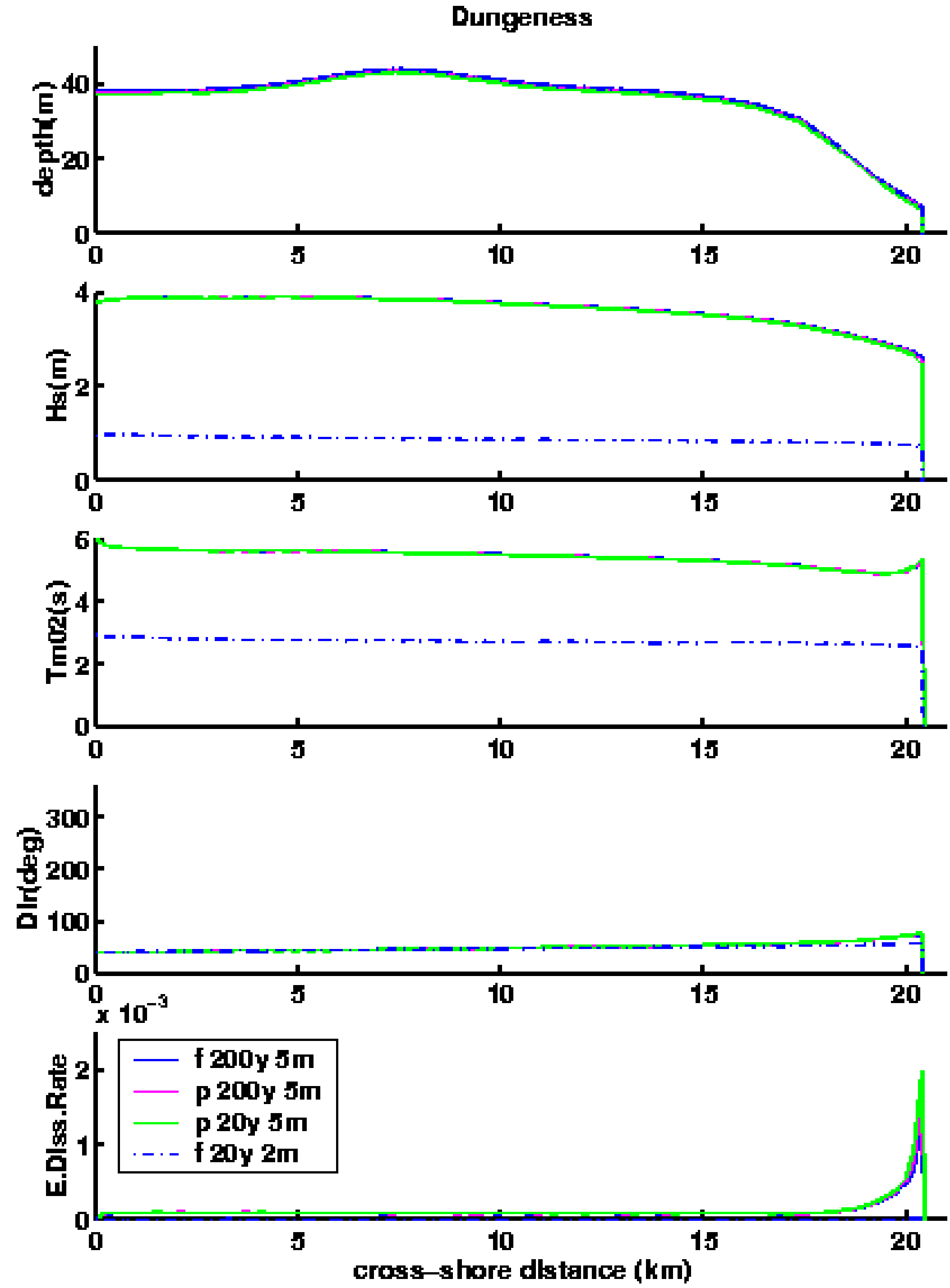

Figure 2.13 Cross-shore sections, showing water depth, wave height, mean wave period ($T_{0,2}$), mean wave direction and energy dissipation rate, for Dungeness

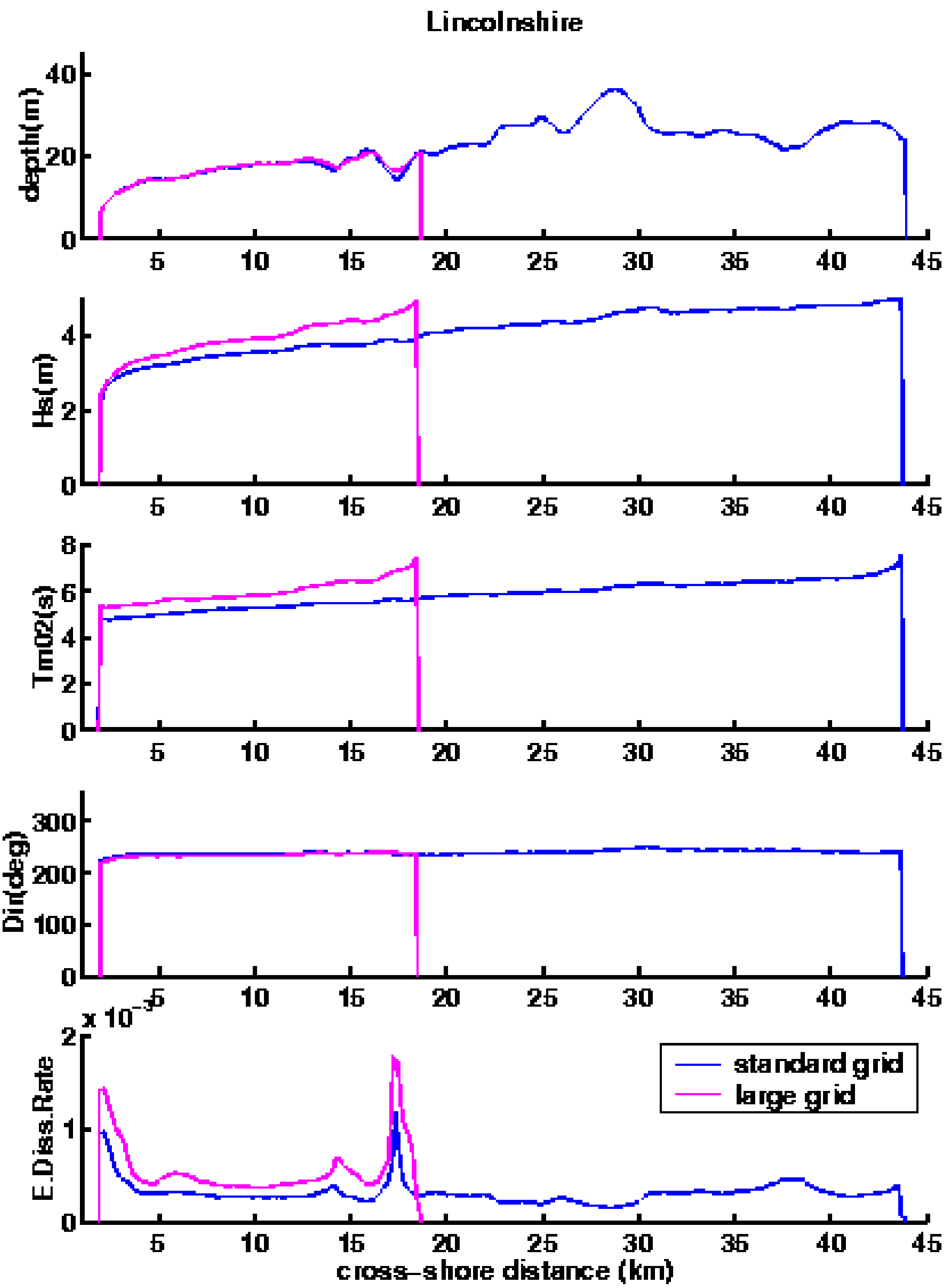

Figure 2.14 **cross-shore sections, showing water depth, wave height, mean wave period ($T_{0,2}$), mean wave direction and energy dissipation rate for Lincolnshire for long and short models**

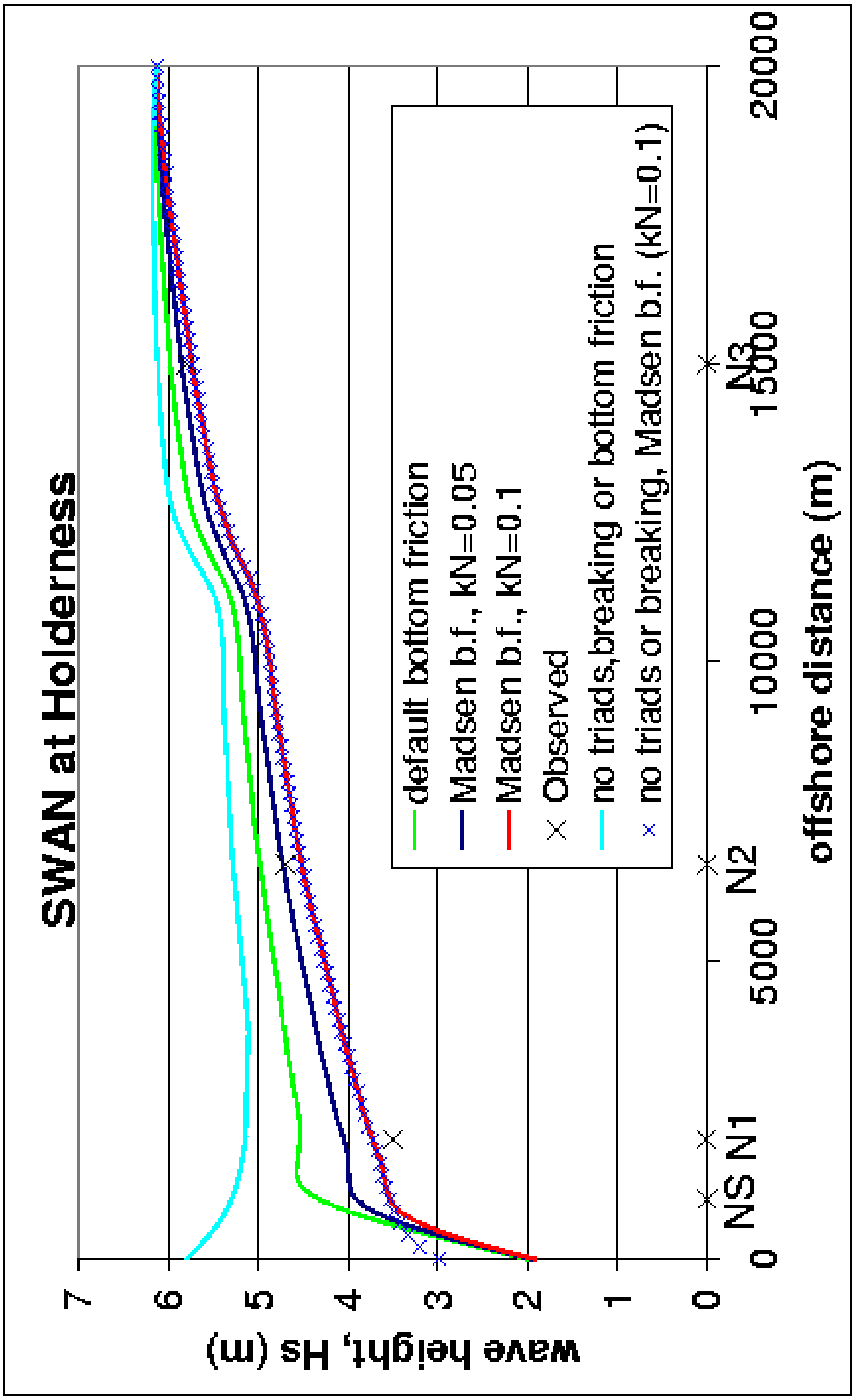

Figure 2.15 Cross-shore sections for Holderness, showing effect of different dissipation terms in SWAN

Appendix 3

COSMOS and OTT results for Lincolnshire

Appendix 3 COSMOS and OTT results for Lincolnshire

The results of the individual model runs for the present and future scenarios, are given in the following tables:

- Table 3.1 for present day results at the seawall
- Table 3.2 for future results at the seawall
- Table 3.3 for present day results at the embankment
- Table 3.4 for future results at the embankment
- Table 3.5 for present day results at the shingle beach
- Table 3.6 for future results at the shingle beach

All elevations are given with respect to ODN (m). All structures have simple cross-sections, comprising of a straight slope from toe to crest. OTT then contains a lower area landwards of the crest that is used to collect the overtopped water. The following labels are used:

RP	Return period of offshore wave and water level pair (years)
Hs	Significant wave height offshore (m)
Tp	Peak wave period offshore (s)
WL	Water Level offshore (m)
Beach slope	Beach slope in front of structure is 1:N with N given
Toe Depth	Elevation of structure toe (m)
Slope	Slope of front face of sea wall, expressed as 1:N with N given
Crest height	Elevation of sea wall crest (m)
Urms toe	Root-mean-square depth-averaged water velocity at toe of structure (m/s)
Umax toe	Maximum instantaneous depth-averaged water velocity at toe of structure (m/s)
Umin toe	Minimum instantaneous depth-averaged water velocity at toe of structure (m/s)
Urms mid	Root-mean-square depth-averaged water velocity at midpoint of structure (m/s)
Umax mid	Maximum instantaneous depth-averaged water velocity at midpoint of structure (m/s)
Umin mid	Minimum instantaneous depth-averaged water velocity at midpoint of structure (m/s)
Qmean	Mean overtopping discharge (m^3/s/m)
Qmax	Maximum instantaneous overtopping flux rate (m^3/s/m)
Vtotal	Total overtopping volume during the test (m^3/m)
Vmax	Maximum overtopping event volume (m^3/m)
No. waves	Total number of waves in numerical model run
NQ	Number of overtopping events during the test

A large number of tests were run for the seawall. Six water level/wave conditions were modelled from each joint probability contour (for present and future scenarios at 20, 50 and 200-year return periods). Therefore there are 18 present day and 18 future sets of results using present day beach slope and toe depth. In addition there are six present day results with the structure toe depth reduced by 0.35m and four present day results with the water level raised by 0.35m (marked with a * in the WL column in table 3.1). Moreover, there are single results for future 20-year and 200-year return periods with a steeper beach, three future results for 50-year return period with a steeper beach, four with a raised crest level, six with a lowered toe and six with a lowered toe and a steeper beach. There are 39 results in total for the future scenario at the smooth sloping wall.

Four water level/wave conditions were modelled from each joint probability contour for the embankment and shingle beach (for present and future scenarios at 20, 50 and 200-year return periods). Therefore there are 12 present day and 12 future sets of results using present day beach slope for each of the embankment and seawall.

The results for mean and maximum overtopping rates and rms velocities, from the results using the present day beach slope, toe depth and crest level at the sloping sea wall at Lincolnshire are shown in Figure 3.1 to Figure 3.4. Figure 3.1 shows the mean overtopping flux rates. The results show that different combinations of wave height and water level (with the same joint exceedence return period) produce different overtopping rates. The wave height/water level combinations with the highest water levels have low waves so rarely overtop. The combinations with the highest offshore wave heights have depth-limited waves at the structure toe but low water depths. Middle combinations have relatively high (possibly depth-limited) waves and higher water levels and one of these gives the highest overtopping rate for a given offshore joint return period. The peak rates were given by offshore wave height/water level pairs with wave heights between 3m and 4m. Figure 3.2 shows the maximum overtopping flux rates, which do not follow nice smooth curves. The variability comes from the nature of the model. OTT is a wave-by-wave numerical model that was run for 1000 wave (peak) periods. A time series of waves was generated from a JONSWAP spectrum at the offshore boundary and was then transformed inshore, onto the structure by OTT. Different runs give different time series, so the maximum instantaneous overtopping rate varies from run to run. This inherent variability makes the statistics for maxima and minima poorly suited to direct comparisons between runs. More reliance will be placed on the average and root-mean-square statistics, where the effect of simulating a time series is less pronounced.

Figure 3.3 shows the root-mean-square velocity at the toe of the sloping sea wall and Figure 3.4 shows the root-mean-square velocity at the midpoint of the sloping sea wall. Figure 3.3 shows smooth variations between adjacent runs, but Figure 3.4 shows more variability. This is related to the position of the model output. The midpoint of the structure is at 3.23m ODN, which is higher than mean water level for the present day runs with higher values of wave height, but is below mean water level for the lower wave heights.

Figure 3.5 shows mean overtopping rates (50-year return period waves) for the following cases:

- Present day conditions with a standard beach, water level, toe depth and crest level, labelled 'Present – 50y – orig'.
- Present day waves with a standard beach, water level, toe depth and crest level, but present day water levels increased by 0.35m. This is the simplest way to represent the effects of climate change. Labelled 'Present – 50y –WL + 35cm'.
- Future conditions with a standard beach, water level, toe depth and crest level. Labelled 'Future(35) – 50y – orig'.
- Future conditions with the standard beach, water level and toe depth, but a raised crest level. Labelled 'Future(35) – 50y – C+35cm'.

The overtopping rates from the present day conditions using water levels raised by 0.35m give results close to those from the future conditions (within about 10%) but very different from the present day results. The results from the future conditions using a structure crest level raised by 0.35m show overtopping rates that are still much larger than the present day results.

Figure 3.6 shows the effect of lowering the structure toe level and the beach steepness on overtopping rates for 50-year return period conditions and the sloping sea wall at Lincolnshire. In all cases the structure front slope and crest level used were the default values. The following results were plotted:

- Present 50yr –original: standard present-day conditions and structure.
- Present 50yr – low toe: present-day condition but toe depth lowered to –0.35m
- Future 50yr – original: future conditions and standard structure
- Future 50yr – low toe: future conditions but toe depth lowered to –0.35m
- Future 50yr (steepened) – original: future conditions and standard structure but steeper beach

- Future 50yr (steepened) – low toe: future conditions with steeper beach and lower toe depth.

Figure 3.6 shows that lowering the beach level (which is the same a lowering the toe depth) lead to significantly higher overtopping rates for both present and future scenarios. Increasing the toe depth by 0.35m had a greater effect than increasing the beach steepness from 1:144 to 1:115. Note that the choice of lowering the beach by 0.35m was made so that the effect could be compared to the effect of sea level rise. It has no scientific validity and is not a prediction for what will happen to beach levels. Nevertheless, the results show that if beach draw-down happens as a result of sea level rise then it will have a significant effect on overtopping rates.

Similar plots, of other quantities and other structures types could also be presented. Instead, however, the highest value (for overtopping rate, rms velocity etc) from the four or six conditions from the same joint probability contour, was used as the worst case from the contour's return period. A better representation would have been achieved if more points from each joint probability contour had been used. However, it was considered that four to six represented an adequate number to give an assessment of the changes that would occur due to climate change. The worst case values of rms velocity at the structure toe and midpoint and the maximum and mean overtopping rate are given in the following tables:

- Table 3.7 for results at the seawall
- Table 3.8 for results at the embankment
- Table 3.9 for results at the shingle beach.

Figure 3.7 shows wort-case rms velocities at the toe of the Lincolnshire sea wall. There is an increase of 7% to 8% between present and future. The effect of coastal steepening is to increase the velocities by 3% to 10% above present day values. The scenarios of future waves and a raised structure crest and of present day waves with a raised water level give velocities between the present and future wave scenarios with the normal crest height. Raising the crest level increases reflections, which will result in a reduction of velocities at some points due to a stronger partial standing wave being set up. The rms velocities at the toe of the structure are highest for the future case with the lowered toe.

The results from the 50-year return period tests are shown in Figure 3.?. This shows that the future damage potential is about 17% higher than the present-day levels. This figure rises to 22% if coastal steepening continues at the present rate and jumps to 35% if the beach level at the toe decreases by 0.35m as well.

Tables

Table 3.1 Results of individual present day model runs for sloping sea wall at Lincolnshire. Runs marked * were made with water level raised 0.35m

RP (yrs)	H_s (m)	T_p (s)	WL (m)	Beach Slope 1:N	Toe depth (m)	slope	Crest height (m)	Urms toe (m/s)	Umax toe (m/s)	Umin toe (m/s)	Urms mid (m/s)	Umax mid (m/s)	Umin mid (m/s)	Qmean (m^3/s)	Qmax (m^3/s)	Vtotal (m^3/m)	Vmax (m^3/m)	No. waves	NQ
20	2	5.1	3.66	144	0	1.623	6.47	0.688	2.37	-1.61	1.792	5.58	-6.43	1.52E-03	0.897	10.52	0.78	1158	88
20	3	6.2	3.43	144	0	1.623	6.47	0.757	2.85	-1.6	1.873	6.88	-7.4	3.42E-03	1.556	26.08	1.73	1170	132
20	4	7.2	3.11	144	0	1.623	6.47	0.758	3.29	-1.63	1.642	7.19	-7.1	2.97E-03	2.215	27.46	2.55	1297	122
20	5	8.0	2.74	144	0	1.623	6.47	0.704	3.52	-1.62	1.354	6.68	-6.2	8.62E-04	1.016	8.75	0.87	1273	47
20	5.4	8.3	2.36	144	0	1.623	6.47	0.646	2.86	-1.59	1.016	5.93	-5.22	5.62E-05	0.4	0.57	0.27	1296	6
20	5.8	8.6	1.9	144	0	1.623	6.47	0.56	2.77	-1.4	0.645	4.62	-4.17	0.00E+00	0	0	0	1285	0
50	2	5.1	3.84	144	0	1.623	6.47	0.708	2.46	-1.61	1.71	6.01	-6.32	3.14E-03	1.419	21.77	1.51	1121	145
50	3	6.2	3.53	144	0	1.623	6.47	0.774	2.69	-1.61	1.902	6.36	-6.43	4.28E-03	1.14	32.62	1.37	1180	177
50	4	7.2	3.25	144	0	1.623	6.47	0.783	3.36	-1.59	1.691	7	-6.88	6.05E-03	1.746	55.85	1.95	1263	189
50	5	8.0	2.99	144	0	1.623	6.47	0.761	3.25	-1.61	1.539	7.25	-6.63	4.21E-03	2.543	42.76	3.97	1294	130
50	5.4	8.3	2.76	144	0	1.623	6.47	0.72	3.07	-1.62	1.408	6.86	-6.47	1.46E-03	1.721	14.8	2.36	1272	55
50	5.8	8.6	2.53	144	0	1.623	6.47	0.679	3.45	-1.59	1.19	6.33	-6.32	5.76E-04	1.167	6.43	1.37	1283	30
50	2	5.1	4.19*	144	0	1.623	6.47	0.728	2.53	-1.56	1.387	5.84	-5.85	1.14E-02	1.791	79.16	1.97	1136	318
50	3	6.2	3.88*	144	0	1.623	6.47	0.821	3.08	-1.6	1.744	6.94	-6.24	1.93E-02	3.123	147.15	4.19	1170	385
50	4	7.2	3.60*	144	0	1.623	6.47	0.829	3.41	-1.56	1.63	7.27	-6.19	1.85E-02	3.624	170.38	5.36	1296	371
50	5	8.0	3.34*	144	0	1.623	6.47	0.808	3.85	-1.58	1.554	8.31	-6.59	1.23E-02	3.027	124.52	4	1305	285
50	2	5.1	3.84	144	-0.35	1.623	6.47	0.727	2.79	-1.62	1.839	6.28	-6.27	5.14E-03	2.242	35.66	2.82	1130	182
50	3	6.2	3.53	144	-0.35	1.623	6.47	0.809	3.34	-1.68	1.838	8.14	-6.22	9.63E-03	3.373	73.48	4.56	1199	229
50	4	7.2	3.25	144	-0.35	1.623	6.47	0.817	3.85	-1.67	1.684	8.12	-6.57	1.04E-02	4.417	96.42	6.95	1260	227
50	5	8.0	2.99	144	-0.35	1.623	6.47	0.79	4.07	-1.66	1.53	8.7	-6.8	6.47E-03	3.818	65.62	5.33	1283	168
50	5.4	8.3	2.76	144	-0.35	1.623	6.47	0.758	3.62	-1.68	1.392	7.39	-6.1	2.95E-03	3.061	29.95	4.88	1286	104
50	5.8	8.6	2.53	144	-0.35	1.623	6.47	0.711	3.56	-1.64	1.193	6.68	-6.42	1.12E-03	1.961	12.55	2.4	1292	55
200	2	5.1	4.05	144	0	1.623	6.47	0.717	2.56	-1.58	1.492	6.11	-5.98	6.79E-03	1.564	47.1	1.72	1132	232
200	3	6.2	3.72	144	0	1.623	6.47	0.807	3.02	-1.59	1.91	6.14	-6.94	1.05E-02	2.459	79.99	3.2	1171	302
200	4	7.2	3.44	144	0	1.623	6.47	0.809	3.25	-1.58	1.676	7.51	-6.48	1.12E-02	2.418	103.67	3.14	1293	275
200	5	8.0	3.21	144	0	1.623	6.47	0.792	3.42	-1.6	1.592	6.98	-6.48	7.37E-03	2.067	74.81	2.78	1293	244
200	5.4	8.3	3.12	144	0	1.623	6.47	0.788	3.63	-1.6	1.637	7.57	-6.71	7.33E-03	3.344	74.38	5.38	1279	189
200	5.8	8.6	3.03	144	0	1.623	6.47	0.766	3.57	-1.56	1.503	7.68	-6.69	5.86E-03	3.316	65.45	5.32	1264	182

Table 3.2 Results of individual future scenario model runs for sloping sea wall at Lincolnshire

RP (yrs)	H_s (m)	T_p (s)	WL (m)	Beach Slope 1:N	Toe depth (m)	slope	Crest height (m)	Urms toe (m/s)	Umax toe (m/s)	Umin toe (m/s)	Urms mid (m/s)	Umax mid (m/s)	Umin mid (m/s)	Qmean (m^3/s)	Qmax (m^3/s)	Vtotal (m^3/m)	Vmax (m^3/m)	No. waves	NQ
20	2	5.1	3.99	144	0	1.623	6.47	0.715	2.2	-1.57	1.551	5.44	-6.32	5.76E-03	1.666	39.97	2.11	1121	204
20	3	6.2	3.77	144	0	1.623	6.47	0.804	2.88	-1.61	1.793	7.03	-6.68	1.31E-02	3.19	100.23	4.45	1155	321
20	3.5	6.7	3.64	144	0	1.623	6.47	0.816	3.3	-1.6	1.782	7.23	-6.52	1.47E-02	2.391	123.02	2.81	1236	311
20	4	7.2	3.5	144	0	1.623	6.47	0.818	3.36	-1.61	1.678	7.25	-6.27	1.54E-02	2.26	142.58	3.61	1300	297
20	4.5	7.6	3.23	144	0	1.623	6.47	0.785	3.5	-1.58	1.591	7.05	-7.48	7.40E-03	2.639	75.1	3.67	1281	223
20	5	8.0	2.95	144	0	1.623	6.47	0.755	3.4	-1.63	1.528	7.03	-6.26	3.09E-03	1.513	31.35	2.17	1293	124
20	4	7.2	3.5	115	0	1.623	6.47	0.847	3.89	-1.58	1.746	8.34	-6.68	1.87E-02	4.465	172.17	6.58	1276	346
50	2	5.1	4.15	144	0	1.623	6.47	0.736	2.43	-1.55	1.421	6.05	-5.81	9.65E-03	1.313	66.91	1.46	1133	314
50	3	6.2	3.9	144	0	1.623	6.47	0.823	3.12	-1.58	1.707	6.91	-6.61	2.26E-02	2.687	172.06	3.6	1200	377
50	3.5	6.7	3.77	144	0	1.623	6.47	0.847	3.35	-1.59	1.695	7.42	-7.03	2.38E-02	3.138	199.88	4.18	1254	420
50	4	7.2	3.63	144	0	1.623	6.47	0.847	3.32	-1.58	1.682	7.66	-7.04	2.17E-02	2.719	199.99	4.35	1258	423
50	4.5	7.6	3.46	144	0	1.623	6.47	0.821	3.43	-1.57	1.55	7.56	-7.05	1.62E-02	3.264	164.87	4.56	1283	342
50	5	8.0	3.28	144	0	1.623	6.47	0.807	3.6	-1.6	1.612	7.08	-7.01	1.11E-02	2.722	112.56	3.59	1292	255
50	3	6.2	3.9	115	0	1.623	6.47	0.841	2.93	-1.58	1.77	6.91	-7.04	2.33E-02	3.151	177.87	4.31	1186	421
50	3.5	6.7	3.77	115	0	1.623	6.47	0.852	3.35	-1.59	1.775	7.58	-6.75	2.42E-02	2.791	203	3.96	1256	425
50	4	7.2	3.63	115	0	1.623	6.47	0.864	3.86	-1.6	1.658	8.29	-6.93	2.62E-02	3.337	241.8	4.57	1273	412
50	2	5.1	4.15	144	0	1.54	6.82	0.709	2.27	-1.58	1.551	5.75	-6.37	3.66E-03	0.958	25.4	0.94	1129	172
50	3	6.2	3.9	144	0	1.54	6.82	0.813	3.08	-1.65	1.843	7.04	-7.02	1.20E-02	2.262	91.49	2.56	1169	272
50	4	7.2	3.63	144	0	1.54	6.82	0.826	3.54	-1.63	1.733	7.43	-6.72	1.30E-02	2.541	120.05	3.11	1281	270
50	5	8.0	3.28	144	0	1.54	6.82	0.794	3.56	-1.64	1.592	7.58	-6.7	5.54E-03	2.733	56.21	3.71	1293	180
50	2	5.1	4.15	144	-0.35	1.623	6.47	0.742	2.66	-1.58	1.655	6.27	-6.51	1.43E-02	2.915	99.43	4.1	1147	336
50	3	6.2	3.9	144	-0.35	1.623	6.47	0.852	3.2	-1.63	1.931	6.72	-7.52	2.95E-02	4.357	225.07	7.69	1204	433
50	3.5	6.7	3.77	144	-0.35	1.623	6.47	0.872	3.49	-1.64	1.881	7.27	-7.13	3.33E-02	5.25	279.55	9.55	1251	440
50	4	7.2	3.63	144	-0.35	1.623	6.47	0.87	4.23	-1.62	1.792	8.08	-7.9	3.17E-02	6.178	292.2	11.25	1271	421
50	4.5	7.6	3.46	144	-0.35	1.623	6.47	0.855	3.7	-1.61	1.694	8.07	-6.9	2.54E-02	4.704	257.71	9.58	1274	388
50	5	8.0	3.28	144	-0.35	1.623	6.47	0.837	3.78	-1.61	1.68	7.7	-7.37	1.71E-02	4.42	173.15	8.4	1273	304
50	2	5.1	4.15	115	-0.35	1.623	6.47	0.759	2.69	-1.61	1.712	5.98	-6.38	1.56E-02	2.884	108.04	4.46	1146	352
50	3	6.2	3.9	115	-0.35	1.623	6.47	0.883	3.56	-1.66	1.976	7.75	-6.99	3.43E-02	4.8	261.39	8.02	1211	460
50	3.5	6.7	3.77	115	-0.35	1.623	6.47	0.907	4.05	-1.67	1.944	7.75	-7.28	4.01E-02	6.12	336.72	10.23	1244	476

Table 3.2 Results of individual future scenario model runs for sloping sea wall at Lincolnshire - continued

RP (yrs)	H_s (m)	T_p (s)	WL (m)	Beach Slope 1:N	Toe depth (m)	slope	Crest height (m)	Urms toe (m/s)	Umax toe (m/s)	Umin toe (m/s)	Urms mid (m/s)	Umax mid (m/s)	Umin mid (m/s)	Qmean (m^3/s)	Qmax (m^3/s)	Vtotal (m^3/m)	Vmax (m^3/m)	No. waves	NQ
50	4	7.2	3.63	115	-0.35	1.623	6.47	0.91	4.33	-1.65	1.872	9.04	-7.26	3.93E-02	6.993	362.51	13.36	1272	456
50	4.5	7.6	3.46	115	-0.35	1.623	6.47	0.897	4.3	-1.64	1.737	8.43	-7.36	3.26E-02	5.619	330.65	10.74	1273	418
50	5	8.0	3.28	115	-0.35	1.623	6.47	0.879	3.82	-1.65	1.714	7.97	-6.86	2.25E-02	4.763	228.88	9.45	1274	343
200	2	5.1	4.32	144	0	1.623	6.47	0.74	2.41	-1.53	1.343	5.62	-5.82	1.75E-02	2.613	121.51	3.08	1141	417
200	3	6.2	4.17	144	0	1.623	6.47	0.854	3.07	-1.56	1.557	6.71	-6.43	3.98E-02	2.745	303.39	4.19	1165	563
200	3.5	6.7	3.99	144	0	1.623	6.47	0.864	3.43	-1.57	1.595	7.48	-5.94	4.07E-02	3.8	341.37	6.54	1262	529
200	4	7.2	3.84	144	0	1.623	6.47	0.858	3.87	-1.57	1.553	7.48	-6.14	3.92E-02	4.361	361.75	7.21	1286	504
200	4.5	7.6	3.68	144	0	1.623	6.47	0.86	3.72	-1.54	1.524	8.01	-6.46	3.31E-02	4.292	335.76	8.06	1271	472
200	5	8.0	3.51	144	0	1.623	6.47	0.841	4.04	-1.57	1.573	7.76	-6.27	2.42E-02	3.642	245.4	5.93	1261	346
200	3.5	6.7	3.99	115	0	1.623	6.47	0.888	3.72	-1.56	1.635	7.3	-6.67	4.91E-02	4.537	412.1	6.51	1253	524

Table 3.3 Results of individual present-day model runs for embankment at Lincolnshire

RP (yrs)	H_s (m)	T_p (s)	WL (m)	Beach Slope 1:N	Toe depth (m)	slope	Crest height (m)	Urms toe (m/s)	Umax toe (m/s)	Umin toe (m/s)	Urms mid (m/s)	Umax mid (m/s)	Umin mid (m/s)	Qmean (m^3/s)	Qmax (m^3/s)	Vtotal (m^3/m)	Vmax (m^3/m)	No. waves	NQ
20	2	5.1	3.66	144	-1.815	3	5.38	0.565	2	-2.23	1.648	6.16	-4.67	3.42E-02	3.329	237.03	6.88	1063	478
20	3	6.2	3.43	144	-1.815	3	5.38	0.82	2.79	-2.31	2.192	8.09	-4.76	8.10E-02	5.682	617.82	13.4	1061	600
20	4	7.2	3.11	144	-1.815	3	5.38	1.06	3.75	-2.32	2.431	9.27	-4.78	1.12E-01	8.264	1032.81	21.64	1142	624
20	5	8.0	2.74	144	-1.815	3	5.38	1.137	4.22	-2.35	2.432	9.16	-4.8	7.88E-02	8.421	800.27	22.66	1157	526
50	2	5.1	3.84	144	-1.815	3	5.38	0.557	2.01	-2.22	1.544	5.62	-4.63	5.23E-02	3.67	362.3	7.83	1054	572
50	3	6.2	3.53	144	-1.815	3	5.38	0.815	2.81	-2.3	2.162	7.81	-4.78	9.81E-02	6.058	748.27	14.76	1067	641
50	4	7.2	3.25	144	-1.815	3	5.38	1.059	3.69	-2.3	2.426	8.57	-4.78	1.42E-01	8.872	1309.03	23.83	1143	680
50	5	8.0	2.99	144	-1.815	3	5.38	1.152	4.29	-2.33	2.462	10.7	-4.79	1.26E-01	9.64	1282.63	28.45	1151	639
200	2	5.1	4.05	144	-1.815	3	5.38	0.546	2.12	-2.19	1.428	5.45	-4.56	8.13E-02	4.039	564.07	8.77	1058	692
200	3	6.2	3.72	144	-1.815	3	5.38	0.807	2.91	-2.28	2.089	7.21	-4.79	1.35E-01	6.756	1032.8	16.68	1070	721
200	4	7.2	3.44	144	-1.815	3	5.38	1.055	3.61	-2.29	2.409	10.3	-4.81	1.91E-01	9.645	1762.75	28.2	1151	767
200	5	8.0	3.21	144	-1.815	3	5.38	1.156	4.28	-2.31	2.472	9.43	-4.79	1.81E-01	10.951	1840.71	32.62	1154	747

Table 3.4 Results of individual future model runs for embankment at Lincolnshire

RP (yrs)	H_s (m)	T_p (s)	WL (m)	Beach Slope 1:N	Toe depth (m)	slope	Crest height (m)	Urms toe (m/s)	Umax toe (m/s)	Umin toe (m/s)	Urms mid (m/s)	Umax mid (m/s)	Umin mid (m/s)	Qmean (m^3/s)	Qmax (m^3/s)	Vtotal (m^3/m)	Vmax (m^3/m)	No. waves	NQ
20	2	5.1	3.99	144	-1.815	3	5.38	0.548	2.13	-2.2	1.459	5.6	-4.58	7.20E-02	3.934	498.97	8.52	1061	670
20	3	6.2	3.77	144	-1.815	3	5.38	0.804	2.9	-2.27	2.066	7.06	-4.79	1.46E-01	6.944	1117.39	17.09	1075	747
20	4	7.2	3.5	144	-1.815	3	5.38	1.053	3.6	-2.28	2.399	9.97	-4.81	2.08E-01	9.947	1923.03	29.22	1150	789
20	5	8.0	2.95	144	-1.815	3	5.38	1.151	4.27	-2.33	2.461	11	-4.79	1.18E-01	9.452	1196.62	27.5	1150	619
50	2	5.1	4.15	144	-1.815	3	5.38	0.54	2.1	-2.18	1.372	5.97	-4.52	9.88E-02	4.295	685.17	9.48	1063	742
50	3	6.2	3.9	144	-1.815	3	5.38	0.796	2.88	-2.26	2.008	8.31	-4.78	1.79E-01	7.328	1366.05	18.12	1076	807
50	4	7.2	3.63	144	-1.815	3	5.38	1.05	3.69	-2.27	2.374	9.33	-4.8	2.49E-01	10.748	2300.79	31.25	1149	841
50	5	8.0	3.28	144	-1.815	3	5.38	1.158	4.27	-2.3	2.473	9.67	-4.8	2.01E-01	11.407	2041.74	33.76	1152	775
200	2	5.1	4.32	144	-1.815	3	5.38	0.531	2.08	-2.16	1.284	5.54	-4.55	1.34E-01	4.785	932.33	11.15	1063	847
200	3	6.2	4.17	144	-1.815	3	5.38	0.781	2.83	-2.23	1.863	7	-4.72	2.62E-01	8.132	1997.04	20.26	1086	916
200	4	7.2	3.84	144	-1.815	3	5.38	1.044	3.63	-2.25	2.322	9.25	-4.76	3.26E-01	11.916	3006.27	34.29	1141	909
200	5	8.0	3.51	144	-1.815	3	5.38	1.161	4.26	-2.29	2.462	10	-4.79	2.78E-01	12.753	2819.99	38.09	1153	857

Table 3.5 Results of individual present-day model runs for shingle beach at Lincolnshire

RP (yrs)	H_s (m)	T_p (s)	WL (m)	Beach Slope 1:N	Toe depth (m)	slope	Crest height (m)	Urms toe (m/s)	Umax toe (m/s)	Umin toe (m/s)	Urms mid (m/s)	Umax mid (m/s)	Umin mid (m/s)	Qmean (m^3/s)	Qmax (m^3/s)	Vtotal (m^3/m)	Vmax (m^3/m)	No. waves	NQ
20	2	5.1	3.66	144	-3.63	5	5.38	0.474	1.81	-1.73	0.878	2.83	-4.56	9.90E-03	2.08	68.67	4.75	1121	209
20	3	6.2	3.43	144	-3.63	5	5.38	0.663	2.73	-2.15	1.351	3.96	-5.22	3.91E-02	4.485	298.27	12.41	1117	364
20	4	7.2	3.11	144	-3.63	5	5.38	0.811	3.34	-2.77	2.027	6.36	-5.29	8.48E-02	7.6	782.3	23.83	1086	471
20	5	8.0	2.74	144	-3.63	5	5.38	0.901	3.64	-3.16	2.414	7.86	-5.28	8.43E-02	8.658	856.07	29.86	1115	445
50	2	5.1	3.84	144	-3.63	5	5.38	0.472	1.8	-1.67	0.844	2.71	-4.57	1.87E-02	2.437	129.33	5.8	1124	312
50	3	6.2	3.53	144	-3.63	5	5.38	0.664	2.72	-2.17	1.319	4.22	-5.21	4.91E-02	4.766	374.63	13.21	1116	419
50	4	7.2	3.25	144	-3.63	5	5.38	0.813	3.33	-2.8	1.966	6.52	-5.28	1.07E-01	8.154	991.56	25.29	1085	526
50	5	8.0	2.99	144	-3.63	5	5.38	0.907	3.65	-3.21	2.329	6.77	6.77	1.28E-01	9.716	1299.56	33.92	1117	526
200	2	5.1	4.05	144	-3.63	5	5.38	0.469	1.79	-1.72	0.811	2.79	-4.11	3.53E-02	2.879	244.92	7.13	1121	454
200	3	6.2	3.72	144	-3.63	5	5.38	0.663	2.73	-2.15	1.351	3.96	-5.22	3.91E-02	4.485	298.27	12.41	1117	364
200	4	7.2	3.44	144	-3.63	5	5.38	0.816	3.32	-2.67	1.894	5.88	-5.28	1.46E-01	8.836	1344.17	28.6	1086	598
200	5	8.0	3.21	144	-3.63	5	5.38	0.914	3.77	-3.25	2.25	7.17	-5.29	1.78E-01	10.907	1806.46	37.21	1120	605

Table 3.6 Results of individual future model runs for shingle beach at Lincolnshire

RP (yrs)	H_s (m)	T_p (s)	WL (m)	Beach Slope 1:N	Toe depth (m)	slope	Crest height (m)	Urms toe (m/s)	Umax toe (m/s)	Umin toe (m/s)	Urms mid (m/s)	Umax mid (m/s)	Umin mid (m/s)	Qmean (m^3/s)	Qmax (m^3/s)	Vtotal (m^3/m)	Vmax (m^3/m)	No. waves	NQ
20	2	5.1	3.99	144	-3.63	5	5.38	0.47	1.79	-1.7	0.819	2.83	-4.11	2.97E-02	2.754	206.22	6.79	1120	415
20	3	6.2	3.77	144	-3.63	5	5.38	0.663	2.69	-2.09	1.249	4.06	-5.04	8.05E-02	5.398	613.81	14.88	1119	538
20	4	7.2	3.5	144	-3.63	5	5.38	0.818	3.32	-2.69	1.869	5.65	-5.28	1.59E-01	9.029	1468.7	29.81	1086	626
20	5	8.0	2.95	144	-3.63	5	5.38	0.906	3.65	-3.2	2.343	6.97	-5.29	1.20E-01	9.521	1220.23	33.29	1116	511
50	2	5.1	4.15	144	-3.63	5	5.38	0.468	1.79	-1.74	0.799	2.74	-4.12	4.66E-02	3.074	322.85	7.64	1124	526
50	3	6.2	3.9	144	-3.63	5	5.38	0.663	2.68	-2.12	1.215	3.97	-5.02	1.03E-01	5.734	785.91	15.74	1118	598
50	4	7.2	3.63	144	-3.63	5	5.38	0.819	3.3	-2.71	1.82	5.5	-5.27	1.91E-01	9.483	1767.48	32	1086	674
50	5	8.0	3.28	144	-3.63	5	5.38	0.915	3.77	-3.26	2.224	7.24	-5.29	1.96E-01	11.286	1993.24	38.22	1121	632
200	2	5.1	4.32	144	-3.63	5	5.38	0.466	1.77	-1.77	0.777	2.66	-4.15	7.15E-02	3.399	495.47	8.44	1123	631
200	3	6.2	4.17	144	-3.63	5	5.38	0.663	2.65	-2.18	1.156	3.83	-4.98	1.65E-01	6.604	1255.93	18.27	1123	715
200	4	7.2	3.84	144	-3.63	5	5.38	0.822	3.29	-2.75	1.744	5.64	-5.28	2.54E-01	10.515	2345	35.03	1091	738
200	5	8.0	3.51	144	-3.63	5	5.38	0.922	3.78	-3.13	2.145	6.67	-5.29	2.66E-01	12.352	2701.49	44.16	1122	714

Table 3.7 Seawall results for Lincolnshire. P= present-day wave/water level conditions, F = future conditions

scenario	Return Period (years)	Waves	Water Level	Beach Slope (1:nnn)	Toe Depth (m)	Crest Elevation (m)	RMS velocity (m/s) at toe	RMS velocity (m/s) at wall midpoint	Mean overtopping discharge ($m^3/m/s$)	Maximum overtopping discharge ($m^3/m/s$)	Maximum overtopping event volume (m^3/m)
20, present	20	P	P	144	0	6.47	0.758	1.873	3.42E-03	2.215	2.55
50, present	50	P	P	144	0	6.47	0.783	1.902	6.05E-03	2.543	3.97
200, present	200	P	P	144	0	6.47	0.809	1.91	1.12E-02	3.344	5.38
20, future	20	F	F	144	0	6.47	0.818	1.793	1.54E-02	3.19	4.45
50, future	50	F	F	144	0	6.47	0.847	1.707	2.38E-02	3.264	4.56
200, future	200	F	F	144	0	6.47	0.864	1.595	4.07E-02	4.361	8.06
20, future -steepened	20	F	F	115	0	6.47	0.847	1.746	1.87E-02	4.465	6.58
50, future -steepened	50	F	F	115	0	6.47	0.864	1.775	2.62E-02	3.337	4.57
200, future - steepened	200	F	F	115	0	6.47	0.888	1.635	4.91E-02	4.537	6.51
future - raised crest	50	F	F	144	0	6.82	0.826	1.843	1.30E-02	2.733	3.71
present waves - raised wl	50	P	F	144	0	6.47	0.829	1.744	1.93E-02	3.624	5.36
present - lowered toe	50	P	P	144	-0.35	6.47	0.817	1.839	1.04E-02	4.417	6.95
future, lowered toe	50	F	F	144	-0.35	6.47	0.872	1.831	3.33E-02	6.078	11.25
future, low toe, steepened	50	F	F	115	-0.35	6.47	0.91	1.976	4.01E-02	6.993	13.36

Table 3.8 Embankment results for Lincolnshire. P= present-day wave/water level conditions, F = future conditions

scenario	RP	Waves	WL	beach slope	toe depth	crest elevation	Urms,toe	Urms,mid	Qmean	Qmax	Vtotal	Vmax
	[years]			[1:nn]	[m]	[m]	[m/s]	[m/s]	[$m^3/m/s$]	[$m^3/m/s$]	[m^3/m]	[m^3/m]
20, present	20	P	P	144	-1.815	5.38	1.137	2.432	0.112	8.4	1032.8	22.66
50, present	50	P	P	144	-1.815	5.38	1.152	2.462	0.142	9.6	1309.0	28.45
200, present	200	P	P	144	-1.815	5.38	1.156	2.472	0.191	11.0	1840.7	32.62
20, future	20	F	F	144	-1.815	5.38	1.151	2.473	0.208	9.9	1923.0	29.22
50, future	50	F	F	144	-1.815	5.38	1.158	2.473	0.249	11.4	2300.8	33.76
200, future	200	F	F	144	-1.815	5.38	1.161	2.462	0.326	12.8	3006.3	38.09

Table 3.9 Shingle beach results for Lincolnshire. P= present-day wave/water level conditions, F = future conditions

scenario	RP	Waves	WL	beach slope	toe depth	crest elevation	Urms,toe	Urms,mid	Qmean	Qmax	Vtotal	Vmax
	[years]			[1:nn]	[m]	[m]	[m/s]	[m/s]	[m^3/m/s]	[m^3/m/s]	[m^3/m]	[m^3/m]
20, present	20	P	P	144	-3.63	5.38	0.901	2.414	0.085	8.7	-	29.86
50, present	50	P	P	144	-3.63	5.38	0.907	2.414	0.128	9.7	-	33.92
200, present	200	P	P	144	-3.63	5.38	0.914	2.414	0.178	10.9	-	37.21
20, future	20	F	F	144	-3.63	5.38	0.906	2.343	0.159	9.5	-	33.29
50, future	50	F	F	144	-3.63	5.38	0.915	2.343	0.196	11.3	-	38.22
200, future	200	F	F	144	-3.63	5.38	0.922	2.343	0.266	12.4	-	44.16

Figures

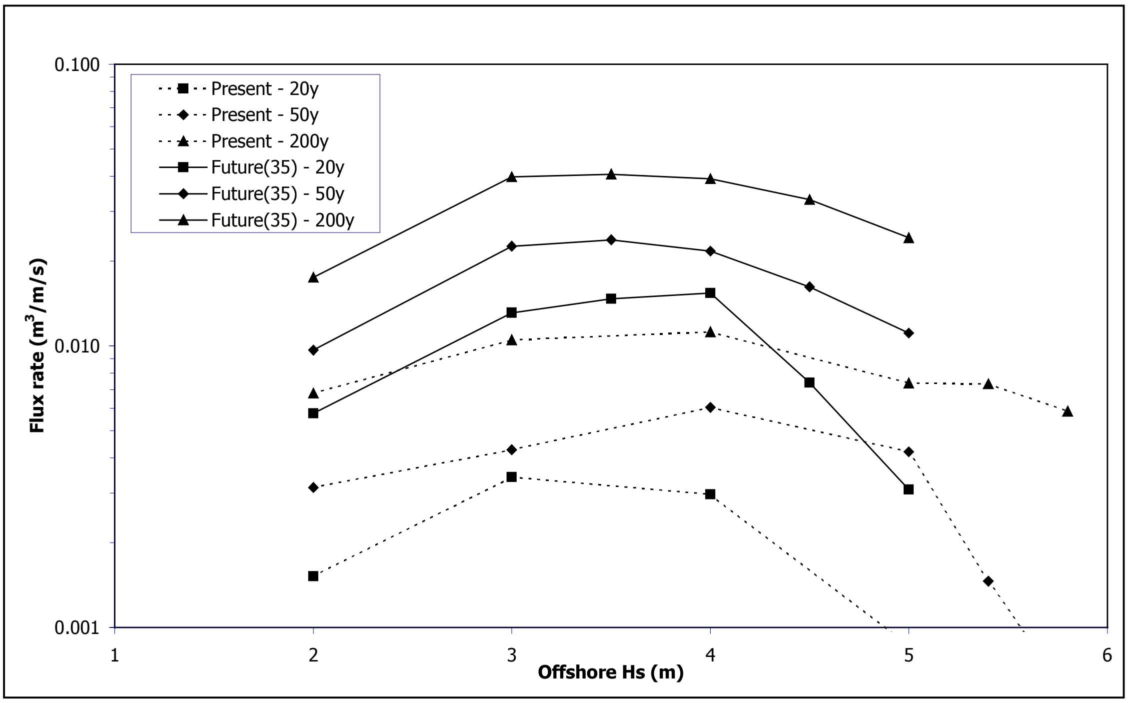

Figure 3.1 Mean overtopping flux rates for sloping sea wall at Lincolnshire

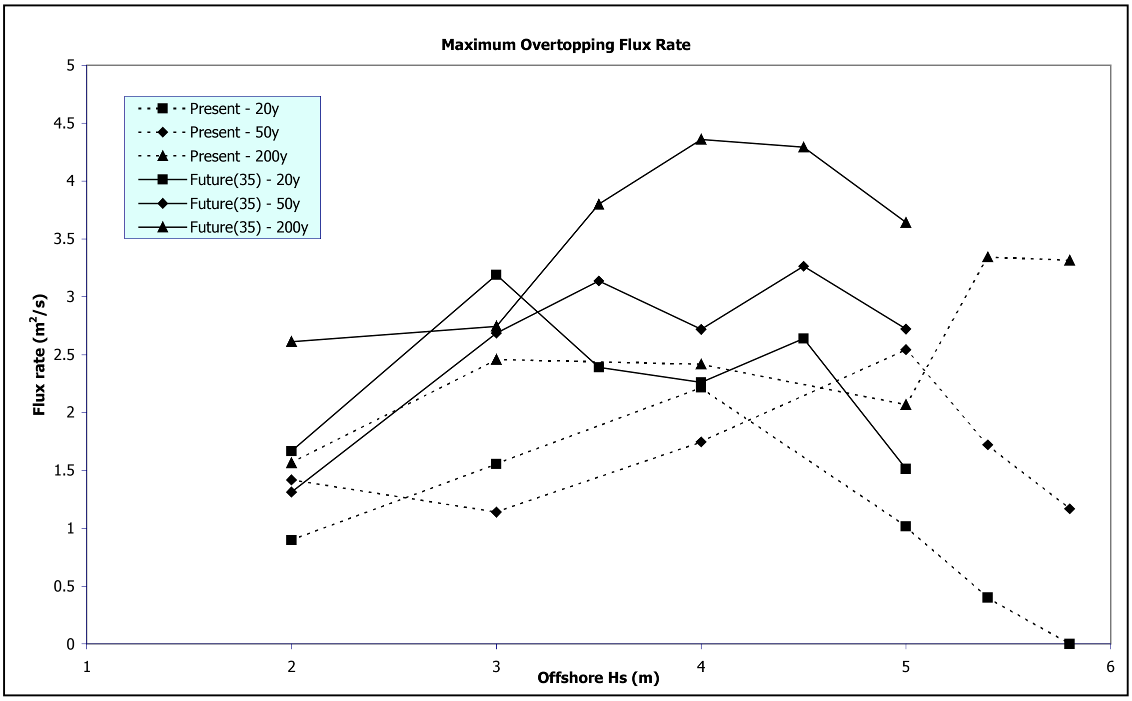

Figure 3.2 Maximum overtopping flux rates for sloping sea wall at Lincolnshire

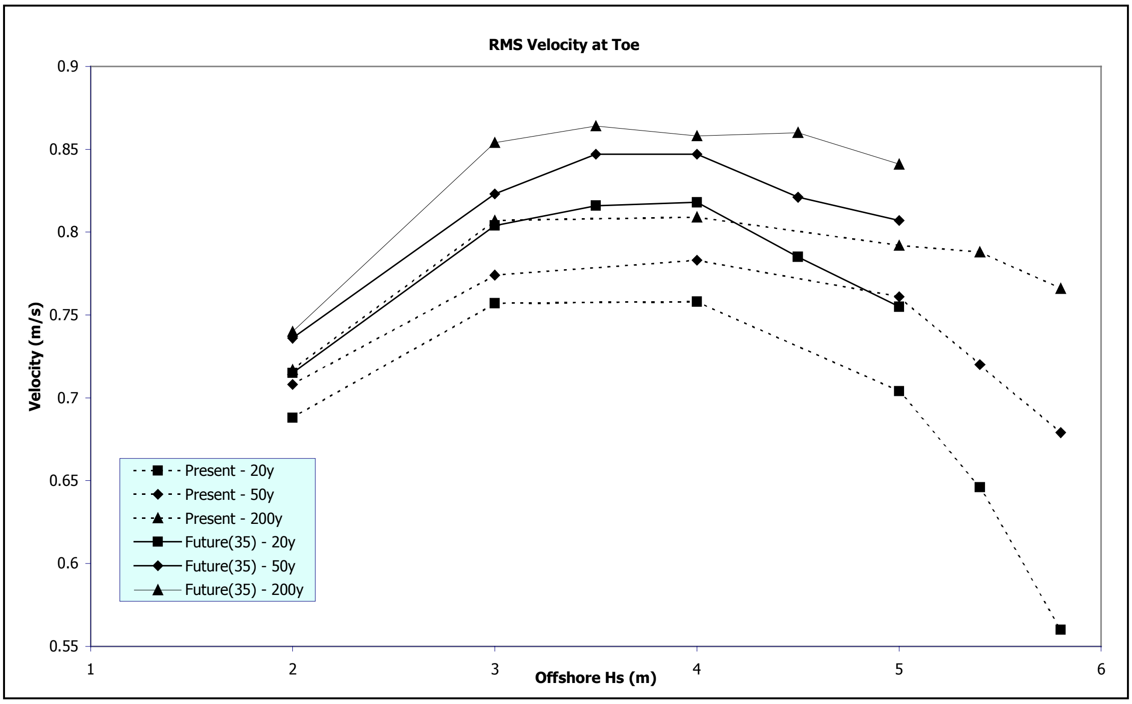

Figure 3.3 Root-mean-square velocity at toe of sloping sea wall at Lincolnshire

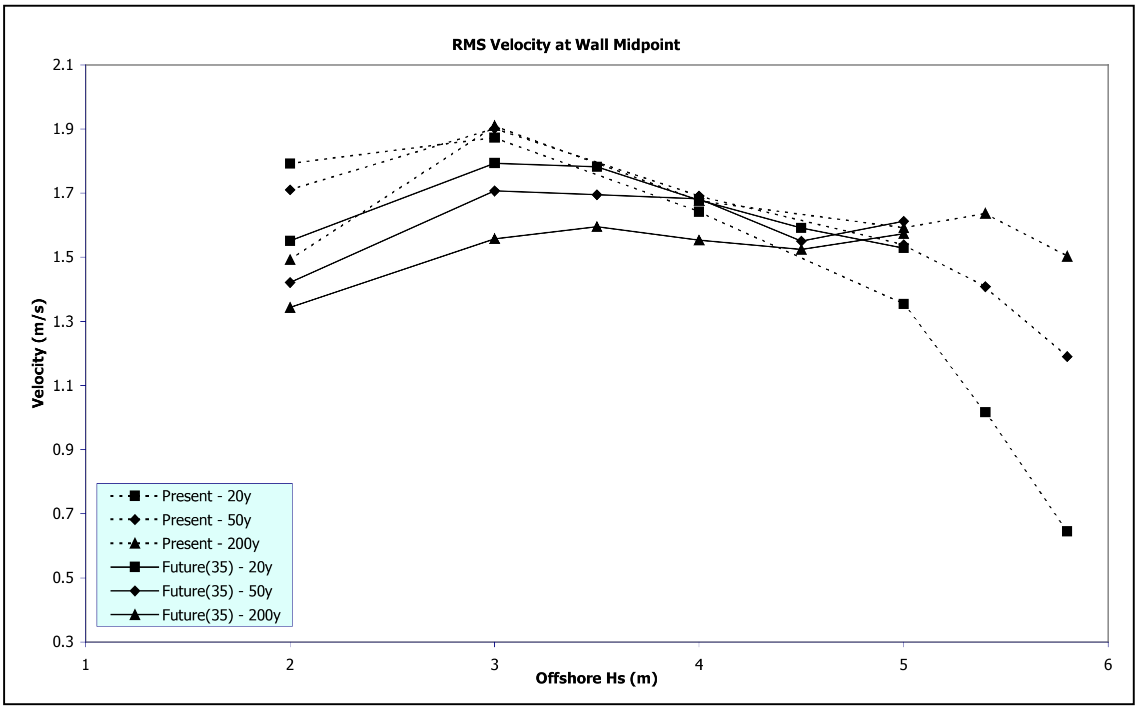

Figure 3.4 Root-mean-square velocity at midpoint of sloping sea wall at Lincolnshire

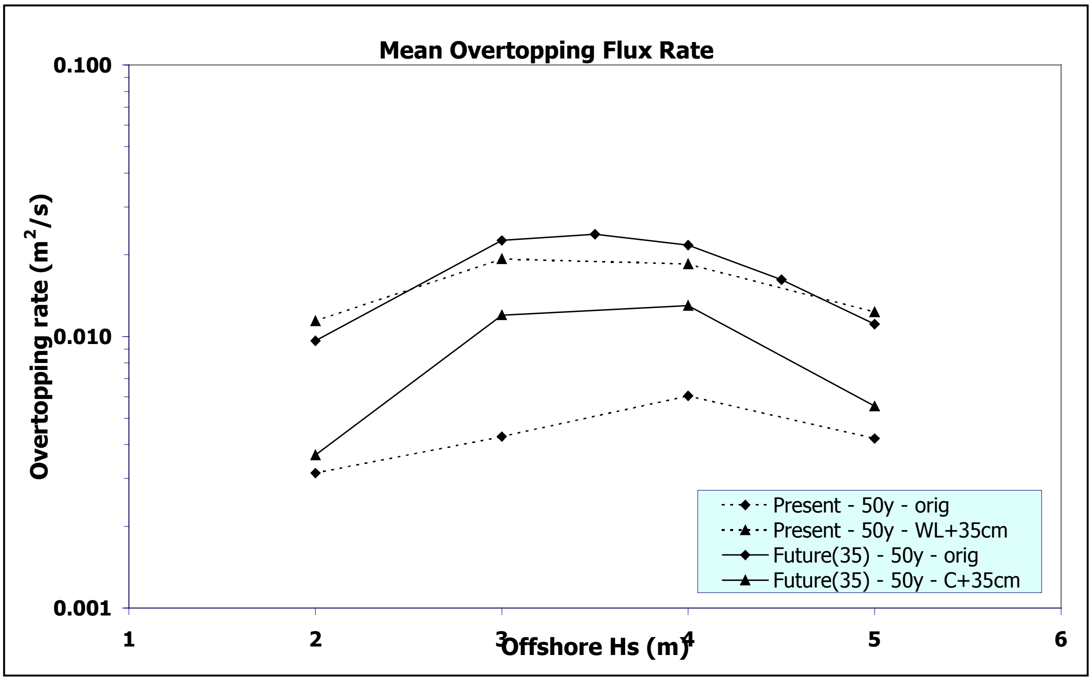

Figure 3.5 **Overtopping rates for present and future scenarios, with 50-year return period and altered crest and water level**

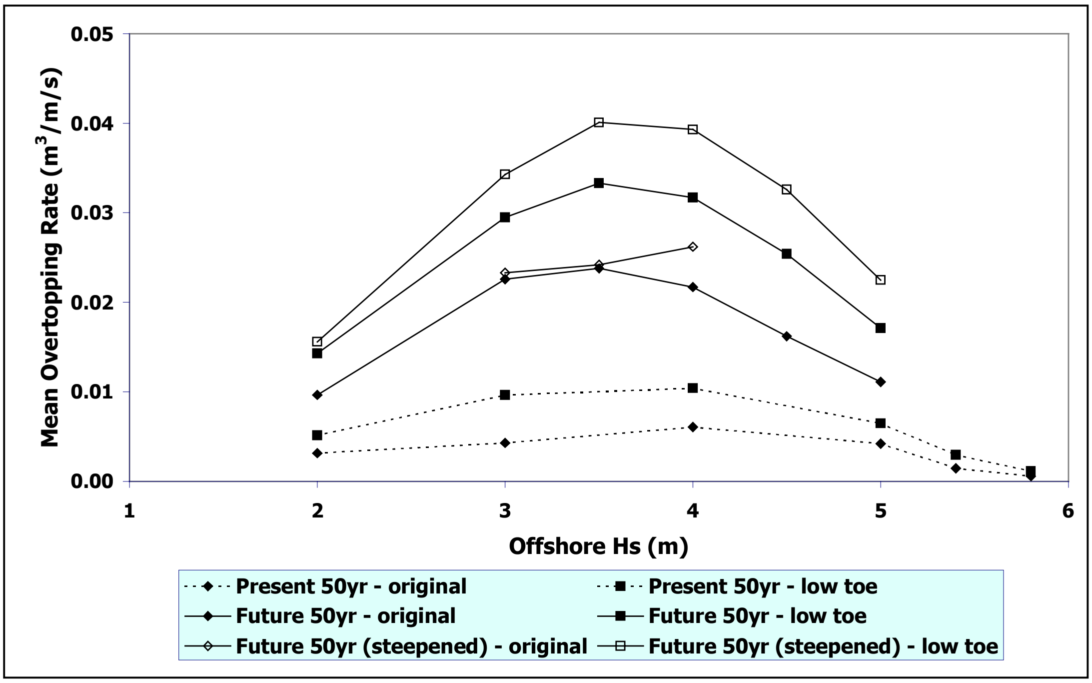

Figure 3.6 **Effect of toe depth and beach steepness on overtopping rates for 50-year return period conditions at Lincolnshire seawall**

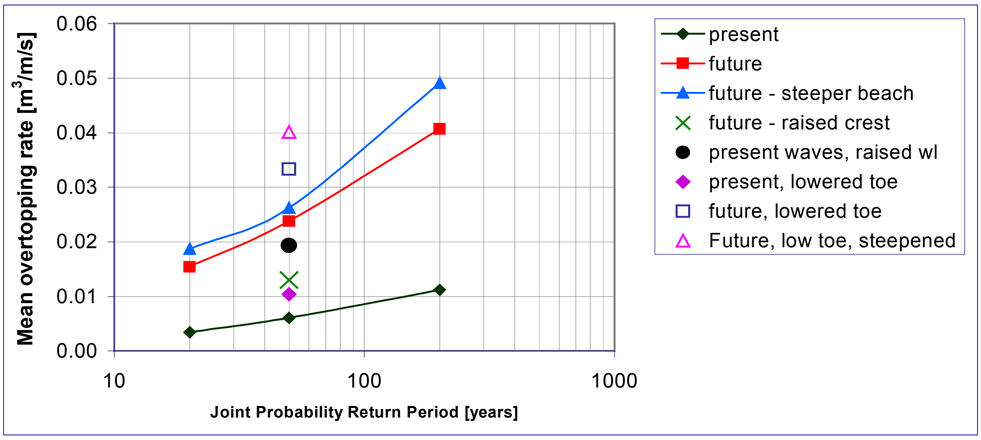

Figure 3.7 Mean overtopping rates at Lincolnshire seawall

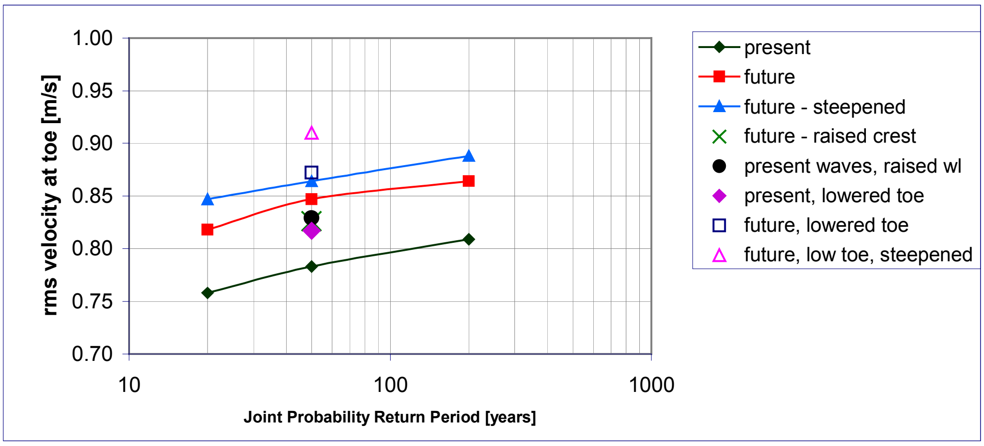

Figure 3.8 Root-mean-square velocities at toe of Lincolnshire seawall

Appendix 4

COSMOS and OTT results for Dungeness

Appendix 4 COSMOS and OTT results for Dungeness

The results of the individual model runs for the present and future scenarios, are given in the following tables:

- Table 4.1 for present day results at the seawall
- Table 4.2 for future results at the seawall
- Table 4.3 for present day results at the embankment
- Table 4.4 for future results at the embankment
- Table 4.5 for present day results at the shingle beach
- Table 4.6 for future results at the shingle beach

All elevations are given with respect to ODN (m). All structures have simple cross-sections, comprising of a straight slope from toe to crest. OTT then contains a lower area landwards of the crest that is used to collect the overtopped water. The labels are explained in Appendix 3.

Four water level/wave conditions were modelled from each joint probability contour (for present and future scenarios at 20, 50 and 200-year return periods). Therefore there are 12 present day and 12 future sets of results. The single highest value was used as a representation of the maximum overtopping rate associated with the offshore return period. A better representation would have been achieved if more than four points from each joint probability contour had been used. However, it was considered that four represented an adequate number to give an assessment of the changes that would occur due to climate change.

Figure 4.1 shows the mean overtopping flux rates from each test using the sloping sea wall at Dungeness to Rye. Figure 4.2 shows the maximum overtopping flux rates from each test using the sloping sea wall at Dungeness to Rye. Figure 4.3 shows the root-mean-square velocity at the toe of the sloping sea wall at Dungeness to Rye and Figure 4.4 shows the root-mean-square velocity at the midpoint of the sloping sea wall.

Similar plots, of other quantities and other structure types could also be presented. Instead, however, the highest value (for overtopping rate, rms velocity etc) from the four conditions from the same joint probability contour, was used as the worst case from the contour's return period. A better representation would have been achieved if more points from each joint probability contour had been used. However, it was considered that four represented an adequate number to give an assessment of the changes that would occur due to climate change. The worst case values of rms velocity at the structure toe and midpoint and the maximum and mean overtopping rate are given in the following tables:

- Table 4.7 for results at the seawall
- Table 4.8 for results at the embankment
- Table 4.9 for results at the shingle beach.

Figure 4,5shows mean overtopping rates for the seawall at Dungeness. The future overtopping rates are between 2.6 and 2.1 times the present day rates (for 20-year return period and 200-year return period). This decrease in relative overtopping rate with increasing return period is probably due to the decrease in relative wave height with increasing return period (Figure 10). Figure 4.6 shows root-mean-square velocities at the toe of the seawall at Dungeness. This translates into percentage increases in scour potential that vary between14% and 19% and percentage increases in damage potential that vary between 9% and 13%. In these cases the scour and damage potential decreases with return period.

Tables

Table 4.1 Results of individual present day model runs for sloping sea wall at Dungeness

RP (yrs)	H_s (m)	T_p (s)	WL (m)	Beach Slope 1:N	Toe depth (m)	slope	Crest height (m)	Urms toe (m/s)	Umax toe (m/s)	Umin toe (m/s)	Urms mid (m/s)	Umax mid (m/s)	Umin mid (m/s)	Qmean (m^2/s)	Qmax (m^2/s)	Vtotal (m^3/m)	Vmax (m^3/m)	No. waves	NQ
20	1	3.4	4.37	142	0	1.623	6.47	0.36	1.14	-1.46	0.953	3.78	-2.28	4.85E-05	0.205	0.21	0.17	1117	4
20	2	4.8	4.24	142	0	1.623	6.47	0.697	2.72	-1.53	1.358	5.68	-5.76	9.57E-03	2.38	60.34	3.09	1137	282
20	3	5.9	4.05	142	0	1.623	6.47	0.828	3.29	-1.55	1.604	6.7	-6.17	2.99E-02	4.505	228.21	7.63	1193	457
20	4	6.8	3.85	142	0	1.623	6.47	0.857	3.67	-1.55	1.65	7.55	-6.35	3.47E-02	5.369	291.09	9.94	1235	459
50	1	3.4	4.5	142	0	1.623	6.47	0.355	1.13	-1.43	0.928	3.76	-2.23	1.28E-04	0.383	0.55	0.28	1129	13
50	2	4.8	4.42	142	0	1.623	6.47	0.7	2.59	-1.5	1.294	5.43	-2.93	1.65E-02	2.73	104.3	3.46	1136	385
50	3	5.9	4.23	142	0	1.623	6.47	0.844	3.26	-1.54	1.509	6.39	-5.63	4.71E-02	4.876	358.95	8.99	1195	558
50	4	6.8	4	142	0	1.623	6.47	0.877	3.62	-1.55	1.618	7.28	-5.75	5.00E-02	5.994	419.54	11.16	1238	540
200	1	3.4	4.7	142	0	1.623	6.47	0.347	1.1	-1.41	0.888	3.72	-2.14	4.86E-04	0.431	2.09	0.39	1130	48
200	2	4.8	4.58	142	0	1.623	6.47	0.703	2.53	-1.49	1.271	4.98	-2.34	2.56E-02	3.012	161.67	3.99	1134	479
200	3	5.9	4.45	142	0	1.623	6.47	0.862	3.64	-1.5	1.458	6.85	-4.65	7.46E-02	5.957	568.99	10.32	1203	707
200	4	6.8	4.26	142	0	1.623	6.47	0.907	4.07	-1.52	1.525	8.16	-5.65	8.67E-02	7.686	727.83	15.19	1242	707

Table 4.2 Results of individual future scenario model runs for sloping sea wall at Dungeness

RP (yrs)	H_s (m)	T_p (s)	WL (m)	Beach Slope 1:N	Toe depth (m)	slope	Crest height (m)	Urms toe (m/s)	Umax toe (m/s)	Umin toe (m/s)	Urms mid (m/s)	Umax mid (m/s)	Umin mid (m/s)	Qmean ($m^3/s/m$)	Qmax ($m^3/s/m$)	Vtotal (m^3/m)	Vmax (m^3/m)	No. waves	NQ
20	1	3.4	4.74	142	0	1.623	6.47	0.346	1.09	-1.41	0.88	3.5	-2.12	6.73E-04	0.448	2.9	0.47	1133	63
20	2	4.8	4.65	142	0	1.623	6.47	0.702	2.5	-1.47	1.259	4.98	-2.98	3.07E-02	3.116	193.58	4.51	1129	528
20	3	5.9	4.5	142	0	1.623	6.47	0.866	3.7	-1.49	1.452	6.55	-4.64	8.24E-02	6.199	628.67	10.61	1206	724
20	4	6.8	4.28	142	0	1.623	6.47	0.909	4.06	-1.52	1.524	7.96	-5.77	9.03E-02	7.798	757.75	15.57	1238	716
50	1	3.4	4.89	142	0	1.623	6.47	0.34	1.07	-1.4	0.849	3.09	-2.17	1.87E-03	0.736	8.06	0.77	1115	128
50	2	4.8	4.83	142	0	1.623	6.47	0.698	2.45	-1.45	1.238	4.84	-2.16	4.73E-02	3.256	298.21	5.55	1122	643
50	3	5.9	4.64	142	0	1.623	6.47	0.875	3.67	-1.48	1.431	7.18	-3.31	1.07E-01	6.795	818.58	12.23	1202	796
50	4	6.8	4.42	142	0	1.623	6.47	0.924	4.02	-1.5	1.507	7.81	-5.26	1.17E-01	8.406	984.64	17.58	1240	782
200	1	3.4	5.2	142	0	1.623	6.47	0.327	1.11	-1.35	0.787	2.91	-1.95	8.55E-03	1.069	36.82	1.06	1107	306
200	2	4.8	5.12	142	0	1.623	6.47	0.688	2.59	-1.39	1.2	4.58	-2.05	8.56E-02	4.176	539.79	6.73	1115	815
200	3	5.9	4.87	142	0	1.623	6.47	0.885	3.62	-1.46	1.41	6.37	-2.53	1.58E-01	7.556	1204.16	15.33	1193	885
200	4	6.8	4.68	142	0	1.623	6.47	0.948	3.96	-1.48	1.487	7.01	-3.29	1.81E-01	9.702	1519.65	20.33	1252	891

Table 4.3 Results of individual present day model runs for embankment at Dungeness

RP (yrs)	H_s (m)	T_p (s)	WL (m)	Beach Slope 1:N	Toe depth (m)	slope	Crest height (m)	Urms toe (m/s)	Umax toe (m/s)	Umin toe (m/s)	Urms mid (m/s)	Umax mid (m/s)	Umin mid (m/s)	Qmean ($m^3/s/m$)	Qmax ($m^3/s/m$)	Vtotal (m^3/m)	Vmax (m^3/m)	No. waves	NQ
20	1	3.4	4.37	142	-1.965	3	5.55	0.248	0.98	-0.94	0.463	1.6	-2.5	3.32E-03	0.808	14.28	1.02	1074	168
20	2	4.8	4.24	142	-1.965	3	5.55	0.481	1.92	-1.99	1.204	4.12	-4.73	6.94E-02	3.562	437.32	7.5	1110	643
20	3	5.9	4.05	142	-1.965	3	5.55	0.771	2.78	-2.34	1.968	7.68	-4.89	1.84E-01	7.336	1401.05	18.36	1074	792
20	4	6.8	3.85	142	-1.965	3	5.55	0.974	3.26	-2.36	2.333	9.65	-4.85	2.60E-01	10.268	2184.52	28.74	1130	833
50	1	3.4	4.5	142	-1.965	3	5.55	0.248	0.96	-0.96	0.449	1.54	-2.51	7.03E-03	0.903	30.26	1.35	1078	265
50	2	4.8	4.42	142	-1.965	3	5.55	0.473	1.89	-2.01	1.125	3.89	-4.7	9.95E-02	3.87	627.42	8.32	1112	738
50	3	5.9	4.23	142	-1.965	3	5.55	0.76	2.74	-2.32	1.868	7.79	-4.86	2.35E-01	7.824	1789.55	19.65	1079	875
50	4	6.8	4	142	-1.965	3	5.55	0.968	3.23	-2.34	2.283	9.02	-4.86	3.15E-01	11.004	2643.67	30.67	1138	884
200	1	3.4	4.7	142	-1.965	3	5.55	0.245	0.95	-1.01	0.429	1.44	-1.94	1.86E-02	1.186	80.14	1.75	1076	495
200	2	4.8	4.58	142	-1.965	3	5.55	0.467	1.87	-2.03	1.063	3.46	-4.65	1.34E-01	4.154	843.04	8.98	1101	841
200	3	5.9	4.45	142	-1.965	3	5.55	0.745	2.69	-2.29	1.749	7.07	-4.81	3.09E-01	8.424	2358.36	21.87	1090	951
200	4	6.8	4.26	142	-1.965	3	5.55	0.957	3.34	-2.31	2.179	8.07	-4.9	4.21E-01	12.118	3533.87	33.64	1139	961

Table 4.4 Results of individual future scenario model runs for embankment at Dungeness

RP (yrs)	H_s (m)	T_p (s)	WL (m)	Beach Slope 1:N	Toe depth (m)	slope	Crest height (m)	Urms toe (m/s)	Umax toe (m/s)	Umin toe (m/s)	Urms mid (m/s)	Umax mid (m/s)	Umin mid (m/s)	Qmean ($m^3/s/m$)	Qmax ($m^3/s/m$)	Vtotal (m^3/m)	Vmax (m^3/m)	No. waves	NQ
20	1	3.4	4.74	142	-1.965	3	5.55	0.244	0.94	-1	0.425	1.42	-1.95	2.21E-02	1.263	94.99	1.82	1077	537
20	2	4.8	4.65	142	-1.965	3	5.55	0.464	1.96	-1.74	1.037	3.31	-4.62	1.51E-01	4.366	952.97	9.32	1103	888
20	3	5.9	4.5	142	-1.965	3	5.55	0.742	2.68	-2.29	1.721	6.84	-4.79	3.28E-01	8.554	2503.82	22.72	1090	964
20	4	6.8	4.28	142	-1.965	3	5.55	0.956	3.34	-2.31	2.17	8	-4.9	4.30E-01	12.23	3611.73	33.87	1140	965
50	1	3.4	4.89	142	-1.965	3	5.55	0.242	0.93	-0.91	0.411	1.37	-1.97	3.92E-02	1.504	168.87	2.11	1085	676
50	2	4.8	4.83	142	-1.965	3	5.55	0.457	1.96	-1.77	0.975	3.05	-3.95	2.04E-01	4.869	1289.06	10.96	1103	955
50	3	5.9	4.64	142	-1.965	3	5.55	0.733	2.64	-2.27	1.645	6.28	-4.75	3.86E-01	9.058	2943.96	24.92	1097	990
50	4	6.8	4.42	142	-1.965	3	5.55	0.95	3.35	-2.29	2.103	7.82	-4.91	4.99E-01	12.811	4184.26	36.26	1142	987
200	1	3.4	5.2	142	-1.965	3	5.55	0.236	0.92	-0.99	0.388	1.57	-2.03	1.05E-01	1.879	451.15	3.37	1095	949
200	2	4.8	5.12	142	-1.965	3	5.55	0.448	1.9	-1.82	0.894	2.8	-3.77	3.17E-01	5.611	2000.37	13.32	1098	1033
200	3	5.9	4.87	142	-1.965	3	5.55	0.722	2.79	-2.24	1.533	5.77	-4.79	4.96E-01	9.936	3780.12	27.55	1101	1023
200	4	6.8	4.68	142	-1.965	3	5.55	0.937	3.39	-2.27	1.982	7.77	-4.9	6.45E-01	13.86	5412.63	42.22	1137	1019

Table 4.5 Results of individual present day model runs for shingle beach at Dungeness

RP (yrs)	H_s (m)	T_p (s)	WL (m)	Beach Slope 1:N	Toe depth (m)	slope	Crest height (m)	Urms toe (m/s)	Umax toe (m/s)	Umin toe (m/s)	Urms mid (m/s)	Umax mid (m/s)	Umin mid (m/s)	Qmean ($m^3/s/m$)	Qmax ($m^3/s/m$)	Vtotal (m^3/m)	Vmax (m^3/m)	No. waves	NQ
20	1	3.4	4.37	142	-3.93	5	5.55	0.217	0.85	-1	0.4	1.45	-1.74	2.43E-04	0.347	1.05	0.52	1104	13
20	2	4.8	4.24	142	-3.93	5	5.55	0.429	1.64	-1.65	0.728	2.63	-3.35	2.56E-02	2.327	161.51	5.4	1107	384
20	3	5.9	4.05	142	-3.93	5	5.55	0.644	2.55	-2.09	1.16	3.84	-5.13	9.80E-02	5.56	747.63	15.82	1118	579
20	4	6.8	3.85	142	-3.93	5	5.55	0.805	3.31	-2.56	1.6	4.81	-5.39	1.80E-01	9.14	1512.27	27.48	1101	650
50	1	3.4	4.5	142	-3.93	5	5.55	0.216	0.84	-0.99	0.394	1.4	-1.79	8.45E-04	0.443	3.64	0.73	1100	53
50	2	4.8	4.42	142	-3.93	5	5.55	0.426	1.62	-1.69	0.71	2.55	-3.38	4.39E-02	2.652	276.93	6.06	1109	501
50	3	5.9	4.23	142	-3.93	5	5.55	0.64	2.51	-2.09	1.121	3.73	-4.89	1.34E-01	6.071	1020.52	17.13	1120	661
50	4	6.8	4	142	-3.93	5	5.55	0.806	3.3	-2.6	1.555	5.18	-5.38	2.21E-01	9.61	1852.08	29.02	1100	700
200	1	3.4	4.7	142	-3.93	5	5.55	0.214	0.82	-0.89	0.384	1.34	-1.55	4.32E-03	0.693	18.58	1.12	1103	174
200	2	4.8	4.58	142	-3.93	5	5.55	0.422	1.61	-1.72	0.696	2.49	-3.41	6.72E-02	3.053	423.5	7.08	1108	627
200	3	5.9	4.45	142	-3.93	5	5.55	0.637	2.48	-2.14	1.079	3.63	-4.85	1.91E-01	6.619	1455.51	18.61	1124	758
200	4	6.8	4.26	142	-3.93	5	5.55	0.805	3.29	-2.51	1.481	4.99	-5.22	3.07E-01	10.672	2574.56	34.21	1096	785

Table 4.6 Results of individual future scenario model runs for shingle beach at Dungeness

RP (yrs)	H_s (m)	T_p (s)	WL (m)	Beach Slope 1:N	Toe depth (m)	slope	Crest height (m)	Urms toe (m/s)	Umax toe (m/s)	Umin toe (m/s)	Urms mid (m/s)	Umax mid (m/s)	Umin mid (m/s)	Qmean ($m^3/s/m$)	Qmax ($m^3/s/m$)	Vtotal (m^3/m)	Vmax (m^3/m)	No. waves	NQ
20	1	3.4	4.74	142	-3.93	5	5.55	0.213	0.82	-0.9	0.382	1.33	-1.56	5.68E-03	0.729	24.47	1.23	1104	210
20	2	4.8	4.65	142	-3.93	5	5.55	0.421	1.6	-1.73	0.691	2.46	-3.42	8.01E-02	3.213	504.96	7.67	1111	661
20	3	5.9	4.5	142	-3.93	5	5.55	0.636	2.48	-2.15	1.069	3.6	-4.84	2.06E-01	6.703	1569.95	18.92	1127	779
20	4	6.8	4.28	142	-3.93	5	5.55	0.805	3.3	-2.52	1.476	4.97	-5.22	3.14E-01	10.716	2638.3	34.54	1097	792
50	1	3.4	4.89	142	-3.93	5	5.55	0.211	0.81	-0.92	0.373	1.29	-1.61	1.43E-02	0.874	61.54	1.59	1102	398
50	2	4.8	4.83	142	-3.93	5	5.55	0.417	1.58	-1.77	0.676	2.4	-3.05	1.21E-01	3.583	764.26	8.92	1109	773
50	3	5.9	4.64	142	-3.93	5	5.55	0.633	2.47	-2.18	1.048	3.54	-4.81	2.53E-01	7.183	1926.18	20.29	1127	838
50	4	6.8	4.42	142	-3.93	5	5.55	0.805	3.3	-2.54	1.442	4.89	-5.2	3.71E-01	11.367	3113.56	36.48	1096	840
200	1	3.4	5.2	142	-3.93	5	5.55	0.209	0.83	-0.95	0.358	1.33	-1.7	6.09E-02	1.369	262.04	2.57	1102	781
200	2	4.8	5.12	142	-3.93	5	5.55	0.409	1.56	-1.66	0.652	2.39	-3.07	2.17E-01	4.297	1368.27	10.34	1111	916
200	3	5.9	4.87	142	-3.93	5	5.55	0.626	2.46	-2.21	1.013	3.69	-4.51	3.47E-01	8.026	2645.33	24.07	1126	910
200	4	6.8	4.68	142	-3.93	5	5.55	0.803	3.29	-2.58	1.383	4.75	-5.16	4.93E-01	12.39	4139.15	39.63	1097	902

Table 4.7 Seawall results for Dungeness to Rye. P= present-day wave/water level conditions, F = future conditions

scenario	Return Period (years)	Waves	WL	Beach Slope (1:nnn)	Toe Depth (m)	Crest elevation (m)	Urms,toe (m/s)	Urms,mid (m/s)	Qmean ($m^3/s/m$)	Qmax ($m^3/s/m$)	Vmax (m^3/m)
20, present	20	P	P	142	0	6.47	0.857	1.65	3.47E-02	5.369	9.94
50, present	50	P	P	142	0	6.47	0.877	1.618	5.00E-02	5.994	11.16
200, present	200	P	P	142	0	6.47	0.907	1.525	8.67E-02	7.686	15.19
20, future	20	F	F	142	0	6.47	0.909	1.524	9.03E-02	7.798	15.57
50, future	50	F	F	142	0	6.47	0.924	1.507	1.17E-01	8.406	17.58
200, future	200	F	F	142	0	6.47	0.948	1.487	1.81E-01	9.702	20.33

Table 4.8 Embankment results for Dungeness to Rye. P= present-day wave/water level conditions, F = future conditions

scenario	Return Period (years)	Waves	WL	Beach Slope (1:nnn)	Toe Depth (m)	Crest elevation (m)	Urms,toe (m/s)	Urms,mid (m/s)	Qmean ($m^3/s/m$)	Qmax ($m^3/s/m$)	Vmax (m^3/m)
20, present	20	P	P	142	-1.965	5.55	0.974	2.333	0.260	10.3	28.74
50, present	50	P	P	142	-1.965	5.55	0.974	2.333	0.315	11.0	30.67
200, present	200	P	P	142	-1.965	5.55	0.974	2.333	0.421	12.1	33.64
20, future	20	F	F	142	-1.965	5.55	0.956	2.17	0.430	12.2	33.87
50, future	50	F	F	142	-1.965	5.55	0.956	2.17	0.499	12.8	36.26
200, future	200	F	F	142	-1.965	5.55	0.956	2.17	0.645	13.9	42.22

Table 4.9 Shingle Beach results for Dungeness to Rye. P= present-day wave/water level conditions, F = future conditions

scenario	Return Period (years)	Waves	WL	Beach Slope (1:nnn)	Toe Depth (m)	Crest elevation (m)	Urms,toe (m/s)	Urms,mid (m/s)	Qmean ($m^3/s/m$)	Qmax ($m^3/s/m$)	Vmax (m^3/m)
20, present	20	P	P	142	-3.93	5.55	0.805	1.6	0.180	9.1	27.48
50, present	50	P	P	142	-3.93	5.55	0.806	1.6	0.221	9.6	29.02
200, present	200	P	P	142	-3.93	5.55	0.806	1.6	0.307	10.7	34.21
20, future	20	F	F	142	-3.93	5.55	0.805	1.476	0.314	10.7	34.54
50, future	50	F	F	142	-3.93	5.55	0.805	1.476	0.371	11.4	36.48
200, future	200	F	F	142	-3.93	5.55	0.805	1.476	0.493	12.4	39.63

Figures

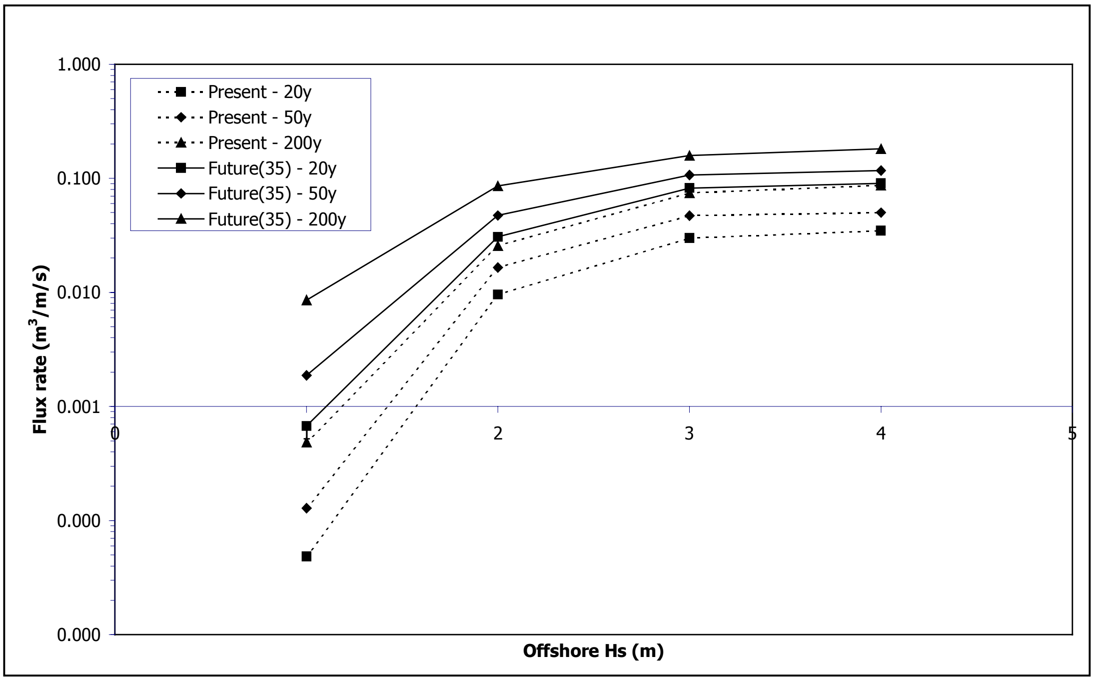

Figure 4.1 **Mean overtopping flux rates for sloping sea wall at Dungeness to Rye**

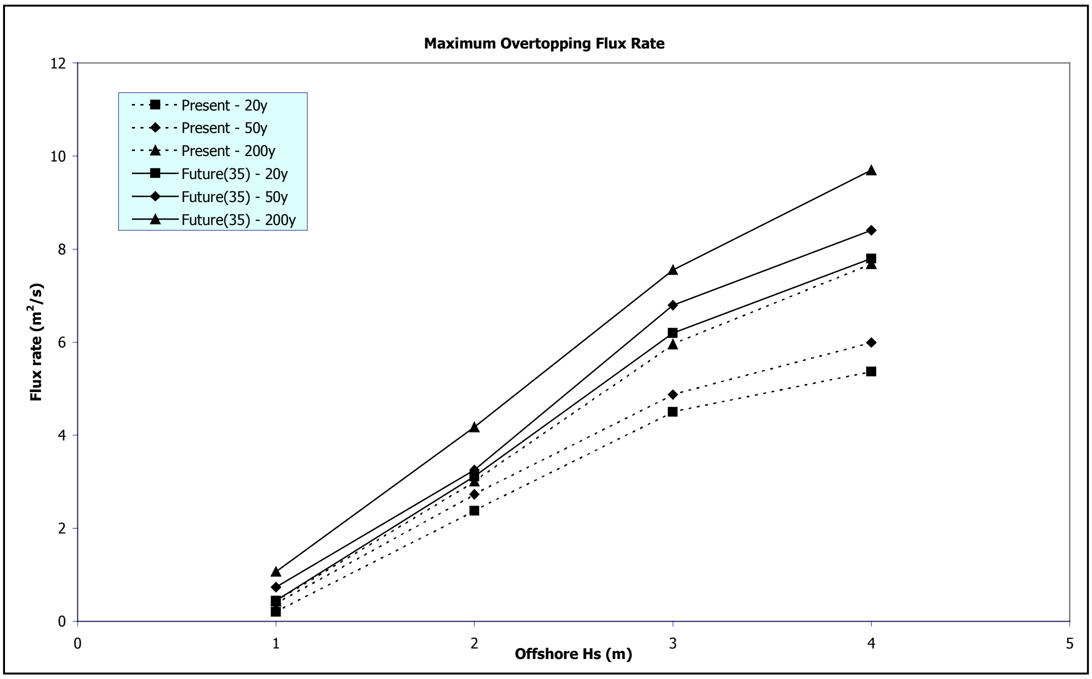

Figure 4.2 **Maximum overtopping flux rates for sloping sea wall at Dungeness to Rye**

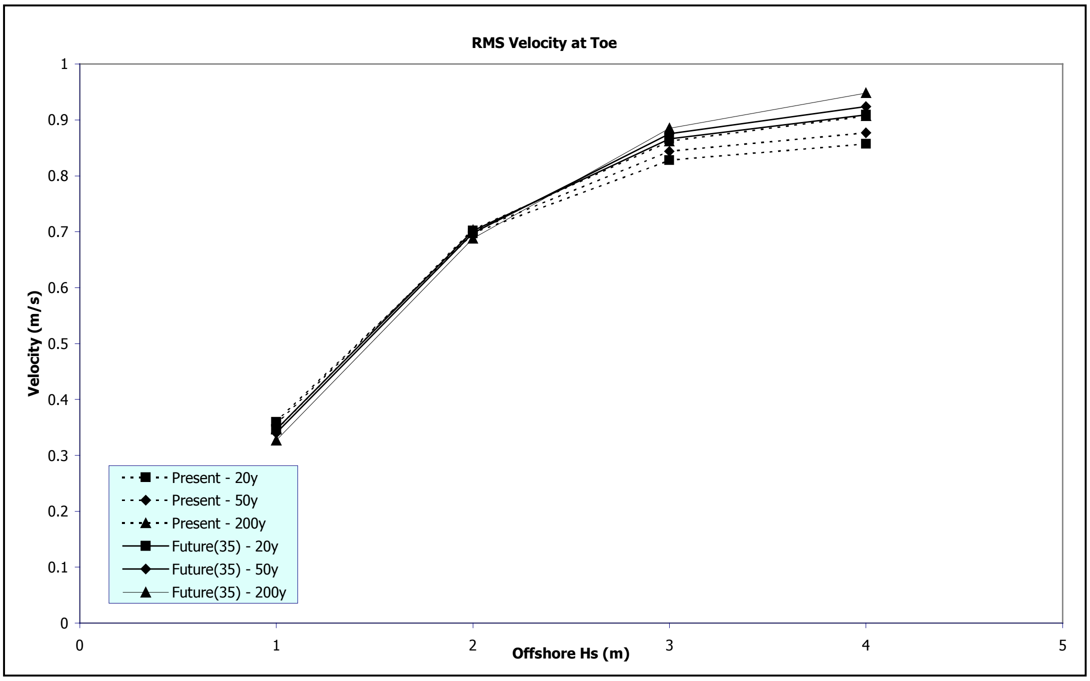

Figure 4.3 **Root-mean-square velocity at toe of sloping sea wall at Dungeness to Rye**

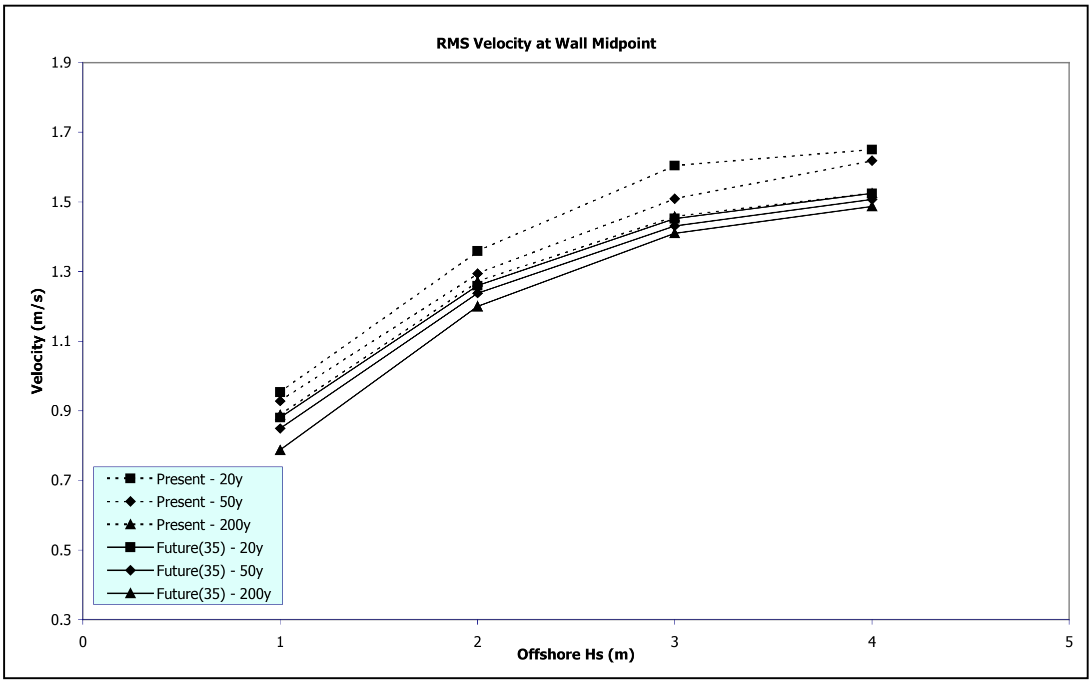

Figure 4.4 **Root-mean-square velocity at midpoint of sloping sea wall at Dungeness to Rye**

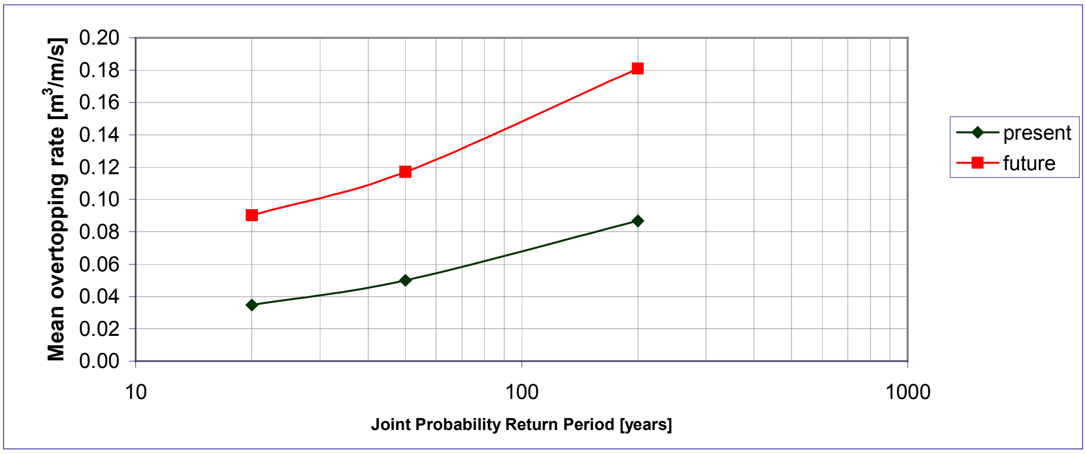

Figure 4.5 **Mean seawall-overtopping rates at Dungeness**

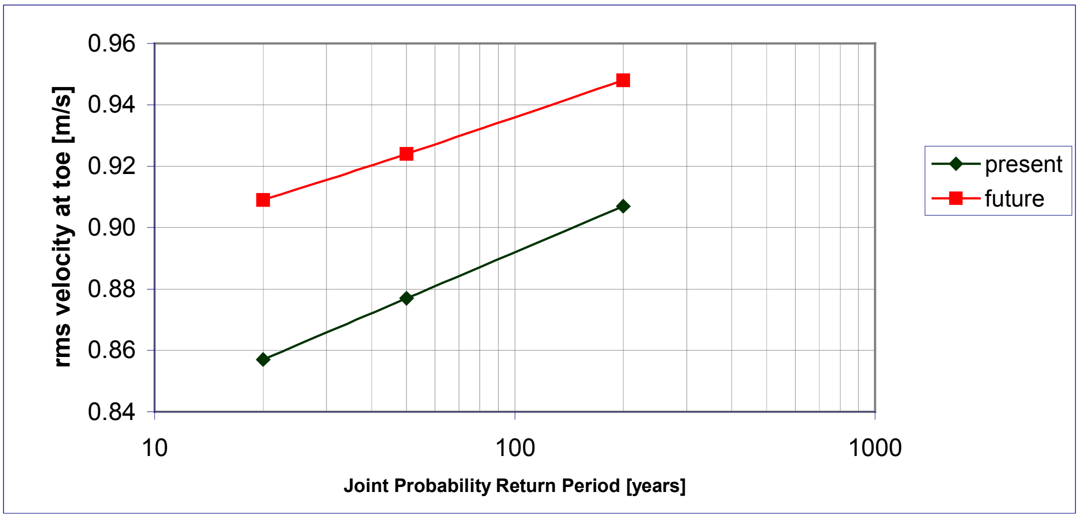

Figure 4.6 **Root-mean-square velocities at toe of seawall at Dungeness**

Appendix 5

COSMOS and OTT results for Lyme Bay

Appendix 5 COSMOS and OTT results for Lyme Bay

The results of the individual model runs for the present and future scenarios, are given in the following tables:

- Table 5.1 for present day results at the seawall
- Table 5.2 for future results at the seawall
- Table 5.3 for present day results at the embankment
- Table 5.4 for future results at the embankment
- Table 5.5 for present day results at the shingle beach
- Table 5.6 for future results at the shingle beach

All elevations are given with respect to ODN (m). All structures have simple cross-sections, comprising of a straight slope from toe to crest. OTT then contains a lower area landwards of the crest that is used to collect the overtopped water. The labels are explained in Appendix 3.

Four water level/wave conditions were modelled from each joint probability contour (for present and future scenarios at 20, 50 and 200-year return periods). Coastal steepening was also modelled for the seawall case. Therefore there are 12 present day and 24 future sets of results for the seawall and 12 cases for present and future for the embankment and shingle beach.

Figure 5.1 shows the mean overtopping flux rates from each test using the sloping sea wall at Lyme Bay. Figure 5.2 shows the maximum overtopping flux rates from each test using the sloping sea wall at Lyme Bay. Figure 5.3 shows the root-mean-square velocity at the toe of the sloping sea wall at Lyme Bay and Figure 5.4 shows the root-mean-square velocity at the midpoint of the sloping sea wall.

The single highest value was used as a representation of the maximum overtopping rate associated with the offshore return period. The worst case values of rms velocity at the structure toe and midpoint and the maximum and mean overtopping rate are given in the following tables:

- Table 5.7 for results at the seawall
- Table 5.8 for results at the embankment
- Table 5.9 for results at the shingle beach.

Figure 5.5 shows mean overtopping rates for the seawall at Lyme Bay. The future overtopping rates are 3.5 and 3.2 times the present day rates (for 50-year and 200-year return period respectively). The future/present overtopping ratios increased to 3.5 and 3.2 for 50-year and 200-year return periods when the coastal steepening scenario was simulated.

This decrease in relative overtopping rate with increasing return period is again probably due to the decrease in relative wave height with increasing return period (Figure 10). Figure 5.6 shows root-mean-square velocities at the toe of the seawall at Lyme Bay. This translates into percentage increases in scour potential that vary between12% and 25% and percentage increases in damage potential that vary between 8% and 14%. Again, the scour and damage potential decrease with return period.

Tables

Table 5.1 Results of individual present day model runs for sloping sea wall at Lyme Bay

RP (yrs)	H_s (m)	T_p (s)	WL (m)	Beach Slope 1:N	Toe depth (m)	slope	Crest height (m)	$Urms_T$ (m/s)	UmaxT (m/s)	Umin toe (m/s)	Urms mid (m/s)	Umax mid (m/s)	Umin mid (m/s)	Qmean (m^3/s)	Qmax (m^3/s)	Vtotal (m^3/m)	Vmax (m^3/m)	No. waves	NQ
20	1	3.4	2.74	206	0	1.623	6.47	0.383	1.03	-1.13	0.884	2.74	-3.57	0.00E+00	0	0	0	1135	0
20	2	4.8	2.65	206	0	1.623	6.47	0.548	2.21	-1.49	1.049	4.22	-4.43	0.00E+00	0	0	0	1195	0
20	3	5.9	2.5	206	0	1.623	6.47	0.574	2.59	-1.61	0.992	4.87	-4.3	1.10E-05	0.146	0.08	0.08	1157	1
20	4	6.8	2.21	206	0	1.623	6.47	0.552	2.6	-1.5	0.803	5.66	-4.44	1.99E-06	0.033	0.02	0.02	1160	1
50	1	3.4	2.93	206	0	1.623	6.47	0.389	1.05	-1.12	1.115	3.91	-5.12	0.00E+00	0	0	0	1136	0
50	2	4.8	2.82	206	0	1.623	6.47	0.572	2.11	-1.51	1.195	5.14	-5.87	7.12E-06	0.052	0.04	0.04	1215	1
50	3	5.9	2.68	206	0	1.623	6.47	0.605	2.52	-1.6	1.14	5.61	-5.18	4.48E-05	0.44	0.34	0.34	1154	1
50	4	6.8	2.43	206	0	1.623	6.47	0.593	2.91	-1.62	0.989	5.87	-5.14	2.94E-05	0.299	0.25	0.25	1178	1
200	1	3.4	3.29	206	0	1.623	6.47	0.394	1.12	-1.28	1.446	4.15	-5.11	0.00E+00	0	0	0	1126	0
200	2	4.8	3.15	206	0	1.623	6.47	0.615	2.39	-1.62	1.478	6.1	-5.87	6.42E-05	0.369	0.4	0.39	1222	2
200	3	5.9	3.06	206	0	1.623	6.47	0.668	2.8	-1.58	1.488	6.46	-6.08	3.23E-04	1.315	2.47	1.27	1146	24
200	4	6.8	2.74	206	0	1.623	6.47	0.65	3.07	-1.57	1.26	5.8	-5.87	1.83E-04	0.832	1.54	1.03	1219	12

Table 5.2 Results of individual future scenario model runs for sloping sea wall at Lyme Bay

RP (yrs)	H_s (m)	T_p (s)	WL (m)	Beach Slope 1:N	Toe depth (m)	slope	Crest height (m)	$Urms_T$ (m/s)	UmaxT (m/s)	Umin toe (m/s)	Urms mid (m/s)	Umax mid (m/s)	Umin mid (m/s)	Qmean (m^3/s)	Qmax (m^3/s)	Vtotal (m^3/m)	Vmax (m^3/m)	No. waves	NQ
20	1	3.4	3.02	206	0	1.623	6.47	0.391	1.07	-1.13	1.21	3.45	-4.77	0.00E+00	0	0	0	1131	0
20	2	4.8	2.92	206	0	1.623	6.47	0.586	2.06	-1.52	1.294	4.75	-5.52	2.17E-05	0.214	0.14	0.14	1223	1
20	3	5.9	2.77	206	0	1.623	6.47	0.619	2.48	-1.58	1.223	5.5	-5.18	5.96E-05	0.621	0.45	0.45	1153	1
20	4	6.8	2.52	206	0	1.623	6.47	0.61	2.83	-1.6	1.07	6.01	-4.79	5.93E-05	0.601	0.5	0.5	1197	1
20	1	3.4	3.02	191	0	1.623	6.47	0.393	1.07	-1.14	1.209	3.36	-5.4	0.00E+00	0	0	0	1126	0
20	2	4.8	2.92	191	0	1.623	6.47	0.591	2.42	-1.55	1.299	4.69	-5.23	2.30E-05	0.233	0.15	0.15	1216	1
20	3	5.9	2.77	191	0	1.623	6.47	0.627	2.48	-1.58	1.233	5.42	-5.23	6.14E-05	0.64	0.47	0.47	1156	1
20	4	6.8	2.52	191	0	1.623	6.47	0.618	2.82	-1.6	1.083	5.67	-5.12	6.46E-05	0.686	0.54	0.54	1199	1
50	1	3.4	3.23	206	0	1.623	6.47	0.394	1.12	-1.26	1.409	3.58	-5.42	0.00E+00	0	0	0	1116	0
50	2	4.8	3.13	206	0	1.623	6.47	0.613	2.4	-1.62	1.456	5.73	-5.5	5.60E-05	0.326	0.35	0.35	1220	2
50	3	5.9	2.92	206	0	1.623	6.47	0.647	2.87	-1.59	1.354	5.44	-6.03	1.30E-04	0.702	1	0.89	1154	7
50	4	6.8	2.68	206	0	1.623	6.47	0.64	3.15	-1.55	1.208	5.77	-5.62	1.13E-04	0.753	0.95	0.8	1211	9
50	1	3.4	3.23	191	0	1.623	6.47	0.395	1.11	-1.27	1.407	3.64	-5.1	0.00E+00	0	0	0	1116	0
50	2	4.8	3.13	191	0	1.623	6.47	0.618	2.4	-1.63	1.46	6.17	-5.45	6.44E-05	0.384	0.41	0.4	1220	2
50	3	5.9	2.92	191	0	1.623	6.47	0.654	2.87	-1.6	1.362	6.04	-6.07	1.55E-04	0.877	1.18	0.98	1156	11
50	4	6.8	2.68	191	0	1.623	6.47	0.647	3.16	-1.56	1.214	5.79	-5.67	1.41E-04	0.75	1.18	0.93	1208	10
200	1	3.4	3.61	206	0	1.623	6.47	0.392	1.19	-1.31	1.541	3.97	-5.5	0.00E+00	0	0	0	1125	0
200	2	4.8	3.52	206	0	1.623	6.47	0.653	2.66	-1.56	1.826	5.28	-6.08	4.40E-04	0.915	2.77	1.12	1158	31
200	3	5.9	3.18	206	0	1.623	6.47	0.69	2.75	-1.62	1.591	5.89	-5.89	7.10E-04	1.57	5.42	1.71	1155	39
200	4	6.8	2.98	206	0	1.623	6.47	0.693	2.98	-1.61	1.51	6.07	-6.11	8.90E-04	1.674	7.47	1.88	1225	48
200	1	3.4	3.61	191	0	1.623	6.47	0.393	1.19	-1.31	1.542	3.91	-5.21	0.00E+00	0	0	0	1124	0
200	2	4.8	3.52	191	0	1.623	6.47	0.657	2.66	-1.57	1.835	5.43	-6.17	4.73E-04	0.905	2.98	1.17	1162	33
200	3	5.9	3.18	191	0	1.623	6.47	0.697	2.75	-1.62	1.595	6.02	-6.32	8.29E-04	1.577	6.32	1.92	1154	43
200	4	6.8	2.98	191	0	1.623	6.47	0.7	2.98	-1.61	1.506	6.42	-6.21	1.04E-03	1.699	8.73	2.13	1225	51

Table 5.3 Results of individual present day model runs for embankment at Lyme Bay

RP (yrs)	H_s (m)	T_p (s)	WL (m)	Beach Slope 1:N	Toe depth (m)	slope	Crest height (m)	Urms toe (m/s)	Umax toe (m/s)	Umin toe (m/s)	Urms mid (m/s)	Umax mid (m/s)	Umin mid (m/s)	Qmean ($m^3/s/m$)	Qmax ($m^3/s/m$)	Vtotal (m^3/m)	Vmax (m^3/m)	No. waves	NQ
20	1	3.4	2.74	206	-1.11	3	4.56	0.273	1.01	-0.86	0.97	3.57	-3.69	3.05E-06	0.012	0.01	0.01	1100	1
20	2	4.8	2.65	206	-1.11	3	4.56	0.607	2.07	-1.86	1.821	6.21	-4	5.86E-03	1.68	36.97	3.04	1131	190
20	3	5.9	2.5	206	-1.11	3	4.56	0.794	2.67	-1.86	1.973	6.62	-4.05	1.66E-02	3.125	126.91	6.62	1088	314
20	4	6.8	2.21	206	-1.11	3	4.56	0.856	2.91	-1.88	1.942	7.86	-4.03	1.16E-02	3.096	97.29	6.55	1098	229
50	1	3.4	2.93	206	-1.11	3	4.56	0.27	0.93	-0.93	0.84	2.97	-3.64	2.70E-05	0.113	0.12	0.12	1087	1
50	2	4.8	2.82	206	-1.11	3	4.56	0.6	2.2	-1.83	1.767	5.51	-4	1.22E-02	2.129	77.08	3.69	1134	285
50	3	5.9	2.68	206	-1.11	3	4.56	0.802	2.65	-1.84	1.98	6.71	-4.04	3.12E-02	3.595	238.25	7.88	1080	460
50	4	6.8	2.43	206	-1.11	3	4.56	0.877	3.01	-1.88	2.009	7.17	-4.02	2.66E-02	3.911	223.33	8.78	1094	395
200	1	3.4	3.29	206	-1.11	3	4.56	0.27	0.98	-0.9	0.668	2.23	-3.38	4.36E-04	0.441	1.88	0.51	1072	47
200	2	4.8	3.15	206	-1.11	3	4.56	0.583	2.19	-1.8	1.628	6.44	-3.9	3.72E-02	2.711	234.26	5.52	1119	527
200	3	5.9	3.06	206	-1.11	3	4.56	0.804	2.76	-1.81	1.938	6.75	-3.99	8.81E-02	4.995	671.89	11.93	1074	682
200	4	6.8	2.74	206	-1.11	3	4.56	0.897	2.99	-1.84	2.036	7.87	-4.02	6.72E-02	5.252	564.22	12.94	1108	593

Table 5.4 Results of individual future scenario model runs for embankment at Lyme Bay

RP (yrs)	H_s (m)	T_p (s)	WL (m)	Beach Slope 1:N	Toe depth (m)	slope	Crest height (m)	Urms toe (m/s)	Umax toe (m/s)	Umin toe (m/s)	Urms mid (m/s)	Umax mid (m/s)	Umin mid (m/s)	Qmean ($m^3/s/m$)	Qmax ($m^3/s/m$)	Vtotal (m^3/m)	Vmax (m^3/m)	No. waves	NQ
20	1	3.4	3.02	206	-1.11	3	4.56	0.271	1.11	-0.95	0.791	2.69	-3.59	4.16E-05	0.203	0.18	0.18	1082	1
20	2	4.8	2.92	206	-1.11	3	4.56	0.595	2.19	-1.83	1.73	6.04	-3.98	1.78E-02	2.334	112.36	4.4	1128	373
20	3	5.9	2.77	206	-1.11	3	4.56	0.804	2.63	-1.83	1.977	6.81	-4.01	4.10E-02	3.904	313.07	8.62	1083	514
20	4	6.8	2.52	206	-1.11	3	4.56	0.884	3.05	-1.87	2.025	7.23	-4.01	3.58E-02	4.172	300.55	9.62	1105	463
50	1	3.4	3.23	206	-1.11	3	4.56	0.27	1.01	-0.88	0.69	2.42	-3.43	2.50E-04	0.336	1.08	0.44	1078	24
50	2	4.8	3.13	206	-1.11	3	4.56	0.585	2.2	-1.81	1.64	6.46	-3.9	3.51E-02	2.679	221.04	5.44	1119	518
50	3	5.9	2.92	206	-1.11	3	4.56	0.805	2.6	-1.83	1.97	7.71	-3.99	6.27E-02	4.526	478.64	10.65	1072	607
50	4	6.8	2.68	206	-1.11	3	4.56	0.894	3.01	-1.85	2.035	8.39	-4	5.72E-02	5.007	480.26	12.3	1104	568
200	1	3.4	3.61	206	-1.11	3	4.56	0.267	1.05	-0.99	0.567	1.72	-2.72	5.80E-03	0.691	24.98	1.09	1087	272
200	2	4.8	3.52	206	-1.11	3	4.56	0.551	2.03	-1.75	1.386	5.97	-3.87	8.86E-02	3.53	558.64	7.44	1125	749
200	3	5.9	3.18	206	-1.11	3	4.56	0.803	2.72	-1.81	1.907	6.72	-3.98	1.14E-01	5.404	872.77	12.96	1080	750
200	4	6.8	2.98	206	-1.11	3	4.56	0.903	3.08	-1.82	2.023	7.01	-4.01	1.17E-01	6.179	982.21	15.78	1122	744

Table 5.5 Results of individual present day model runs for shingle beach at Lyme Bay

RP (yrs)	H_s (m)	T_p (s)	WL (m)	Beach Slope 1:N	Toe depth (m)	slope	Crest height (m)	Urms toe (m/s)	Umax toe (m/s)	Umin toe (m/s)	Urms mid (m/s)	Umax mid (m/s)	Umin mid (m/s)	Qmean ($m^3/s/m$)	Qmax ($m^3/s/m$)	Vtotal (m^3/m)	Vmax (m^3/m)	No. waves	NQ
20	1	3.4	2.74	206	-2.22	5	4.56	0.254	0.95	-1	0.515	1.7	-2.5	0.00E+00	0	0	0	1097	0
20	2	4.8	2.65	206	-2.22	5	4.56	0.494	2.16	-1.55	1.189	3.3	-4.41	1.34E-03	1.183	8.44	2.46	1100	47
20	3	5.9	2.5	206	-2.22	5	4.56	0.632	2.81	-2.21	1.774	5.87	-4.45	1.45E-02	3.162	110.4	8.56	1115	199
20	4	6.8	2.21	206	-2.22	5	4.56	0.697	3.08	-2.55	2.061	6.29	-4.44	1.42E-02	3.649	119.31	10.17	1094	185
50	1	3.4	2.93	206	-2.22	5	4.56	0.251	1.06	-0.92	0.488	1.54	-2.15	0.00E+00	0	0	0	1097	0
50	2	4.8	2.82	206	-2.22	5	4.56	0.497	2.14	-1.59	1.103	3.12	-4.32	3.25E-03	1.405	20.48	3.05	1098	92
50	3	5.9	2.68	206	-2.22	5	4.56	0.641	2.79	-2.1	1.691	5.5	-4.44	2.59E-02	3.694	197.87	9.94	1114	302
50	4	6.8	2.43	206	-2.22	5	4.56	0.708	3.07	-2.46	2	6.45	-4.45	2.90E-02	4.335	243.38	12.92	1093	297
200	1	3.4	3.29	206	-2.22	5	4.56	0.25	1.01	-1.02	0.458	1.58	-1.94	4.70E-05	0.147	0.2	0.19	1100	2
200	2	4.8	3.15	206	-2.22	5	4.56	0.501	2.05	-1.57	0.969	2.79	-4.27	1.37E-02	1.983	86.52	4.61	1098	260
200	3	5.9	3.06	206	-2.22	5	4.56	0.655	2.75	-2.2	1.519	4.65	-4.44	7.13E-02	4.906	544.06	14.08	1114	515
200	4	6.8	2.74	206	-2.22	5	4.56	0.725	3.04	-2.54	1.884	6.1	-4.46	6.61E-02	5.595	554.51	16.53	1092	468

Table 5.6 Results of individual future scenario model runs for shingle beach at Lyme Bay

RP (yrs)	H_s (m)	T_p (s)	WL (m)	Beach Slope 1:N	Toe depth (m)	slope	Crest height (m)	Urms toe (m/s)	Umax toe (m/s)	Umin toe (m/s)	Urms mid (m/s)	Umax mid (m/s)	Umin mid (m/s)	Qmean ($m^3/s/m$)	Qmax ($m^3/s/m$)	Vtotal (m^3/m)	Vmax (m^3/m)	No. waves	NQ
20	1	3.4	3.02	206	-2.22	5	4.56	0.25	1.05	-0.94	0.481	1.47	-2.19	2.38E-07	0.002	0	0	1098	0
20	2	4.8	2.92	206	-2.22	5	4.56	0.499	2.11	-1.51	1.056	3.01	-4.31	5.24E-03	1.551	33	3.37	1099	134
20	3	5.9	2.77	206	-2.22	5	4.56	0.644	2.78	-2.13	1.647	5.33	-4.44	3.38E-02	3.934	257.86	10.54	1113	347
20	4	6.8	2.52	206	-2.22	5	4.56	0.711	3.06	-2.48	1.968	6.41	-4.46	3.76E-02	4.712	315.38	14.15	1090	347
50	1	3.4	3.23	206	-2.22	5	4.56	0.25	1.02	-1.01	0.463	1.62	-1.91	3.15E-05	0.099	0.14	0.14	1099	1
50	2	4.8	3.13	206	-2.22	5	4.56	0.5	2.05	-1.56	0.976	2.81	-4.27	1.27E-02	1.951	80.06	4.51	1098	237
50	3	5.9	2.92	206	-2.22	5	4.56	0.649	2.76	-2.16	1.577	4.94	-4.44	5.05E-02	4.366	385.39	12.35	1113	438
50	4	6.8	2.68	206	-2.22	5	4.56	0.719	3.05	-2.52	1.905	6.48	-4.46	5.70E-02	5.375	478.35	15.94	1090	440
200	1	3.4	3.61	206	-2.22	5	4.56	0.247	0.95	-0.98	0.442	1.45	-1.76	9.85E-04	0.419	4.24	0.66	1102	56
200	2	4.8	3.52	206	-2.22	5	4.56	0.491	1.93	-1.53	0.852	2.82	-3.96	4.43E-02	2.532	279.17	5.93	1098	528
200	3	5.9	3.18	206	-2.22	5	4.56	0.659	2.99	-2.08	1.463	4.87	-4.44	9.30E-02	5.323	709.74	15.21	1114	587
200	4	6.8	2.98	206	-2.22	5	4.56	0.738	3.26	-2.46	1.783	6.23	-4.45	1.12E-01	6.5	937.24	20.33	1089	594

Table 5.7 Seawall results for Lyme Bay. P= present-day wave/water level conditions, F = future conditions

scenario	Return Period (years)	Waves	WL	Beach Slope (1:nnn)	Toe Depth (m)	Crest elevation (m)	Urms,toe (m/s)	Urms,mid (m/s)	Qmean (m^3/s/m)	Qmax (m^3/s/m)	Vmax (m^3/m)
20, present	20	P	P	206	0	6.47	0.574	1.049	1.99E-06	0.146	0.08
50, present	50	P	P	206	0	6.47	0.605	1.195	4.48E-05	0.440	0.34
200, present	200	P	P	206	0	6.47	0.668	1.488	3.23E-04	1.315	1.27
20, future	20	F	F	206	0	6.47	0.619	1.294	5.93E-05	0.621	0.50
50, future	50	F	F	206	0	6.47	0.647	1.456	1.30E-04	0.753	0.89
200, future	200	F	F	206	0	6.47	0.693	1.826	8.90E-04	1.674	1.88
20, future -steepened	20	F	F	191	0	6.47	0.627	1.083	6.46E-05	0.686	0.54
50, future -steepened	50	F	F	191	0	6.47	0.654	1.362	1.55E-04	0.877	0.98
200, future - steepened	200	F	F	191	0	6.47	0.700	1.835	1.04E-03	1.699	2.13

Table 5.8 Embankment results for Lyme Bay. P= present-day wave/water level conditions, F = future conditions

scenario	Return Period (years)	Waves	WL	Beach Slope (1:nnn)	Toe Depth (m)	Crest elevation (m)	Urms,toe (m/s)	Urms,mid (m/s)	Qmean (m^3/s/m)	Qmax (m^3/s/m)	Vmax (m^3/m)
20, present	20	P	P	206	-1.11	4.56	0.856	1.973	0.017	3.13	6.62
50, present	50	P	P	206	-1.11	4.56	0.877	2.009	0.031	3.91	8.78
200, present	200	P	P	206	-1.11	4.56	0.897	2.036	0.088	5.25	12.94
20, future	20	F	F	206	-1.11	4.56	0.884	2.025	0.041	4.17	9.62
50, future	50	F	F	206	-1.11	4.56	0.894	2.035	0.063	5.01	12.3
200, future	200	F	F	206	-1.11	4.56	0.903	2.035	0.117	6.18	15.78

Table 5.9 Shingle Beach results for Lyme Bay. P= present-day wave/water level conditions, F = future conditions

scenario	Return Period (years)	Waves	WL	Beach Slope (1:nnn)	Toe Depth (m)	Crest elevation (m)	Urms,toe (m/s)	Urms,mid (m/s)	Qmean (m^3/s/m)	Qmax (m^3/s/m)	Vmax (m^3/m)
20, present	20	P	P	206	-2.22	4.56	0.697	2.061	0.015	3.65	10.17
50, present	50	P	P	206	-2.22	4.56	0.708	2.061	0.038	4.34	12.92
200, present	200	P	P	206	-2.22	4.56	0.725	2.061	0.071	5.60	16.53
20, future	20	F	F	206	-2.22	4.56	0.711	1.968	0.038	4.71	14.15
50, future	50	F	F	206	-2.22	4.56	0.719	1.968	0.057	5.38	15.94
200, future	200	F	F	206	-2.22	4.56	0.738	1.968	0.112	6.50	20.33

Figures

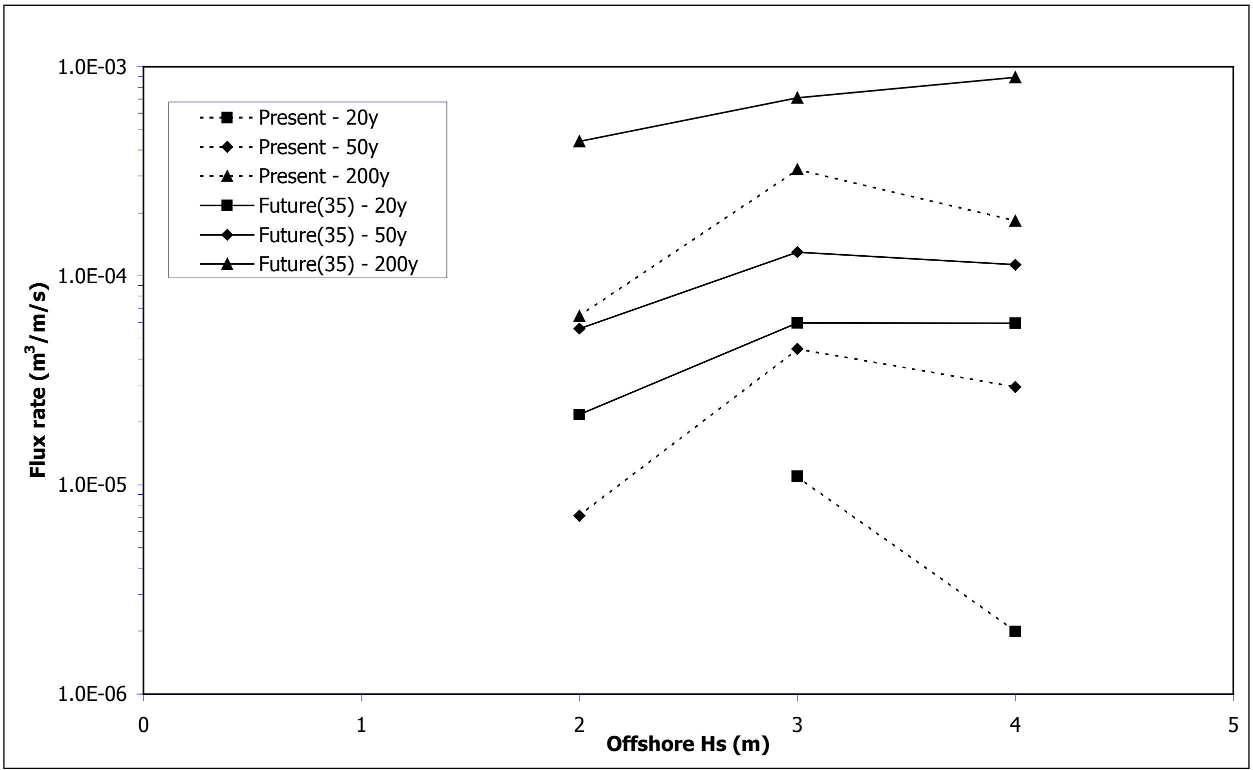

Figure 5.1. Mean overtopping flux rates for sloping sea wall at Lyme Bay

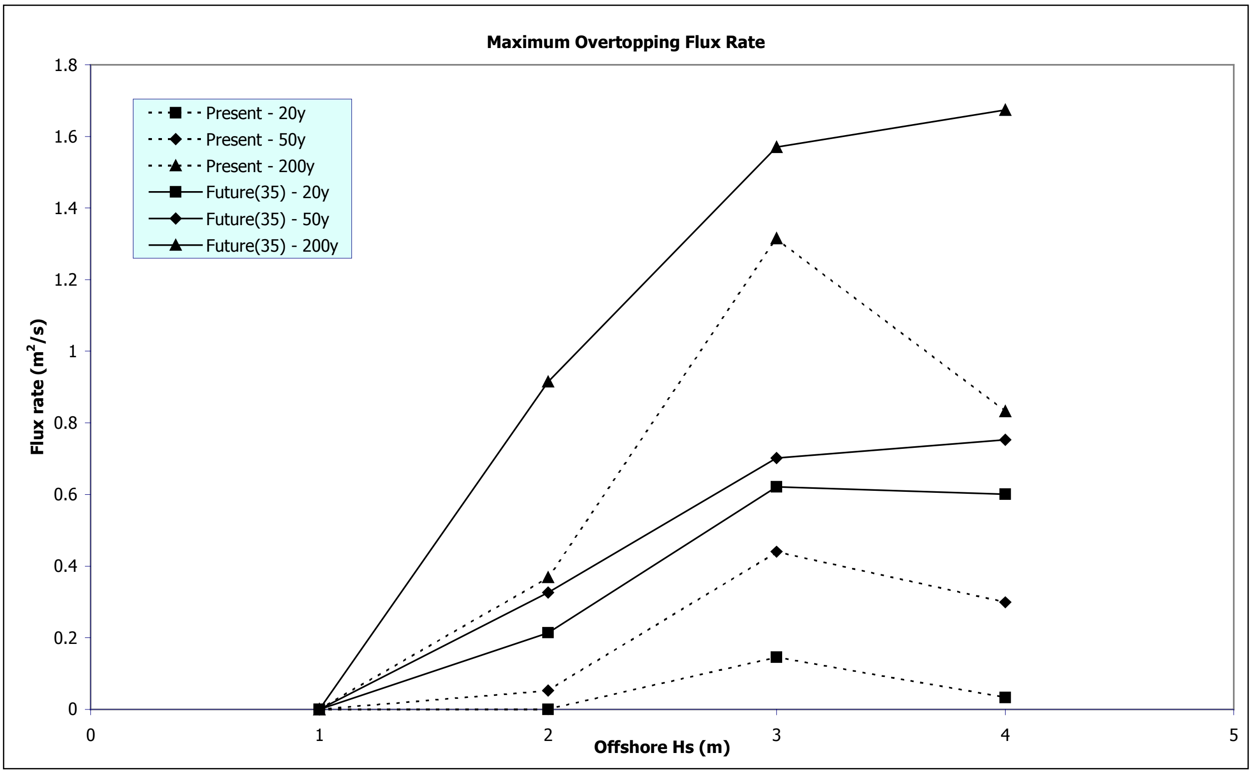

Figure 5.2 Maximum overtopping flux rates for sloping sea wall at Lyme Bay

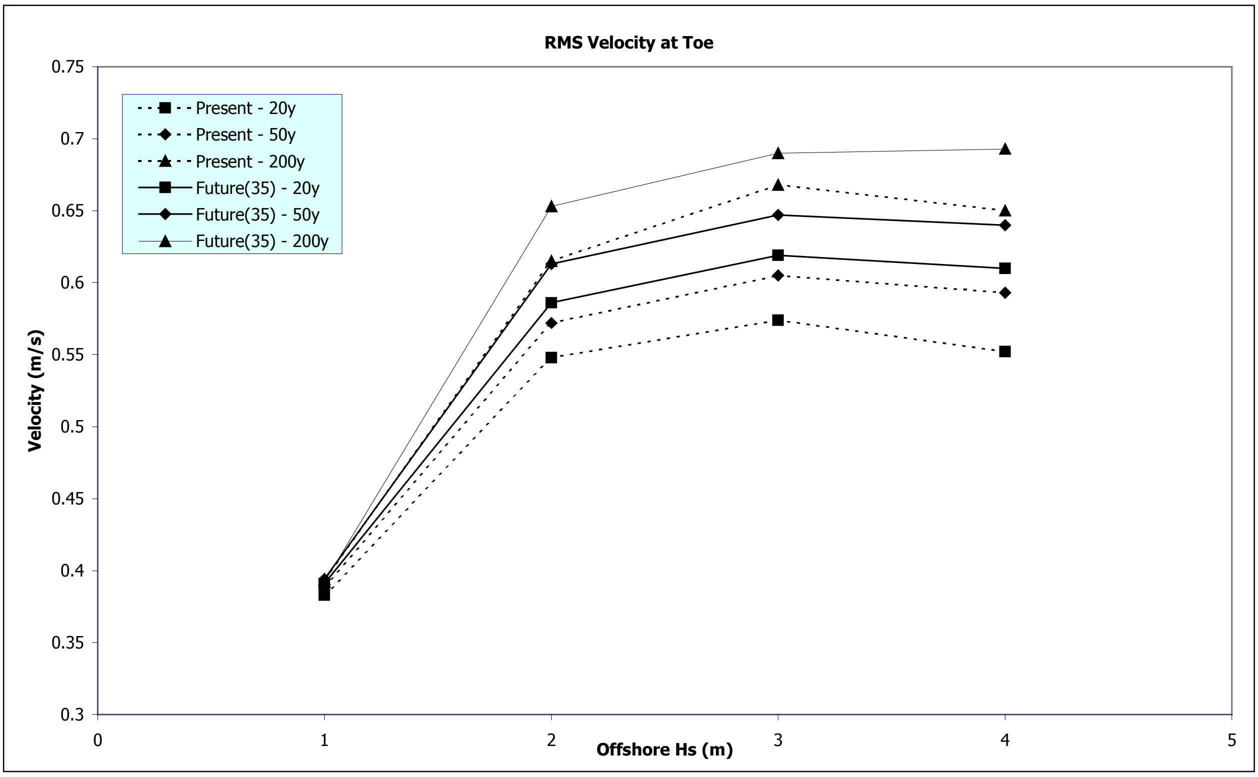

Figure 5.3. Root-mean-square velocity at toe of sloping sea wall at Lyme Bay

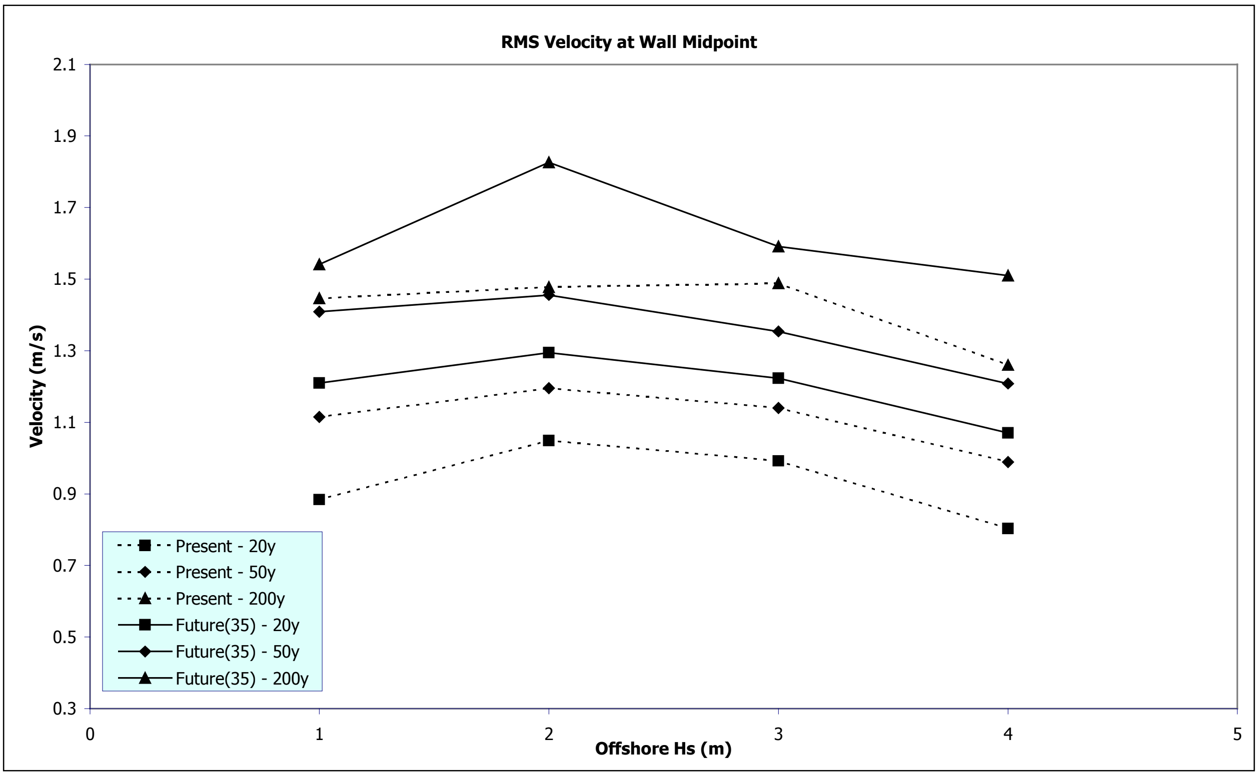

Figure 5.4. Root-mean-square velocity at midpoint of sloping sea wall at Lyme Bay

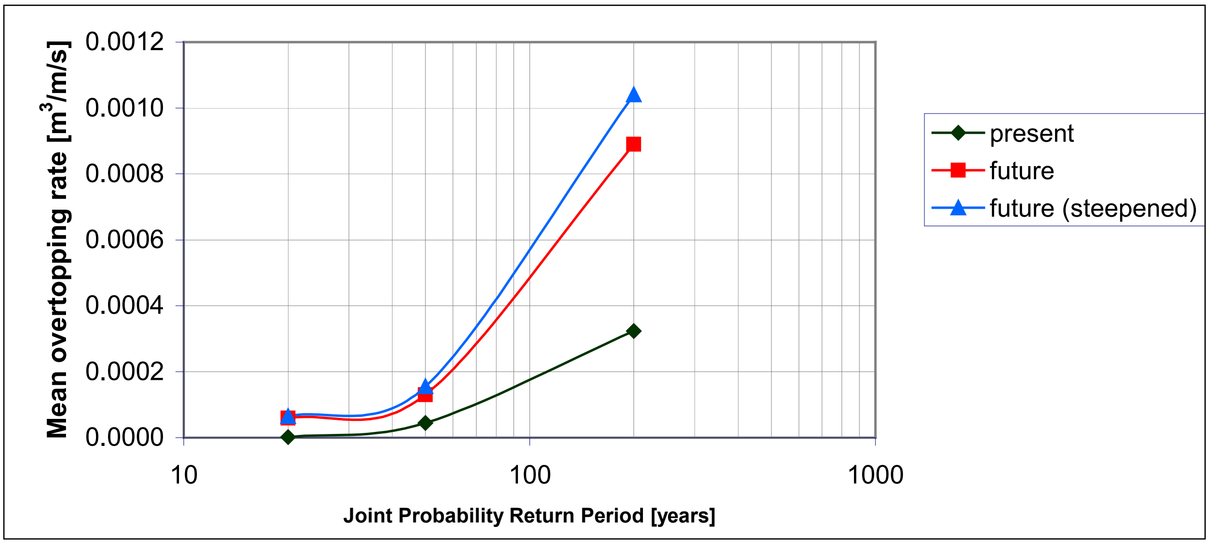

Figure 5.5 Mean seawall-overtopping rates at Lyme Bay

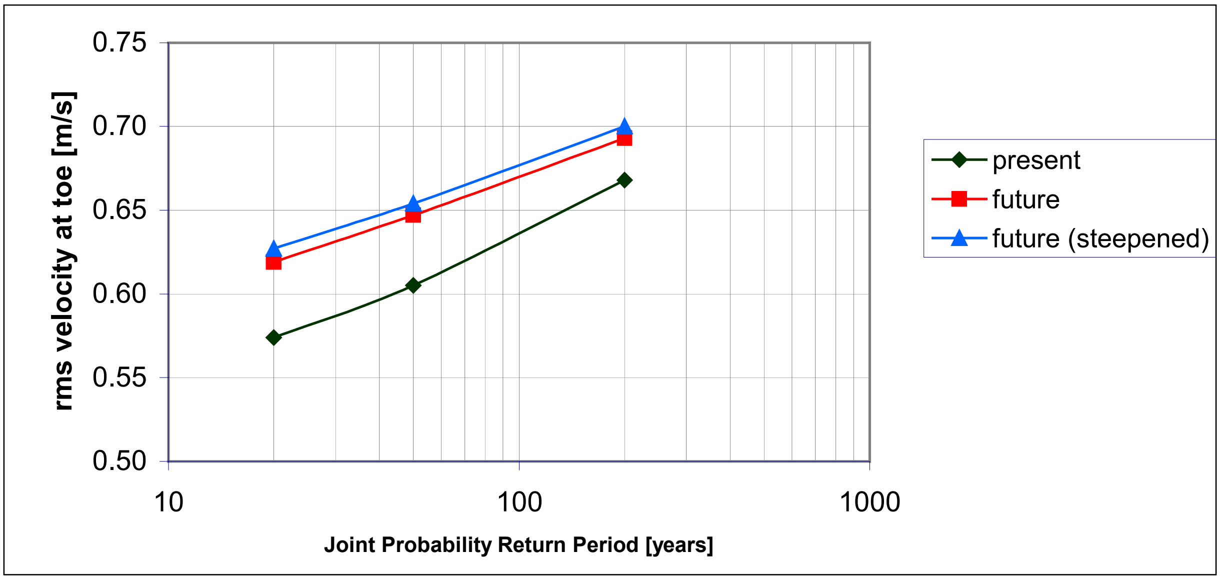

Figure 5.6 Root-mean-square velocities at toe of seawall at Lyme Bay

Appendix 6

COSMOS and OTT results for Swansea Bay

Appendix 6 COSMOS and OTT results for Swansea Bay

The results of the individual model runs for the present and future scenarios, are given in the following tables:

- Table 6.1 for present day results at the seawall
- Table 6.2 for future results at the seawall
- Table 6.3 for present day results at the embankment
- Table 6.4 for future results at the embankment
- Table 6.5 for present day results at the shingle beach
- Table 6.6 for future results at the shingle beach

All elevations are given with respect to ODN (m). All structures have simple cross-sections, comprising of a straight slope from toe to crest. OTT then contains a lower area landwards of the crest that is used to collect the overtopped water. The labels are explained in Appendix 3.

Four water level/wave conditions were modelled from each joint probability contour (for present, future and future+steepened beach scenarios at 20, 50 and 200-year return periods). Therefore there are 12 present day and 24 future sets of results.

Figure 6.1 shows the mean overtopping flux rates from each test using the sloping sea wall at Swansea Bay. Figure 6.2 shows the maximum overtopping flux rates from each test using the sloping sea wall at Swansea Bay. Figure 6.3 shows the root-mean-square velocity at the toe of the sloping sea wall at Swansea Bay and Figure 6.4 shows the root-mean-square velocity at the midpoint of the sloping sea wall.

The single highest value was used as a representation of the maximum overtopping rate associated with the offshore return period. The worst case values of rms velocity at the structure toe and midpoint and the maximum and mean overtopping rate are given in the following tables:

- Table 6.7 for results at the seawall
- Table 6.8 for results at the embankment
- Table 6.9 for results at the shingle beach.

Figure 6.5 shows mean overtopping rates for the seawall at Swansea Bay. The future overtopping rates are 1.4 and 1.3 times the present day rates (for 20-year and 200-year return period respectively). The future/present overtopping ratios increased to 1.6 when the coastal steepening scenario was simulated. Figure 6.5 shows root-mean-square velocities at the toe of the seawall at Swansea Bay. This translates into increases in scour potential around 6% and increases in damage potential around 4%. These percentages do not change significantly with return period. Swansea Bay is the only region where wave heights did not drop in the future model run (Figure 10). There were large increases in scour and damage potential when the coastal steepening scenario was modelled.

Tables

Table 6.1 Results of individual present day model runs for sloping sea wall at Swansea Bay

RP (yrs)	H_s (m)	T_p (s)	WL (m)	Beach Slope 1:N	Toe depth (m)	slope	Crest height (m)	$Urms_T$ (m/s)	UmaxT (m/s)	Umin toe (m/s)	Urms mid (m/s)	Umax mid (m/s)	Umin mid (m/s)	Qmean (m^3/s)	Qmax (m^3/s)	Vtotal (m^3/m)	Vmax (m^3/m)	No. waves	NQ
20	2	5.1	5.32	54	0	1.623	6.47	0.806	3.09	-1.49	1.378	5.63	-2.3	2.04E-01	6.523	1287.02	11.24	1121	974
20	3	6.3	5.19	54	0	1.623	6.47	1.089	4.61	-1.53	1.629	7.96	-3.53	4.56E-01	15.414	3827.11	36.17	1238	1063
20	4	7.2	5.06	54	0	1.623	6.47	1.186	5.49	-1.52	1.737	9.21	-5.45	5.60E-01	18.259	5166.73	47.45	1199	1065
20	5	8.1	4.68	54	0	1.623	6.47	1.216	6.1	-1.56	1.801	9.64	-5.62	4.97E-01	19.867	5046.62	53.37	1214	1023
50	2	5.1	5.43	54	0	1.623	6.47	0.806	3.1	-1.47	1.365	5.79	-2.26	2.46E-01	7.056	1548.31	11.81	1120	1016
50	3	6.3	5.3	54	0	1.623	6.47	1.089	4.58	-1.51	1.613	7.73	-3.15	5.09E-01	15.94	4273.64	38.53	1235	1088
50	4	7.2	5.16	54	0	1.623	6.47	1.189	5.46	-1.53	1.733	9.5	-5.34	6.16E-01	18.823	5684.12	49.15	1202	1091
50	5	8.1	4.85	54	0	1.623	6.47	1.229	6.05	-1.54	1.786	9.77	-5.2	5.90E-01	21.045	5988.09	57.02	1213	1059
200	2	5.1	5.64	54	0	1.623	6.47	0.786	2.99	-1.43	1.321	5.38	-2.13	3.22E-01	7.654	2031.34	14.64	1111	1078
200	3	6.3	5.5	54	0	1.623	6.47	1.091	5.1	-1.47	1.593	8.26	-3.17	6.16E-01	16.909	5166.84	41.64	1227	1133
200	4	7.2	5.3	54	0	1.623	6.47	1.194	5.49	-1.52	1.718	9.38	-3.49	6.99E-01	19.584	6447.44	51.49	1213	1115
200	5	8.1	5.11	54	0	1.623	6.47	1.25	5.98	-1.55	1.768	10	-5.87	7.48E-01	22.96	7595.4	65.47	1206	1106

Table 6.2 Results of individual future scenario model runs for sloping sea wall at Swansea Bay

RP (yrs)	H_s (m)	T_p (s)	WL (m)	Beach Slope 1:N	Toe depth (m)	slope	Crest height (m)	$Urms_T$ (m/s)	UmaxT (m/s)	Umin toe (m/s)	Urms mid (m/s)	Umax mid (m/s)	Umin mid (m/s)	Qmean (m^3/s)	Qmax (m^3/s)	Vtotal (m^3/m)	Vmax (m^3/m)	No. waves	NQ
20	2	5.1	5.72	54	0	1.623	6.47	0.779	2.96	-1.41	1.305	5.21	-2.09	3.55E-01	7.814	2236.86	15.54	1116	1099
20	3	6.3	5.6	54	0	1.623	6.47	1.087	5.04	-1.46	1.581	8.24	-3.25	6.73E-01	17.323	5643.58	43.01	1212	1137
20	4	7.2	5.44	54	0	1.623	6.47	1.197	5.46	-1.5	1.697	8.52	-3.29	7.87E-01	20.282	7263.62	53.7	1210	1141
20	5	8.1	4.94	54	0	1.623	6.47	1.238	6.04	-1.53	1.776	10.8	-5.58	6.42E-01	21.688	6519.81	58.91	1212	1077
20	2	5.1	5.72	30	0	1.623	6.47	0.817	3.05	-1.51	1.384	6.34	-2.28	3.84E-01	7.9	2421	15.97	1141	1105
20	3	6.3	5.6	30	0	1.623	6.47	1.163	5.12	-1.57	1.698	8.05	-3.65	7.33E-01	17.399	6152.23	42.98	1198	1147
20	4	7.2	5.44	30	0	1.623	6.47	1.319	5.78	-1.65	1.889	10.5	-6.21	9.23E-01	23.39	8516.49	64.14	1214	1142
20	5	8.1	4.94	30	0	1.623	6.47	1.407	7.2	-1.72	2.041	11.4	-6.87	8.45E-01	27.79	8578.35	78.64	1199	1089
50	2	5.1	5.83	54	0	1.623	6.47	0.766	2.9	-1.39	1.28	5.27	-2.05	4.03E-01	8.05	2540.22	16.52	1128	1120
50	3	6.3	5.73	54	0	1.623	6.47	1.085	5.01	-1.44	1.566	7.56	-2.12	7.52E-01	17.795	6306.71	44.62	1196	1153
50	4	7.2	5.55	54	0	1.623	6.47	1.199	5.47	-1.49	1.685	8.21	-3.23	8.62E-01	20.759	7952.95	55.41	1207	1150
50	5	8.1	5.18	54	0	1.623	6.47	1.255	5.98	-1.54	1.768	9.68	-5.05	7.95E-01	23.822	8069.09	68.99	1206	1114
50	2	5.1	5.83	30	0	1.623	6.47	0.804	3	-1.49	1.355	6.55	-2.21	4.35E-01	8.433	2743.35	16.61	1142	1124
50	3	6.3	5.73	30	0	1.623	6.47	1.156	5.07	-1.55	1.68	7.67	-3.1	8.15E-01	17.85	6835.63	44.16	1199	1162
50	4	7.2	5.55	30	0	1.623	6.47	1.319	5.74	-1.64	1.877	11.2	-4.96	1.00E+00	24.12	9241.42	66.59	1209	1151
50	5	8.1	5.18	30	0	1.623	6.47	1.418	7.11	-1.69	1.997	11.2	-6.27	1.01E+00	29.451	10280.73	83.9	1197	1122
200	2	5.1	5.96	54	0	1.623	6.47	0.752	2.84	-1.37	1.248	5.49	-1.98	4.67E-01	8.316	2944.28	17.44	1133	1136
200	3	6.3	5.93	54	0	1.623	6.47	1.072	4.94	-1.4	1.534	7.39	-3.12	8.77E-01	18.247	7359.81	46.43	1194	1169
200	4	7.2	5.73	54	0	1.623	6.47	1.206	5.47	-1.47	1.678	9.44	-3.26	9.96E-01	22.446	9192.02	60.74	1207	1167
200	5	8.1	5.41	54	0	1.623	6.47	1.27	5.94	-1.51	1.77	11.4	-3.28	9.62E-01	26.153	9767.13	76.95	1188	1145
200	2	5.1	5.96	30	0	1.623	6.47	0.789	2.93	-1.48	1.317	6.1	-2.17	5.02E-01	8.974	3166.77	17.28	1134	1140
200	3	6.3	5.93	30	0	1.623	6.47	1.138	4.98	-1.52	1.639	8.07	-2.44	9.39E-01	18.787	7879.36	45.62	1180	1177
200	4	7.2	5.73	30	0	1.623	6.47	1.316	6.23	-1.61	1.851	10.2	-5.61	1.14E+00	25.184	10499.62	70.04	1202	1166
200	5	8.1	5.41	30	0	1.623	6.47	1.427	7.06	-1.65	1.982	11.4	-6.29	1.19E+00	30.967	12072.86	89.8	1179	1150

Table 6.3 Results of individual present day model runs for embankment at Swansea Bay

RP (yrs)	H_s (m)	T_p (s)	WL (m)	Beach Slope 1:N	Toe depth (m)	slope	Crest height (m)	$Urms_T$ (m/s)	UmaxT (m/s)	Umin toe (m/s)	Urms mid (m/s)	Umax mid (m/s)	Umin mid (m/s)	Qmean (m^3/s)	Qmax (m^3/s)	Vtotal (m^3/m)	Vmax (m^3/m)	No. waves	NQ
20	2	5.1	5.32	54	-2.56	3	6.14	0.526	2.3	-2.02	1.083	3.28	-4.57	2.85E-01	6.562	1794.58	14.49	1079	956
20	3	6.3	5.19	54	-2.56	3	6.14	0.908	3.26	-2.77	1.979	7.55	-5.39	6.92E-01	15.092	5807.59	45.34	1143	1009
20	4	7.2	5.06	54	-2.56	3	6.14	1.172	4.22	-2.79	2.449	10.5	-5.47	9.63E-01	21.741	8892.05	71.41	1123	1023
20	5	8.1	4.68	54	-2.56	3	6.14	1.415	5.05	-2.86	2.862	11.4	-5.48	1.03E+00	26.015	10431.41	89.01	1117	1017
50	2	5.1	5.43	54	-2.56	3	6.14	0.53	2.3	-2.05	1.069	3.25	-4.54	3.37E-01	7.111	2124.09	16.07	1078	972
50	3	6.3	5.3	54	-2.56	3	6.14	0.9	3.23	-2.76	1.925	7.12	-5.4	7.56E-01	15.606	6343.93	46.66	1141	1025
50	4	7.2	5.16	54	-2.56	3	6.14	1.164	4.23	-2.78	2.404	11.2	-5.46	1.03E+00	22.279	9514.29	73.01	1122	1041
50	5	8.1	4.85	54	-2.56	3	6.14	1.406	5.07	-2.84	2.812	10.9	-5.48	1.15E+00	27.05	11662.09	94.59	1115	1033
200	2	5.1	5.64	54	-2.56	3	6.14	0.525	2.25	-1.79	1.015	3.21	-4.45	4.35E-01	7.794	2741.32	18.63	1081	1008
200	3	6.3	5.5	54	-2.56	3	6.14	0.887	3.2	-2.74	1.829	6.77	-5.42	8.82E-01	16.459	7403.59	49.07	1141	1051
200	4	7.2	5.3	54	-2.56	3	6.14	1.155	4.24	-2.77	2.342	10.7	-5.45	1.13E+00	23.091	10432.67	75.31	1121	1049
200	5	8.1	5.11	54	-2.56	3	6.14	1.393	5.1	-2.81	2.726	12.1	-5.47	1.35E+00	28.724	13743.96	101.75	1117	1062

Table 6.4 Results of individual future scenario model runs for embankment at Swansea Bay

RP (yrs)	H_s (m)	T_p (s)	WL (m)	Beach Slope 1:N	Toe depth (m)	slope	Crest height (m)	$Urms_T$ (m/s)	UmaxT (m/s)	Umin toe (m/s)	Urms mid (m/s)	Umax mid (m/s)	Umin mid (m/s)	Qmean (m^3/s)	Qmax (m^3/s)	Vtotal (m^3/m)	Vmax (m^3/m)	No. waves	NQ
20	2	5.1	5.72	54	-2.56	3	6.14	0.521	2.23	-1.8	0.997	3.19	-4.42	4.78E-01	8.056	3010.27	19.36	1081	1009
20	3	6.3	5.6	54	-2.56	3	6.14	0.881	3.2	-2.73	1.786	6.34	-5.42	9.51E-01	16.852	7983.45	50.2	1138	1043
20	4	7.2	5.44	54	-2.56	3	6.14	1.146	4.25	-2.76	2.272	9.84	-5.43	1.24E+00	23.887	11433.93	77.53	1120	1050
20	5	8.1	4.94	54	-2.56	3	6.14	1.401	5.08	-2.83	2.783	10.8	-5.48	1.22E+00	27.68	12352.04	97.14	1114	1055
50	2	5.1	5.83	54	-2.56	3	6.14	0.519	2.21	-1.82	0.975	3.18	-4.37	5.41E-01	8.396	3409.49	20.3	1082	1005
50	3	6.3	5.73	54	-2.56	3	6.14	0.874	3.21	-2.72	1.73	6.09	-5.42	1.05E+00	17.386	8783.23	51.67	1131	1037
50	4	7.2	5.55	54	-2.56	3	6.14	1.138	4.26	-2.75	2.225	9.27	-5.41	1.33E+00	24.431	12257.77	79.3	1119	1045
50	5	8.1	5.18	54	-2.56	3	6.14	1.39	5.11	-2.81	2.708	12.1	-5.47	1.41E+00	29.172	14333.23	103.38	1119	1063
200	2	5.1	5.96	54	-2.56	3	6.14	0.516	2.18	-1.85	0.948	3.16	-3.85	6.26E-01	8.747	3944.05	21.32	1081	989
200	3	6.3	5.93	54	-2.56	3	6.14	0.857	3.2	-2.69	1.641	6.3	-5.41	1.19E+00	17.958	10012.45	53.44	1128	1039
200	4	7.2	5.73	54	-2.56	3	6.14	1.129	4.27	-2.73	2.147	8.53	-5.39	1.48E+00	25.404	13666.7	81.97	1117	1052
200	5	8.1	5.41	54	-2.56	3	6.14	1.381	5.09	-2.78	2.624	12.9	-5.48	1.62E+00	30.587	16401.47	109.18	1117	1063

Table 6.5 Results of individual present day model runs for shingle beach at Swansea Bay

RP (yrs)	H_s (m)	T_p (s)	WL (m)	Beach Slope 1:N	Toe depth (m)	slope	Crest height (m)	$Urms_T$ (m/s)	Umax T (m/s)	Umin toe (m/s)	Urms mid (m/s)	Umax mid (m/s)	Umin mid (m/s)	Qmean (m^3/s)	Qmax (m^3/s)	Vtotal (m^3/m)	Vmax (m^3/m)	No. waves	NQ
20	2	5.1	5.32	54	-5.12	5	6.14	0.471	1.78	-1.95	0.805	2.89	-3.82	1.73E-01	4.329	1090.22	12.33	1112	745
20	3	6.3	5.19	54	-5.12	5	6.14	0.727	2.82	-2.71	1.318	4.48	-5.54	4.63E-01	10.53	3883.92	36.44	1102	842
20	4	7.2	5.06	54	-5.12	5	6.14	0.908	3.7	-3.09	1.745	5.9	-5.81	6.93E-01	15.873	6395.5	58.08	1095	847
20	5	8.1	4.68	54	-5.12	5	6.14	1.095	4.43	-3.74	2.26	7.13	-5.92	8.25E-01	21.5	8369.08	85.99	1111	846
50	2	5.1	5.43	54	-5.12	5	6.14	0.469	1.77	-1.96	0.794	2.86	-3.83	2.09E-01	4.574	1318.55	12.96	1113	774
50	3	6.3	5.3	54	-5.12	5	6.14	0.725	2.82	-2.74	1.302	4.43	-5.53	5.18E-01	10.956	4350.53	37.59	1101	837
50	4	7.2	5.16	54	-5.12	5	6.14	0.906	3.7	-3.1	1.72	5.81	-5.81	7.54E-01	16.33	6956.68	61.12	1099	839
50	5	8.1	4.85	54	-5.12	5	6.14	1.096	4.44	-3.57	2.213	6.91	-5.92	9.33E-01	22.348	9465.76	90.35	1112	856
200	2	5.1	5.64	54	-5.12	5	6.14	0.465	1.77	-1.99	0.779	2.8	-3.41	2.95E-01	5.062	1857.21	16.22	1115	747
200	3	6.3	5.5	54	-5.12	5	6.14	0.719	2.81	-2.6	1.265	4.34	-5.28	6.33E-01	11.642	5315.57	39.91	1099	807
200	4	7.2	5.3	54	-5.12	5	6.14	0.904	3.69	-3.12	1.685	5.71	-5.79	8.44E-01	16.85	7793.79	64.6	1099	824
200	5	8.1	5.11	54	-5.12	5	6.14	1.093	4.46	-3.6	2.138	6.74	-5.92	1.11E+00	23.605	11309.88	96.32	1114	846

Table 6.6 Results of individual future scenario model runs for shingle beach at Swansea Bay

RP (yrs)	H_s (m)	T_p (s)	WL (m)	Beach Slope 1:N	Toe depth (m)	slope	Crest height (m)	$Urms_T$ (m/s)	Umax T (m/s)	Umin toe (m/s)	Urms mid (m/s)	Umax mid (m/s)	Umin mid (m/s)	Qmean (m^3/s)	Qmax (m^3/s)	Vtotal (m^3/m)	Vmax (m^3/m)	No. waves	NQ
20	2	5.1	5.72	54	-5.12	5	6.14	0.464	1.77	-2.01	0.773	2.77	-3.42	3.34E-01	5.347	2106.22	17.78	1113	728
20	3	6.3	5.6	54	-5.12	5	6.14	0.717	2.8	-2.62	1.248	4.3	-5.26	6.98E-01	11.981	5856.96	45.08	1099	782
20	4	7.2	5.44	54	-5.12	5	6.14	0.902	3.69	-3.13	1.652	5.64	-5.78	9.42E-01	17.469	8694.24	67.38	1098	803
20	5	8.1	4.94	54	-5.12	5	6.14	1.095	4.45	-3.58	2.185	6.92	-5.92	9.92E-01	22.769	10072.94	92.42	1112	849
50	2	5.1	5.83	54	-5.12	5	6.14	0.463	1.77	-2.03	0.764	2.74	-3.43	3.96E-01	5.708	2495.73	26.56	1114	572
50	3	6.3	5.73	54	-5.12	5	6.14	0.714	2.8	-2.63	1.231	4.42	-5.24	7.89E-01	12.453	6624.29	57.63	1100	746
50	4	7.2	5.55	54	-5.12	5	6.14	0.9	3.68	-3.15	1.627	5.58	-5.61	1.03E+00	17.829	9461.68	70.17	1103	773
50	5	8.1	5.18	54	-5.12	5	6.14	1.093	4.46	-3.61	2.12	6.7	-5.92	1.17E+00	23.927	11852.53	97.73	1116	837
200	2	5.1	5.96	54	-5.12	5	6.14	0.461	1.77	-2.04	0.756	2.83	-3.44	4.85E-01	6.118	3056.43	771.91	1117	9
200	3	6.3	5.93	54	-5.12	5	6.14	0.702	2.77	-2.64	1.192	4.29	-5.21	9.39E-01	13.031	7879.96	88.59	1097	404
200	4	7.2	5.73	54	-5.12	5	6.14	0.899	3.67	-2.99	1.594	5.49	-5.59	1.18E+00	18.83	10859.33	82.88	1102	731
200	5	8.1	5.41	54	-5.12	5	6.14	1.092	4.47	-3.63	2.054	7	-5.85	1.36E+00	25.168	13789.32	102.65	1123	795

Table 6.7 Seawall results for Swansea Bay. P= present-day wave/water level conditions, F = future conditions

scenario	Return Period (years)	Waves	WL	Beach Slope (1:nnn)	Toe Depth (m)	Crest elevation (m)	Urms,toe (m/s)	Urms,mid (m/s)	Qmean ($m^3/s/m$)	Qmax ($m^3/s/m$)	Vmax (m^3/m)
20, present	20	P	P	54	0	6.47	1.216	1.801	5.60E-01	19.867	53.37
50, present	50	P	P	54	0	6.47	1.229	1.786	6.16E-01	21.045	57.02
200, present	200	P	P	54	0	6.47	1.25	1.768	7.48E-01	22.96	65.47
20, future	20	F	F	54	0	6.47	1.238	1.776	7.87E-01	21.688	58.91
50, future	50	F	F	54	0	6.47	1.255	1.768	8.62E-01	23.822	68.99
200, future	200	F	F	54	0	6.47	1.27	1.77	9.96E-01	26.153	76.95
20, future -steepened	20	F	F	30	0	6.47	1.407	2.041	9.23E-01	27.79	78.64
50, future -steepened	50	F	F	30	0	6.47	1.418	1.997	1.01E+00	29.451	83.9
200, future - steepened	200	F	F	30	0	6.47	1.427	1.982	1.19E+00	30.967	89.8

Table 6.8 Embankment results for Swansea Bay. P= present-day wave/water level conditions, F = future conditions

scenario	Return Period (years)	Waves	WL	Beach Slope (1:nnn)	Toe Depth (m)	Crest elevation (m)	Urms,toe (m/s)	Urms,mid (m/s)	Qmean ($m^3/s/m$)	Qmax ($m^3/s/m$)	Vmax (m^3/m)
20, present	20	P	P	54	-2.56	6.14	1.415	2.862	1.030	26.0	89.01
50, present	50	P	P	54	-2.56	6.14	1.415	2.783	1.150	27.1	94.59
200, present	200	P	P	54	-2.56	6.14	1.415	2.783	1.350	28.7	101.75
20, future	20	F	F	54	-2.56	6.14	1.401	2.783	1.240	27.7	97.14
50, future	50	F	F	54	-2.56	6.14	1.401	2.783	1.410	29.2	103.38
200, future	200	F	F	54	-2.56	6.14	1.401	2.783	1.620	30.6	109.18

Table 6.9. Shingle Beach results for Swansea Bay. P= present-day wave/water level conditions, F = future conditions

scenario	Return Period (years)	Waves	WL	Beach Slope (1:nnn)	Toe Depth (m)	Crest elevation (m)	Urms,toe (m/s)	Urms,mid (m/s)	Qmean ($m^3/s/m$)	Qmax ($m^3/s/m$)	Vmax (m^3/m)
20, present	20	P	P	54	-5.12	6.14	1.095	2.26	0.825	21.5	85.99
50, present	50	P	P	54	-5.12	6.14	1.096	2.26	0.933	22.3	90.35
200, present	200	P	P	54	-5.12	6.14	1.096	2.26	1.110	23.6	96.32
20, future	20	F	F	54	-5.12	6.14	1.095	2.185	0.992	22.8	92.42
50, future	50	F	F	54	-5.12	6.14	1.095	2.185	1.170	23.9	97.73
200, future	200	F	F	54	-5.12	6.14	1.095	2.185	1.360	25.2	102.65

Figures

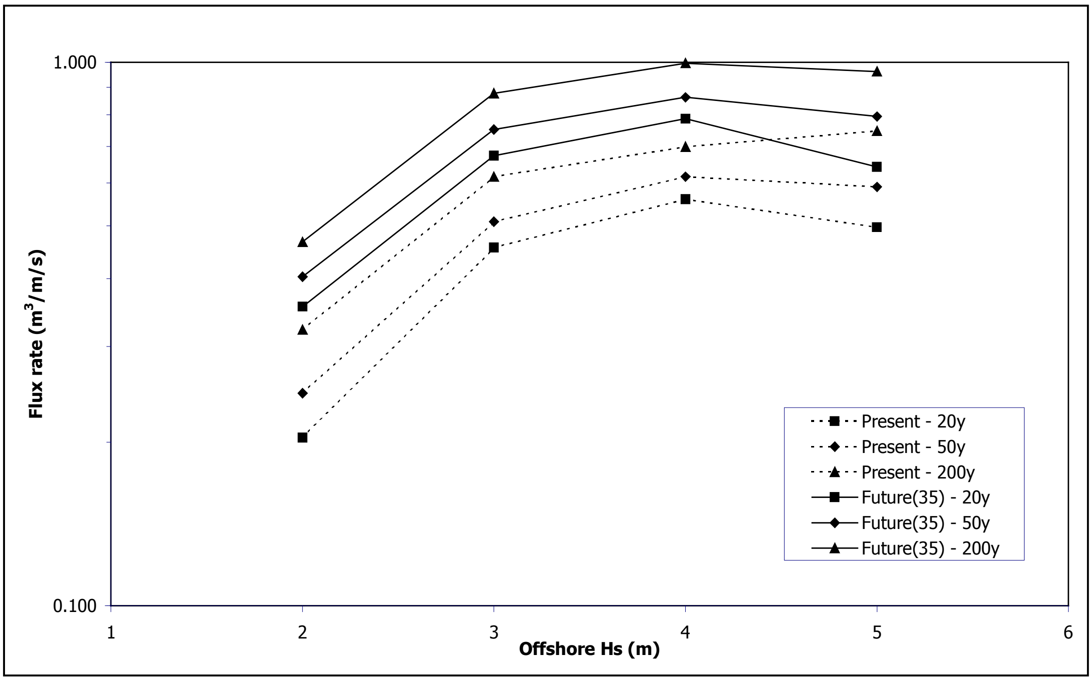

Figure 6.1 Mean overtopping flux rates for sloping sea wall at Swansea Bay

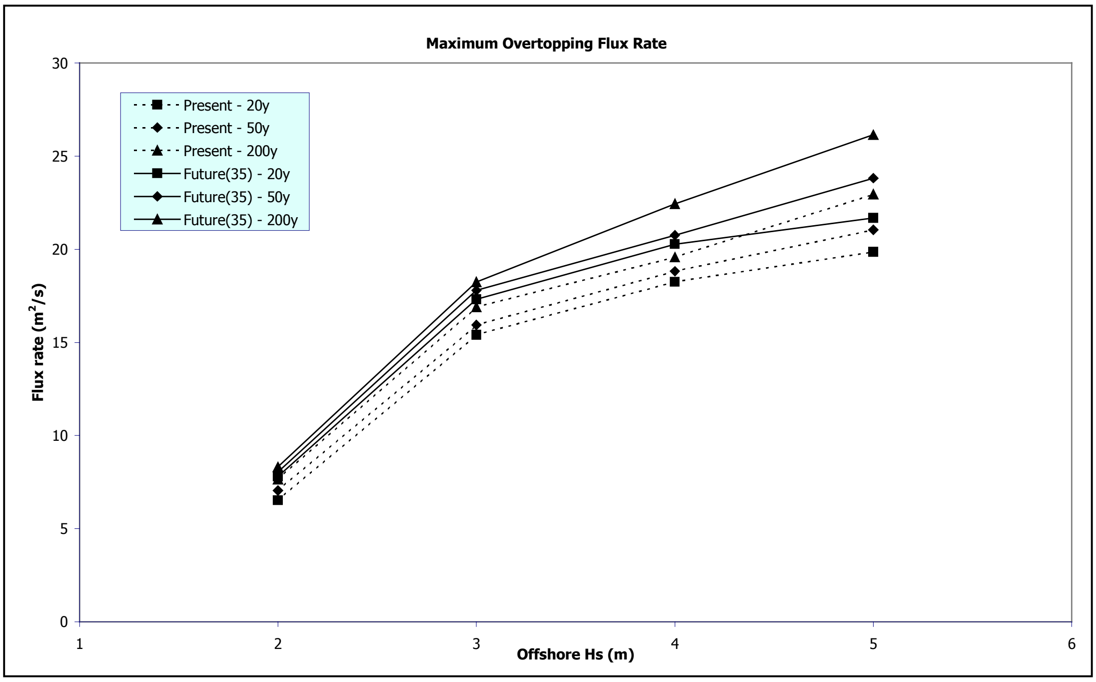

Figure 6.2 Maximum overtopping flux rates for sloping sea wall at Swansea Bay

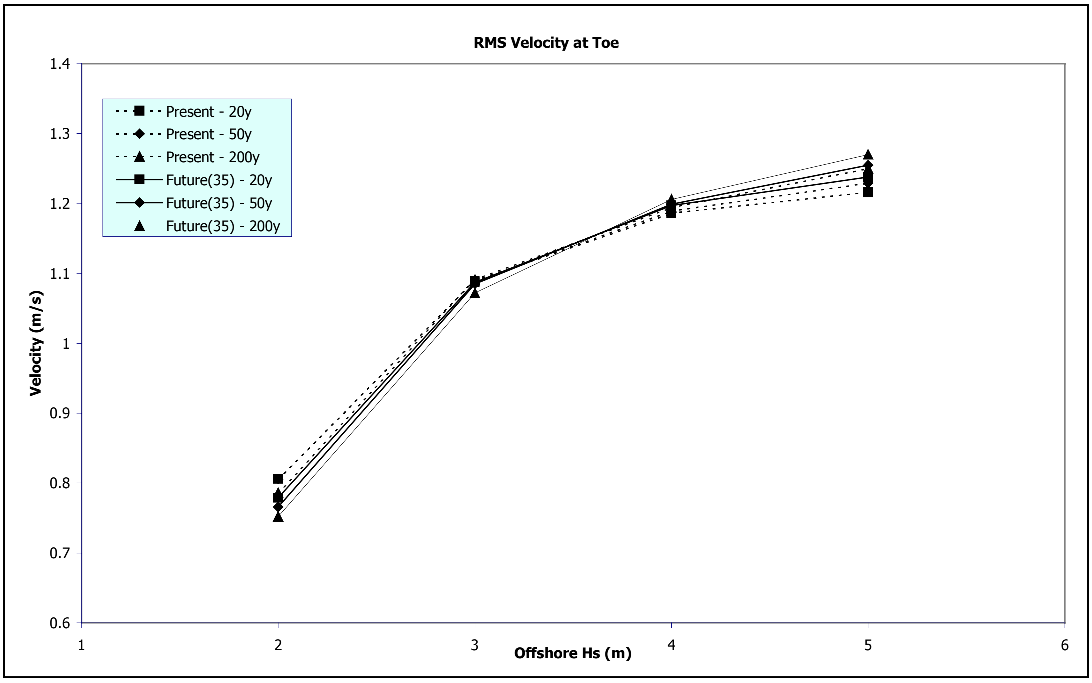

Figure 6.3 Root-mean-square velocity at toe of sloping sea wall at Swansea Bay

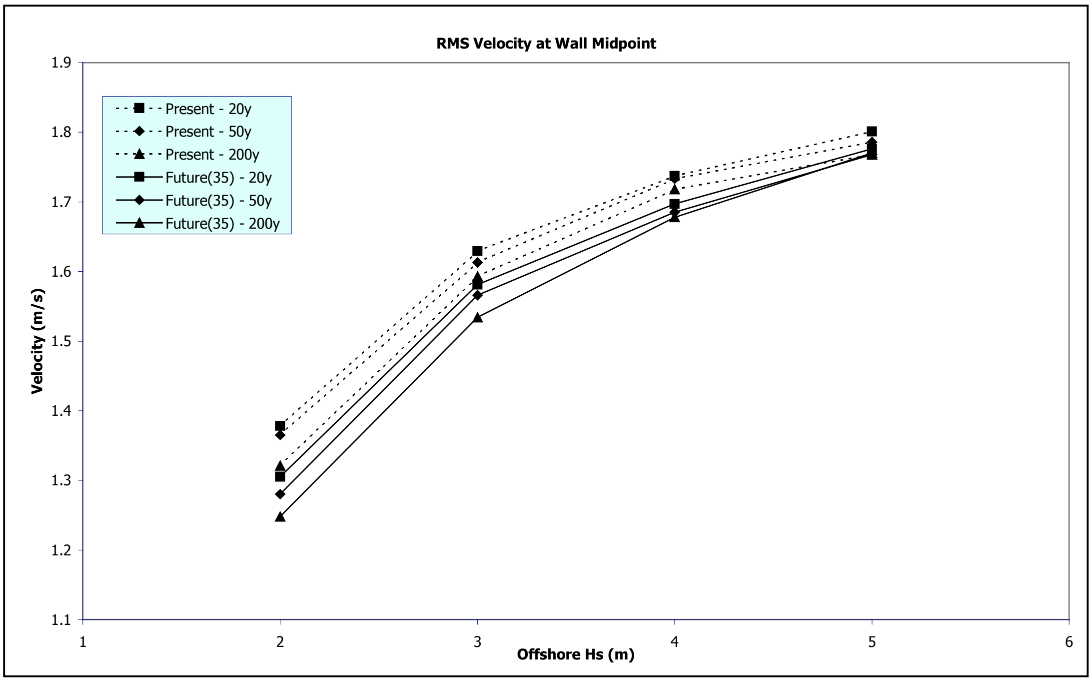

Figure 6.4 Root-mean-square velocity at midpoint of sloping sea wall at Swansea Bay

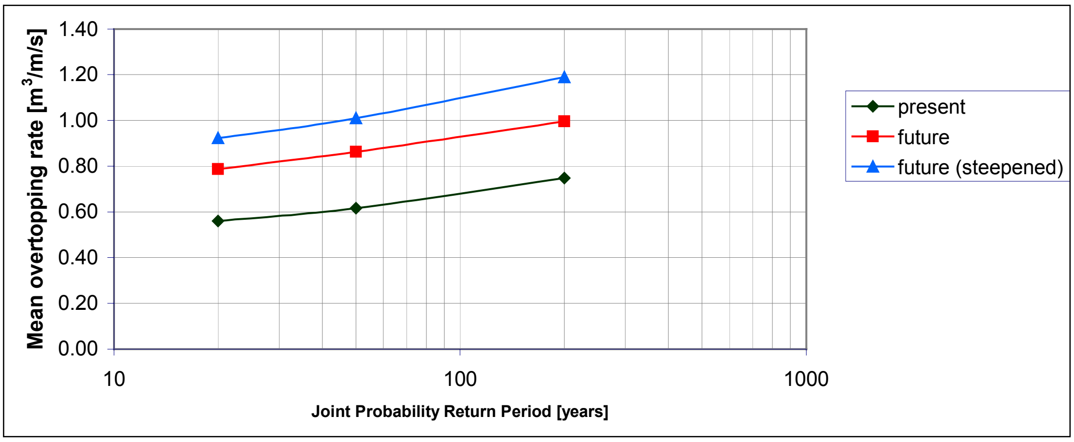

Figure 6.5 **Mean seawall-overtopping rates at Swansea Bay**

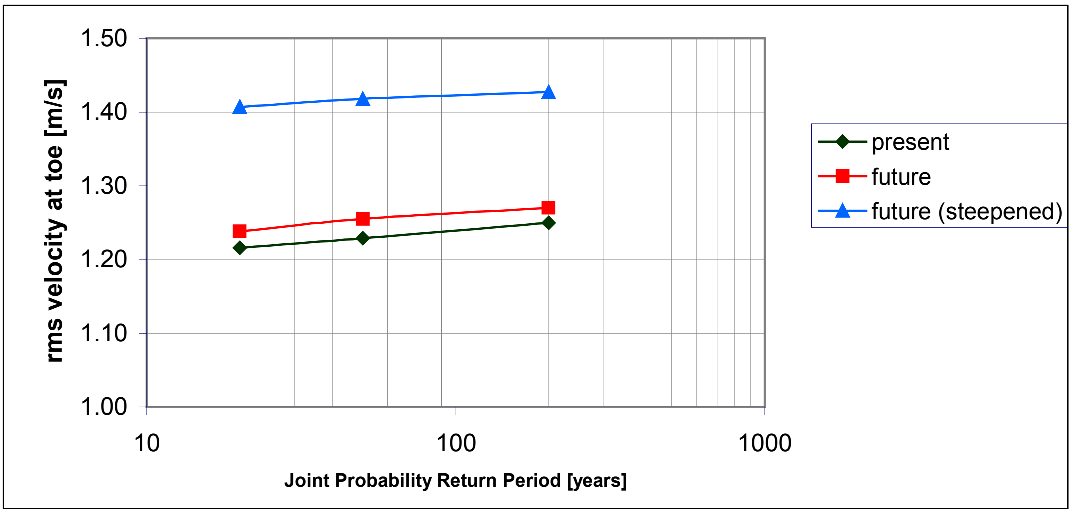

Figure 6.6 **Root-mean-square velocities at toe of seawall at Swansea Bay**

Appendix 7

COSMOS and OTT results for Fylde

Appendix 7 COSMOS and OTT results for Fylde

The results of the individual model runs for the present and future scenarios, are given in the following tables:

- Table 7.1 for present day results at the seawall
- Table 7.2 for future results at the seawall
- Table 7.3 for present day results at the embankment
- Table 7.4 for future results at the embankment
- Table 7.5 for present day results at the shingle beach
- Table 7.6 for future results at the shingle beach

All elevations are given with respect to ODN (m). All structures have simple cross-sections, comprising of a straight slope from toe to crest. OTT then contains a lower area landwards of the crest that is used to collect the overtopped water. The labels are explained in Appendix 3.

Four water level/wave conditions were modelled from each joint probability contour (for present and future scenarios at 20, 50 and 200-year return periods). Therefore there are 12 present day and 12 future sets of results. Figure 7.1 shows the mean overtopping flux rates from each test using the sloping sea wall at Fylde. Figure 7.2 shows the maximum overtopping flux rates from each test using the sloping sea wall at Fylde. Figure 7.3 shows the root-mean-square velocity at the toe of the sloping sea wall at Fylde and Figure 7.4 shows the root-mean-square velocity at the midpoint of the sloping sea wall.

The single highest value was used as a representation of the maximum overtopping rate associated with the offshore return period. The worst case values of rms velocity at the structure toe and midpoint and the maximum and mean overtopping rate are given in the following tables:

- Table 7.7 for results at the seawall
- Table 7.8 for results at the embankment
- Table 7.9 for results at the shingle beach.

Figure 7.5 shows mean overtopping rates for the seawall at Fylde. The future overtopping rates are 2.0 to 1.7 times the present day rates. Figure 7.6 shows root-mean-square velocities at the toe of the seawall at Fylde. This translates into increases in scour potential between 8% and 13%. The increases in damage potential are between 5% and 9%.

Tables

Table 7.1 Results of individual present day model runs for sloping sea wall at Fylde

RP (yrs)	H_s (m)	T_p (s)	WL (m)	Beach Slope 1:N	Toe depth (m)	slope	Crest height (m)	Urms toe (m/s)	Umax toe (m/s)	Umin toe (m/s)	Urms mid (m/s)	Umax mid (m/s)	Umin mid (m/s)	Qmean (m^2/s)	Qmax (m^2/s)	Vtotal (m^3/m)	Vmax (m^3/m)	No. waves	NQ
20	1	3.2	5.3	100	0	1.623	6.47	0.363	1.17	-1.37	0.85	2.94	-1.99	2.10E-02	1.536	90.29	1.97	1103	501
20	2	4.6	5.17	100	0	1.623	6.47	0.741	2.57	-1.46	1.341	5.49	-2.2	1.32E-01	5.356	757.67	7.98	1153	875
20	3	5.6	4.81	100	0	1.623	6.47	0.943	4	-1.52	1.551	6.93	-3.32	1.78E-01	8.535	1234.46	16.39	1153	895
20	4	6.5	4.37	100	0	1.623	6.47	0.997	4.17	-1.54	1.634	7.59	-5.96	1.59E-01	10.514	1331.96	20.97	1243	824
50	1	3.2	5.5	100	0	1.623	6.47	0.352	1.1	-1.34	0.799	2.89	-1.94	3.96E-02	1.959	170.67	2.3	1111	673
50	2	4.6	5.43	100	0	1.623	6.47	0.721	2.48	-1.43	1.295	4.86	-2.07	2.00E-01	5.927	1148.48	10.74	1126	976
50	3	5.6	5.04	100	0	1.623	6.47	0.948	3.92	-1.48	1.526	6.55	-3.37	2.48E-01	9.255	1722.27	18.86	1155	961
50	4	6.5	4.52	100	0	1.623	6.47	1.014	4.74	-1.54	1.616	8.95	-5.03	2.01E-01	11.538	1683.09	25.46	1240	871
200	1	3.2	5.84	100	0	1.623	6.47	0.329	1.17	-1.28	0.704	2.43	-1.8	9.67E-02	2.257	416.39	3.47	1114	921
200	2	4.6	5.76	100	0	1.623	6.47	0.692	2.35	-1.35	1.22	5.07	-1.97	3.17E-01	6.736	1814.01	12.56	1119	1084
200	3	5.6	5.38	100	0	1.623	6.47	0.95	3.78	-1.47	1.492	6.1	-2.21	3.86E-01	11.037	2674.65	21.43	1164	1059
200	4	6.5	4.89	100	0	1.623	6.47	1.042	4.68	-1.48	1.582	8.19	-3.33	3.33E-01	13.442	2798.3	31.41	1218	991

Table 7.2 Results of individual future scenario model runs for sloping sea wall at Fylde

RP (yrs)	H_s (m)	T_p (s)	WL (m)	Beach Slope 1:N	Toe depth (m)	slope	Crest height (m)	Urms toe (m/s)	Umax toe (m/s)	Umin toe (m/s)	Urms mid (m/s)	Umax mid (m/s)	Umin mid (m/s)	Qmean (m^2/s)	Qmax (m^2/s)	Vtotal (m^3/m)	Vmax (m^3/m)	No. waves	NQ
20	1	3.2	5.68	100	0	1.623	6.47	0.341	1.06	-1.31	0.75	2.58	-1.87	6.52E-02	2.147	280.67	2.63	1112	813
20	2	4.6	5.57	100	0	1.623	6.47	0.709	2.43	-1.41	1.266	4.62	-2.05	2.45E-01	6.145	1404.59	11.62	1122	1028
20	3	5.6	5.31	100	0	1.623	6.47	0.95	3.8	-1.48	1.497	6.26	-2.24	3.56E-01	10.641	2467.44	20.95	1167	1036
20	4	6.5	4.85	100	0	1.623	6.47	1.039	4.67	-1.49	1.588	8.16	-3.22	3.17E-01	13.297	2660.61	30.85	1226	976
50	1	3.2	5.92	100	0	1.623	6.47	0.324	1.16	-1.26	0.681	2.36	-1.76	1.16E-01	2.424	499.58	3.87	1110	976
50	2	4.6	5.79	100	0	1.623	6.47	0.689	2.34	-1.35	1.211	5.07	-1.96	3.29E-01	6.858	1885.55	12.7	1114	1092
50	3	5.6	5.53	100	0	1.623	6.47	0.948	3.69	-1.42	1.473	6.45	-2.14	4.55E-01	11.743	3153.26	22.71	1160	1097
50	4	6.5	5.01	100	0	1.623	6.47	1.053	4.67	-1.49	1.576	7.53	-3.3	3.87E-01	14.439	3247.93	33.01	1227	1023
200	1	3.2	6.45	100	0	1.623	6.47	0.294	1.06	-1.16	0.545	1.98	-1.61	3.22E-01	3.654	1388.36	5.28	1104	981
200	2	4.6	6.31	100	0	1.623	6.47	0.644	2.4	-1.26	1.074	4.35	-1.72	6.10E-01	8.562	3494.96	16.69	1098	1226
200	3	5.6	5.85	100	0	1.623	6.47	0.935	3.93	-1.35	1.439	6.53	-1.99	6.42E-01	13.146	4454.28	29.47	1150	1129
200	4	6.5	5.33	100	0	1.623	6.47	1.069	4.61	-1.44	1.565	7.14	-2.13	5.48E-01	16.965	4597.07	41.56	1216	1097

Table 7.3 Results of individual present day model runs for embankment at Fylde

RP (yrs)	H_s (m)	T_p (s)	WL (m)	Beach Slope 1:N	Toe depth (m)	slope	Crest height (m)	Urms toe (m/s)	Umax toe (m/s)	Umin toe (m/s)	Urms mid (m/s)	Umax mid (m/s)	Umin mid (m/s)	Qmean (m^2/s)	Qmax (m^2/s)	Vtotal (m^3/m)	Vmax (m^3/m)	No. waves	NQ
20	1	3.2	5.3	100	-2.3	3	6.93	0.272	1.03	-1.12	0.492	1.74	-2.52	9.55E-04	0.733	4.11	0.89	1088	54
20	2	4.6	5.17	100	-2.3	3	6.93	0.505	2.06	-1.77	1.17	3.54	-5.45	4.98E-02	3.736	285.5	7.3	1104	488
20	3	5.6	4.81	100	-2.3	3	6.93	0.756	2.94	-2.92	2.085	7.34	-5.54	1.31E-01	7.492	907.92	17.81	1065	607
20	4	6.5	4.37	100	-2.3	3	6.93	1.064	3.73	-2.98	2.747	9	-5.64	2.11E-01	11.948	1773.77	32.28	1132	651
50	1	3.2	5.5	100	-2.3	3	6.93	0.271	1.01	-1.03	0.475	1.72	-2.55	3.37E-03	0.863	14.49	1.33	1082	124
50	2	4.6	5.43	100	-2.3	3	6.93	0.501	2	-1.77	1.089	3.17	-4.92	8.44E-02	4.233	483.59	8.66	1106	606
50	3	5.6	5.04	100	-2.3	3	6.93	0.752	3.11	-2.9	1.967	7.41	-5.56	1.79E-01	8.28	1242.15	20.06	1068	681
50	4	6.5	4.52	100	-2.3	3	6.93	1.059	3.72	-2.97	2.712	10.7	-5.65	2.52E-01	12.566	2116.01	33.91	1137	694
200	1	3.2	5.84	100	-2.3	3	6.93	0.269	0.98	-1.09	0.451	1.58	-2	1.66E-02	1.42	71.49	1.92	1083	375
200	2	4.6	5.76	100	-2.3	3	6.93	0.496	1.92	-1.74	0.999	3.14	-4.79	1.50E-01	4.923	858.36	10.04	1108	771
200	3	5.6	5.38	100	-2.3	3	6.93	0.741	3.07	-2.88	1.794	6.03	-5.58	2.71E-01	9.3	1881.46	22.81	1065	813
200	4	6.5	4.89	100	-2.3	3	6.93	1.044	3.9	-2.94	2.585	10.4	-5.63	3.71E-01	14.096	3113.25	41.01	1132	815

Table 7.4 Results of individual future scenario model runs for embankment at Fylde

RP (yrs)	H_s (m)	T_p (s)	WL (m)	Beach Slope 1:N	Toe depth (m)	slope	Crest height (m)	Urms toe (m/s)	Umax toe (m/s)	Umin toe (m/s)	Urms mid (m/s)	Umax mid (m/s)	Umin mid (m/s)	Qmean (m^2/s)	Qmax (m^2/s)	Vtotal (m^3/m)	Vmax (m^3/m)	No. waves	NQ
20	1	3.2	5.68	100	-2.3	3	6.93	0.27	1	-1.06	0.463	1.64	-2.25	8.33E-03	1.182	35.87	1.64	1083	225
20	2	4.6	5.57	100	-2.3	3	6.93	0.499	1.96	-1.74	1.049	3.25	-4.86	1.09E-01	4.489	625.46	9.28	1108	672
20	3	5.6	5.31	100	-2.3	3	6.93	0.744	3.07	-2.88	1.827	6.29	-5.58	2.50E-01	9.088	1734.33	22.28	1065	787
20	4	6.5	4.85	100	-2.3	3	6.93	1.045	3.87	-2.94	2.598	10.5	-5.63	3.57E-01	13.978	2995	40.21	1132	802
50	1	3.2	5.92	100	-2.3	3	6.93	0.269	0.97	-1.1	0.445	1.55	-2.01	2.27E-02	1.526	97.59	2.16	1080	443
50	2	4.6	5.79	100	-2.3	3	6.93	0.496	2.07	-1.74	0.992	3.12	-4.77	1.57E-01	5.028	900.53	10.16	1107	782
50	3	5.6	5.53	100	-2.3	3	6.93	0.738	3.05	-2.87	1.722	5.48	-5.58	3.23E-01	9.78	2236.3	23.95	1076	864
50	4	6.5	5.01	100	-2.3	3	6.93	1.04	3.9	-2.92	2.543	10.1	-5.62	4.17E-01	14.586	3499.81	43.28	1135	846
200	1	3.2	6.45	100	-2.3	3	6.93	0.258	0.97	-1.01	0.412	1.71	-1.74	1.11E-01	2.341	480.07	3.81	1098	902
200	2	4.6	6.31	100	-2.3	3	6.93	0.487	2.13	-1.72	0.892	2.84	-4.06	3.38E-01	6.577	1938.08	14.66	1106	970
200	3	5.6	5.85	100	-2.3	3	6.93	0.731	3.08	-2.84	1.588	5.23	-5.57	4.54E-01	10.672	3145.64	26.37	1086	941
200	4	6.5	5.33	100	-2.3	3	6.93	1.027	3.88	-2.9	2.407	9.25	-5.58	5.60E-01	16.292	4701.57	48.35	1132	936

Table 7.5 Results of individual present day model runs for shingle beach at Fylde

RP (yrs)	H_s (m)	T_p (s)	WL (m)	Beach Slope 1:N	Toe depth (m)	slope	Crest height (m)	Urms toe (m/s)	Umax toe (m/s)	Umin toe (m/s)	Urms mid (m/s)	Umax mid (m/s)	Umin mid (m/s)	Qmean (m^2/s)	Qmax (m^2/s)	Vtotal (m^3/m)	Vmax (m^3/m)	No. waves	NQ
20	1	3.2	5.3	100	-4.6	5	6.93	0.228	0.91	-0.96	0.428	1.48	-2.01	5.81E-05	0.182	0.25	0.25	1104	1
20	2	4.6	5.17	100	-4.6	5	6.93	0.463	1.84	-1.81	0.809	2.88	-3.4	1.17E-02	2.198	66.85	4.88	1115	182
20	3	5.6	4.81	100	-4.6	5	6.93	0.703	2.67	-2.33	1.189	4.13	-4.96	4.73E-02	4.983	328.15	13.09	1126	356
20	4	6.5	4.37	100	-4.6	5	6.93	0.897	3.57	-2.82	1.767	5.67	-6.04	1.05E-01	9.15	879.88	29.6	1107	447
50	1	3.2	5.5	100	-4.6	5	6.93	0.227	0.91	-0.99	0.417	1.43	-1.75	1.69E-04	0.337	0.73	0.53	1103	8
50	2	4.6	5.43	100	-4.6	5	6.93	0.46	1.84	-1.86	0.793	2.76	-3.47	2.64E-02	2.632	151.06	5.83	1114	339
50	3	5.6	5.04	100	-4.6	5	6.93	0.702	2.65	-2.38	1.155	4.01	-4.99	7.43E-02	5.744	514.87	15.59	1125	454
50	4	6.5	4.52	100	-4.6	5	6.93	0.899	3.56	-2.85	1.726	5.51	-6.04	1.30E-01	9.834	1089.11	31.53	1106	495
200	1	3.2	5.84	100	-4.6	5	6.93	0.224	0.88	-1.02	0.398	1.51	-1.85	2.29E-03	0.687	9.87	1.18	1108	103
200	2	4.6	5.76	100	-4.6	5	6.93	0.457	1.84	-1.93	0.773	2.63	-3.17	6.44E-02	3.451	368.84	7.87	1118	537
200	3	5.6	5.38	100	-4.6	5	6.93	0.697	2.64	-2.46	1.116	3.86	-5.05	1.35E-01	6.794	935.41	18.55	1123	606
200	4	6.5	4.89	100	-4.6	5	6.93	0.902	3.53	-2.77	1.63	5.3	-5.94	2.11E-01	11.471	1774	35.89	1104	630

Table 7.6 Results of individual future scenario model runs for shingle beach at Fylde

RP (yrs)	H_s (m)	T_p (s)	WL (m)	Beach Slope 1:N	Toe depth (m)	slope	Crest height (m)	Urms toe (m/s)	Umax toe (m/s)	Umin toe (m/s)	Urms mid (m/s)	Umax mid (m/s)	Umin mid (m/s)	Qmean (m^2/s)	Qmax (m^2/s)	Vtotal (m^3/m)	Vmax (m^3/m)	No. waves	NQ
20	1	3.2	5.68	100	-4.6	5	6.93	0.225	0.89	-1.01	0.406	1.38	-1.81	6.35E-04	0.541	2.74	0.79	1107	41
20	2	4.6	5.57	100	-4.6	5	6.93	0.459	1.84	-1.89	0.786	2.71	-3.43	3.94E-02	2.99	225.53	6.43	1115	416
20	3	5.6	5.31	100	-4.6	5	6.93	0.698	2.64	-2.44	1.122	3.89	-5.04	1.20E-01	6.611	833.59	18.02	1123	572
20	4	6.5	4.85	100	-4.6	5	6.93	0.902	3.54	-2.77	1.639	5.32	-5.92	2.01E-01	11.284	1687.4	35.46	1105	611
50	1	3.2	5.92	100	-4.6	5	6.93	0.223	0.87	-1.02	0.395	1.5	-1.88	3.95E-03	0.75	16.99	1.35	1109	152
50	2	4.6	5.79	100	-4.6	5	6.93	0.456	1.84	-1.93	0.772	2.62	-3.18	6.92E-02	3.52	396.78	8.1	1116	554
50	3	5.6	5.53	100	-4.6	5	6.93	0.697	2.64	-2.49	1.1	3.8	-4.64	1.71E-01	7.22	1188.08	19.7	1123	662
50	4	6.5	5.01	100	-4.6	5	6.93	0.901	3.52	-2.8	1.604	5.25	-5.87	2.45E-01	11.935	2052.83	37.26	1101	660
200	1	3.2	6.45	100	-4.6	5	6.93	0.219	0.88	-1.01	0.373	1.4	-1.69	5.51E-02	1.536	237.39	2.87	1106	699
200	2	4.6	6.31	100	-4.6	5	6.93	0.448	1.82	-1.99	0.742	2.73	-2.92	2.07E-01	4.923	1185.9	10.79	1121	837
200	3	5.6	5.85	100	-4.6	5	6.93	0.693	2.62	-2.56	1.071	3.67	-4.67	2.72E-01	8.422	1886.09	21.86	1126	769
200	4	6.5	5.33	100	-4.6	5	6.93	0.902	3.51	-2.86	1.534	5.11	-5.84	3.51E-01	13.132	2945.19	40.56	1097	751

Table 7.7 Seawall results for Fylde. P= present-day wave/water level conditions, F = future conditions

scenario	Return Period (years)	Waves	WL	Beach Slope (1:nnn)	Toe Depth (m)	Crest elevation (m)	Urms,toe (m/s)	Urms,mid (m/s)	Qmean ($m^3/s/m$)	Qmax ($m^3/s/m$)	Vmax (m^3/m)
20, present	20	P	P	100	0	6.47	0.997	4.17	1.78E-01	10.514	20.97
50, present	50	P	P	100	0	6.47	1.014	4.74	2.48E-01	11.538	25.46
200, present	200	P	P	100	0	6.47	1.042	4.68	3.86E-01	13.442	31.41
20, future	20	F	F	100	0	6.47	1.039	4.67	3.56E-01	13.297	30.85
50, future	50	F	F	100	0	6.47	1.053	4.67	4.55E-01	14.439	33.01
200, future	200	F	F	100	0	6.47	1.069	4.61	6.42E-01	16.965	41.56

Table 7.8 Embankment results for Fylde

scenario	Return Period (years)	Waves	WL	Beach Slope (1:nnn)	Toe Depth (m)	Crest elevation (m)	Urms,toe (m/s)	Urms,mid (m/s)	Qmean ($m^3/s/m$)	Qmax ($m^3/s/m$)	Vmax (m^3/m)
20, present	20	P	P	100	-2.3	6.93	1.064	2.747	0.211	11.9	32.28
50, present	50	P	P	100	-2.3	6.93	1.064	2.747	0.252	12.6	33.91
200, present	200	P	P	100	-2.3	6.93	1.064	2.747	0.371	14.1	41.01
20, future	20	F	F	100	-2.3	6.93	1.045	2.598	0.357	14.0	40.21
50, future	50	F	F	100	-2.3	6.93	1.045	2.598	0.417	14.6	43.28
200, future	200	F	F	100	-2.3	6.93	1.045	2.598	0.560	16.3	48.35

Table 7.9 Shingle Beach results for Fylde

scenario	Return Period (years)	Waves	WL	Beach Slope (1:nnn)	Toe Depth (m)	Crest elevation (m)	Urms,toe (m/s)	Urms,mid (m/s)	Qmean ($m^3/s/m$)	Qmax ($m^3/s/m$)	Vmax (m^3/m)
20, present	20	P	P	100	-4.6	6.93	0.897	1.767	0.105	9.2	29.6
50, present	50	P	P	100	-4.6	6.93	0.899	1.767	0.130	9.8	31.53
200, present	200	P	P	100	-4.6	6.93	0.902	1.767	0.211	11.5	35.89
20, future	20	F	F	100	-4.6	6.93	0.902	1.639	0.201	11.3	35.46
50, future	50	F	F	100	-4.6	6.93	0.902	1.639	0.245	11.9	37.26
200, future	200	F	F	100	-4.6	6.93	0.902	1.639	0.351	13.1	40.56

Figures

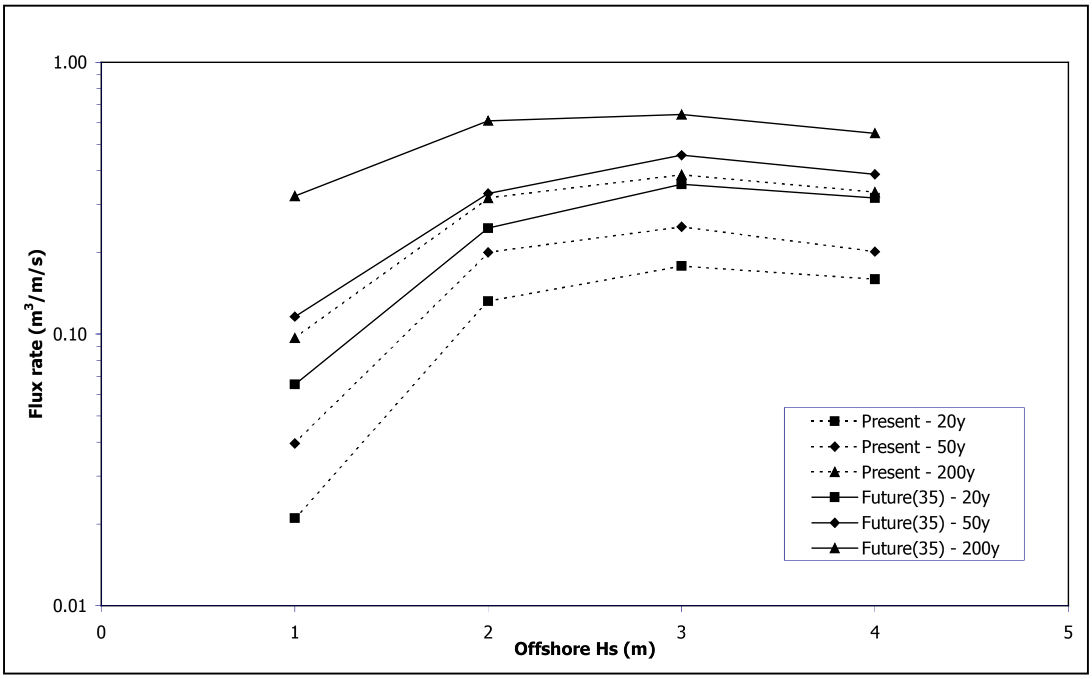

Figure 7.1 Mean overtopping flux rates for sloping sea wall at Fylde

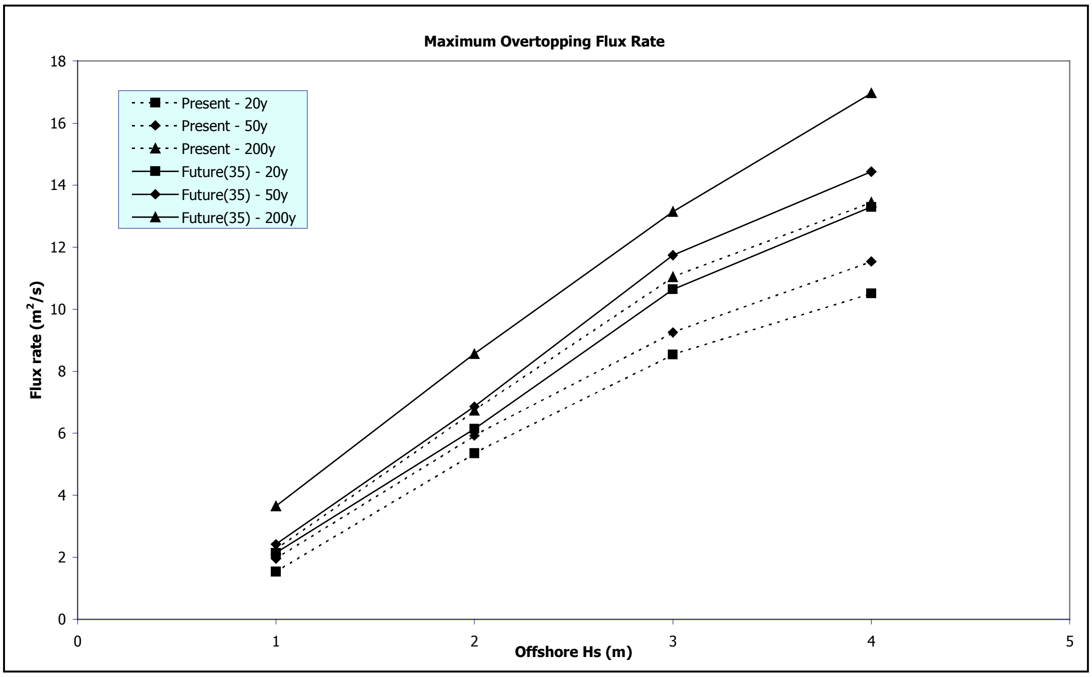

Figure 7.2 Maximum overtopping flux rates for sloping sea wall at Fylde

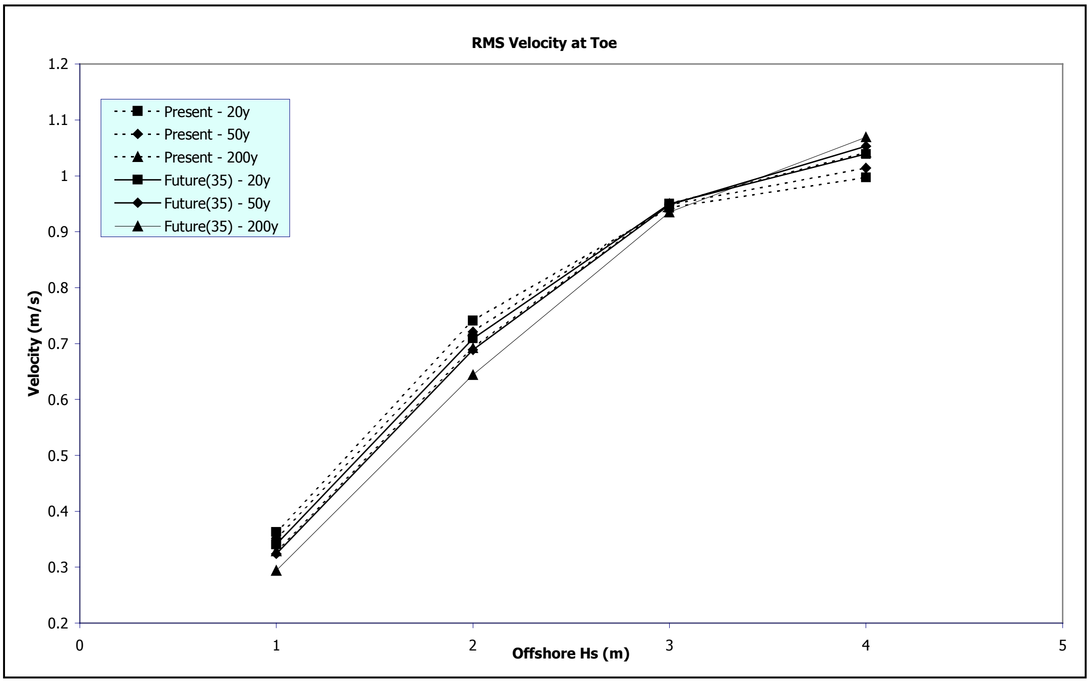

Figure 7.3 Root-mean-square velocity at toe of sloping sea wall at Fylde

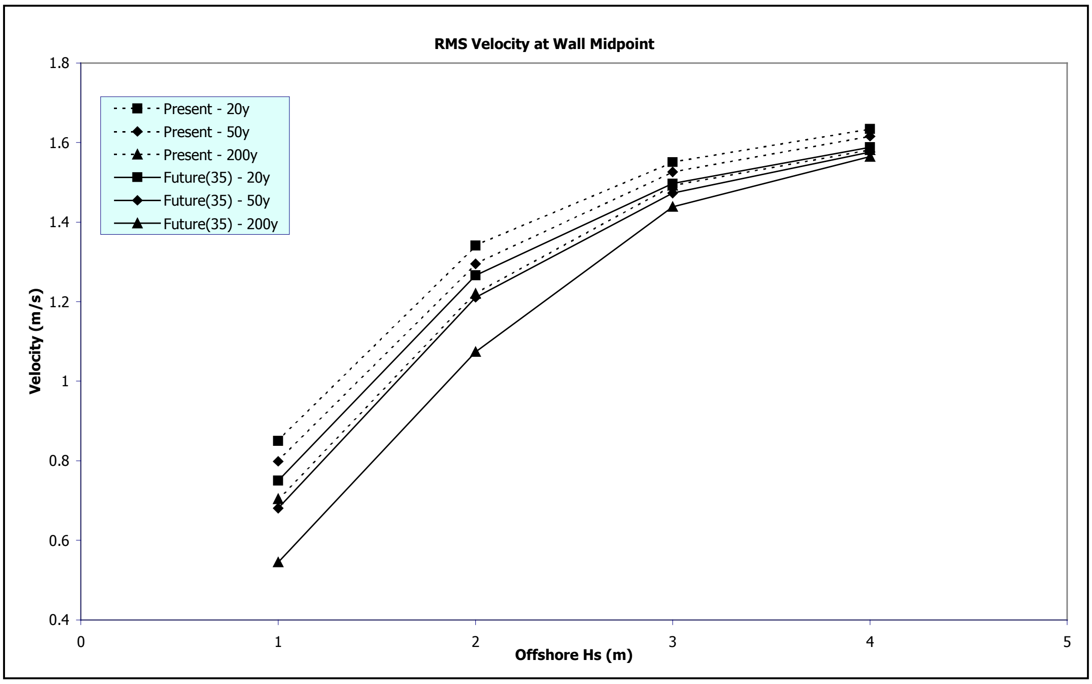

Figure 7.4 Root-mean-square velocity at midpoint of sloping sea wall at Fylde

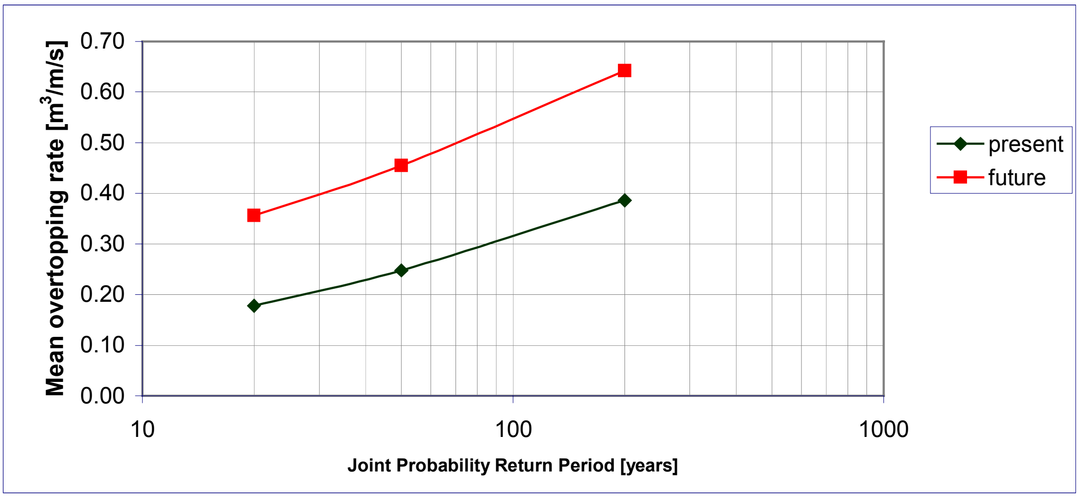

Figure 7.5 **Mean seawall-overtopping rates at Fylde**

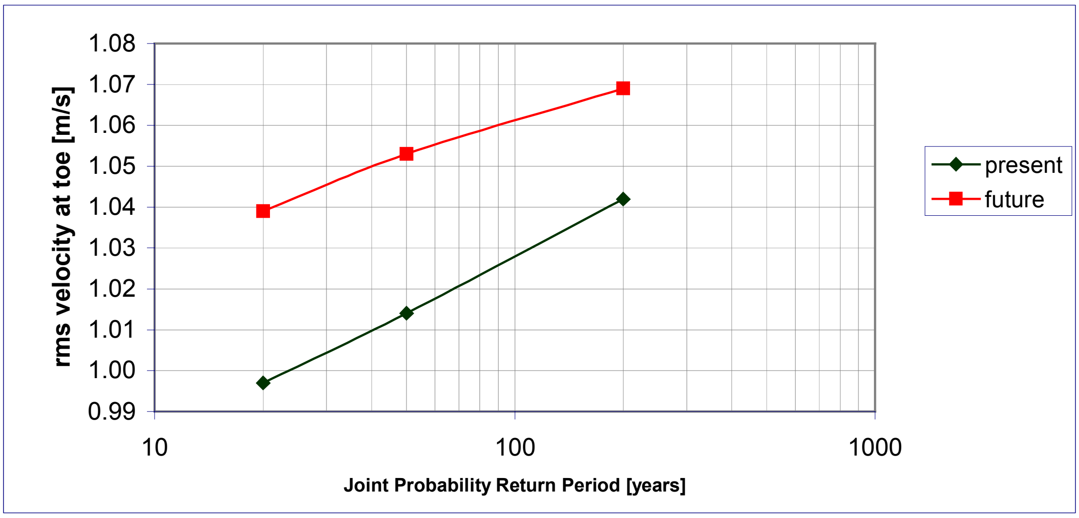

Figure 7.6 **Root-mean-square velocities at toe of seawall at Fylde**

Appendix 8

Longshore drift rates

Appendix 8 Longshore Drift Rates.

This appendix contains time series and plots of mean annual nett drift rates, expressed in metres cubed per year through a cross-shore profile.

Table 1 Mean annual nett drift rates [m3/year] at Lincolnshire and Dungeness

Year	Lincolnshire present	Lincolnshire future	Dungeness (180°) present	Dungeness (180°) future	Dungeness (225°) present	Dungeness (225°) future
1	-349986	-162260	114388	175769	35782	31638
2	140586	-398455	107530	116748	2236	35362
3	-275725	-253983	132886	133493	36610	50535
4	-366874	-450095	104964	84670	34879	23165
5	-386197	-318722	93280	137501	19416	46550
6	-331451	-641222	141082	90670	33671	39828
7	-192859	-9423	105234	121229	4860	8108
8	-267670	-271239	148345	121742	49174	34493
9	-653864	-181070	114351	119916	31493	27322
10	-11475	-230072	159131	147472	51364	26790
11	-523215	-1016778	80619	146238	8842	31859
12	269811	-187899	96673	166518	3057	47155
13	-196962	-124190	101505	80116	12131	10135
14	-377862	-454954	138393	112303	40153	40973
15	-673390	-228355	81106	149494	28667	41960
16	-98534	-147690	181332	140236	47040	4917
17	-347877	-195912	109362	109612	4222	28028
18	-375599	-85848	129128	134936	49149	21827
19	-326112	-775737	66658	95156	14708	21917
20	-608685	-466682	86177	173572	20161	62827
21	-467495	-80387	125289	124830	50006	18387
22	-264780	-452018	164413	149790	33984	46965
23	-575612	-262577	74639	150896	23655	52916
24	-659672	-613760	66021	68517	12226	22112
25	-147194	-291843	141694	158709	36901	40539
26	-140876	-27858	138165	117961	16808	34624
27	-1483337	-465898	111166	109368	40577	17409
28	-273391	-322292	106044	107266	35767	29705
29	-382391	-281280	106486	128326	26543	23635

Table 2 Mean annual nett drift rates [m^3/year]at Lyme Bay, Swansea Bay and Fylde

Year	Lyme Bay (180°) present	Lyme Bay (180°) future	Swansea Bay (180°) present	Swansea Bay (180°) future	Swansea Bay (225°) present	Swansea Bay (225°) future	Fylde present	Fylde future
1	87920	197451	1707458	2870396	254208	326970	-502725	-1059088
2	105026	125142	1664174	2138230	-111526	429576	-669234	-699202
3	144437	131539	2047924	1997155	250451	330096	-680475	-705360
4	117187	80802	1735343	1545752	403518	208469	-360523	-762710
5	85299	131185	1412976	2048612	178212	464670	-395140	-751752
6	126678	69006	1812022	1308459	191711	274908	-422953	-373033
7	105402	125528	1804378	1764089	-8238	191180	-922620	-531340
8	147943	99804	2052353	1787116	400570	306521	-393899	-600912
9	98581	126836	1772615	2026673	270142	292946	-645952	-547061
10	153643	136709	2122116	1843902	336187	162260	-635740	-889150
11	76672	114875	1437171	1866997	166545	146187	-388634	-855872
12	100659	164905	1774108	2273492	-7705	342041	-741270	-584433
13	95897	66811	1658316	1355808	169446	-16587	-714152	-552769
14	138283	104124	2079632	1743809	174895	423641	-529661	-394841
15	77622	149355	1319471	2401014	233550	423848	-520801	-1082157
16	208154	175199	2809404	2372091	284546	230801	-1146630	-747357
17	114702	122722	1522446	2120182	26767	246558	-427132	-1290086
18	138406	140144	2016188	2161934	418492	303484	-746444	-907191
19	63860	74852	1071522	1309126	213623	122563	-264268	-507891
20	61618	145273	1289544	2340256	270415	369023	-447780	-763541
21	104324	125332	1758560	1965771	404081	311974	-370664	-696274
22	179293	135649	2638730	2129546	258195	507153	-1275624	-566703
23	73459	149239	1120770	2238685	210910	420287	-186686	-610684
24	39441	60035	828872	1164944	-30855	312294	-602792	-263827
25	129493	174693	2024403	2600135	336795	561733	-738720	-738978
26	153040	105175	2289946	1811721	67869	163747	-1044888	-945273
27	113954	94921	1988629	1470680	441778	113163	-449356	-783390
28	101739	76007	1619457	1447341	397568	130761	-232319	-530045
29	90417	119927	1488926	1919878	171316	161572	-642945	-972316

Figures

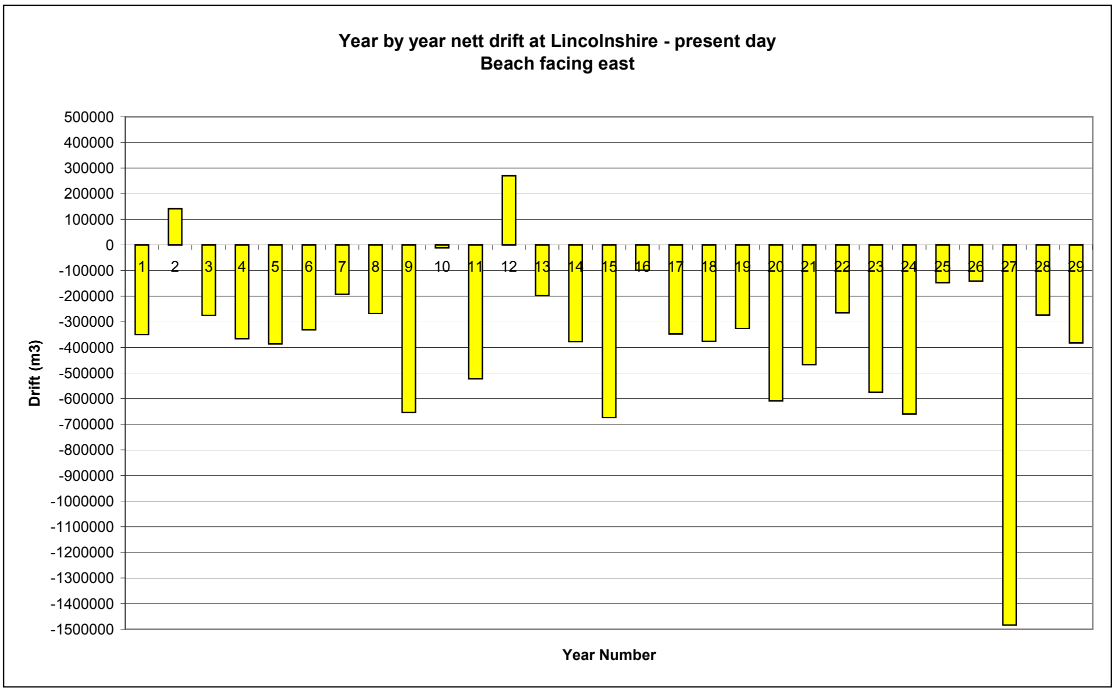

Figure 8.1 Present day scenario nett annual drift rates at Lincolnshire

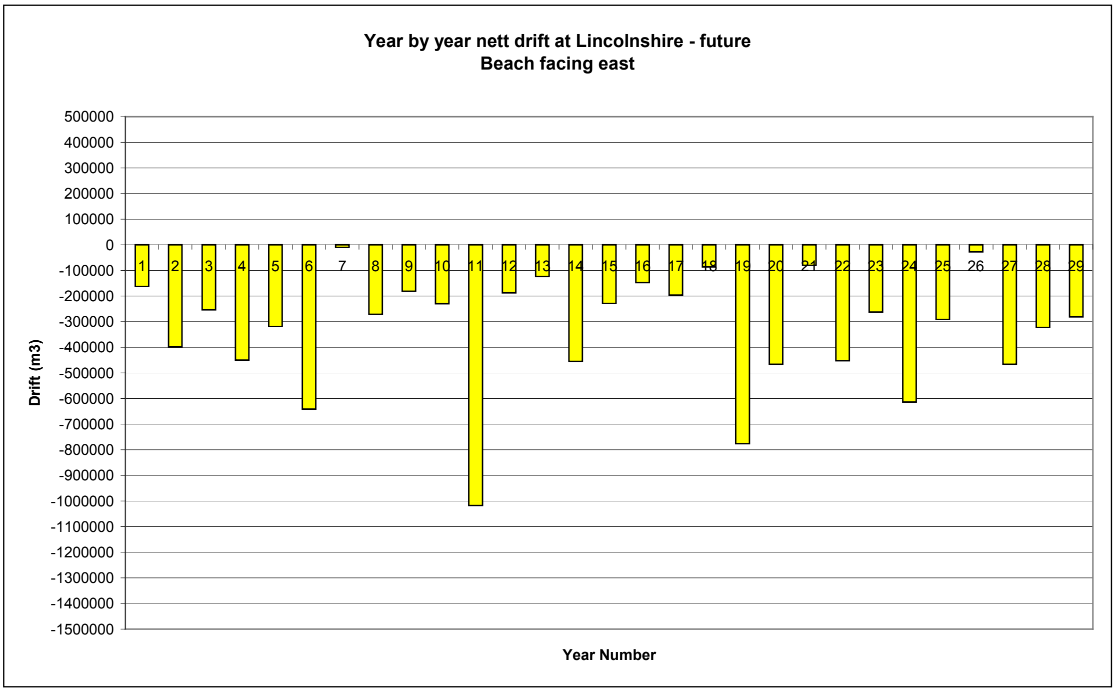

Figure 8.2 Future scenario nett annual drift rates at Lincolnshire

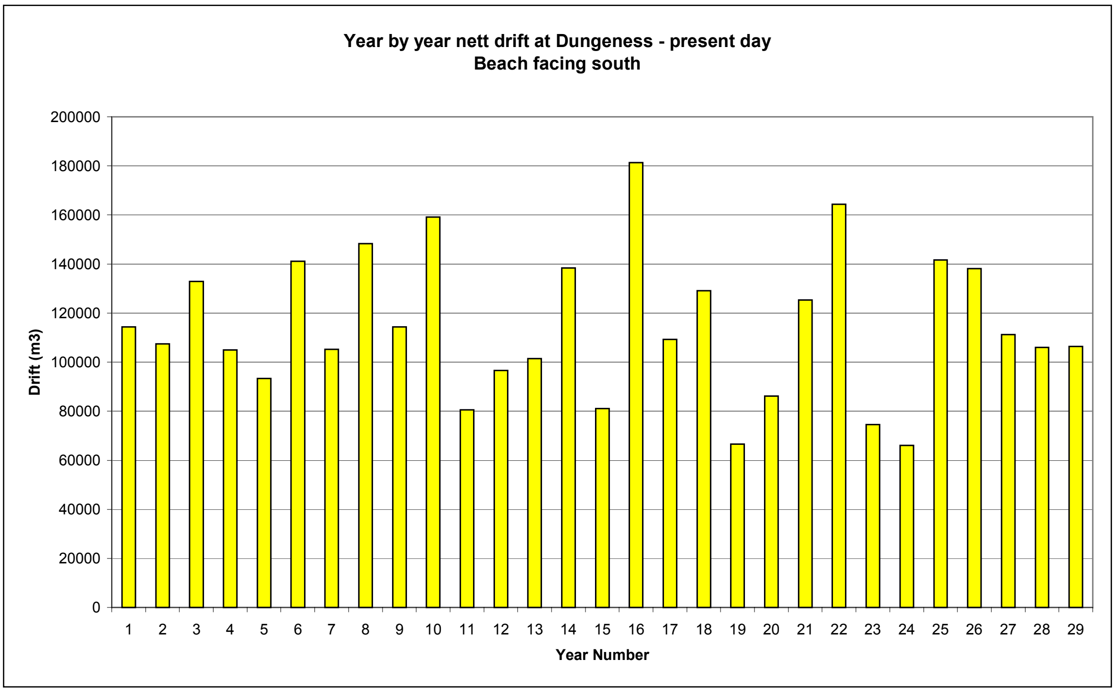

Figure 8.3 Present day scenario nett annual drift rates at Dungeness (beach facing 180°)

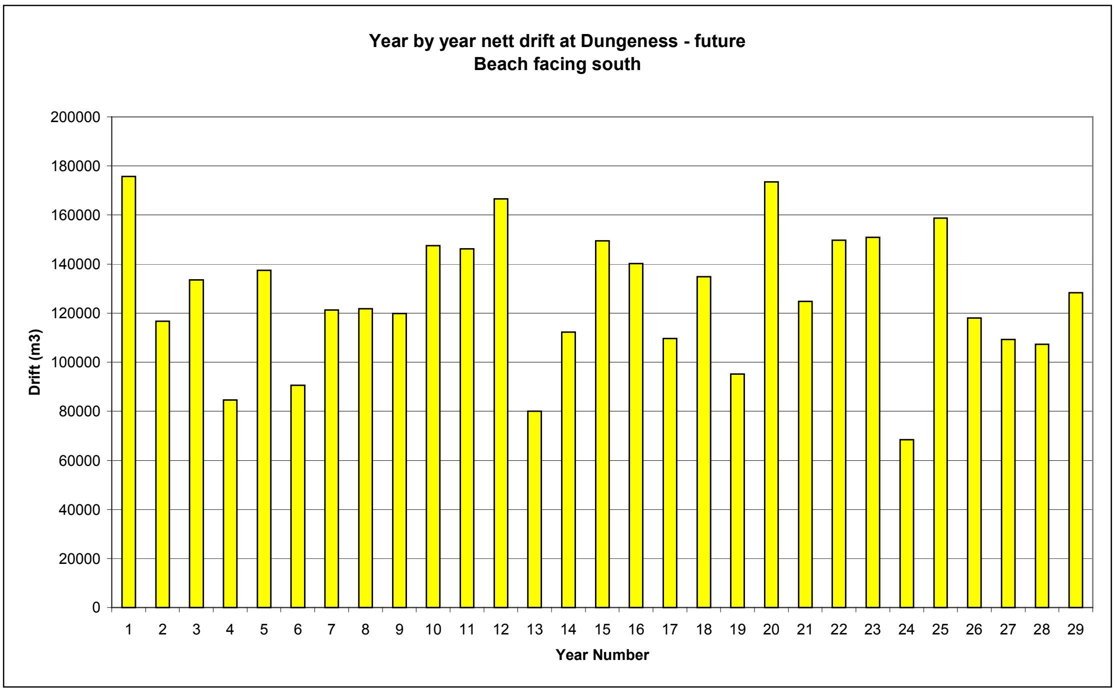

Figure 8.4 Future scenario nett annual drift rates at Dungeness (beach facing 180°)

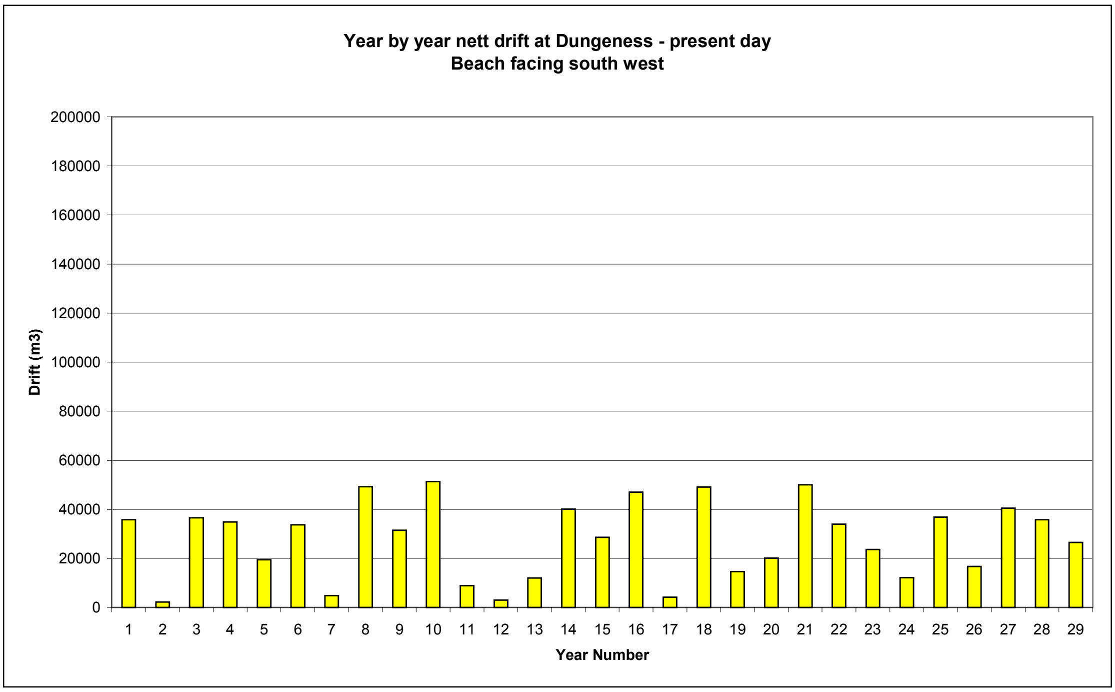

Figure 8.5 Present day scenario nett annual drift rates at Dungeness (beach facing 225°)

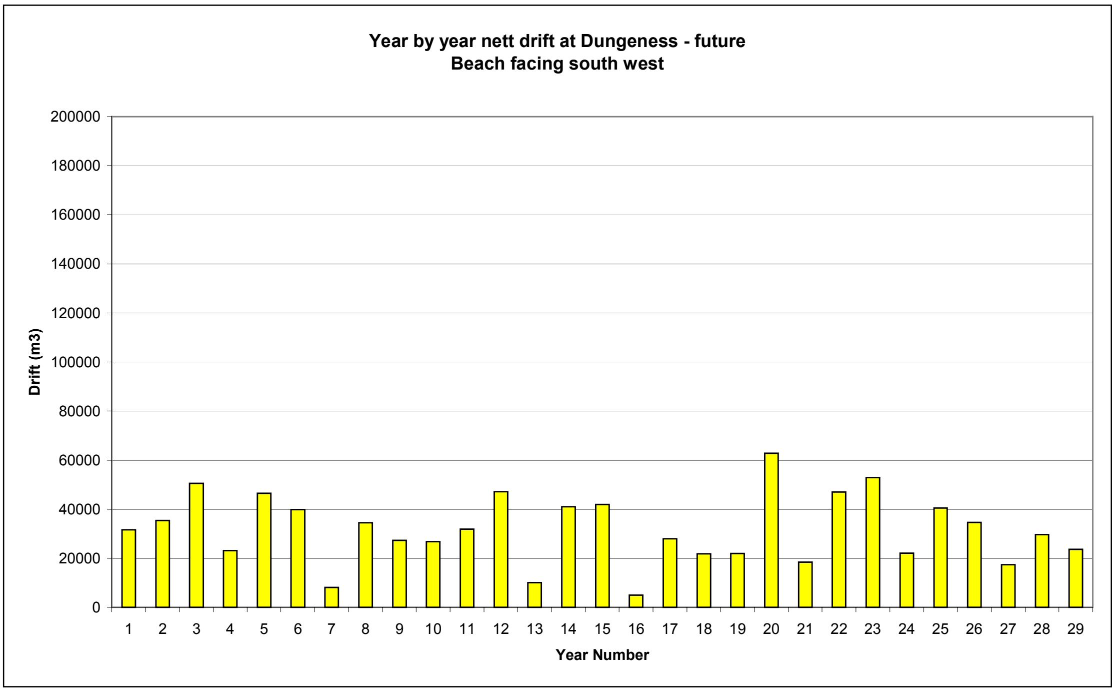

Figure 8.6 Future scenario nett annual drift rates at Dungeness (beach facing 225°)

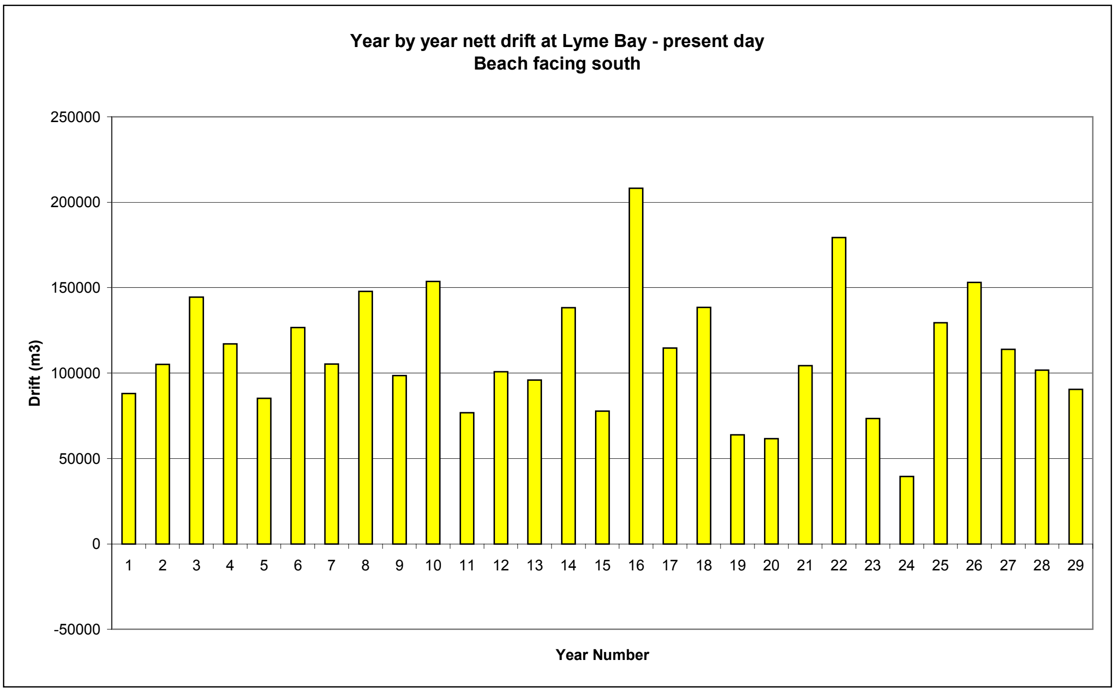

Figure 8.7 Present day scenario nett annual drift rates at Lyme Bay (beach facing 180°)

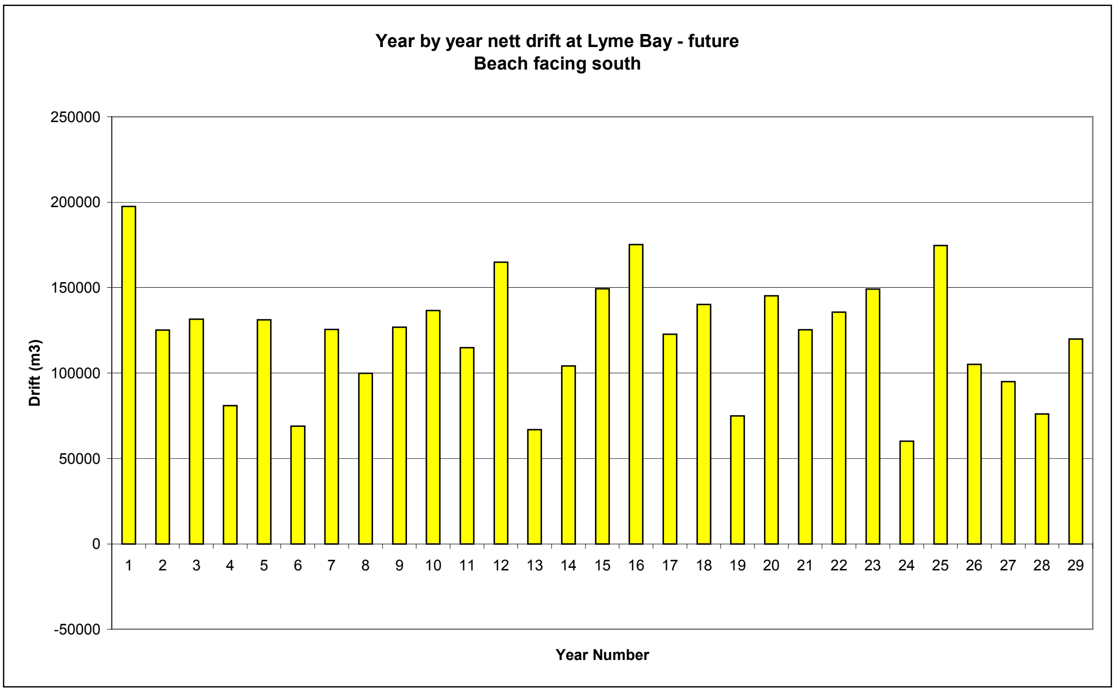

Figure 8.8 Future scenario nett annual drift rates at Lyme Bay (beach facing 180°)

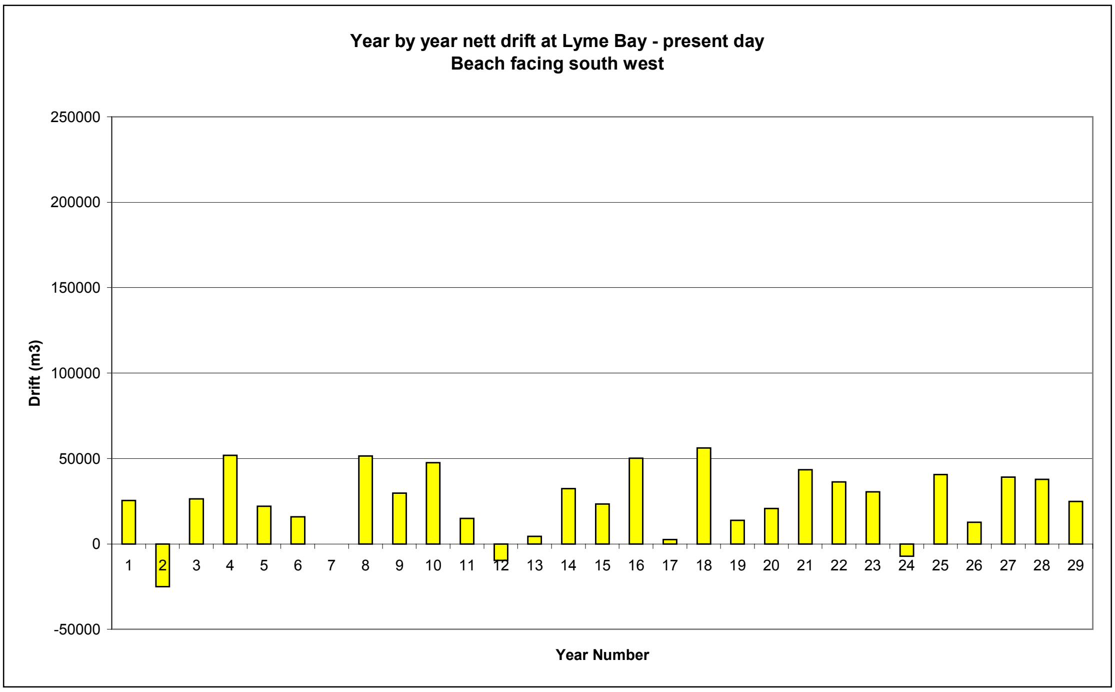

Figure 8.9 Present day scenario nett annual drift rates at Lyme Bay (beach facing 225°)

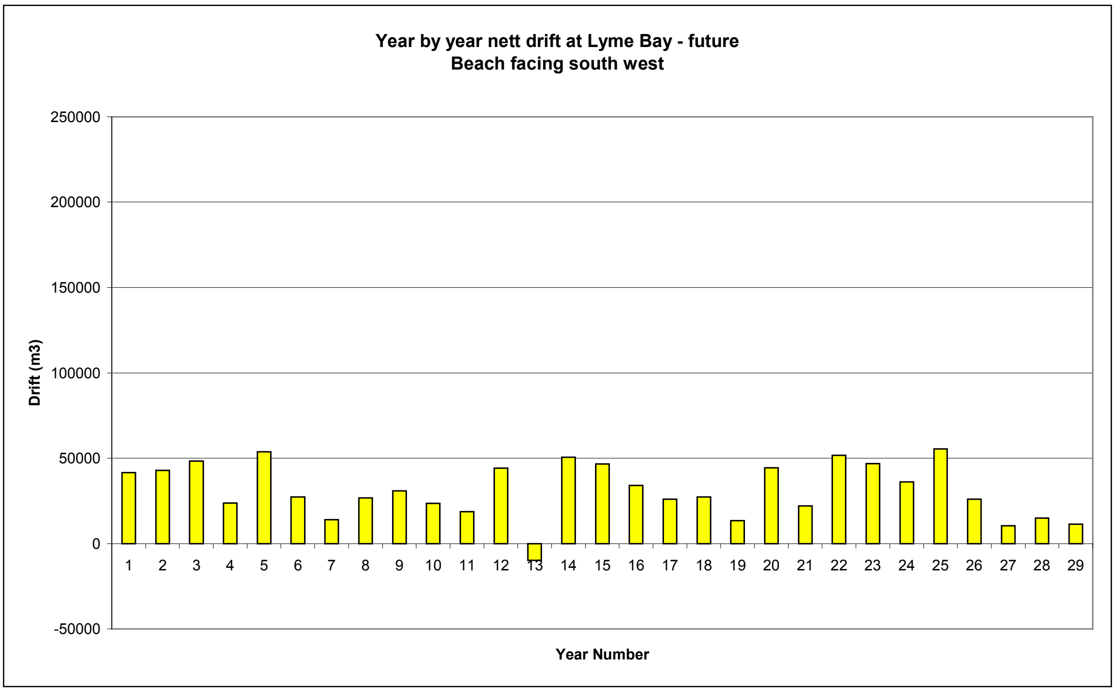

Figure 8.10 Future scenario nett annual drift rates at Lyme Bay (beach facing 225°)

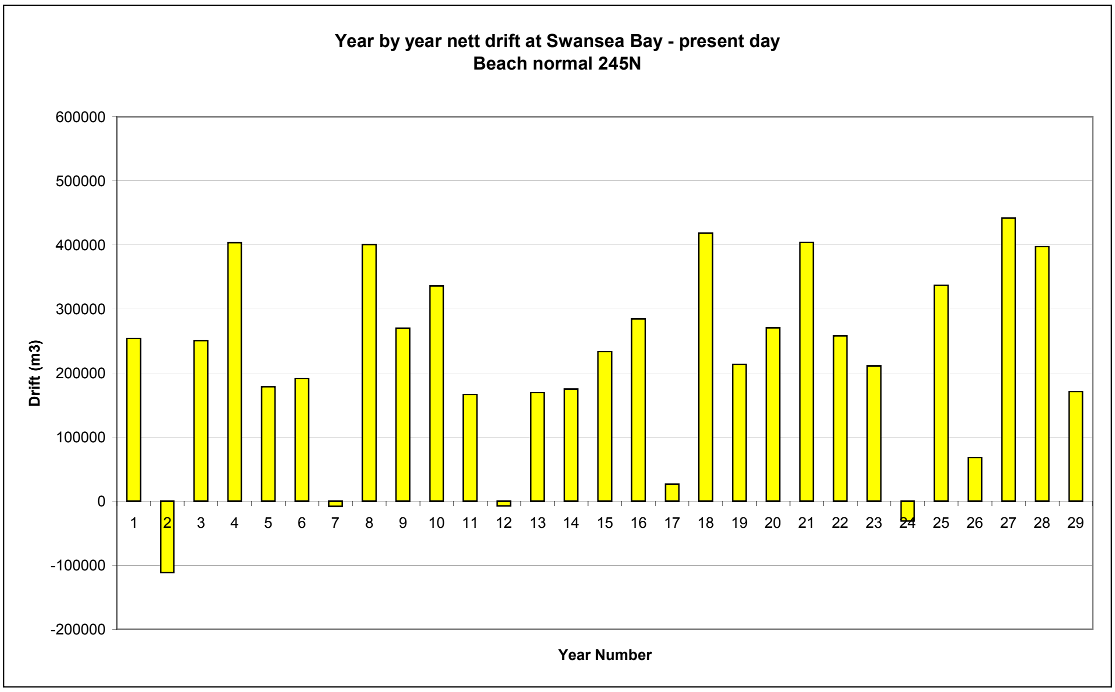

Figure 8.11 Present day scenario nett annual drift rates at Swansea Bay

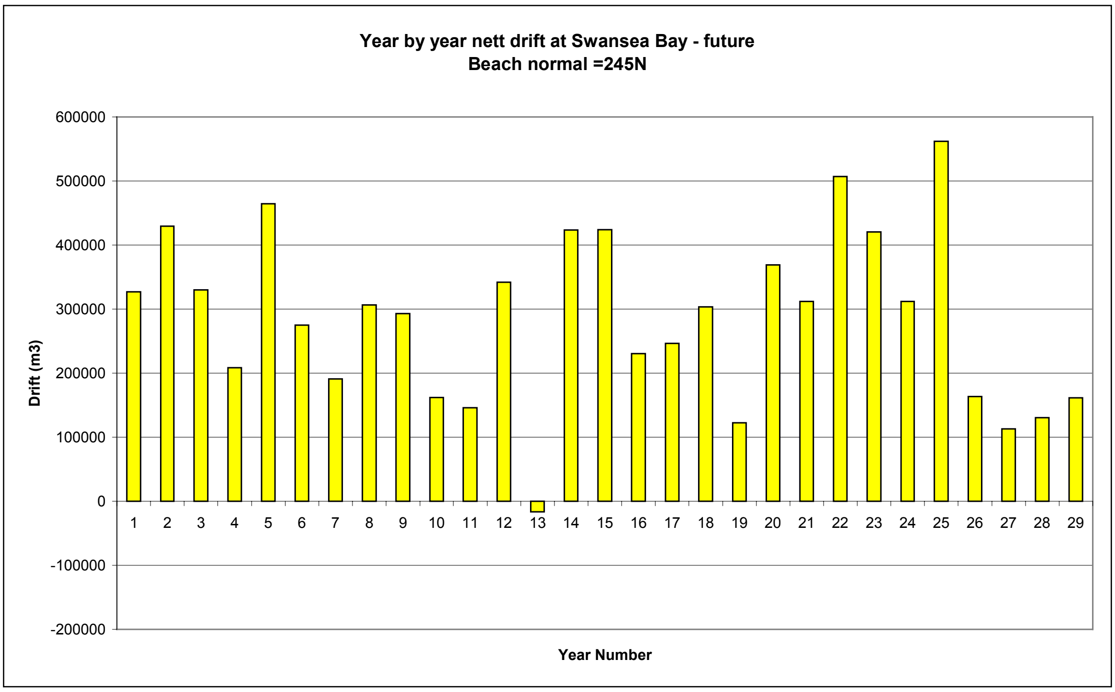

Figure 8.12 Future scenario nett annual drift rates at Swansea Bay

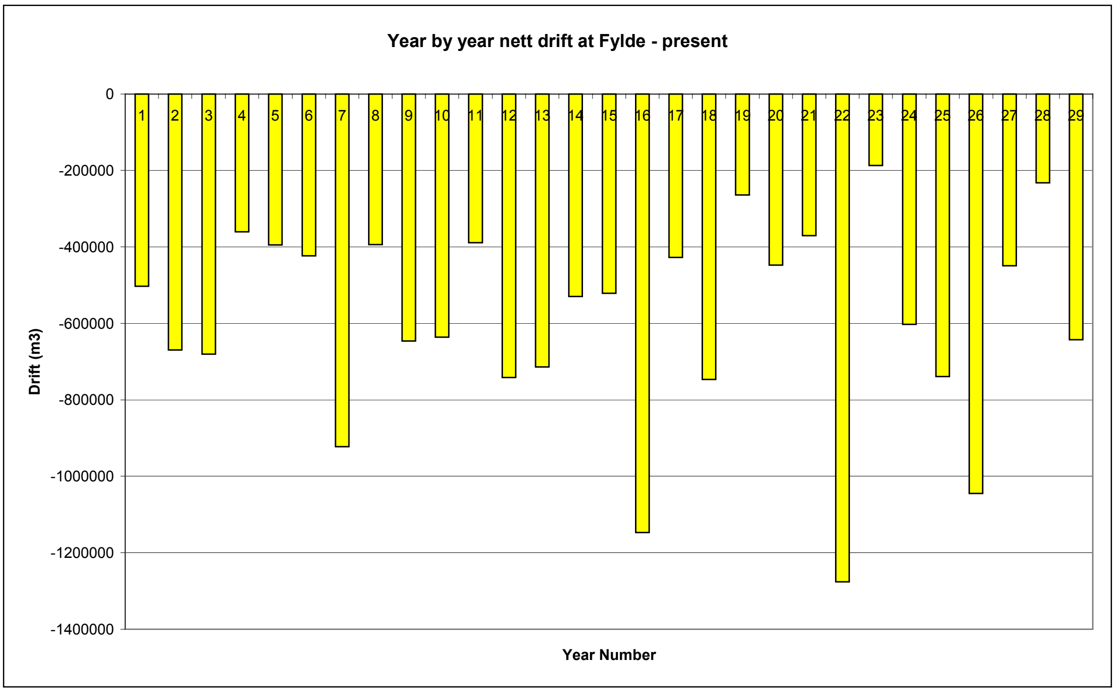

Figure 8.13 Present day scenario nett annual drift rates at Fylde

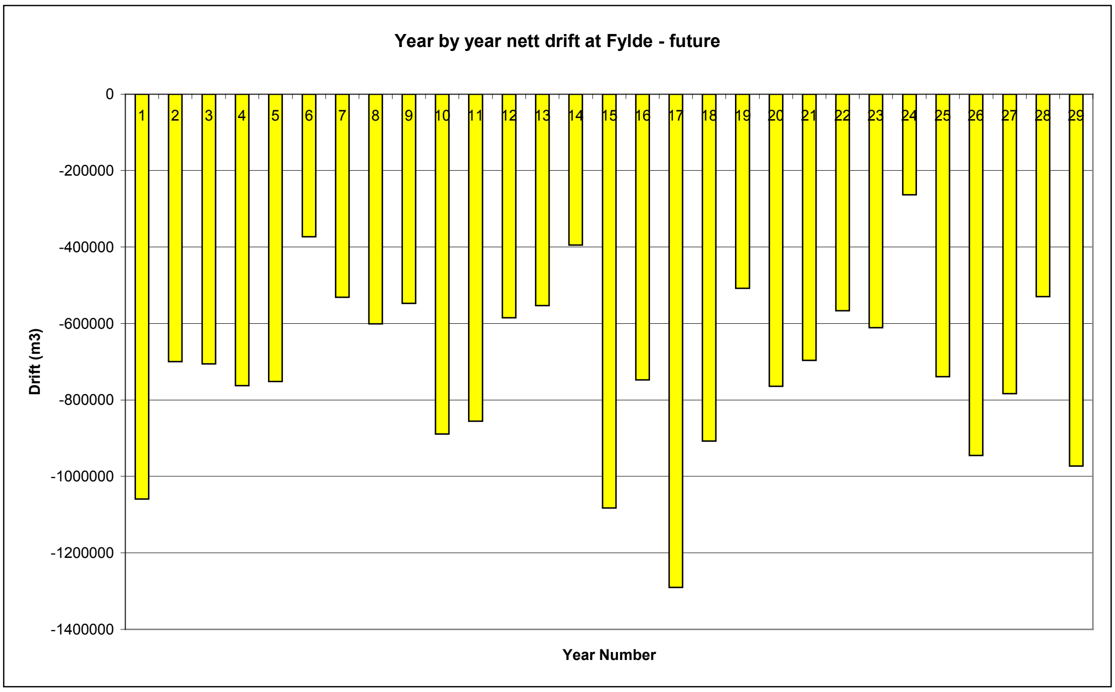

Figure 8.14 Future scenario nett annual drift rates at Fylde

Appendix 9

Statistical analysis of coastal defence response functions

Appendix 9 Overtopping rates from statistical analysis

The present and future overtopping rates were calculated for embankment and shingle beach at all five sites using the statistical analysis of the coastal defence response functions method (Section 7). The rates and their ratios are shown for a number of return periods for Lincolnshire, Dungeness to Rye, Lyme Bay, Swansea Bay and Fylde in Table 9.1 to Table 9.5 respectively. The following definitions apply:

- Q_p is the mean overtopping rate for present day conditions
- Q_f is the mean overtopping rate for future conditions
- Bank signifies that calculations were made for the standard embankment (details in Table 2)
- Shingle signifies that calculations were made for the standard shingle beach (details in Table 2)

Table 9.1 Overtopping rates and ratios at Lincolnshire

Return period [years]	Qp bank [$m^3/s/m$]	Qf bank [$m^3/s/m$]	Qf/Qp bank [-]	Qp shingle [$m^3/s/m$]	Qf shingle [$m^3/s/m$]	Qf/Qp shingle [-]
0.1	0.068	0.104	1.53	0.010	0.016	1.60
0.2	0.123	0.172	1.40	0.023	0.036	1.57
0.5	0.186	0.254	1.37	0.047	0.073	1.55
1	0.231	0.321	1.39	0.072	0.111	1.54
2	0.282	0.382	1.35	0.101	0.160	1.58
5	0.356	0.472	1.33	0.152	0.230	1.51
10	0.405	0.552	1.36	0.190	0.290	1.53
20	0.459	0.612	1.33	0.234	0.351	1.50
50	0.542	0.734	1.35	0.296	0.457	1.54
100	0.650	0.793	1.22	0.394	0.529	1.34
200	0.769	0.887	1.15	0.500	0.618	1.24
500	0.885	1.127	1.27	0.612	0.848	1.39

Table 9.2 Overtopping rates and ratios at Dungeness to Rye

Return period [years]	Qp bank [$m^3/s/m$]	Qf bank [$m^3/s/m$]	Qf/Qp bank [-]	Qp shingle [$m^3/s/m$]	Qf shingle [$m^3/s/m$]	Qf/Qp shingle [-]
0.1	0.218	0.405	1.86	0.054	0.150	2.78
0.2	0.301	0.552	1.83	0.096	0.249	2.59
0.5	0.399	0.708	1.77	0.162	0.392	2.42
1	0.471	0.816	1.73	0.219	0.505	2.31
2	0.539	0.918	1.70	0.277	0.623	2.25
5	0.623	1.057	1.70	0.360	0.782	2.17
10	0.693	1.143	1.65	0.417	0.904	2.17
20	0.762	1.258	1.65	0.475	1.051	2.21
50	0.880	1.471	1.67	0.601	1.269	2.11
100	0.973	1.630	1.68	0.700	1.494	2.13
200	1.078	1.764	1.64	0.788	1.690	2.14
500	1.300	2.025	1.56	1.075	2.620	2.44

Table 9.3 Overtopping rates and ratios at Lyme Bay

Return period [years]	Qp bank [$m^3/s/m$]	Qf bank [$m^3/s/m$]	Qf/Qp bank [-]	Qp shingle [$m^3/s/m$]	Qf shingle [$m^3/s/m$]	Qf/Qp shingle [-]
0.1	0.041	0.080	1.95	0.007	0.019	2.71
0.2	0.059	0.106	1.80	0.012	0.029	2.42
0.5	0.083	0.142	1.71	0.021	0.044	2.10
1	0.103	0.171	1.66	0.028	0.058	2.07
2	0.123	0.199	1.62	0.036	0.073	2.03
5	0.154	0.238	1.55	0.050	0.095	1.90
10	0.182	0.278	1.53	0.064	0.119	1.86
20	0.218	0.329	1.51	0.082	0.150	1.83
50	0.307	0.409	1.33	0.132	0.209	1.58
100	0.376	0.478	1.27	0.185	0.271	1.46
200	0.457	0.583	1.28	0.251	0.356	1.42
500	0.701	0.882	1.26	0.463	0.607	1.31

Table 9.4 Overtopping rates and ratios at Swansea Bay

Return period [years]	Qp bank [$m^3/s/m$]	Qf bank [$m^3/s/m$]	Qf/Qp bank [-]	Qp shingle [$m^3/s/m$]	Qf shingle [$m^3/s/m$]	Qf/Qp shingle [-]
0.1	0.445	0.655	1.47	0.146	0.278	1.90
0.2	0.691	0.960	1.39	0.287	0.500	1.74
0.5	0.974	1.288	1.32	0.500	0.802	1.60
1	1.184	1.530	1.29	0.685	1.049	1.53
2	1.372	1.747	1.27	0.877	1.294	1.48
5	1.592	2.008	1.26	1.153	1.667	1.45
10	1.735	2.212	1.27	1.339	1.910	1.43
20	1.875	2.395	1.28	1.517	2.213	1.46
50	2.053	2.601	1.27	1.744	2.518	1.44
100	2.190	2.718	1.24	1.986	2.735	1.38
200	2.280	2.859	1.25	2.178	3.219	1.48
500	2.372	3.229	1.36	2.313	3.855	1.67

Table 9.5 Overtopping rates and ratios at Fylde

Return period [years]	Qp bank [$m^3/s/m$]	Qf bank [$m^3/s/m$]	Qf/Qp bank [-]	Qp shingle [$m^3/s/m$]	Qf shingle [$m^3/s/m$]	Qf/Qp shingle [-]
0.1	0.091	0.148	1.63	0.008	0.019	2.38
0.2	0.132	0.208	1.58	0.016	0.033	2.06
0.5	0.195	0.293	1.50	0.031	0.061	1.97
1	0.244	0.359	1.47	0.048	0.087	1.81
2	0.292	0.424	1.45	0.068	0.119	1.75
5	0.357	0.516	1.45	0.099	0.166	1.68
10	0.402	0.583	1.45	0.125	0.209	1.67
20	0.467	0.672	1.44	0.150	0.263	1.75
50	0.565	0.812	1.44	0.212	0.366	1.73
100	0.656	0.947	1.44	0.259	0.481	1.86
200	0.829	1.213	1.46	0.364	0.859	2.36
500	0.930	1.489	1.60	0.539	1.366	2.53